

REPORT ON HIGH ENERGY ARCING FAULT EXPERIMENTS

Experimental Results from Open Box Enclosures

Date Published: December 2021

Prepared by:
G. Taylor
Office of Nuclear Regulatory Research

A.D. Putorti Jr.
National Institute of Standards and Technology

C. LaFleur
Sandia National Laboratories

Mark Henry Salley, NRC Project Manager

This report was published as National Institute of Standards and Technology (NIST) Technical Note 2198 as part of a series of experiments funded by the U.S. Nuclear Regulatory Commission's Office of Nuclear Regulatory Research. The report has been re-published as an NRC Research Information Letter (RIL).

Sandia National Laboratories is a multimission laboratory managed and operated by National Technology & Engineering Solutions of Sandia, LLC, a wholly owned subsidiary of Honeywell International Inc., for the U.S. Department of Energy's National Nuclear Security Administration under contract DE-NA0003525.

Disclaimer

Legally binding regulatory requirements are stated only in laws, NRC regulations, licenses, including technical specifications, or orders; not in Research Information Letters (RILs). A RIL is not regulatory guidance, although NRC's regulatory offices may consider the information in a RIL to determine whether any regulatory actions are warranted.

Certain commercial equipment, instruments, or materials are identified in this paper in order to specify the experimental procedure adequately. Such identification is not intended to imply recommendation or endorsement by the US Nuclear Regulatory Commission or the National Institute of Standards and Technology, or Sandia National Laboratories, nor is it intended to imply that the materials or equipment identified are necessarily the best available for the purpose.

Report on High Energy Arcing Fault Experiments

Experimental Results from Open Box Enclosures

Anthony D. Putorti Jr.
Scott Bareham
Christopher Brown
Wai Cheong Tam
Edward Hnetkovsky
Andre Thompson
Michael Selepak
Philip Deardorff
*National Institute of
Standards and Technology*

Kenneth Hamburger
Nicholas Melly
Kenneth Miller
Gabriel Taylor
*U.S. Nuclear Regulatory
Commission*

Kenneth Armijo
Paul Clem
Alvaro Augusto Cruz-Cabrera
Byron Demosthenous
Austin Glover
Chris LaFleur
Raymond Martinez
James Taylor
Rana Weaver
Caroline Winters
Sandia National Laboratories

This publication is available free of charge from:
<https://doi.org/10.6028/NIST.TN.2198>

December 2021



U.S. Department of Commerce
Gina M. Raimondo, Secretary

National Institute of Standards and Technology
*James K. Olthoff, Performing the Non-Exclusive Functions and Duties of the Under Secretary of Commerce
for Standards and Technology & Director, National Institute of Standards and Technology*

Certain commercial entities, equipment, or materials may be identified in this document in order to describe an experimental procedure or concept adequately. Such identification is not intended to imply recommendation or endorsement by the National Institute of Standards and Technology, nor is it intended to imply that the entities, materials, or equipment are necessarily the best available for the purpose.

**National Institute of Standards and Technology Technical Note 2198
Natl. Inst. Stand. Technol. Tech. Note 2198, 537 pages (December 2021)
CODEN: NTNOEF**

**This publication is available free of charge from:
<https://doi.org/10.6028/NIST.TN.2198>**

Abstract

This report documents an experimental program to investigate High Energy Arcing Fault (HEAF) phenomena. The experiments provide data to better characterize the arc to improve the prediction of arc energy emitted during a HEAF event. An open box allows for direct observation of the arc, jet, enclosure breach, material loss, and electrical properties.

The experiments were performed at KEMA Labs located in Chalfont, Pennsylvania. The experimental design, setup, and execution were completed by staff from the U.S. Nuclear Regulatory Commission (NRC), the U.S. National Institute of Standards and Technology (NIST), Sandia National Laboratories (SNL) and KEMA Labs. In addition, representatives from the Electric Power Research Institute (EPRI) observed some of the experimental setup and execution.

The HEAF experiments were performed between August 22, 2019 and September 18, 2019 on near-identical 51 cm (20 in) cubic metal boxes suspended from a Unistrut support structure. A three-phase arcing fault was initiated at the ends of the conductors oriented vertically and located at the center of the box. Either aluminum or copper was used for the conductors. The low-voltage experiments used 1 000 volts AC, while the medium-voltage experiments used 6 900 volts AC consistent with other recently completed experiments [1]. Durations of the experiment ranged from 1 s to 5 s with fault currents ranging from 1 kA to 30 kA. Real-time electrical operating conditions, including voltage, current, and frequency, were measured during the experiments. Heat fluxes and incident energies were measured with plate thermometers, plate calorimeters, and slug calorimeters at various locations around the electrical enclosures. The experiments were documented with normal and high-speed videography, infrared imaging, and photography.

Key words

High Energy Arcing Fault, Arc Flash, Electrical Enclosure, Electric Arc, Fire Probabilistic Risk Assessment

Table of Contents

1. Introduction	1
1.1. Background	1
1.2. Objectives	2
1.3. Scope	2
1.4. Approach	2
2. Experimental Method.....	1
2.1. Experiment Planning	1
2.2. Experiment Facility	2
2.3. Open Box.....	5
2.4. Instrumentation.....	7
2.4.1. Overview of Instruments	7
2.4.2. Optical Emission Spectroscopy	10
2.4.3. Digital Imaging.....	10
2.4.4. Calorimetry.....	13
2.4.5. d-Dot Sensors	23
2.4.6. Conductivity Sensors.....	25
2.4.7. Voltage Holdoff Strength	26
2.4.8. Mass Loss Measurements.....	28
2.4.9. Electrical Data Acquisition and Processing	29
3. Low-Voltage Experiment Results.....	34
3.1. Low-Voltage Experiment Results with Copper Electrodes	35
3.1.1. Experiment ID: OB01(a)	36
3.1.2. Experiment ID: OB01(b).....	38
3.1.3. Experiment ID: OB02	41
3.1.4. Experiment ID: OB03	44
3.1.5. Experiment ID: OB04	46
3.1.6. Experiment ID: OB09	50
3.2. Low-Voltage Experiment Results with Aluminum Electrodes	52
3.2.1. Experiment ID: OB05	53
3.2.2. Experiment ID: OB06	55
3.2.3. Experiment ID: OB07	57
3.2.4. Experiment ID: OB08	60
3.2.5. Experiment ID: OB10	63

3.3. Summary of Low-Voltage Box Experiments	65
4. Medium-Voltage Experiment Results.....	69
4.1. Medium-Voltage Experimental Results with Copper Electrodes	70
4.1.1. Experiment ID: OBMV04	70
4.1.2. Experiment ID: OBMV05	74
4.2. Medium-Voltage Experiment Results with Aluminum Electrodes.....	78
4.2.1. Experiment ID: OBMV01	78
4.2.2. Experiment ID: OBMV02	82
4.2.3. Experiment ID: OBMV03	88
4.2.4. Experiment ID: OBMV06	92
4.3. Summary of Medium-Voltage Open Box Experiments	97
5. Summary and Conclusion.....	99
5.1. Summary	99
5.2. Conclusions	100
References.....	102
Appendix A: Engineering Drawings	105
A.1 Experiments Facility.....	105
A.2 Support Drawings.....	111
Appendix B: Measurement Plots.....	115
Appendix C: KEMA Experiment Report.....	160

List of Tables

Table 1. Low-voltage box experimental matrix.....	7
Table 2. Medium-voltage box experimental matrix.....	7
Table 3. List of measurement equipment.....	8
Table 4. Expanded uncertainty for IR imager temperatures.....	13
Table 5. Low-voltage circuit calibration.....	34
Table 6. Low-voltage experiments - planned nominal experiment parameters.....	34
Table 7. Medium-voltage experiments - planned nominal experiment parameters.....	35
Table 9. Experiment OB01(a) parameters.....	36
Table 10. Experiment OB01(a) plate calorimeter measurements.....	37
Table 11. Experiment OB01(b) parameters.....	39
Table 12. Experiment OB01(b) plate calorimeter measurements.....	40
Table 13. Experiment OB02 parameters.....	41
Table 14. Experiment OB02 plate calorimeter measurements.....	43
Table 15. Experiment OB03 parameters.....	44
Table 16. Experiment OB03 plate calorimeter measurements.....	46
Table 17. Experiment OB04 parameters.....	47
Table 18. Experiment OB04 plate calorimeter measurements.....	49
Table 19. Experiment OB09 parameters.....	50
Table 20. Experiment OB09 plate calorimeter measurements.....	52
Table 21. Experiment OB05 parameters.....	53
Table 22. Experiment OB05 plate calorimeter measurements.....	54
Table 23. Experiment OB06 parameters.....	55
Table 24. Experiment OB06 plate calorimeter measurements.....	56
Table 25. Experiment OB07 experiment parameters.....	57
Table 26. Experiment OB07 plate calorimeter measurements.....	59
Table 27. Experiment OB08 parameters.....	60
Table 28. Experiment OB08 plate calorimeter measurements.....	62
Table 29. Experiment OB10 parameters.....	63
Table 30. Experiment OB10 plate calorimeter measurements.....	64
Table 31. Summary of low-voltage box experiments.....	67
Table 32. Low-voltage box experiment comparison of measured electrical energy and calculated energy from calorimeter heat rise.....	68
Table 33. Medium-voltage circuit calibration.....	69
Table 34. Medium-voltage experiments planned nominal parameters.....	69
Table 35. Experiment OBMV04 parameters.....	71
Table 36. Experiment OBMV04 thermal measurements.....	73
Table 37. Experiment OBMV05 parameters.....	74
Table 38. Experiment OBMV05 thermal measurements.....	76
Table 39. Experiment OBMV01 parameters.....	78
Table 40. Experiment OBMV01 thermal measurements.....	80
Table 41. Experiment OBMV02 parameters.....	82
Table 42. Experiment OBMV02 thermal measurements.....	84
Table 43. Experiment OBMV03 parameters.....	88
Table 44. Experiment OBMV03 thermal measurements.....	91
Table 45. Experiment OBMV06 parameters.....	93

Table 46. Experiment OBMV06 thermal measurements.	95
Table 47. Summary of medium-voltage open box experiment results.	97
Table 48. Medium-voltage box experiment summary of thermal measurements.	98
Table 49. Summary of low-voltage and medium-voltage experiment parameters.	99

List of Figures

Fig. 1. Isometric drawing of test cell #7 (left) and location of test cell #7 (right with respect to KEMA facility).....	3
Fig. 2. Isometric drawing of test cell # 9 (left) and location of test cell #9 (right with respect to KEMA facility).....	4
Fig. 3. Open box configuration low-voltage experiments (left – isometric, center – 1.3 cm (0.5 in) copper electrode, right – 2.5 cm (1 in) aluminum electrode).....	5
Fig. 4. Open box configuration medium-voltage experiments (left - isometric, center – aluminum 10.2 cm (4 in) bars, right – copper 7.62 cm (3 in) bars).....	6
Fig. 5. Plan view of instrumentation locations (note that locations and instruments used varied by experiment and illustration is not to scale). Three cameras (labeled ‘C’ are shown in the far left of the figure and were approximately 5.8 m from the open box.	9
Fig. 6. Instrumentation cluster covered with heat resisting fabric for protection during experiments (from left-to-right, air breakdown, plate calorimeter, d-dot, air conductivity, high speed IR, and visible videography).	9
Fig. 7. The spectrometer is mounted to the top of the base plate.	10
Fig. 8. High-speed high-resolution imaging (left – IR image, center - IR image fused with visible image, right – visible image).	11
Fig. 9. Thermal imagers used inside and outside the test cell (left – thermal imaging cameras located approximately 27 m from the open box, right – imaging cameras located within the test cell, from left to right: thermal, high speed visible, thermal).	12
Fig. 10. Plate calorimeter apparatus in its thermal protected configuration	14
Fig. 11. Exploded view of modified plate thermometer (left); cross-sectional view of modified plate thermometer placed on cone calorimeter sample holder (right).	15
Fig. 12. Cross-section of ASTM Slug (top) nominal dimensions in millimeters, photo of device being prepared in the field (bottom). Note that the two bolts on each side of the device are used for mounting to the DIN rail of the instrumentation rack.....	18
Fig. 13. Thermal capacitance style slug, illustration (top left), photo of device being prepared in the field (top right), dimensional drawings showing internal construction (bottom left and right). All nominal dimensions in mm.	20
Fig. 14. Calorimeter arrays used during medium-voltage experiments (left – horizontal array, center - array location within cell, right – vertical array).	21
Fig. 15. Calorimeter configuration during the medium-voltage experiments. Approximate dimensions in mm.	22
Fig. 16. Data acquisition system configuration with EMI rejection.....	23
Fig. 17. d-Dot sensors arrangement prior to experiment. Note all sensors oriented in same axis based on results from earlier experiment indicating the largest measured signal.....	24
Fig. 18. Parallel plate sensors with a perforated screen design to eliminate EMI.	25

Fig. 19. Breakdown sensor (left – electrode configuration, middle – safety jumper, right – operational experiment).....	27
Fig. 20. Measured waveform spark gap from experiment.....	27
Fig. 21. High voltage breakdown strength: pre-HEAF ($E_{BD}=28.5\text{kV/cm} \pm 2.2$ kV/cm).	28
Fig. 22. Example of mass loss measurement using surface area estimated by computer software (363 cm^2 estimated area in example photo shown).....	29
Fig. 23. Zero-sequence voltage (Experiment OB08).....	30
Fig. 24. Original and modified device voltage when wye-neutral was not connected to ground (Experiment OB04).	31
Fig. 25. Original and modified device voltage when wye-neutral was connected to ground via impedance (Experiment OB04).	32
Fig. 26. Line-to-ground voltage at generator (top), at open box (middle), and modified open box voltage (bottom) (experiment ob08).....	33
Fig. 27. Experiment OB01(a) pre-experiment (left) and post-experiment (right) copper electrodes. Phase sequence from left-to-right is C-B-A.	37
Fig. 28. Thermal (left) and visible (right) video still shot during arc ($t = 1.97\text{s}$)	37
Fig. 29. Experiment OB01(b) pre-experiment (left) and post-experiment (right) copper electrodes. Phase sequence from left-to-right is C-B-A.	40
Fig. 30. Experiment OB02 pre-experiment (left) and post-experiment (right) copper electrodes. Phase sequence from left-to-right is C-B-A.	42
Fig. 31. Experiment OB02 enclosure breach. (bottom side breach (left), top side breach with electrode holder removed (right)).	42
Fig. 32. Experiment OB02 thermal (left) and visible (right) video still shots during the arc ($t = 1.47\text{ s}$).	43
Fig. 33. Experiment OB03 pre-experiment (left) and post-experiment (right) copper electrodes. Phase sequence from left-to-right is C-B-A.	45
Fig. 34. Experiment OB03 enclosure breach (from left-to-right: top, left side, bottom, right side).	45
Fig. 35. Experiment OB03 still shots from the high speed visible video during the arc (Left 0.02 s , Center 1.50 s , Right 3.06 s)	45
Fig. 36. Experiment OB04 pre-experiment (left) and post-experiment (right) copper electrodes. Phase sequence from left to right is C-B-A.	47
Fig. 37. Experiment OB04 enclosure breach (left – bottom side; right – top side).....	48
Fig. 38. Experiment OB04 electrode deflection post-experiment.	48
Fig. 39. Experiment OB04 visible video still shot during the arc (Left 0.09 s ; Center 0.51 s ; Right 1.08 s).	49
Fig. 40. Experiment OB09 pre-experiment (left) and post-experiment (right) copper electrodes. Phase sequence from left-to-right is C-B-A.	51
Fig. 41. Experiment OB09 thermal (left) and visible (right) video still shots during the arc ($t = 0.06\text{ s}$).	51
Fig. 42. Experiment OB05 pre-experiment (left) and post-experiment (right) aluminum electrodes. Phase sequence from left-to-right is C-B-A.	54
Fig. 43. Experiment OB05 thermal (left) and visible (right) video still shot during the arc ($t = 0.33\text{s}$).	54

Fig. 44. Experiment OB06 pre-experiment (left) and post-experiment (right) aluminum electrodes. Phase sequence from left-to-right is C-B-A.	56
Fig. 45. Experiment OB06 enclosure breach (Left –bottom and sides; Right – rear top side).....	56
Fig. 46. Experiment OB07 pre-experiment (left) and post-experiment (right) aluminum electrodes. Phase sequence from left-to-right is C-B-A.	58
Fig. 47. Experiment OB07 enclosure breach (Left – bottom and sides; Right – rear top side).....	58
Fig. 48. Experiment OB07 thermal (left) and visible (right) video still shot during the arc ($t = 0.06$ s).	59
Fig. 49. Experiment OB08 pre-experiment (left) and post-experiment (right) aluminum electrodes. Phase sequence from left-to-right is C-B-A. Note the center electrode was ejected free from the box during the experiment.....	61
Fig. 50. Experiment OB08 enclosure breach (Left –bottom and sides; Right – rear top).	61
Fig. 51. Experiment OB08 aluminum electrodes post-experiment (top three, bottom electrode is from another experiment and included for comparison).	62
Fig. 52. Experiment OB10 pre-experiment (left) and post-experiment (right) aluminum electrodes. Phase sequence from left-to-right is C-B-A.	64
Fig. 53. Experiment OB10 thermal (left) and visible (right) video still shot during arc ($t = 0.06$ s).	64
Fig. 54. Comparison of actual electrical energy input and calculated calorimeter energy with power law fits indicated by dashed lines for aluminum (Al) and copper (Cu) electrodes.	66
Fig. 55. Experiment OBMV04 pre-experiment (left) and post-experiment (right) copper electrodes. Phase sequence from left to right is C-B-A.	72
Fig. 56. Experiment OBMV04 enclosure breach (Left-to-right: Right side, back side, left side).	72
Fig. 57. Experiment OBMV04 copper electrode remanence post-experiment.	72
Fig. 58. Experiment OBMV05 pre-experiment (top) and post-experiment (bottom, left-to-right, left side from outside, front, right side from outside).Phase sequence from left to right is C-B-A.....	75
Fig. 59. Experiment OBMV05 copper electrodes post-experiment.	75
Fig. 60. Experiment OBMV01 pre-experiment (top) and post-experiment (bottom left – side, bottom center – back, bottom right - side). Phase sequence from left to right is C-B-A.	79
Fig. 61. Experiment OBMV01 aluminum electrode post-experiment.	79
Fig. 62. Air conductivity measurement during OBMV01.....	81
Fig. 63. Experiment OBMV02 pre-experiment (left) and post-experiment (right) aluminum electrodes. Phase sequence from left to right is C-B-A.....	83
Fig. 64. Experiment OBMV2 enclosure breach (Left-to-right: left side, bottom side, right side).	83
Fig. 65. Experiment OBMV02 aluminum electrodes post-experiment.	84
Fig. 66. Breakdown experiment prior to Experiment OBMV02.	85
Fig. 67. Breakdown experiment during Experiment OBMV02.	86

Fig. 68. Air conductance measurements during experiment OBMV02.	86
Fig. 69. Experiment OBMV03 pre-experiment (left) and post-experiment (right) aluminum electrodes. Phase sequence from left to right is C-B-A.	89
Fig. 70. Experiment OBMV03 enclosure breach (left-to-right: Left side, back side, right side, top).	89
Fig. 71. Experiment OBMV03 aluminum electrode post-experiment.	90
Fig. 72. Experiment OBMV03 air conductance measurement.	92
Fig. 73. Experiment OBMV06 pre-experiment (left) and post-experiment (right) aluminum electrodes. Phase sequence from left to right is C-B-A.	94
Fig. 74. Experiment OBMV6 enclosure breach (Left-to-right: left side, back side, bottom side, and right side).	94
Fig. 75. Experiment OBMV06 aluminum electrodes post-experiment.	94
Fig. 76. Isometric drawing of test cell #7.	105
Fig. 77. Plan view of Experiment Cell #7. Low-voltage power connections located on right side of drawing.	106
Fig. 78. Elevation view of test cell #7. Low-voltage power connections located on right side of drawing.	107
Fig. 79. Isometric drawing of test cellCell #9	108
Fig. 80. Plan view of test cellCell #9.	109
Fig. 81. Elevation view of test cellCell #9. Breaker shown in drawing is part of KEMA protection system and is not the open box.	110
Fig. 82. Electrode holder used in open box experiments. All nominal dimensions shown in inches.	112
Fig. 83. Drawing KPT-MB-4657, ASTM Calorimeter Assembly.	113
Fig. 84. Drawing KPT-MA-4599, ASTM Calorimeter Cup.	114
Fig. 85. Spectrum from Experiment OB01(a).	115
Fig. 86. Spectrum from Experiment OB01(b), early.	116
Fig. 87. Spectrum from Experiment OB01(b), mid-experiment (left) and late (right).	116
Fig. 88. Experiment OB05 spectra.	117
Fig. 89. Experiment OB07 spectral profiles, an early profile with spectral features (top), transition spectral features (bottom left), and a broadband emission spectrum (bottom right).	119
Fig. 90. Experiment OB08 spectra showing an early profile with spectral features (top), transition spectral features (bottom left), and a broadband emission spectra (bottom right).	120
Fig. 91. Experiment OB09 spectra at the beginning of the experiment (left) and near the end (right).	121
Fig. 92. Experiment OB10 spectra an early profile (left) and a late profile (right).	122
Fig. 93. Experiment OBMV01 spectrum from early in the experiment (left) and later in the experiment (right).	122
Fig. 94. Spectrum from Experiment OBMV02.	123
Fig. 95. Spectrum from Experiment OBMV03.	123
Fig. 96. Experiment OBMV05 spectrum early in the experiment (left) and later in the experiment (right).	124
Fig. 97. Voltage and current measurements for Experiment OB01(a).	126
Fig. 98. Transient current profiles for Experiment OB01(a).	127

Fig. 99. Voltage and current measurements for Experiment OB01(b).....	128
Fig. 100. Transient current profiles for Experiment OB01(b).....	129
Fig. 101. Experiment OB02 voltage and current measurements.	130
Fig. 102. Experiment OB02 transient current profiles.	131
Fig. 103. Experiment OB03 voltage and current measurements.	132
Fig. 104. Experiment OB03 transient current profiles.	133
Fig. 105. Experiment OB04 voltage and current measurements.	134
Fig. 106. Experiment OB04 transient current profiles.	135
Fig. 107. Experiment OB05 voltage and current measurements.	136
Fig. 108. Experiment OB05 transient current profiles.	137
Fig. 109. Experiment OB06 voltage and current measurements.	138
Fig. 110. Experiment OB06 transient current profiles.	139
Fig. 111. Experiment OB07 voltage and current measurements.	140
Fig. 112. Experiment OB07 transient current profiles.	141
Fig. 113. Experiment OB08 voltage and current measurements.	142
Fig. 114. Experiment OB08 transient current profiles.	143
Fig. 115. Experiment OB09 voltage and current measurements.	144
Fig. 116. Experiment OB09 transient current profiles.	145
Fig. 117. Experiment OB10 voltage and current measurements.	146
Fig. 118. Experiment OB10 transient current profiles.	147
Fig. 119. Experiment OBMV01 voltage and current measurements.....	148
Fig. 120. Experiment OBMV01 transient current profiles.	149
Fig. 121. Experiment OBMV01 power and energy profiles.	149
Fig. 122. Experiment OBMV02 voltage and current measurements.....	150
Fig. 123. Experiment OBMV02 transient current profiles.	151
Fig. 124. Experiment OBMV02 power and energy profiles.	151
Fig. 125. Experiment OBMV03 voltage and current measurements.....	152
Fig. 126. Experiment OBMV03 transient current profiles.	153
Fig. 127. Experiment OBMV03 power and energy profiles.	153
Fig. 128. Experiment OBMV04 voltage and current measurements.....	154
Fig. 129. Experiment OBMV04 transient current profiles.	155
Fig. 130. Experiment OBMV04 power and energy profiles.	155
Fig. 131. Experiment OBMV05 voltage and current measurements.....	156
Fig. 132. Experiment OBMV05 transient current profiles.	157
Fig. 133. Experiment OBMV05 power and energy profiles.	157
Fig. 134. Experiment OBMV06 voltage and current measurements.....	158
Fig. 135. Experiment OBMV06 transient current profiles.	159
Fig. 136. Experiment OBMV06 power and energy profiles.	159

EXECUTIVE SUMMARY

PRIMARY AUDIENCE: Fire protection, electrical and probabilistic risk assessment engineers conducting or reviewing fire risk assessments related to high energy arcing faults.

SECONDARY AUDIENCE: Engineers, reviewers, utility managers, and other stakeholders who conduct, review, or manage fire protection programs and need to understand the underlying technical basis for the hazards associated with high energy arcing faults.

KEY RESEARCH QUESTION: How does the energy of electrical arcs change with variation of influencing parameters (e.g., current, voltage, duration, and electrode material)?

RESEARCH OVERVIEW

Operating experience has shown that high energy arcing faults pose a hazard to the safe operation of nuclear facilities. Current regulations and probabilistic risk assessment methods were developed using limited information, and these uncertainties required the use of safety margins to bound the hazard. Experiments aimed at providing additional data to improve realism identified a concern that high energy arcing faults involving aluminum may increase the hazard potential. Due to the limited number of experiments where this phenomenon was observed, the NRC pursued additional experiments focused on assessing the specific impact of aluminum on the hazard. This report documents a set of experiments performed in 2019.

A series of open box electrical arcing experiments were performed under a variety of conditions believed to influence the arc energy characteristics. These influencing parameters included conductor material type, arc duration, fault current, system voltage, and conductor size. Each experiment consisted of an arcing fault initiated and sustained within a five-sided cubical metal enclosure. Numerous measurements were taken to characterize the environment within and surrounding the box, including external heat flux, external incident energy, electromagnetic field, air breakdown strength, and mass loss of electrical conductors and steel box enclosure. Photometric equipment and techniques were deployed to capture the event using a combination of devices to characterize the thermal environment, particulate trajectory and velocity, and event timing.

This report documents the experiments performed, including the experimental methods, experiment facility, open box, instrumentation, experiment observations, and results. Videos and photometric data files are provided by laboratories contracted to the NRC, and information on accessing that information is identified. This report does not provide detailed evaluation of the results or comparisons of the results to other methods or data. Those efforts will be documented in subsequent report(s).

KEY FINDINGS

This research yields a data set of information to characterize the effects of electrical arcing faults involving aluminum or copper electrodes. The results from this research include:

- External heat flux and incident energy measurements which provide direct comparison between aluminum and copper electrodes.

- Mass loss data was collected for the electrodes and the steel enclosure. This information can be subsequently used to evaluate or develop prediction models to support hazard modeling.
 - For the electrodes, more mass was lost for copper electrodes than aluminum when normalized to an equivalent electrical experimental energy.
 - The steel box enclosure mass lost was observed to be larger for the aluminum electrode experiments versus the copper electrode experiments when normalized to an equivalent electrical experimental energy.
- Air conductivity and breakdown strength measurements were made during a number of experiments. For the experimental conditions and locations investigated, the results indicated that the conductive cloud was unlikely to cause equipment arc over.
- Surface conductivity measurement of HEAF byproduct surface deposition showed a decrease in resistance. Impact on plant safety equipment is not likely, but highly dependent on the design, configuration, location, and sensitivity of the equipment.
- For the experimental conditions and locations investigated, the electromagnetic interference measurements showed that the EMI signature was small and not likely to impact sensitive plant equipment.

WHY THIS MATTERS

This report provides empirical evidence to assist U.S. NRC staff and stakeholders who are evaluating the adequacy of current methods. The information provided will support advances in state-of-the-art methods and tools to assess the high energy arcing fault hazard in nuclear facilities. This information may also be applicable to fossil fuel and alternative energy facilities and other buildings with low-voltage and medium-voltage electrical distribution equipment such as switchgear and bus duct.

HOW TO APPLY RESULTS

Engineers and scientist advancing hazard and fire probabilistic risk assessment methods should focus on Section 3 and 4 of this report.

LEARNING AND ENGAGEMENT OPPORTUNITIES

Users of this report may be interested in the following learning opportunities:

Nuclear Energy Agency (NEA) HEAF Project to conduct experiments in order to explore the basic configurations, failure modes and effects of HEAF events. Primary objectives include (1) development of a peer-reviewed guidance document that could be readily used to assist regulators of participants, and (2) joint nuclear safety project report covering all testing and data captured. More information on the project and opportunities to participate in the program can be found online at <https://www.oecd-nea.org/>.

CITATIONS

This report was prepared by the following:

National Institute of Standards and Technology (NIST)
Engineering Laboratory; Fire Research Division
Gaithersburg, Maryland 20899

Anthony D. Putorti Jr.
Scott Bareham
Christopher Brown
Wai Cheong Tam
Edward Hnetkovsky
Andre Thompson
Michael Selepak
Phil Deardorff

Sandia National Laboratories (SNL)
Albuquerque, New Mexico 87185

Kenneth Armijo
Alvaro Augusto Cruz-Cabrera
Paul Clem
Byron Demosthenous
Austin Glover
Chris LaFleur
Ray Martinez
James Taylor
Rana Weaver
Caroline Winters

U.S. Nuclear Regulatory Commission
Washington, DC 20555-0001

Kenneth Hamburger
Nicholas Melly
Kenneth Miller
Gabriel Taylor

ABBREVIATIONS AND ACRONYMS

AC	alternating current
ASTM	ASTM International
AWG	American Wire Gauge
DC	direct current
DIN	Deutsches Institut für Normung
EMI	electro-magnetic interference
EPRI	Electric Power Research Institute
GI	generic issue
GIRP	Generic Issue Review Panel
HEAF	high energy arcing fault
IEEE	Institute of Electrical and Electronic Engineers
IN	information notice
IR	infra-red
ISO	International Organization for Standardization
MD	management directive
NEA	Nuclear Energy Agency
NIST	National Institute of Standards and Technology
NRC	Nuclear Regulatory Commission
OECD	Organisation for Economic Co-operation and Development
OBMV	open box medium-voltage
PIRT	Phenomena Identification and Ranking Table
PRA	probabilistic risk assessment
PT	plate thermometer
RES	Office of Nuclear Regulatory Research
RIL	research information letter
SNL	Sandia National Laboratories
TTL	transistor-transistor logic
T _{cap}	Tungsten slug calorimeter
U.S.	United States of America

1. Introduction

Infrequent events such as fires at a nuclear power plant can pose a significant risk to safe plant operations. Licensees combat this risk by having robust fire protection programs designed to minimize the likelihood and consequences of fire. These programs provide reasonable assurance of adequate protection of the facility from known fire hazards. However, several hazards remain subject to a larger degree of uncertainty, requiring significant safety margins in plant analyses.

One such hazard comprises an electrical arcing fault involving electrical distribution equipment and components comprised of aluminum. While the electrical faults and subsequent fires are considered in existing fire protection programs, recent research [2] has indicated that the presence of aluminum during the electrical fault can exacerbate the damage potential of the event. The extended damage capacity could exceed the protection provided by existing fire protection features for specific fire scenarios and increase plant risk estimated in fire probabilistic risk assessments (PRAs).

The U.S. Nuclear Regulatory Commission (NRC) Office of Nuclear Regulatory Research (RES) studies fire and explosion hazards to ensure the safe operation of nuclear facilities. This includes developing data, tools, and methodologies to support risk and safety assessments. Through recent research efforts and collaboration with international partners, a non-negligible number of reportable high energy arcing fault (HEAF) events have been identified as occurring in nuclear facilities [2]. HEAF events pose a unique hazard in nuclear facilities, and additional research in this area is needed to ensure that the hazard is accurately characterized and assessed for its impact on nuclear safety.

1.1. Background

In June 2013, an OECD/NEA report [3] on international operating experience documented 48 HEAF events, accounting for approximately 10 percent of the total fire events reported. These HEAF events are often accompanied by loss of essential power and complicated shutdowns. Existing PRA methodology for HEAF analysis is prescribed in NUREG/CR-6850 “EPRI/NRC-RES Fire PRA Methodology for Nuclear Power Facilities Vol. 2 [4],” and its Supplement 1 [5]. To confirm these methods, the NRC led an international experimental campaign from 2014 to 2016. This experimental campaign is referred to as “Phase 1 experiments.” The results of these experiments [6] uncovered a potential increase in hazard posed by aluminum components in or near electrical equipment, as well as unanalyzed equipment failure mechanisms.

In response to this new information, the NRC performed a thorough review of U.S. operating experience with a focus on instances where HEAF-like events have occurred in the presence of aluminum. This review uncovered six events where aluminum effects like those observed in the experiments were present. An Information Notice 2017-004, “High Energy Arcing Faults in Electrical Equipment Containing Aluminum Components (IN 2017-04)” detailing the relevant aspects of the licensee event reports and Phase 1 experiments was published in August of 2017 [2].

Additionally, the staff in the Office of Nuclear Regulatory Research (RES) proposed a potential safety concern as a generic issue (GI) in a letter dated May 6, 2016 [7]. The Generic Issue Review Panel (GIRP) completed its screening evaluation [8] for proposed Generic Issue (GI) PRE-GI-018, “High-Energy Arc Faults (HEAFs) Involving Aluminum,” and concluded that the proposed issue met all seven screening criteria outlined in Management Directive (MD) 6.4, “Generic Issues Program.” Therefore, the GIRP recommended that this issue continue into the Assessment Stage of the GI program. The GIRP has completed an assessment plan, issued July 10, 2019 [9]. Though the HEAF research project will result in updated fire PRA guidance for all arcing faults, much of the HEAF research program exists to resolve PRE-GI-018 in accordance with the assessment plan.

These actions resulted in the identification of a need for more data to better understand the hazard. The NRC developed an experimental plan in collaboration with its international collaborative partners under the OECD/NEA program and based on information from a Phenomena Identification and Ranking Table (PIRT) exercise performed in 2017 [10].

On August 31, 2021, the NRC closed the proposed generic issue PRE-GI-018, “High Energy Arc Faults involving Aluminum,” [11] based on the fact that the proposed GI did not meet one of the seven screening criteria. The GIRP concluded that the risk and safety significance of HEAFs involving aluminum cannot be adequately determined without performing additional, long-term research to develop the methodology for such a determination. As such, Criterion 5 of the screening criteria in NRC Management Directive 6.4 is no longer being met, and the proposed GI exited the program.

1.2. Objectives

The research objectives for this experimental series include: 1) observe and record electrical arc behavior to support model development and refinement, 2) measure arc optical emissions, 3) measure electric field, 4) evaluate arc effluent impact on air breakdown strength, and 5) measure the air conductivities of the arc effluent.

1.3. Scope

The scope of this research includes performing experiments to characterize low and medium electric arc using a variety of instrumentation. This effort involves measurement and documentation of electrical and thermal parameters, along with physical evidence. Detailed data analysis for specific applications is beyond the scope of this report.

1.4. Approach

The approach taken for this work follows practices from past efforts but makes several deviations to achieve the objectives. Specifically, the electrical arc is initiated using a three-phase power system. The arc persists for a specified duration, current, and system voltage. Measurements taken prior to, during, and after the experiments are performed to assess specific characteristics of the arc and the influence of parameter variation. KEMA Labs provided electrical energy for the experiment at the specified experimental parameters (system voltage, current, duration). Measurements internal and external to the arc were made using robust measurement devices fielded by the National Institute of Standards and Technology (NIST), KEMA Labs, and Sandia National Laboratories (SNL). Measurements

were recorded, scaled, and reported. Feedback received during the developmental stage of this project was incorporated into the experimental approach.

2. Experimental Method

This section provides information on methods used to perform the experiments¹, including experiment planning, an overview of the experiment facility, the experimental apparatus, and the various instrumentation that were used.

2.1. Experiment Planning

The experiments are designed to complement small-scale arc experiments that were performed at SNL in 2018 and 2019 [12]. The small-scale experiments were limited in the amount of energy that could be delivered to the arc. The experiments performed at KEMA Labs provide more representative energy (voltage, current, and duration) to ensure that the small-scale experimental results are applicable and to understand the impacts of changes in the configuration. In addition, three-phase faults were performed instead of single-phase to ground faults. The small-scale experimental results are documented in SAND2019-11145, “Electrical Arc Fault Particle Size Characterization [12].”

The experiment plan was developed in 2019. Lessons learned from the Phase 1 experiments [6], results from the Phenomena Identification and Ranking Table (PIRT) exercise [10], the literature, and input from the SNL modeling team were used to develop the initial experimental plan. Feedback was received and discussed with the Electric Power Research Institute (EPRI). These discussions resulted in changes to the plan that provided improvements to the overall approach and confidence in the execution of the effort. In addition to the experiments that support model development, additional needs were identified through stakeholder feedback. These include a better understanding of the electrical conductivity characteristics of the arc effluent and the strength of the electromagnetic field of the arc. Two additional experimental plans were developed to address those aspects.

The key parameters that the experimental plan evaluates include:

- Material – copper vs. aluminum electrical conductors
- Voltage – low-voltage vs. medium-voltage
- Current – selection of credible arcing current(s)
- Duration – low-to-mid range HEAF duration(s)

¹ The term ‘test’ implies the use of a standardized test method promulgated by a standards development organization such as the International Organization for Standardization (ISO), ASTM International, Institute of Electrical and Electronics Engineers (IEEE), etc. The experiments described in this report are not standardized tests and were specifically developed to examine HEAF phenomena. The term ‘test’ is used in some contexts to preserve continuity with previous programs or to describe facilities where standard tests are frequently performed. Standard test methods, where they exist, are used for some measurements.

2.2. Experiment Facility

The full-scale experiments were performed at KEMA Labs (referred to in the remainder of this report as “KEMA”), located in Chalfont, Pennsylvania. Two sets of experiments were performed, one in August and the other in September of 2019. The laboratory was chosen for its ability to meet the requirements of the program, specifically the required voltage and current to sustain an electrical arc within the test enclosure.

The test cells were approximately 10 m by 9 m by 8 m high, open on one side. The open side of the test cell faces the operator control room which is equipped with impact resistant glazing

Two different test cells were used during this experiment series. Test Cell #7 was used in August to perform the low-voltage experiments. Test Cell #9 was used in September for the medium-voltage experiments. The test cells are shown in Fig. 1 and Fig. 2. Detailed drawings of the facility are provided in Appendix A. Drawings of the test cells are courtesy of KEMA Labs.

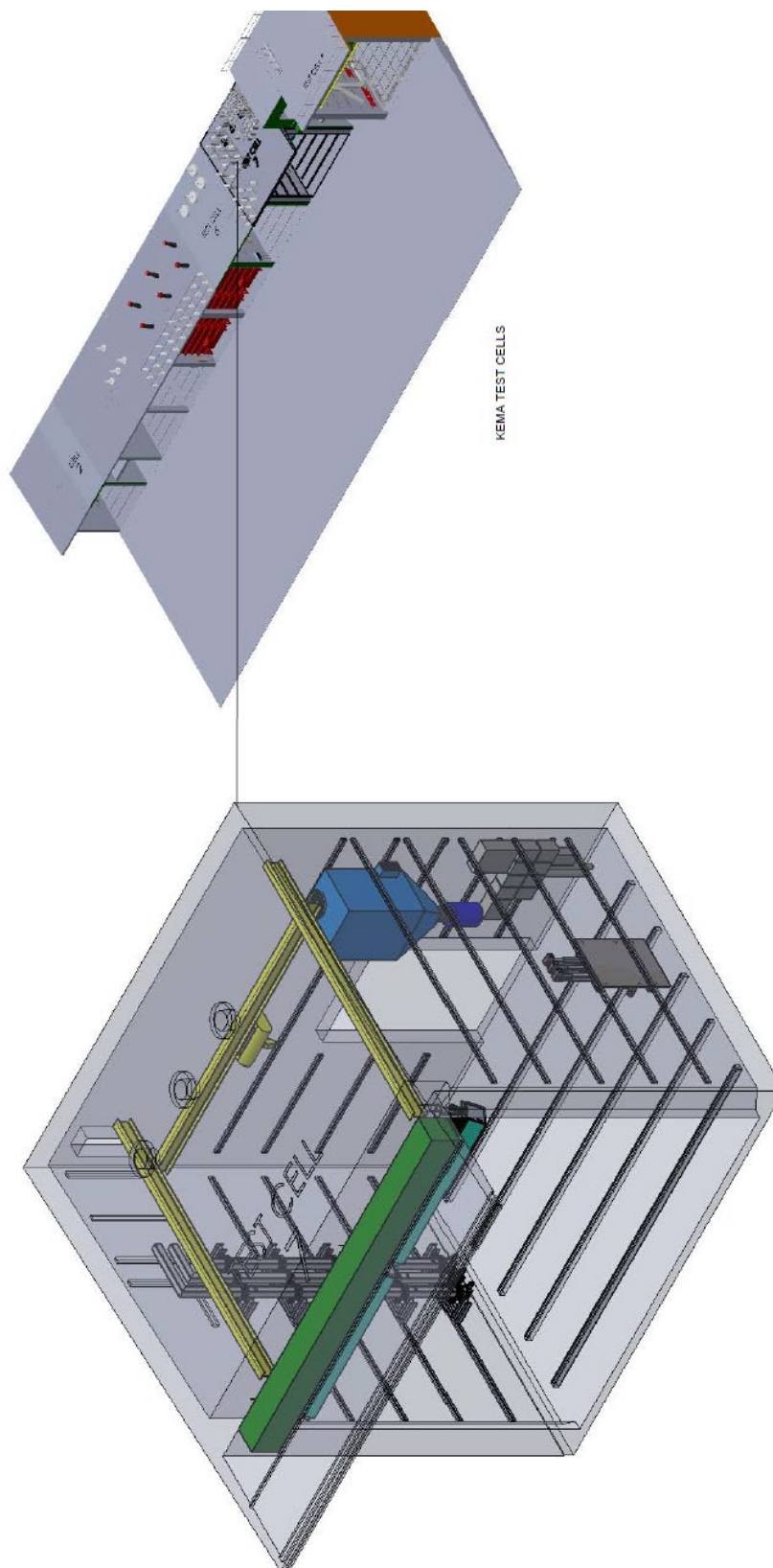


Fig. 1. Isometric drawing of Test Cell #7 (left) and location of Test Cell #7 (right with respect to KEMA facility).

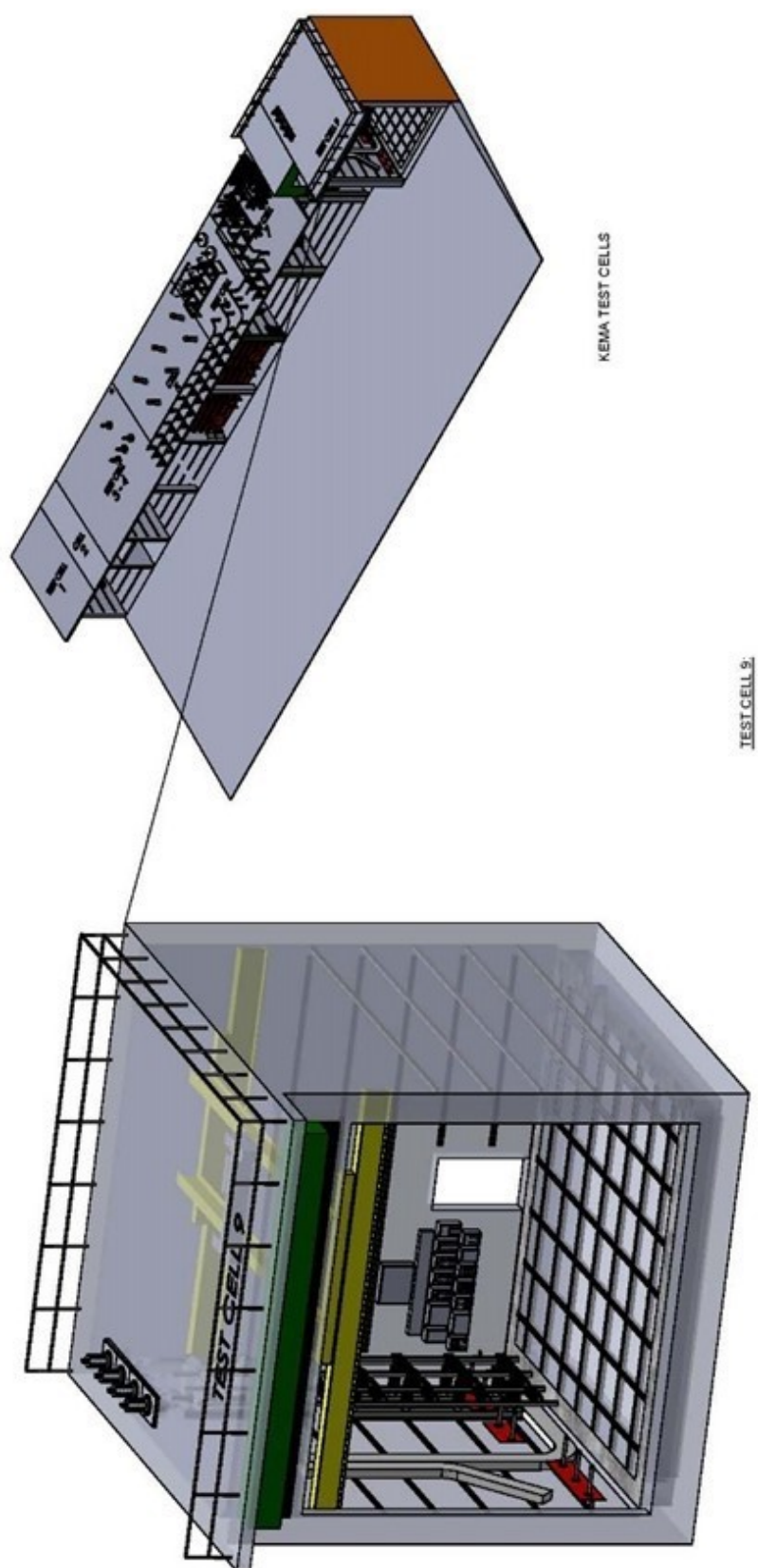


Fig. 2. Isometric drawing of Test Cell # 9 (left) and location of Test Cell #9 (right with respect to KEMA facility).

2.3. Open Box

The open box is shown in Fig. 3 for low-voltage and Fig. 4 for medium-voltage experiments. The box dimensions were approximately 51 cm by 51 cm by 51 cm (20 in by 20 in by 20 in). The box was made of sheet steel with a nominal thickness of 0.18 cm (0.07 in). Three electrodes were spaced approximately 8.9 cm (3.5 in) on center for low-voltage and approximately 13 cm (5.0 in) on center for the medium-voltage experiments. The ends of the electrodes were near the centerline of the box (approximately 25 cm (10 in) from top and bottom). The electrodes were held in place by a prefabricated two-piece insulator block that affixed to the top of the box through a rectangular opening. The bottom of the box was elevated approximately 127 cm (50 in) from the floor.

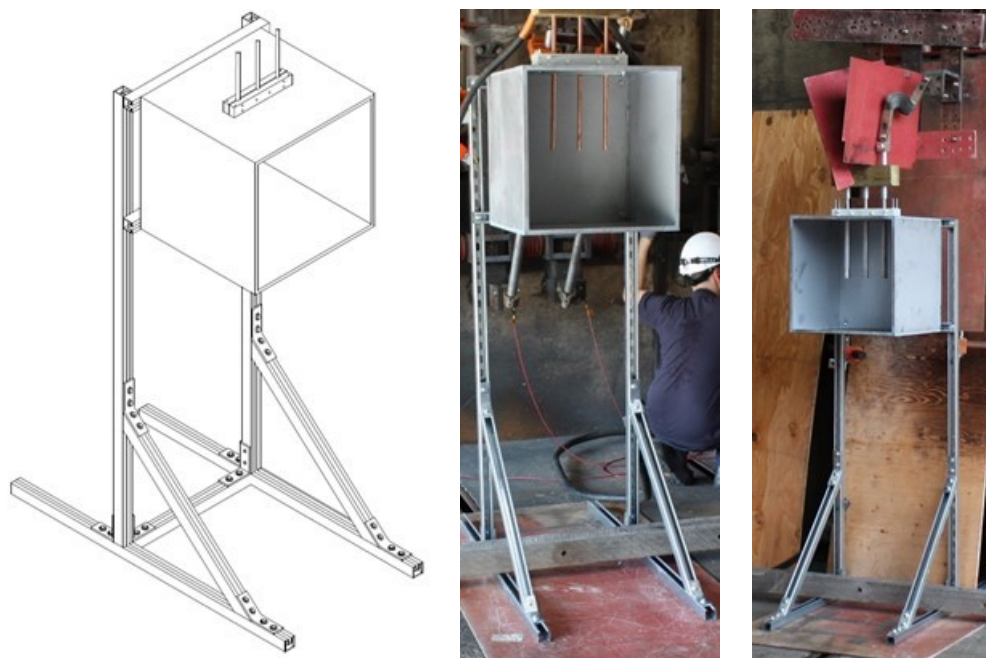


Fig. 3. Open box configuration low-voltage experiments (isometric (left), 1.3 cm (0.5 in) copper electrode (center), 2.5 cm (1 in) aluminum electrode (right)).

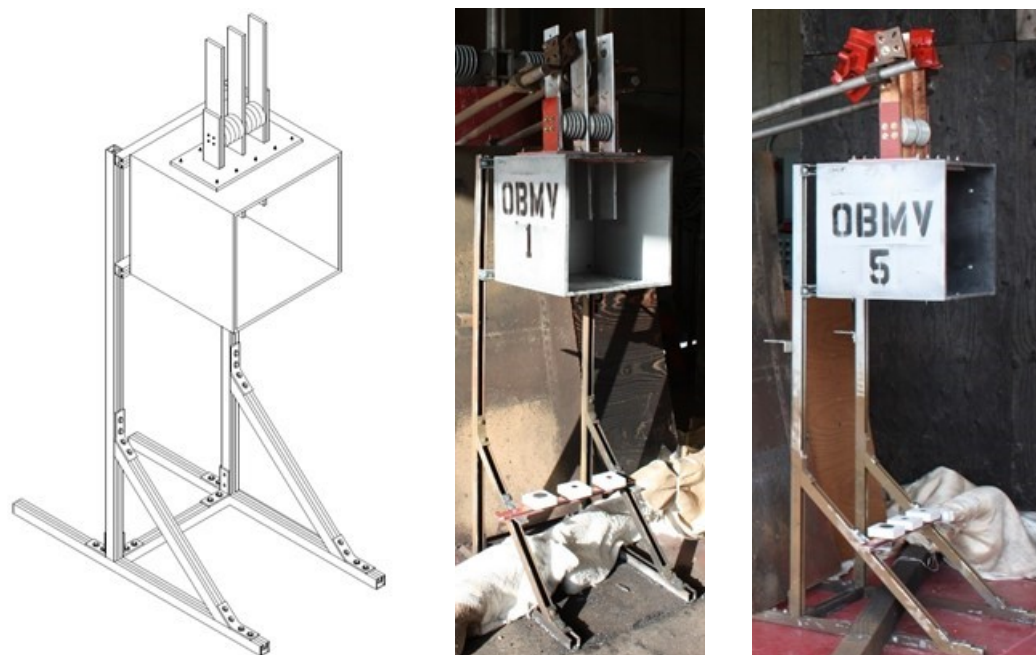


Fig. 4. Open box configuration medium-voltage experiments (isometric (left), aluminum 10.2 cm (4 in) bars (center), copper 7.62 cm (3 in) bars (right)).

One series of low-voltage experiments was performed in August 2019. The experiments are shown in Table 1. The experiments used 1 000 V(AC) instead of a more typical 480 V(AC) or 600 V(AC) system voltage to ensure that the arc could be maintained for the desired experiment duration. During an arc, the system voltage will collapse and be dependent on arc and system impedance. The selection of a higher low-voltage was made to support arc restrike for the planned experimental duration, rather than influence arc energy. The experiment currents were varied between a nominal 1 kA and 30 kA, with experiment durations between approximately 1 s and 4 s. Aluminum or copper electrodes for the low-voltage experiments were cylindrical rods with nominal diameters of 1.3 cm (0.5 in) or 2.5 cm (1.0 in). The larger rod was milled down to a nominal 1.3 cm (0.5 in) in the center of the rod to allow for a single rod support bracket to be used for all low-voltage box experiments.

The second series of experiments was performed at medium-voltage levels in September 2019. The experiments are shown in Table 2. The medium-voltage experiments used 6 900 V (AC), with various arc currents and experimental durations to allow for comparisons to the low-voltage experiments and for evaluation of material effects (aluminum versus copper). Nominal currents of either 15 kA or 30 kA and nominal durations of 1 s, 2 s, or 5 s were used. The electrodes for the medium-voltage experiments were rectangular bars approximately 1.3 cm (0.5 in) thick and 7.6 cm (3.0 in) wide for copper electrodes and approximately 10.2 cm (4.0 in) wide for aluminum electrodes. One exception was OBMV6, a repeat of OBMV1, which used 7.6 cm (3.0 in) wide aluminum bars.

Table 1. Low-voltage box experimental matrix.

EXPERIMENT	Rod Material		Rod Diameter (cm)		Voltage	Current	Duration
#	Al	Cu	1.3	2.5	kV	kA	s
OB01a		X	X		1.0	1.0	2.0
OB01b		X	X		1.0	1.0	2.0
OB02		X		X	1.0	15.0	2.0
OB03		X		X	1.0	15.0	4.0
OB04		X		X	1.0	30.0	1.0
OB05	X		X		1.0	1.0	2.0
OB06	X			X	1.0	15.0	2.0
OB07	X			X	1.0	15.0	4.0
OB08	X			X	1.0	30.0	1.0
OB09		X	X		1.0	5.0	2.0
OB10	X		X		1.0	5.0	2.0

Table 2. Medium-voltage box experimental matrix.

EXPERIMENT	Bar Material		Bar Width (cm)		Voltage	Current	Duration
#	Al	Cu	7.6	10.2	kV	kA	s
OBMV01	X			X	6.9	15	2
OBMV02	X			X	6.9	30	1
OBMV03	X			X	6.9	15	5
OBMV04		X	X		6.9	15	2
OBMV05		X	X		6.9	30	5
OBMV06	X		X		6.9	15	2

2.4. Instrumentation

Thermal, optical emission, electromagnetic, conductivity, and electrical measurements were made using a variety of instruments and techniques. This section provides an overview of each, along with the methods and location of measurement.

2.4.1. Overview of Instruments

Table 3 lists the measurement equipment arranged throughout the test cell and the corresponding measurements. A general configuration is shown in Fig. 5 followed by a photograph in Fig. 6. A brief description of each device follows.

Table 3. List of measurement equipment.

Measurements	Instrument / Technique
Temperature	Infrared (IR) Imaging, Plate Thermometer (PT)
Electromagnetic Interference	Free-Field d-Dot Sensors
Air Conductivity	Planar Conductivity Sensors
Air Breakdown Strength	Breakdown Sensors
Heat Flux (time-varying)	Plate Thermometer (PT)
Heat Flux (average)	Plate Thermometer (PT), Thermal Capacitance Slug (T_{cap} slug), Plate calorimeter
Incident Energy	ASTM Slug Calorimeter (slug), Thermal Capacitance Slug (T_{cap} slug)
Arc Plasma / Fire Dimensions	Videography, IR Imaging
Surface Deposit Analysis	Sample Collection (carbon tape), Post-Experiment Laboratory Analysis (Energy Dispersive Spectroscopy)
Qualitative Information	High Speed / High Dynamic Range Imaging

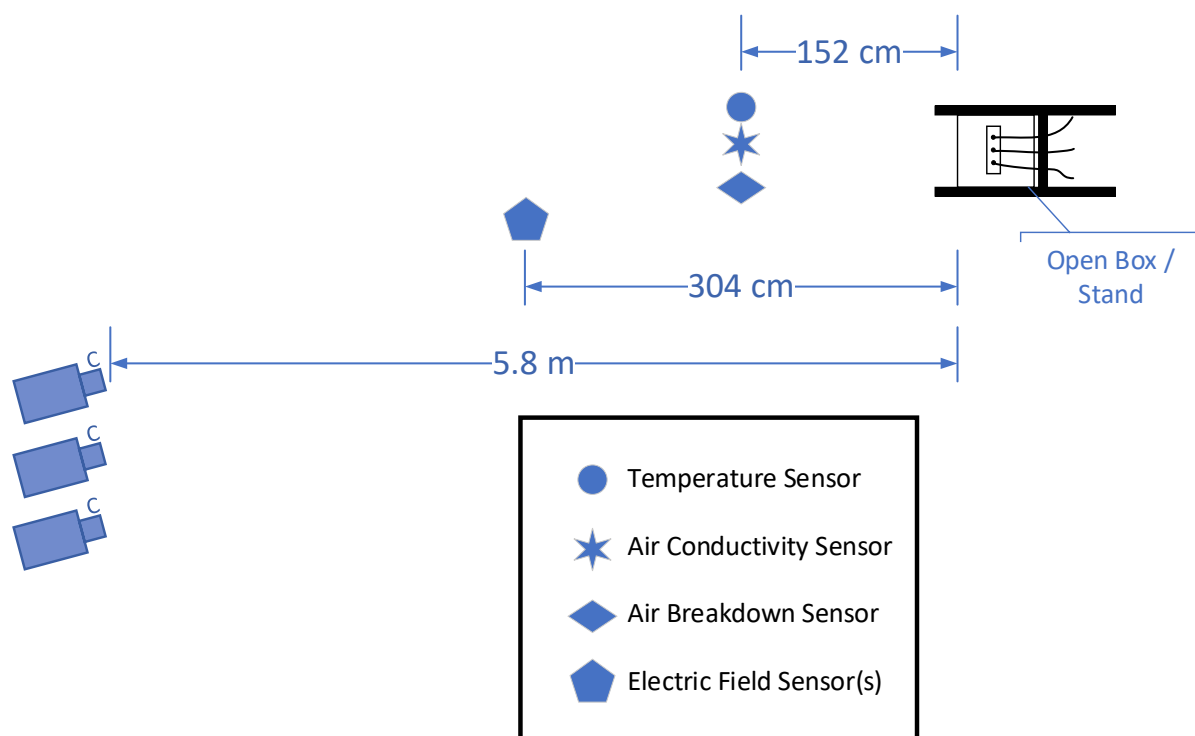


Fig. 5. Plan view of instrumentation locations (note that locations and instruments used varied by experiment and illustration is not to scale). Three cameras (labeled ‘C’ are shown in the far left of the figure and were approximately 5.8 m from the open box.



Fig. 6. Instrumentation cluster covered with heat resisting fabric for protection during experiments (from left-to-right, air breakdown, plate calorimeter, d-dot, air conductivity, high speed IR, and visible videography).

2.4.2. Optical Emission Spectroscopy

An Ocean Optics HR4000 Spectrometer was used to monitor the spectral radiation profile emitted from the arcing fault at a data acquisition rate of 100 Hz for the entire experimental duration. A UV-VIS optical fiber collects light from the arc and disperses it by wavelength/energy using a grating and it is imaged onto a detector. This provides information on how many photons of a given energy are present during the collection time. This energy is specific to the emitting species and the temperature and density of the emitter. By analyzing the emission spectra produced, quantitative time-resolved measurements are produced of both the arc temperature and surrounding graybody temperature. Emission spectra also provide species identification in the arc and the surrounding gas environment. The resulting temperature measurements will be used for model validation and will be made available for comparison to all physical and analytical models. The spectrometer is shown in Fig. 7. Spectrometer results are presented in Appendix B.



Fig. 7. The spectrometer is mounted to the top of the base plate.

2.4.3. Digital Imaging

NIST and SNL fielded numerous imaging technologies to provide high-speed quantitative and qualitative imaging during this HEAF experimental series evolution. The measurement methods included visible high-speed and high-definition imaging, high-speed high dynamic range visible imaging, and high-speed thermal imaging. The equipment fielded by NIST included high-definition video cameras and a high-definition thermal imager like that used in the Phase 1 experiments [6] and 2018 medium-voltage HEAF experiments [1] to capture high-definition visible and high-speed thermal images. NIST also fielded a high speed, high dynamic range, thermal imager equipped with a rotating filter wheel. Equipment fielded by SNL was a subset of equipment fielded in the 2018 experiment [1]. The equipment selection was scaled down based on results and lessons learned. SNL reports document the approach, and uncertainties [13].

The processed images can be accessed from the NRC RIL website²:

<https://www.nrc.gov/reading-rm/doc-collections/research-info-letters/index.html>

² The RIL website can be accessed by visiting <http://www.NRC.gov>, selecting the “NRC Library” >> “Document Collections” >> “Research Information Letters”.

2.4.3.1. High-Speed Videography

One video camera provided high-speed high-resolution quantitative and qualitative imaging of the arcing fault in the open box. The camera was located on the opposite side of the cell from the open box and adjacent to the thermal imaging camera(s). The camera view included the open side of the box under experiment. Images from this camera were used with data fusion products to visualize instrumentation data (current and voltage) and imaging measurements. All imaging was time-synchronized to the start of the arcing event via a trigger signal from KEMA Labs. Fusion of the short-wave high-speed infrared imager with the high-resolution high-speed visible imager provided quantitative temperature data in the overlaid images. A color legend shows the calibrated temperature range with uncertainties. A screenshot of the video compilation is shown in Fig. 8.

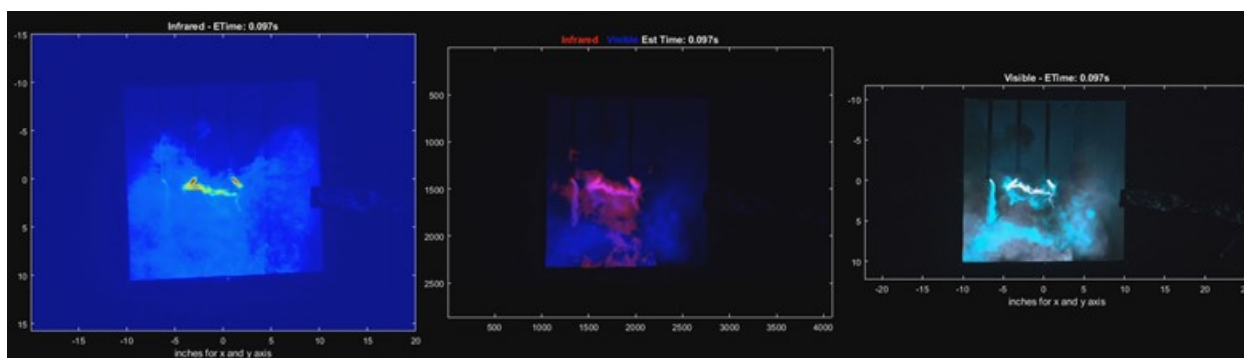


Fig. 8. High-speed high-resolution imaging (IR image (left), IR image fused with visible image (center), visible image (right)).

2.4.3.2. High-Definition Videography

High-definition (HD) video imaging was used to provide additional angles for each experiment. In the experimental cell, video cameras were placed in protective housings and located on the floor or attached to the test cell wall. Their wide view angle and proximity provided high resolution and detail of the early portion of the experiments. However, as the experiment progressed the effluent quickly obscured the camera view. A second set of HD video cameras were located approximately 27 m (90 ft) from the front of the cell adjacent to the thermal imaging cameras. The camera placement and zoom allowed for a macroscopic view of the entire experimental cell or an area surrounding the open box. These cameras were located orthogonal to the action camera attached to the test cell wall. Half of these cameras were equipped with IR pass filters to better image the plasma and fire from the HEAF to improve the image captured during an arcing event.

2.4.3.3. Thermography

Up to four thermal imaging cameras were used per experiment. Two of the cameras were supplied by NIST, while the other two were provided by SNL. The camera settings such as frame-rate, thermal calibration range, and resolution were varied. The cameras were also placed in different locations. The NIST cameras were located outside the test cell

approximately 27 meters (90 ft) from and orthogonal to the front face of the KEMA experimental cell. The SNL cameras were located in the experimental cell and were housed within a mechanically ventilated protective metal enclosure. The thermal imagers used in this series are shown in Fig. 9.



Fig. 9. Thermal imagers used inside and outside the test cell (thermal imaging cameras located approximately 27 m from the open box (left), imaging cameras located within the test cell (right), from left to right: thermal, high speed visible, thermal).

2.4.3.4. SNL Imaging

The SNL thermal imagers were each housed in an enclosure that provided protection for the camera and networking components. An opening in the box allowed for the camera lenses to protrude out of the enclosure. The camera locations, non-orthogonal axis, and distance from the HEAF effluent provided protection for the camera and lens. During the medium-voltage open box experiments, however, a thermal imaging camera lens was impacted by molten metal. Subsequent medium-voltage open box experiments were therefore configured such that the camera lens was not in direct alignment to the HEAF effluent using a mirror and concrete barrier.

2.4.3.5. NIST Imaging

The NIST thermal imagers were only used during the medium-voltage experiments. The thermal imaging was performed with two main goals. The first goal was to obtain qualitative information about the development and movement of the arc, the development of plumes of hot gases and HEAF products issuing from the open box, the impingement of the arc jets on the targets and thermal transducers, and the penetrations formed in the enclosure. The second goal was to provide quantitative measurements of box temperatures during and after the HEAF event. The thermal imaging measurements were performed by a FLIR model SC8243 imaging system and a Telops MS M350 imaging system.

The FLIR thermal imager was equipped with a 50 mm f/4.0 lens, with an InSb detector that had a nominal response range from 3 μm to 5 μm and a nominal pixel pitch of 18 μm by 18 μm . The imager can operate in full resolution mode of 1024 pixels by 1024 pixels at approximately 125 frames per second and can cover the temperature range of approximately -20 $^{\circ}\text{C}$ to 1500 $^{\circ}\text{C}$ (-4 $^{\circ}\text{F}$ to 2732 $^{\circ}\text{F}$) using dynamic range extension techniques. For these experiments, to complement the imaging performed by SNL imagers, the resolution was

lowered to 319 x 255 pixels, and the temperature range was limited to approximately 250 °C to 600 °C so that the frame rate could be increased to approximately 400 Hz.

The Telops thermal imager was equipped with a 50 mm f/2.3 lens, with a detector that has a nominal response range from 3.0 μm to 4.9 μm and a nominal pixel pitch of 16 μm by 16 μm . The imager was operated in full resolution mode of 640 pixels by 512 pixels at approximately 350 frames per second. The video capture was performed using a spinning filter wheel with eight positions, filled with two consecutive series of four different transmittance neutral density filters. A dynamic range extension technique was applied, where the images from each series of four filters were captured, and post-processing software combined the images into one image with an expanded temperature range. After the dynamic range extension was applied, the video images were 640 x 512 pixels in size, covering from approximately - 0 °C to 2500 °C (- 4 °F to 4532 °F), with an effective video frame rate of approximately 88 Hz.

The uncertainty of the temperature results from the FLIR and Telops imagers were both specified by the manufacturer as ± 2 °C or ± 2 percent, with a 99 percent confidence interval. Using the NIST Uncertainty Machine [14], the expanded uncertainty in the temperature measurements of the metal surfaces is given in Table 4. Details of the uncertainty analysis can be found in the previous HEAF report [1].

Table 4. Expanded uncertainty for IR imager temperatures.

Surface	Mean Emissivity	Temperature (°C)	Uncertainty (°C)	Confidence	Coverage Factor	Approximate Uncertainty Contribution
Paint	0.94	100	± 2.6	95%	1.7	Imager: 30% Emissivity: 70%
Paint	0.94	650	± 10.5	95%	1.9	Imager: 70% Emissivity: 30%
Oxidized Steel	0.80	100	± 3.0	95%	1.8	Imager: 20% Emissivity: 80%
Oxidized Steel	0.80	650	± 11.1	95%	1.9	Imager: 65% Emissivity: 35%

2.4.4. Calorimetry

Several types of calorimeters were used in these experiments. For all experiments, an SNL provided plate calorimeter was used. This device was used in the previous small-scale experiments allowing direct comparisons. During the medium-voltage box experiments,

several thermal capacitance slug calorimeters (T_{cap}), ASTM calorimeters, and plate thermometers were used. The types and configurations were selected based on the expected thermal exposure and ability of the device to survive.

2.4.4.1. Plate calorimeter

A plate calorimeter was placed near the open end of the box to measure heat flux. The surface area of the square copper plate was 25.8 cm^2 (4 in^2). Type K thermocouples were used due to their high maximum temperature of $1250 \text{ }^\circ\text{C}$ ($2192 \text{ }^\circ\text{F}$) and display a manufacturer specified uncertainty of $\pm 1.1 \text{ }^\circ\text{C}$ ($\pm 2.0 \text{ }^\circ\text{F}$). The thickness of the copper plate varied between experiments and were either nominally 1 mm (0.04 in) or 3 mm (0.12 in) thick black copper plates. The thickness varied based on the energy of the experiment, projected temperature rise based on copper plate heat capacity, and the expected ability of the sensor to survive up to $400 \text{ }^\circ\text{C}$ ($750 \text{ }^\circ\text{F}$). The data acquisition system measurement uncertainty was $\pm 0.1 \text{ }^\circ\text{C}$ ($\pm 0.2 \text{ }^\circ\text{F}$). These plate calorimeters have been used in other experiments [12, 15, 16]. The plate calorimeter support structure was covered for thermal protection as shown in Fig. 10. One plate calorimeter was used in each experiment, and its location varied between approximately 0.5 m (18 in), 1.8 m (72 in), or 3.0 m (120 in) from the enclosure.



Fig. 10. Plate calorimeter apparatus in its thermal protected configuration.

The energy generated by the arc, Q , can be estimated using the measured plate calorimeter temperature increase ΔT (K):

$$\frac{Q}{4\pi R^2} = \rho_{Cu} C_{Cu} \delta_{Cu} \Delta T \quad (1)$$

where ρ_{Cu} is the density of copper (g/m^3), C_{Cu} is the heat capacity of copper ($\text{J}/(\text{g}\cdot\text{K})$), δ_{Cu} is the copper plate thickness (m), and $4\pi R^2$ is the surface area (m^2) to which arc energy is radiated at a calorimeter distance R (m). This calculation assumes 100 % absorption of

incident radiation on the black copper calorimeter plates and a spherically symmetric distribution of energy.

2.4.4.2. Plate Thermometer

Modified plate thermometers (PTs) are robust thermal sensors that can survive in hostile HEAF environments [1, 6, 17]. They were chosen for heat flux measurements in the HEAF experiments due to their rugged construction, low cost, lack of cooling water, and known emissivity and convective heat flux coefficients.

The modified plate thermometer used in the HEAF experiments is shown in Fig. 11. It consists of two 0.51 mm (0.02 in) nominal diameter (24 AWG) Type K thermocouple wires welded directly to the rear of a 0.787 mm \pm 0.051 mm (0.031 in \pm 0.002 in, 99 percent confidence interval per manufacture specifications) thick Inconel 600 plate, approximately 100 mm (3.94 in) by 100 mm (3.94 in) in size. The plate is backed by a mineral fiber blanket approximately 25.4 mm (1.0 in) thick to minimize heat loss. Machine screws with ceramic washers allow for legs to be attached at the rear of the plate thermometer to simplify installation onto instrumentation racks.

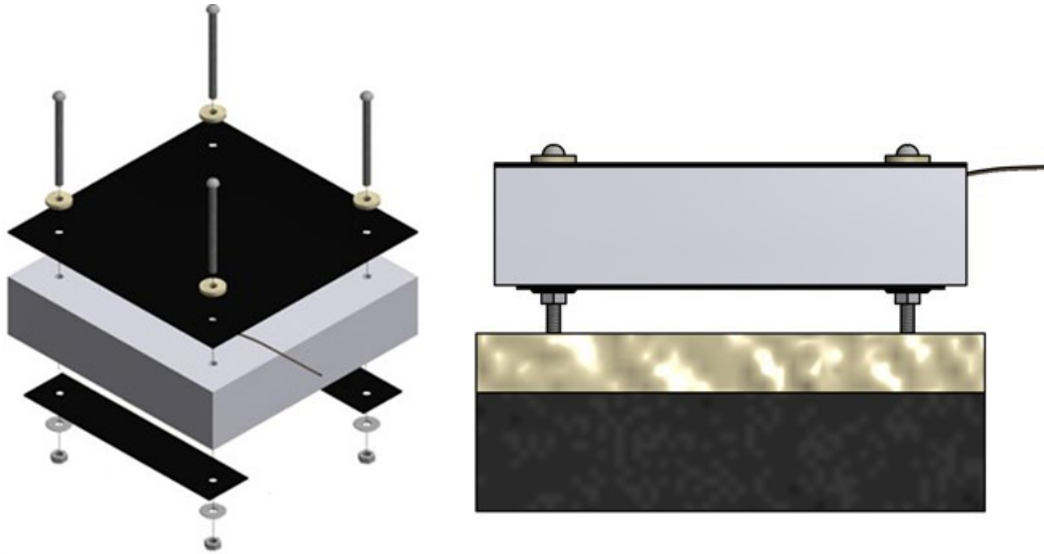


Fig. 11. Exploded view of modified plate thermometer (left); cross-sectional view of modified plate thermometer placed on cone calorimeter sample holder (right).

The incident heat flux on a plate thermometer can be calculated from a heat balance using the following equation, a rearrangement of Equation 18 from Ingason and Wickstrom [21]:

$$\dot{q}_{inc}'' = \sigma \cdot T_{PT}^4 + \frac{(h_{PT} + K_{cond})(T_{PT} - T_{\infty})}{\epsilon_{PT}} + \frac{\rho_{PT} \cdot C_{PT} \cdot \delta \cdot \left(\frac{\Delta T_{PT}}{\Delta t}\right)}{\epsilon_{PT}} \quad (2)$$

Here \dot{q}_{inc}'' is the incident heat flux, σ is the Stefan-Boltzmann Constant, $5.670 \times 10^{-8} \text{ W}/(\text{m}^2 \cdot \text{K}^4)$, T_{PT} is the temperature of the plate (K), h_{PT} is the convection heat transfer coefficient, $10 \text{ W}/(\text{m}^2 \cdot \text{K})$, K_{cond} is the conduction correction factor determined from

NIST cone calorimeter data, $4 \text{ W}/(\text{m}^2 \cdot \text{K})$, T_∞ is the ambient temperature (K), ϵ_{PT} is the plate emissivity, 0.85 at 480°C as rolled and oxidized and specified by the alloy manufacturer, ρ_{PT} is the alloy plate density, $8470 \text{ kg}/\text{m}^3$ from the alloy manufacturer, C_{PT} is the alloy plate heat capacity, $502 \text{ J}/(\text{kg} \cdot \text{K})$ at 300°C from the alloy manufacturer, δ is the alloy plate thickness, 0.79 mm (0.03 in), and Δt is the data acquisition time step of 0.1 s .

The gauge heat flux can also be calculated and is the heat flux listed in the tables of this report. The gauge heat flux is the heat flux that would be reported by an ideal water-cooled transducer such as a Schmidt-Boelter or Gardon gauge operating at a constant temperature of T_{gauge} . The gauge heat flux, \dot{q}''_{gauge} , is calculated from [18]:

$$\dot{q}''_{\text{gauge}} = \sigma \cdot T_{\text{PT}}^4 + \frac{(h_{\text{PT}} + K_{\text{cond}})(T_{\text{PT}} - T_\infty)}{\epsilon_{\text{PT}}} + \frac{\rho_{\text{PT}} \cdot C_{\text{PT}} \cdot \delta \cdot \left(\frac{\Delta T_{\text{PT}}}{\Delta t}\right)}{\epsilon_{\text{PT}}} - \sigma \cdot T_{\text{gauge}}^4 \quad (3)$$

Type A evaluation of uncertainty is performed by the statistical analysis of a series of measurements. Type B evaluation of uncertainty is based on scientific judgement using relevant available information such as manufacturer specifications, calibration data, handbook data, previous experiments, and knowledge of the behaviors of materials and measurement equipment [19, 20, 21].

The plate thermometer temperature increase, ΔT_{PT} , is reported along with the gauge heat flux. The uncertainty in the temperature of the Type K thermocouple wire is given by the manufacturer as $\pm 1.1^\circ\text{C}$ or 0.4 percent with a 99 percent confidence interval [22]. The expanded uncertainty in a PT temperature change of 0°C to 1250°C is 0.3 percent, with a coverage factor of 2 , which corresponds to a confidence interval of 95 percent [19]. The expanded uncertainty in the heat flux measurement is $\pm 1 \text{ kW}/\text{m}^2$ or ± 5 percent, with a coverage factor of 2 , which corresponds to a confidence interval of 95 percent. Additional detail on the uncertainty determination can be found in the previous report [1].

2.4.4.3. ASTM Slug Calorimeters (Slug)

Incident energy was measured using slug calorimeters described in ASTM F1959 [24] and shown in Fig. 12. These instruments are customarily used to measure radiant energy and determine the arc flash hazard to personnel in the area of electrical enclosures. Due to the characteristics of the HEAF phenomena, which can result in convective arc jets, the calorimeters are reacting to convective heat transfer in addition to radiant heat transfer. ASTM slug calorimeters consist of a copper disc with a nominal thickness of 1.6 mm (0.063 in) and nominal diameter of 40 mm (1.6 in). An iron-constantan thermocouple (Type J), composed of two 0.255 mm (0.01 in) nominal diameter (30 AWG) wires, is soldered to the back of the copper disc using silver solder. The ASTM standard specifies that the copper disc be installed in an insulation board. The KEMA slug calorimeters were installed in a G-11 fiberglass epoxy phenolic cup, which was then placed in a calcium silicate board holder nominally 100 mm by 100 mm by 32 mm thick (4 in by 4 in by 1.25 in nominal thickness) for mounting on the instrument rack. The instruments were provided by KEMA. The slug temperatures were reported by the KEMA data acquisition system at a rate of 20 Hz .

The incident energy absorbed by the slug calorimeter during the HEAF experiments is calculated according to the methodology in ASTM F1959 [24]. The method reports the net heat absorbed over the arc duration and assumes that there are no losses from the disc due to re-radiation, convection, or conduction to the disc holder. The absorptivity of the disc is assumed to be one.

The total energy per unit area, Q'' , is calculated by:

$$Q'' = \frac{m \cdot \overline{C_p} \cdot (T_f - T_i)}{A} \quad (4)$$

where m is the mass of the copper disc, $\overline{C_p}$ is the average heat capacity of the copper disc, T_f is the temperature of the disc at the end of the arc, T_i is the temperature of the disc before the arc, and A is the front surface area of the disc. The total energy per unit area resulting from the arc is reported in a summary table for each sensor location in each experiment. The ASTM F1959 standard also refers to the total energy per unit area as incident energy (cal/cm² or kJ/m²).

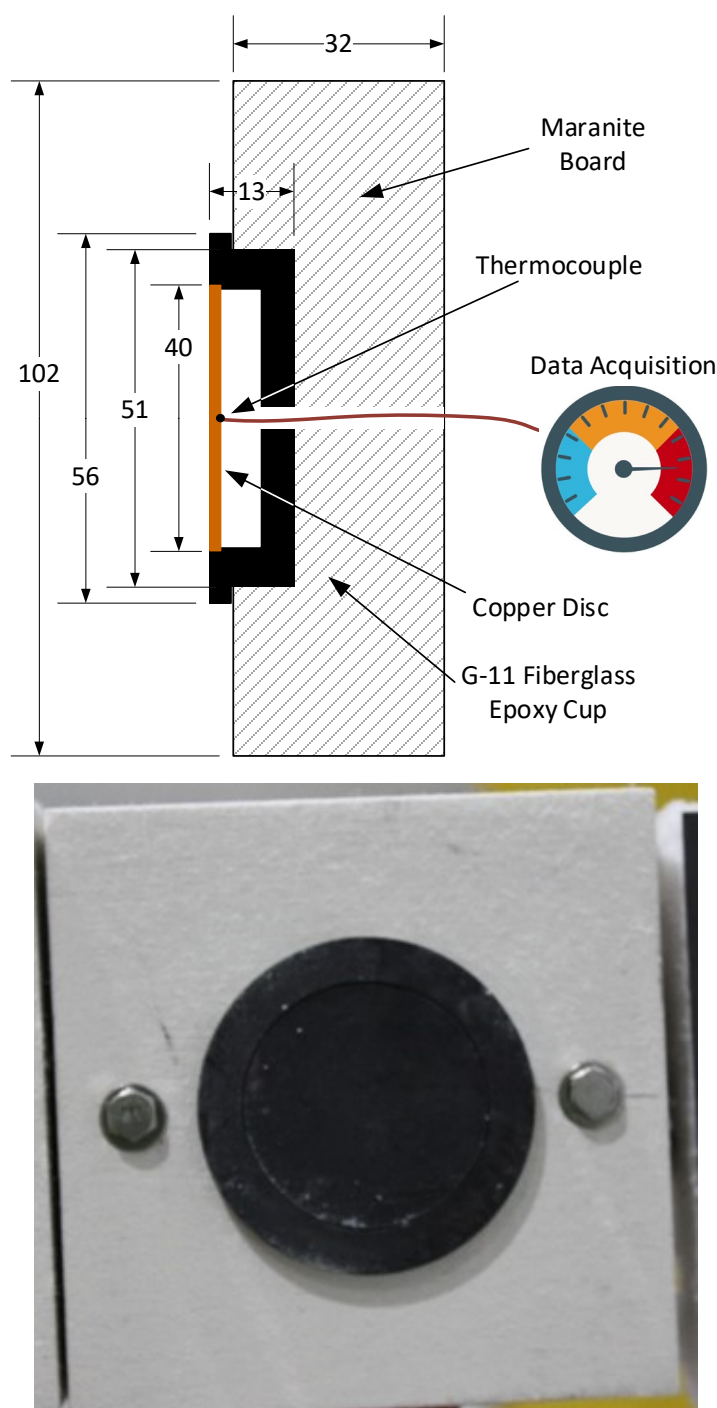


Fig. 12. Cross-section of ASTM Slug (top) nominal dimensions in millimeters, photo of device being prepared in the field (bottom). Note that the two bolts on each side of the device are used for mounting to the DIN rail of the instrumentation rack.

The Type B standard uncertainty in the thermocouple measurement, derived from typical thermocouple manufacturer data, with a coverage factor of 2, is 2.2 °C or 0.75 percent. The ASTM calculation method assumes that the absorptivity of the disc is 1.0; however, inspection of the discs over the course of the experiments suggests that the emissivity may

vary from approximately 0.9 to 1.0, in a rectangular probability distribution. The expanded uncertainty in the incident energy measurement is $\pm 18 \text{ kJ/m}^2$ or ± 4 percent, with a coverage factor of 2, which corresponds to a confidence interval of 95 percent. Additional detail on the uncertainty determination can be found in the previous report [1].

2.4.4.4. Thermal Capacitance Slugs (T_{cap} slug)

Tungsten thermal capacitance slugs (T_{cap} slug) were used to measure the heat flux and incident energy during the HEAF experiment. These sensors were developed as a result of experience gained in Phase 1, where the thermal conditions during some experiments exceeded the measurement capabilities and caused destruction of the ASTM slug calorimeters and modified plate thermometers. A cross section of a T_{cap} slug is shown in Fig. 13, which is a modified example of the thermal capacitance slug described in ASTM E457-08 [25]. The slug is composed of a tungsten cylinder approximately 15 mm (0.59 in) long mounted in calcium silicate board. A type K thermocouple is attached to the rear of the tungsten to measure the temperature during heating. The development of the T_{cap} is described in the previous report [1].

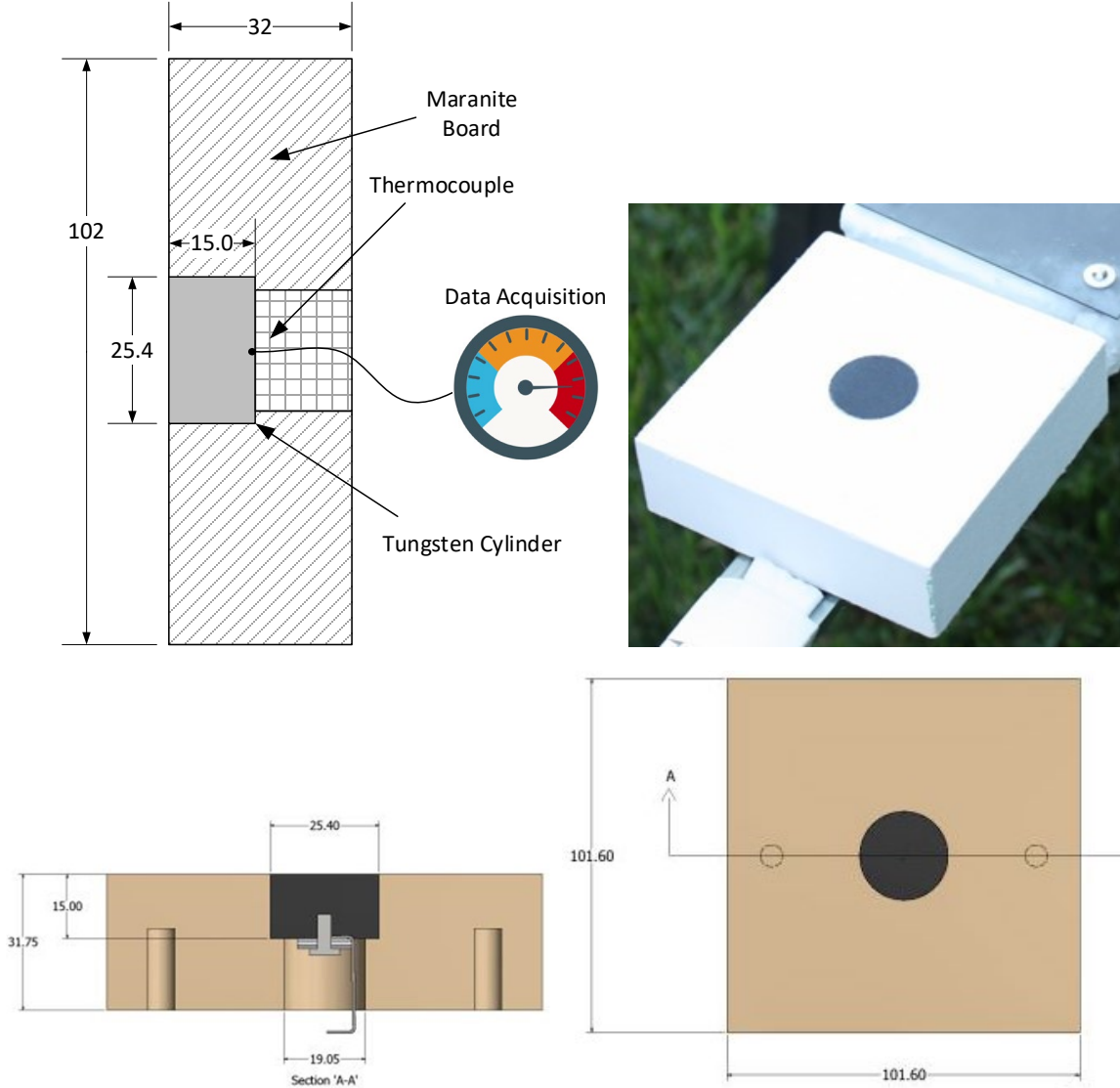


Fig. 13. Thermal capacitance style slug, illustration (top left), photo of device being prepared in the field (top right), dimensional drawings showing internal construction (bottom left and right). All nominal dimensions in mm.

The maximum heat flux was determined from Equation (5), where \dot{q}'' is the heat flux into the surface of the tungsten slug (kW/m^2), ρ is the density of the tungsten slug (kg/m^3), $\overline{C_p}$ is the average heat capacity of the tungsten slug (kJ/[kg K]), l is the thickness (m), ΔT is the change in temperature of the tungsten slug ($^{\circ}\text{C}$), and Δt is the corresponding change in time (s).

$$\dot{q}'' = \rho \cdot \overline{C_p} \cdot l \cdot \left(\frac{\Delta T}{\Delta t} \right) \quad (5)$$

An uncertainty analysis using Type A and Type B components was performed on the T_{cap} slug at 50 kW/m^2 and 5 MW/m^2 using the NIST Uncertainty Machine [14] with cone calorimeter data and fire dynamics simulator (FDS) [23] simulations. The expanded

uncertainty in the heat flux measurement is $\pm 1.5 \text{ kW/m}^2$ or ± 2.9 percent, with a coverage factor of 2, which corresponds to a confidence interval of 95 percent.

The expanded uncertainty of the incident energy over the measurement range is estimated at $\pm 2.4 \text{ KJ/m}^2$ or ± 5 percent, with a 95 percent confidence interval, which includes the estimated error due to conduction effects. Additional details on the development of the T_{cap} , heat transfer analysis, and uncertainty determinations can be found in the previous report [1].

2.4.4.5. Placement of NIST and KEMA instrumentation for medium-voltage open box experiments

During the medium-voltage open box experiments, two small arrays of sensors were deployed by NIST. A vertical array was placed approximately 165 cm (65 in) from the front of the box surface. The array was attached to a stand, and the sensor cables were routed and protected in the stand U-channel using thermal ceramic fiber and GPO3 (red board). The vertical array consisted of one copper slug, one tungsten slug, and one Inconel plate thermometer. A horizontal array was placed directly below the box approximately 84 cm (33 in) from the bottom surface of the box. This array was attached to the stand that supported the open box. The horizontal array consisted of two tungsten slug calorimeters and one copper slug calorimeter. Plate thermometers were not used in the horizontal configuration due to the expected damage. The sensor arrays are shown in Fig. 14 and Fig. 15. The expanded uncertainty in the measurement of the distance from the vertical instrumentation stand to the open box is $\pm 13 \text{ mm}$ (0.5 in) with a coverage factor of 2 and an estimated confidence interval of 95 percent. The expanded uncertainty in the measurement of the other distances in Fig. 15 is $\pm 13 \text{ mm}$ (0.5 in) with a coverage factor of 2 and an estimated confidence interval of 95 percent.

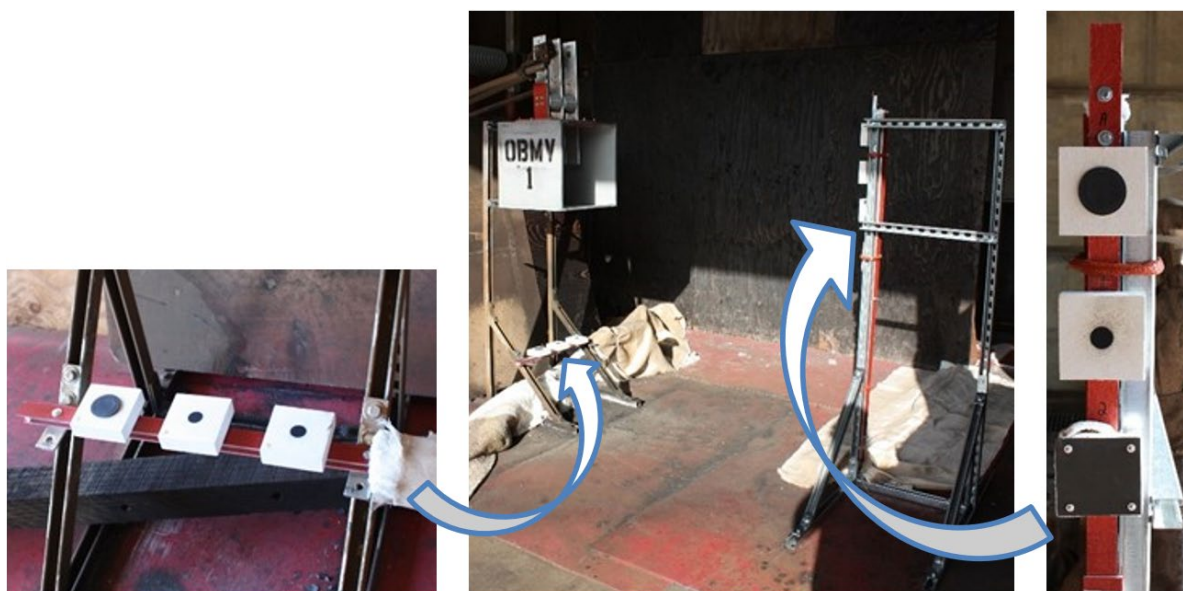


Fig. 14. Calorimeter arrays used during medium-voltage experiments (horizontal array (left), array location within cell (center), vertical array (right)).

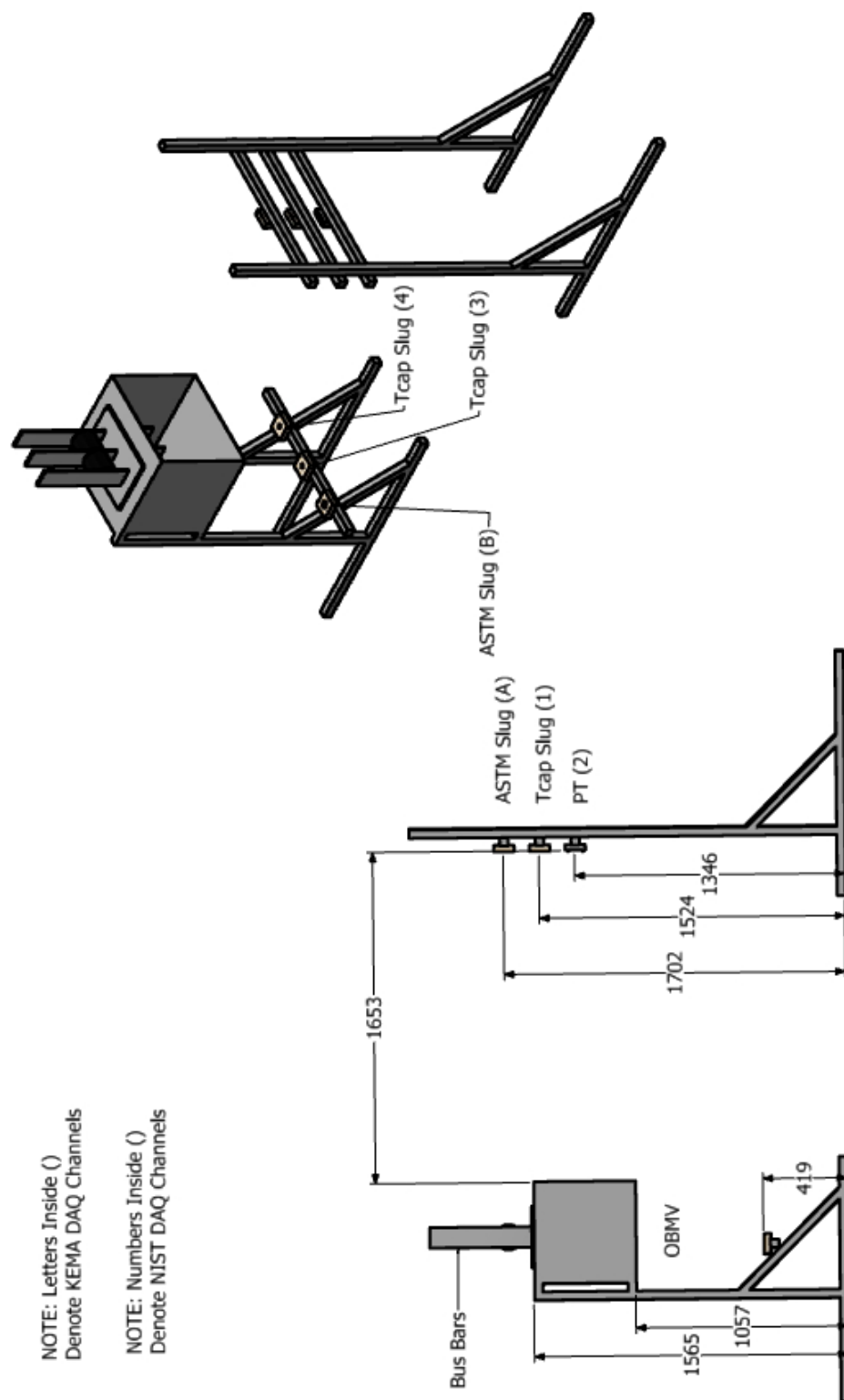


Fig. 15. Calorimeter configuration during the medium-voltage experiments. Approximate dimensions in mm.

2.4.4.6. Data Acquisition System

The NIST data acquisition system used a combination of shielding, grounding, isolation, and system configuration that reduced the impact of electromagnetic interference (EMI), as shown in Fig. 16. This data acquisition system was used for the plate thermometer and T_{cap} instruments and is described in the literature [1, 6, 17]. A TTL signal with a known delay time was used to synchronize to the KEMA data acquisition and control system.

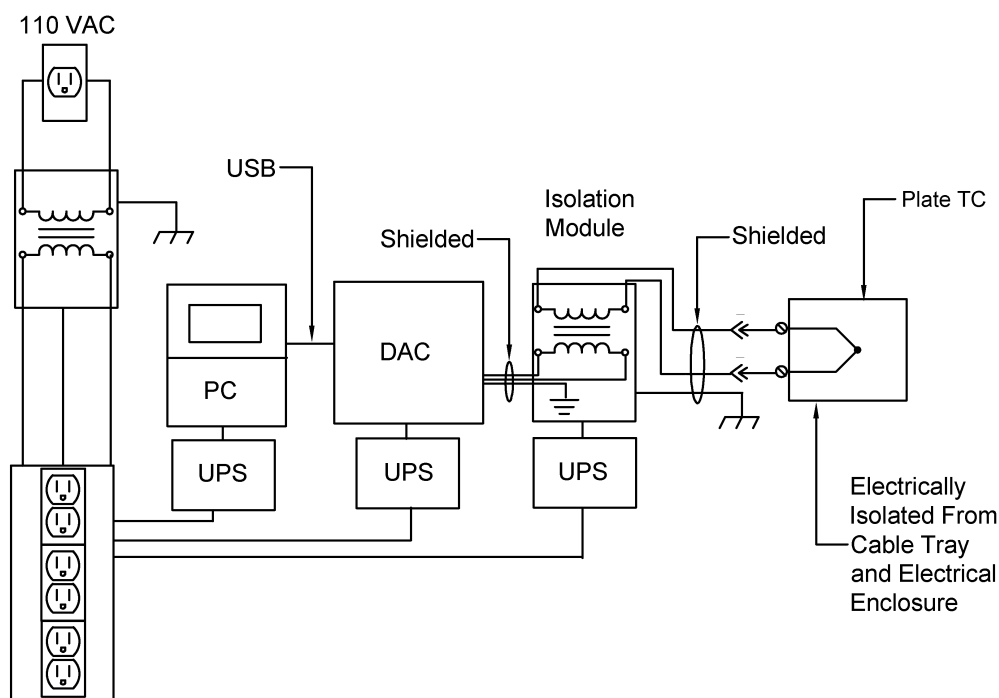


Fig. 16. Data acquisition system configuration with EMI rejection.

2.4.5. d-Dot Sensors

During an arc, significant electromagnetic interference may potentially be generated, which could couple to nearby electronics. The electrical field content of the arc event as a function of frequency was measured using free-field d-Dot sensors, which quantify the electrical field (kV/m) as a function of frequency from 10 kHz to 1.5 GHz. These frequencies correspond to wavelengths of 4 cm (2.5 GHz) to 30 km (10 kHz) which may efficiently couple to nearby cables or metallic traces. Because of space limitation, an RF filter/wave guide was not used. As such, a baseline measurement was required to be made prior to each experiment such that background signals were removed from HEAF measured signals. The sensor cable, optical link, and DAQ were configured to eliminate EMI corruption. This included the use of triple coaxial cable, fiber optic cable, and a DAQ module that was shielded and grounded. Generated field intensity data was transmitted to spectrum analyzers outside the experiment chamber using fiber optic links to minimize EMI coupling from transmission lines.

Probes were initially placed in “far field” outside the predicted thermal plume region to limit thermal damage to the probe and associated cabling. Based on the data from the initial experiments, the probes were positioned in different locations from the open box for subsequent experiments. This allowed for an evaluation of spatial influences on the measured field strength. A photo of the d-Dot sensors prepared for an experiment is presented in Fig. 17.



Fig. 17. d-Dot sensors arrangement prior to experiment. Note all sensors oriented in same axis based on results from earlier experiment indicating the largest measured signal.

For the electrical field measurements, the measurement uncertainty due to the collection oscilloscope was ± 8 mV for a trigger level set above ambient RF noise of 52 mV. No trigger was observed for any of the open box testing at an acquisition rate of 5 GS/s. The electric field level for the Prodyn AD-70 free field d-Dot sensors [26] is given by

$$E(t) = \frac{1}{RA_{eq}\epsilon_0} \int_{t_i}^{t_f} v(t)dt \quad (6)$$

where v is the sensor output (V), ϵ_0 is the permittivity of free space, R is the sensor characteristic load impedance in ohms and A is the equivalent sensor area (m^2), given as:

$$\begin{aligned} R &= 100 \, \Omega \\ A_{eq} &= 10^{-3} \, m^2 \end{aligned}$$

EPRI specifies a transient equipment susceptibility field limit of 152 dBV/m, equivalent to 40 V/m [28]. For comparison, the US military electric field susceptibility standards [27], specifies testing safety critical equipment under 200 V/m fields. The maximum field level at which no trigger occurred (e.g., $E = 11.8 \, V/m \pm 1.8 \, V/m$ uncertainty) appears below the levels of concern for military electronics but could be repeated with specific regard to transient equipment susceptibility field level testing.

2.4.6. Conductivity Sensors

Previous experiments have identified that HEAF effluent, consisting of gases, particles, fume, and plasma, resulted in unacceptable insulation resistance between uninsulated and non-enclosed power conductors. This observation questions the impact of HEAF effluent on the functionality of nuclear power plant electrical equipment. Understanding the impact of HEAF effluent on the performance of safety equipment is desired to better understand the hazard.

A conductivity sensor designed specifically for pulsed power research was used in the open box experiments. The sensor measures free charge and was fully enclosed with a perforated screen design to eliminate electromagnetic interference (EMI). The sensor geometry is shown in Fig. 18.

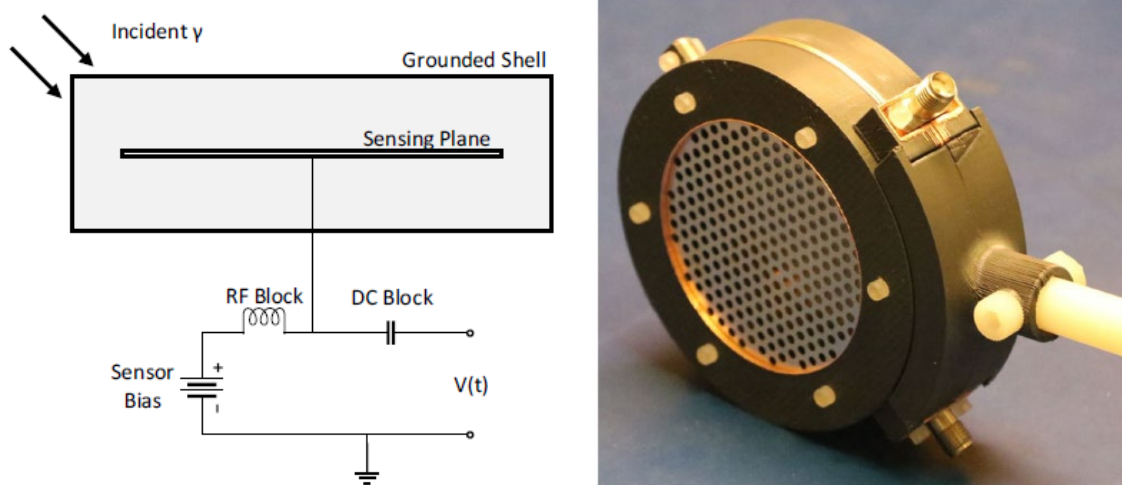


Fig. 18. Parallel plate sensors with a perforated screen design to eliminate EMI.

The sensor was formed from a hollow grounded cylinder with a suspended metal disk. A sensor bias (10 V) was applied to the disk through a radio frequency (RF) block. As conductive particulates entered the chamber, the time change of resistance was measured as a voltage change through a DC block; the higher the conductivity or conductance, the higher the voltage was measured between the perforated sensor plates. A maximum of two sensors was used in an experiment. The grounded shell and use of coaxial cable to fiber link or metal-clad EMI-shielded cables were used to ensure EMI reduction. The use of these sensors in pulse power applications (similar environment to HEAF experiments from an electrical interference perspective) have previously shown successful results. The expanded uncertainty in the medium-voltage air conductivity measurement, limited by the resolution of the data acquisition digital oscilloscope used [28], is 9×10^{-6} S with a 95 % confidence interval.

2.4.7. Voltage Holdoff Strength

To evaluate HEAF generated effluent air-vapor voltage holdoff properties, an approach based on ASTM D2477 [31] was followed. Two conical electrodes as shown in Fig. 19 were used. The effective gap between the electrode tips was approximately 0.5 cm (0.2 in). A fast ramp of 10 kV/s was used instead of a steady or stepped ramp as in ASTM D2477 to enable multiple measurements of breakdown strength during a 2 s to 8 s experiment. The limited duration of a HEAF event limits the applicability of the steady or stepped approach; a fast ramp with multiple breakdown events enables statistical breakdown voltage measurements during a single HEAF experiment. The uncertainty of the breakdown voltage measurement is ± 200 V (0.2 kV) limited by the resolution of the data acquisition digital oscilloscope used [28]. A set of six ramp sequences was used during experiments as shown in Fig. 20. Current viewing transformers and a voltage monitor were connected to oscilloscopes to acquire air breakdown voltage data prior to (baseline) and during HEAF events to quantify any changes in breakdown or holdoff strength. Pre-HEAF air breakdown measurements are shown in Fig. 21, which measured a breakdown field of approximately $28.5 \text{ kV/cm} \pm 2.2 \text{ kV/cm}$. This is consistent with typical air breakdown strengths of 25 kV/cm to 30 kV/cm and a holdoff well above the 0.7 kV/cm to 1.1 kV/cm NEC-allowed electrical field operation levels of concern.

The voltage holdoff strength of air is normally 25 kV/cm to 30 kV/cm dependent on gas density, temperature, and composition. During a HEAF, high temperatures causing decreased air density and the presence of metal particulates would be expected to reduce the holdoff strength of air. An air breakdown field holdoff of less than 0.7 kV/cm to 1.1 kV/cm during HEAF events would be a significant concern. HEAFs could produce environmental conditions where the holdoff strength is not enough to maintain dielectric isolation between electrical power conductors, depending on component design.

A criterion for required voltage holdoff strength was based on discussions with EPRI regarding NEC table 490.24 [30], which specifies minimum clearance of live parts as a function of nominal voltage rating. The values in NEC table 490.24 [30] relevant to medium-voltage equipment include minimum phase-to-ground clearances of 10 cm (4 in) at 7.2 kV and 12.5 cm (5 in) at 13.8 kV. These equate to NEC-allowed maximum design electrical fields of 0.72 kV/cm to 1.10 kV/cm.



Fig. 19. Breakdown sensor (electrode configuration (left), safety jumper (center), operational experiment (right)).

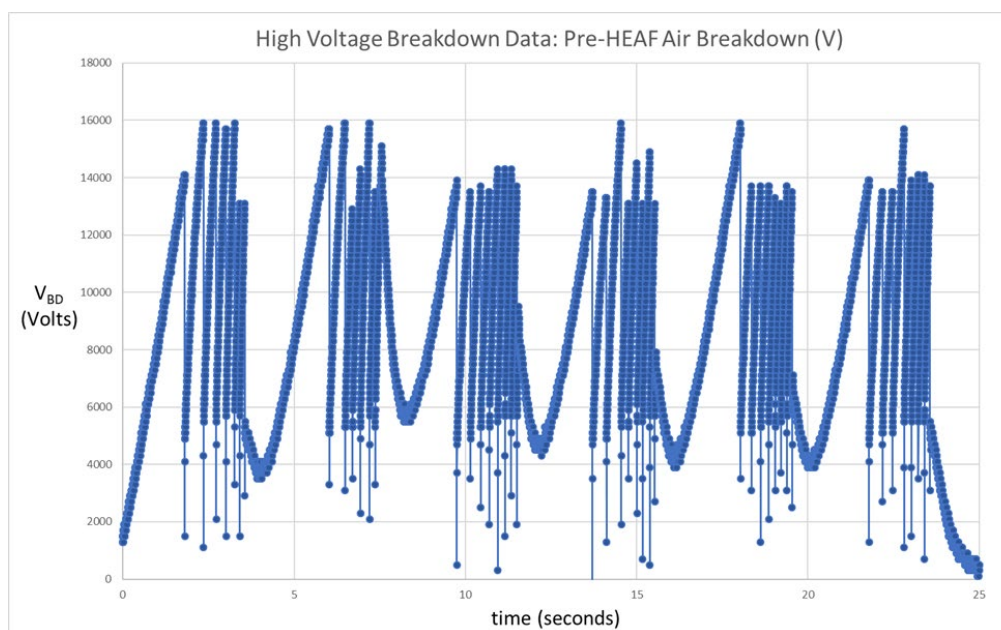


Fig. 20. Measured waveform spark gap from experiment.

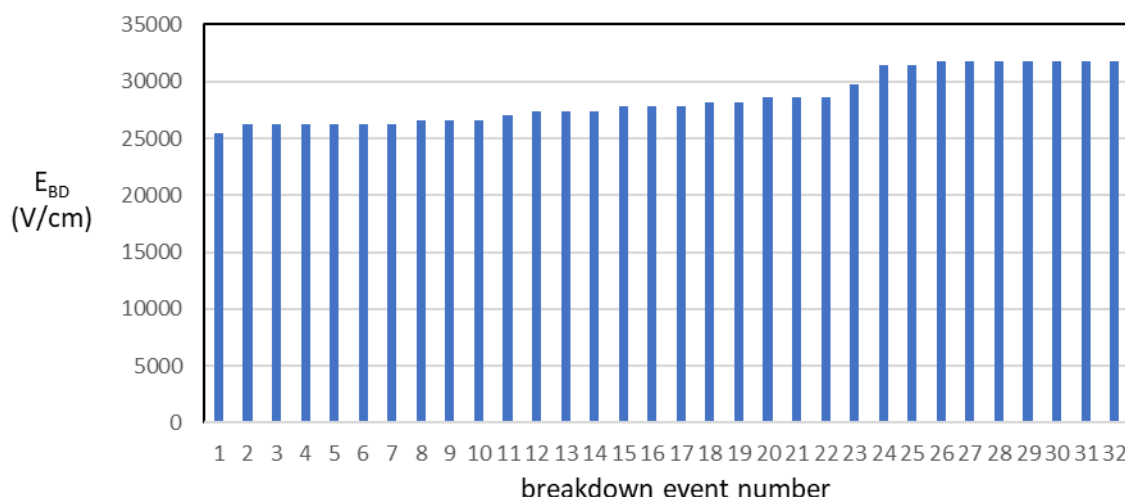


Fig. 21. High-voltage breakdown strength: pre-HEAF ($E_{BD}=28.5\text{kV/cm} \pm 2.2 \text{ kV/cm}$).

2.4.8. Mass Loss Measurements

Mass loss measurements of electrode material were made using an electronic mass balance with a measurement range of approximately 0 kg to 41 kg. The mass balance (NIST Scale 2) has an expanded uncertainty, derived from manufacturer specifications of $\pm 1 \text{ g}$, with a 95 percent confidence interval. Calibrated masses of approximately 50 g to 40.970 kg were used to verify the performance of the mass balance. Initial (pre-experiment) and final (post-experiment) measurements were made of masses of the electrode. The electrode mass loss is reported in the experiment result Sections 3 and 4.

Mass loss measurements of the steel enclosure were also planned; however, during the measurements it was noted that the masses of several enclosures were greater after the experiment than prior to the experiment. It was determined that the electrode material was plated onto the enclosure resulting in an inaccurate measurement of the actual enclosure material loss. The plated and melted electrode material was not easily removed, and an alternative way to estimate material loss was used. The alternative required the use of photo images with reference measurements and a computer software program. This method provided a reasonable measure of mass loss but had a higher level of uncertainty. The expanded uncertainty in mass measurements using the alternative technique based on area was estimated at ± 10 percent with a 95 percent confidence interval. An example of the approach is shown in Fig. 22.

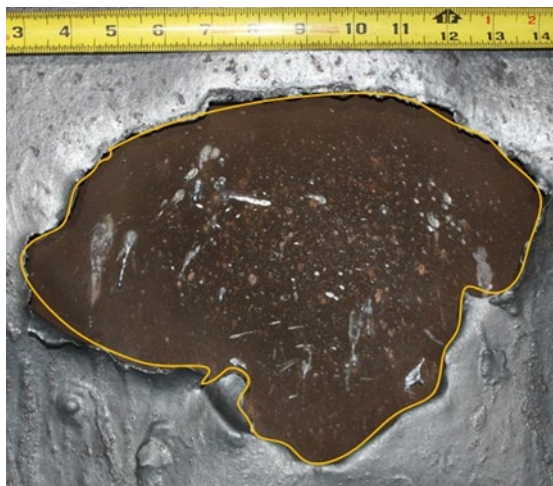


Fig. 22. Example of mass loss measurement using surface area estimated by computer software (363 cm² estimated area in example photo shown).

2.4.9. Electrical Data Acquisition and Processing

Electrical measurements were made by KEMA. Line-to-ground voltages were measured in two locations, one at the generator and just prior to the open box in the test cell and two at the open box. Unless otherwise stated, the line-to-ground voltage reported here was measured at the box. Current measurements were made downstream from any transformer, not in the test cell upstream of the open box. The uncertainty in the measurements made by KEMA Labs were ± 3 percent.

All experiments were run in a wye connection. However, early experiments were run with the wye neutral not connected to ground via impedance. Since the voltages were referenced to ground, the wye neutral and ground did not have a common reference, thus the neutral was floating. This becomes a problem in reporting the actual line-to-neutral voltage at the device. After this was identified, subsequent experiments were performed with the wye-neutral connected to ground via impedance to ensure a common reference. To address the issue for the initial experiments, a post-processing technique was identified by KEMA and is presented below with an example case.

The zero-sequence voltage was calculated by adding all device phase voltages together. An example is shown in Fig. 23 along with the measured device voltage for each phase. The next one-third of this zero-sequence voltage was removed from each of the device voltage waveforms. Fig. 24 and Fig. 25 show how the voltage waveforms are modified for a case where the wye-neutral was not and was connected to ground via impedance. For the cases where the generator neutral was connected to ground via impedance, similarity of the pre- and post-waveforms demonstrated correctness of the MATLAB algorithm and technique. For completeness, a final figure showing the generator, device, and post-processed device voltage waveforms are shown in Fig. 26 from Experiment OB08. MATLAB code used for processing is presented in the previous report [1].

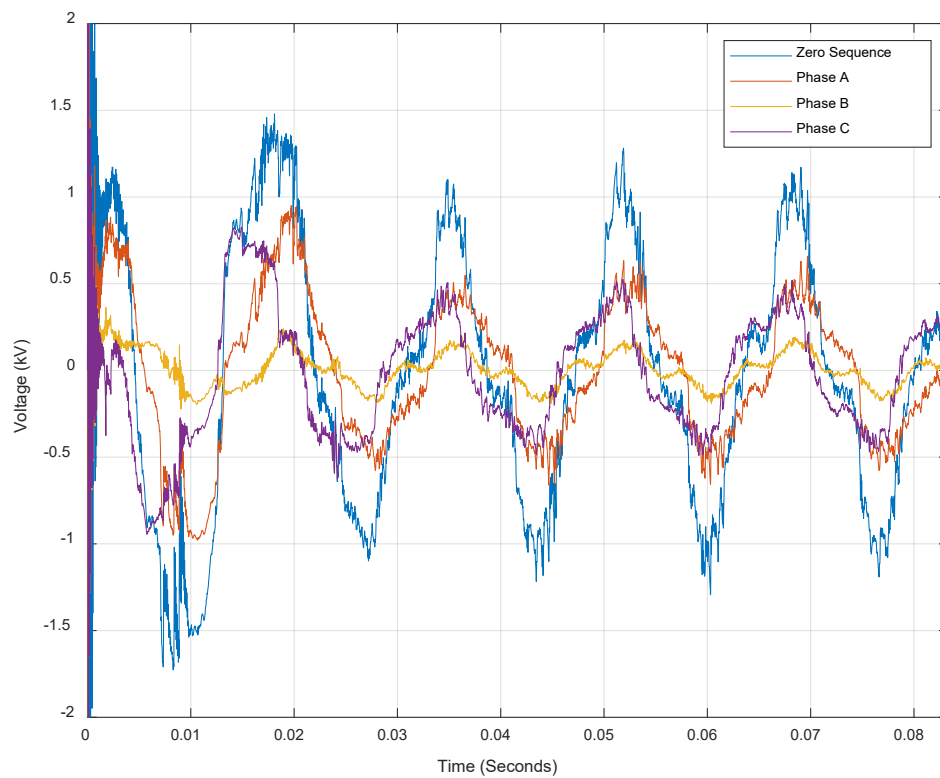


Fig. 23. Zero-sequence voltage (Experiment OB08).

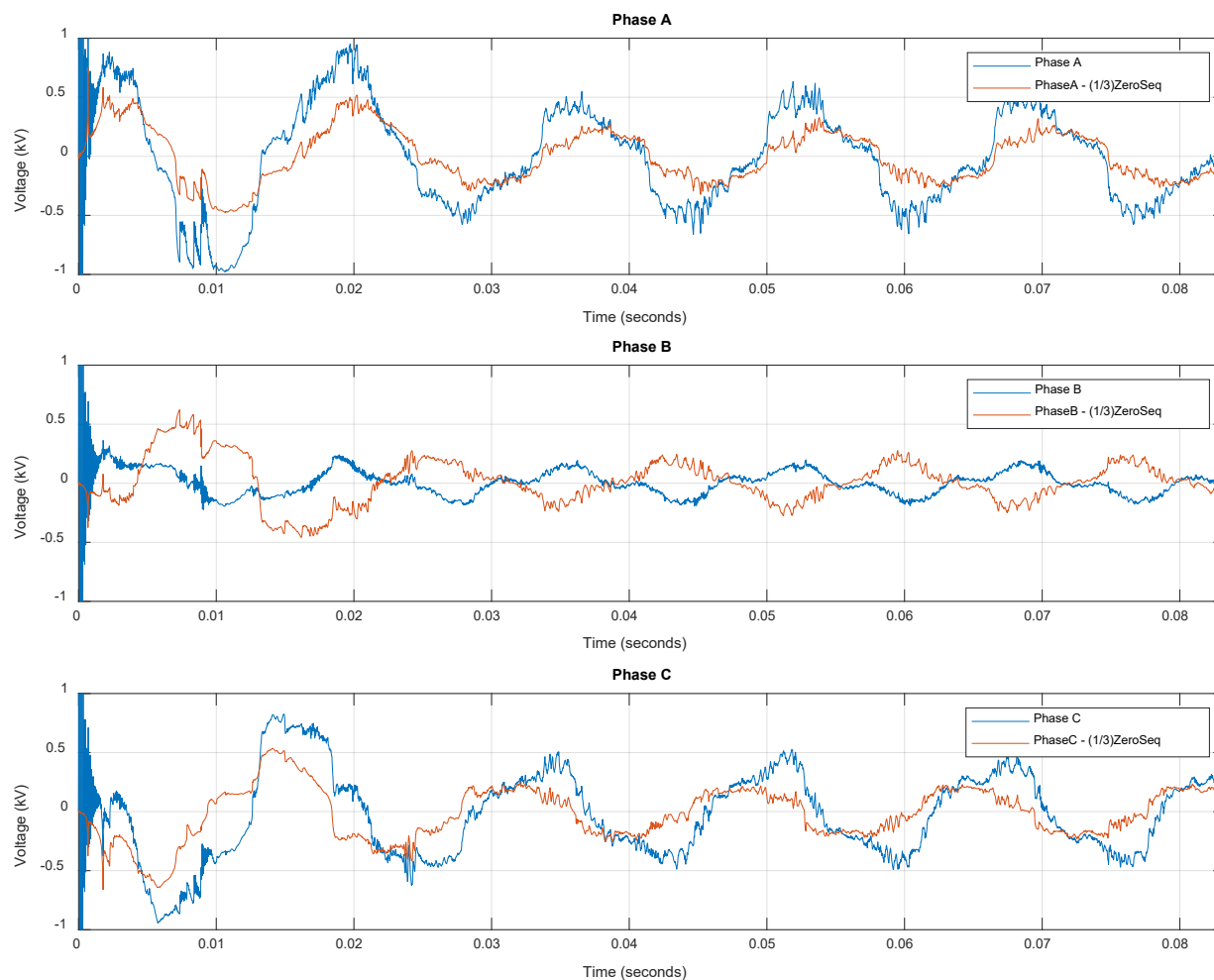


Fig. 24. Original and modified device voltage when wye-neutral was not connected to ground (Experiment OB04).

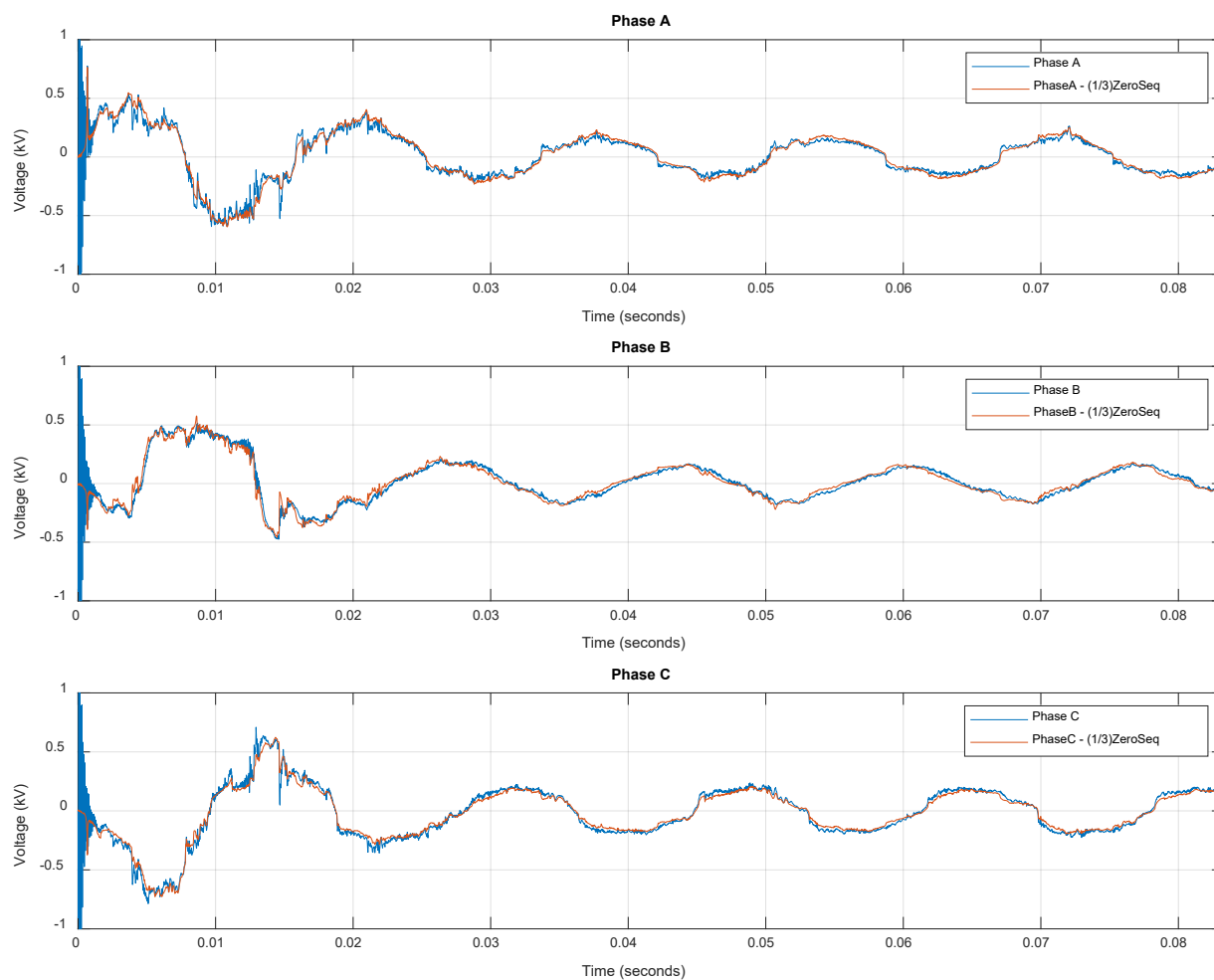


Fig. 25. Original and modified device voltage when wye-neutral was connected to ground via impedance (Experiment OB04).

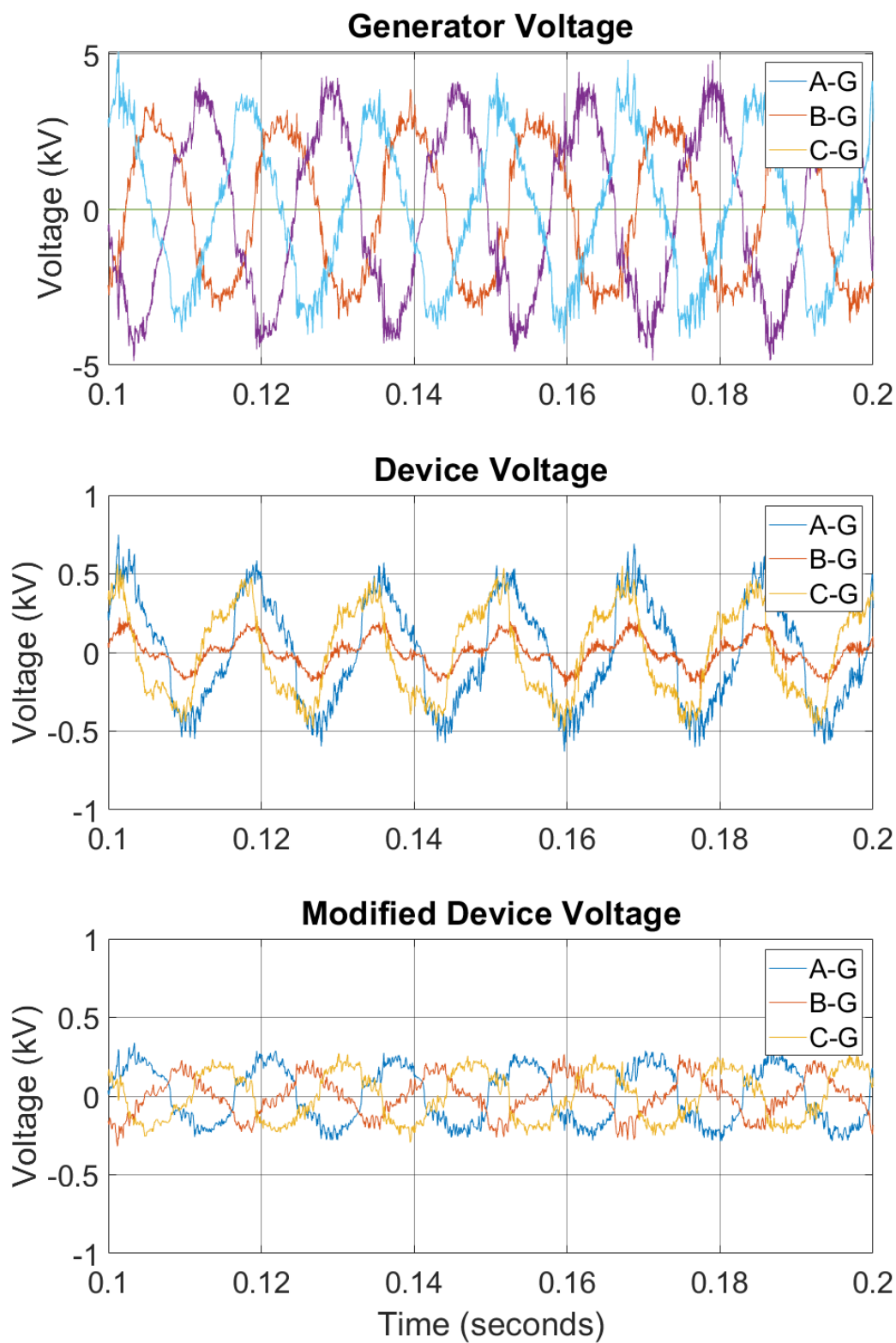


Fig. 26. Line-to-ground voltage at generator (top), at open box (middle), and modified open box voltage (bottom) (experiment OB08).

3. Low-Voltage Experiment Results

KEMA performed calibration runs to ensure that the power circuits selected met the desired experimental parameters. The calibrations were measured at a shorting bus within the laboratory's facility, and the actual experimental conditions were slightly different because of the additional circuit length to the open box and that of the open box equipment. The resulting circuit calibrations are presented in Table 5, with detail provided in the KEMA report (Appendix C).

Table 5. Low-voltage circuit calibration.

Voltage (V)	Current Symmetrical (kA)	Current Peak (kA)	Circuit
1 000	1.04	2.9	190822-7001
1 000	5.05	14.9	190822-7002
1 064	30.0	79.1	190823-7001
1 009	15.0	40.4	190823-7002
6 900	15.3	42.9	190916-9002
6 900	30.6	86.5	190916-9004

The circuit calibrations were performed for about 10 cycles to ensure stabilization of the waveform. The duration of the arc during actual experiments was determined by the ability to maintain the arc within the enclosure and the breaking of the circuit by the laboratory's protective device(s). Provided that the arc did not prematurely extinguish prior to the desired arc time, the laboratory ensured that the arc duration parameter was met by automatically triggering their protective devices to open at the specified duration. Because there was a delay in the opening of the circuit (breaker opening time), the actual durations were longer than the desired durations. Table 6 and Table 7 present the experimental parameter variations planned for this series of experiments.

Table 6. Low-voltage experiments - planned nominal experiment parameters.

Experiment #	Rod Material		Rod Diameter (cm)		System Voltage (kV)	Current (kA)	Duration (s)	Notes
	Al	Cu	1.3	2.5				
OB01(a)		X	X		1.0	1.0	2.0	Shorting wire issue
OB01(b)		X	X		1.0	1.0	2.0	Repeat of OB01(a)
OB02		X		X	1.0	15.0	2.0	
OB03		X		X	1.0	15.0	3.0	
OB04		X		X	1.0	30.0	1.0	
OB05	X		X		1.0	1.0	2.0	

Experiment #	Rod Material		Rod Diameter (cm)		System Voltage (kV)	Current (kA)	Duration (s)	Notes
	Al	Cu	1.3	2.5				
OB06	X			X	1.0	15.0	2.0	
OB07	X			X	1.0	15.0	1.5	
OB08	X			X	1.0	30.0	1.0	
OB09		X	X		1.0	5.0	2.0	
OB10	X		X		1.0	5.0	2.0	

Table 7. Medium-voltage experiments - planned nominal experiment parameters.

Experiment #	Rod Material		Bus size (cm)		System Voltage (kV)	Current (kA)	Duration (s)
	Al	Cu	7.6	10.2			
OBMV1	X			X	6.9	15.0	2
OBMV2	X			X	6.9	30.0	1
OBMV3	X			X	6.9	15.0	5
OBMV4		X	X		6.9	15.0	5
OBMV5		X	X		6.9	30.0	2

3.1. Low-Voltage Experiment Results with Copper Electrodes

Experiments OB01(a) through OB04 and OB09 are presented in this subsection. All of these experiments used copper electrodes.

For each experiment, the following information is provided:

- Experiment specifications
- Electrode length and mass
- Photo of pre- and post-experiment configuration
- Photo of enclosure breach (if applicable)
- Voltage and current profile
- SNL Measurements (if applicable)
- Notes
- Observations

A summary of the low-voltage box experiments is presented at the end of this section Table 30.

3.1.1. Experiment ID: OB01(a)

This was the first open box experiment performed. During the performance of this experiment, it was determined that the low current resulted in an excessively long time for the shorting wire to vaporize. This resulted in a three-phase bolted short for over one-half of the experimental time. The shorting wire used was based on the IEEE guidance [32]. Because the experiment didn't achieve the objectives, this experiment was designated as "OB01(a)," and an identical experiment, designated as "OB01(b)," with a different shorting wire was conducted.

This experiment was performed on August 22, 2019. The experiment parameters are presented in Table 8. Photos of Experiment OB01(a) are presented in Fig. 27. Thermal and visual video stills are provided in Fig. 28. Test OB01(a) used KEMA test circuit S01. The KEMA report identifies this experiment as 190822-7003.

Table 8. Experiment OB01(a) parameters.

Electrical Parameter	Target	Actual	Other
Voltage (V _{L-L})	1 000	1 029	347 (Arc)
Current (A)	1 000	1 052	
Duration (ms)	2 000	2 010	660 (Arc)
Energy (MJ)		0.201	
Other Parameters			
Electrode Length Loss (cm)	0.5 (Phase A)	1.1 (Phase B)	0.3 (Phase C)
Electrode Mass Loss (g)	Not recorded due to limited arcing duration		
Electrode Material	Copper		
Electrode Diameter	1.27 cm (0.5 in)		
Electrode Spacing	8.9 cm (3.5 in) on center		
Shorting Wire	1 – 10 AWG (2.6 mm diameter), k-strand tinned copper		
Box Electrical Configuration	Connected to Neutral		
Generator Configuration	Generator Neutral Floating		
Enclosure Breach	None		



Fig. 27. Experiment OB01(a) pre-experiment (left) and post-experiment (right) copper electrodes. Phase sequence from left-to-right is C-B-A.

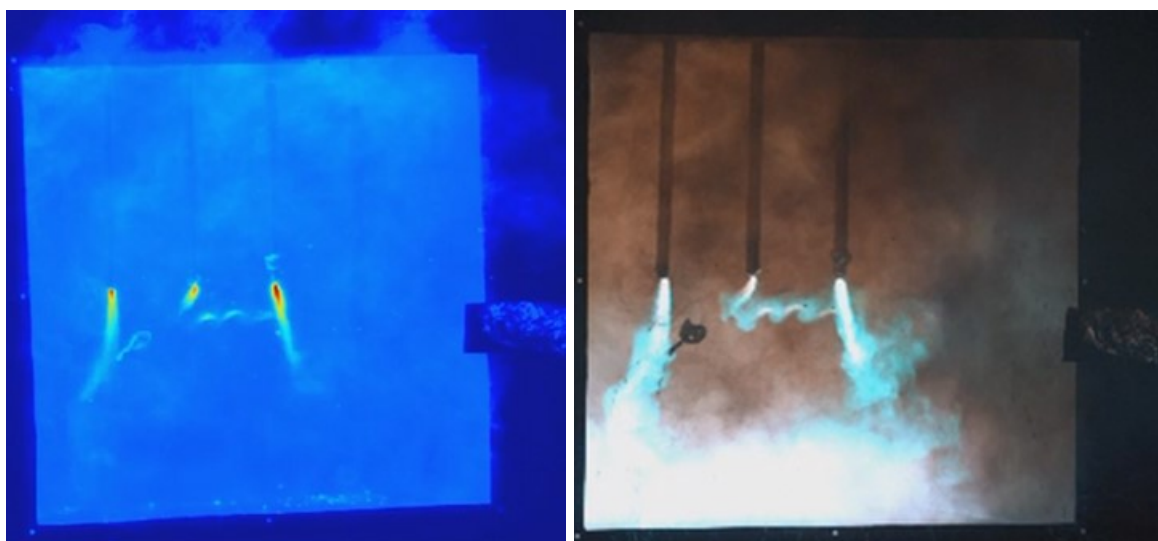


Fig. 28. Thermal (left) and visible (right) video still shot during arc ($t = 1.97\text{s}$).

SNL used a plate calorimeter to measure the incident energy during the experiment, and the approximate measurements are presented in Table 9.

Table 9. Experiment OB01(a) plate calorimeter measurements.

Distance from Electrode (cm)	Thickness (mm)	ΔT ($^{\circ}\text{C}$)	Measured Incident Energy (MJ/m^2)	Calculated Energy (MJ)
45.7	1	21.6	0.07	0.20

Observations and Notes

As can be observed from the photo (Fig. 27), there was minimal material loss from the electrodes, and the enclosure was not breached. Due to the minimal material loss, mass measurements were not made. For this experiment a single uninsulated conductor, 2.6 mm nominal diameter (10 AWG) size with Type K-strand tinned copper, was used as the shorting wire. From video evidence and the electrical measurements, the low current resulted in a significant amount of time (approximately 1.35 s) for the shorting wire to become vaporized. Therefore, the arc was only present for approximately 0.7 s versus the desired 2 s experiment duration. As such, the experiment was re-run as Experiment OB01(b) using a smaller gauge shorting wire.

3.1.2. Experiment ID: OB01(b)

This experiment was a repeat of Experiment OB01(a) except that the IEEE guidance [32] for low-voltage experiments was not followed. The guidance uses a larger cross-sectional conductor in low-voltage experiments to ensure that sufficient conductive material is available to maintain the arc. Maintaining arcs at low-voltage is more difficult than at medium-voltage, hence the guidance to use more material. However, at the low current for these experiments, the recommended shorting wire acted as a slow blow fuse rather than an arc initiator. The following approach was followed to provide the desired arc duration and a better arc initiation mechanism while attempting to ensure sufficient conductive medium. The shorting wire recommended for medium-voltage experiments was used. However, instead of using a single strand, a double strand configuration was used. Given the low current levels, it was believed at the time and confirmed through later experiments that the smaller diameter conductor would provide a better arc initiation mechanism. This approach was found to initiate the arc in less than one cycle.

This experiment was performed on August 22, 2019. The experiment parameters are presented in Table 10. Photos of Experiment OB01(b) are presented in Fig. 29. Experiment OB01(b) used KEMA experiment circuit S01. The KEMA Experiment report identifies this experiment as 190822-7004.

Table 10. Experiment OB01(b) parameters.

Electrical Parameter	Target	Actual	Other
Voltage (V_{L-L})	1 000	1 028	308 (arc)
Current (A)	1 000	1 030	
Duration (ms)	2 000	2 020	
Energy (MJ)		0.736	
Other Parameters			
Electrode Length Loss (cm)	0.5 (Phase A)	0.4 (Phase B)	0.6 (Phase C)
Electrode Mass Loss (g) ³	5.5	12.0	7.0
Electrode Material	Copper		
Electrode Diameter	1.27 cm (0.5 in)		
Electrode Spacing	8.9 cm (3.5 in) on center		
Shorting Wire	2 – 24 AWG (0.51 mm diameter), single strand tinned copper		
Box Electrical Configuration	Neutral		
Generator Configuration	Neutral not Grounded		
Enclosure Breach	None		

³ Mass loss for both Test OB01(a) and OB01(b)



Fig. 29. Experiment OB01(b) pre-experiment (left) and post-experiment (right) copper electrodes. Phase sequence from left-to-right is C-B-A.

SNL used a plate calorimeter to measure the incident energy during the experiment, and the approximate measurements are presented in Table 11.

Table 11. Experiment OB01(b) plate calorimeter measurements.

Distance from Electrode (cm)	Thickness (mm)	ΔT (°C)	Measured Incident Energy (MJ/m ²)	Calculated Energy (MJ)
45.7	1	45.1	0.16	0.41

Observations and Notes

The use of the smaller arcing wire reduced the amount of time to vaporize the wire under these low current conditions. Review of the current and voltage profiles indicated that the 0.51 mm nominal diameter (24 AWG) arc wire was vaporized in approximately 4.44 ms versus the 1 350 ms from experiment OB01(a). The steel enclosure did not breach. The copper electrodes from Experiment OB01(a) were reused for this experiment. The electrodes were not repositioned due to the minimal amount of material lost during the previous experiment. Care must be used when evaluating the material lost from experiment OB01(a) and experiment OB01(b) because the electrode mass loss reported in Table 10 was a combination of both experiments.

3.1.3. Experiment ID: OB02

This experiment was performed on August 30, 2019. The electrical characteristics are presented in Table 12. Photos of Experiment OB02 are presented in Fig. 30 through Fig. 32. Experiment OB02 used KEMA experiment circuit S03. The KEMA experiment report identifies this experiment as 190830-7001.

Table 12. Experiment OB02 parameters .

Electrical Parameter	Target	Actual	Other
Voltage (V_{L-L})	1 000	1 008	271 (arc)
Current (A)	15 000	14 016	
Duration (ms)	2 000	2 020	
Energy (MJ)		11.989	
Other Parameters			
Electrode Length Loss (cm)	5.1 (Phase A)	6.4 (Phase B)	4.9 (Phase C)
Electrode Mass Loss (g)	189.5	369.0	204.0
Electrode Material	Copper		
Electrode Diameter	2.54 cm (1.0 in)		
Electrode Spacing	8.9 cm (3.5 in) on center		
Shorting Wire	2 – 24 AWG (0.51 mm diameter), single strand tinned copper		
Box Electrical Configuration	Neutral		
Generator Configuration	Neutral tied to ground via impedance		
Enclosure Breach	Yes, Bottom and Top		
Enclosure Mass Loss (g)	386		



Fig. 30. Experiment OB02 pre-experiment (left) and post-experiment (right) copper electrodes. Phase sequence from left-to-right is C-B-A.



Fig. 31. Experiment OB02 enclosure breach. (bottom side breach (left), top side breach with electrode holder removed (right)).

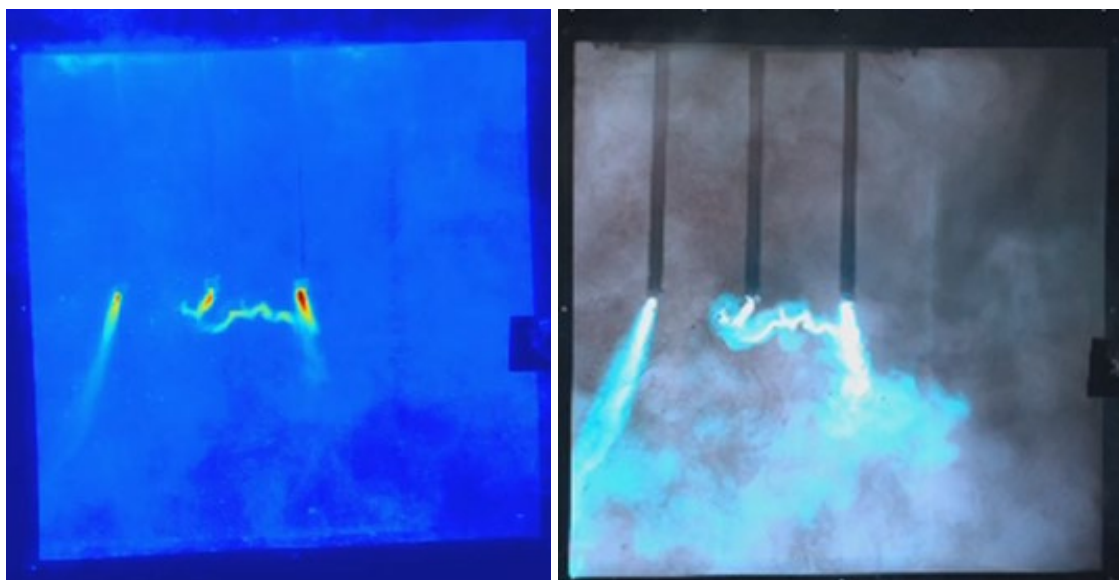


Fig. 32. Experiment OB02 thermal (left) and visible (right) video still shots during the arc ($t = 1.47$ s).

SNL used a plate calorimeter to measure the incident energy during the experiment. The approximate measurements are presented in Table 13.

Table 13. Experiment OB02 plate calorimeter measurements.

Distance from Electrode (cm)	Thickness (mm)	ΔT ($^{\circ}\text{C}$)	Measured Incident Energy (MJ/m^2)	Calculated Energy (MJ)
182.8	3	10.2	0.11	4.46

Observations and Notes

The steel enclosure breached at the bottom and top. The estimated mass loss from the enclosure was approximately 386 g, and a total breach opening on all sides was approximately 275 cm^2 (bottom opening of approximately 248 cm^2 and a top opening of approximately 26 cm^2).

3.1.4. Experiment ID: OB03

This experiment was performed on August 30, 2019. The electrical characteristics are presented in Table 14. Photos of Experiment OB03 are presented in Fig. 33 through Fig. 35. Experiment OB03 used KEMA experiment circuit S03. The KEMA Experiment report identifies this experiment as 190830-7002.

Table 14. Experiment OB03 parameters.

Electrical Parameter	Target	Actual	Other
Voltage (V_{L-L})	1 000	1 008	314 (arc)
Current (A)	15 000	13 804	
Duration (ms)	3 000	3 030	
Energy (MJ)		19.886	
Other Parameters			
Electrode Length Loss (cm)	9.8 (Phase A)	12.1 (Phase B)	8.6 (Phase C)
Electrode Mass Loss (g)	444	515	368
Electrode Material	Copper		
Electrode Diameter	2.54 cm (1.0in)		
Electrode Spacing	8.9 cm (3.5 in) on center		
Shorting Wire	2 – 24 AWG (0.51 mm diameter), single strand tinned copper		
Box Electrical Configuration	Neutral		
Generator Configuration	Neutral tied to ground via impedance		
Enclosure Breach	Bottom, side, back, top		
Enclosure Mass Loss (g)	1 799		



Fig. 33. Experiment OB03 pre-experiment (left) and post-experiment (right) copper electrodes. Phase sequence from left-to-right is C-B-A.

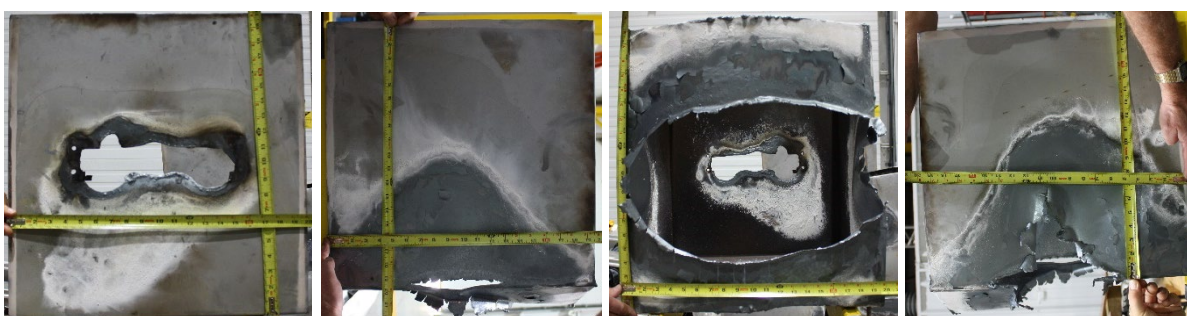


Fig. 34. Experiment OB03 enclosure breach (from left-to-right: top, left side, bottom, right side).

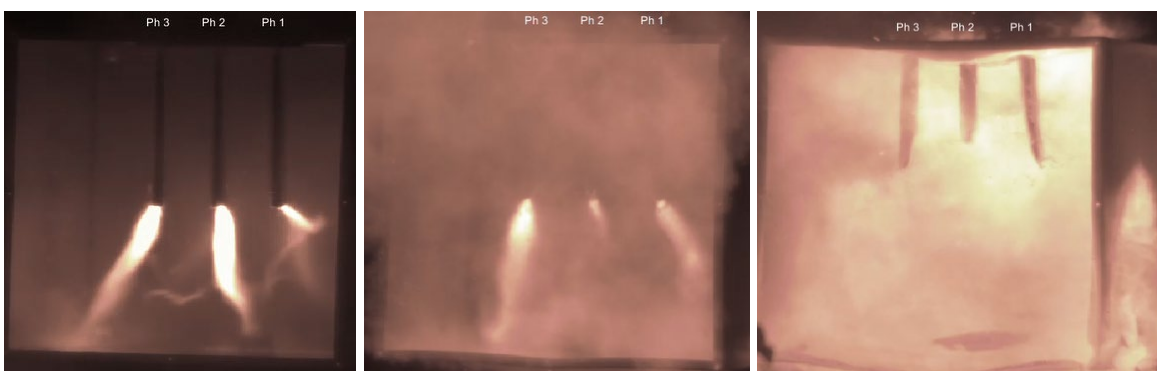


Fig. 35. Experiment OB03 still shots from the high speed visible video during the arc (0.02 s (left), 1.50 s (center), 3.06 s (right)).

SNL used a plate calorimeter to measure the incident energy during the experiment, and the approximate measurements are presented in Table 15.

Table 15. Experiment OB03 plate calorimeter measurements.

Distance from Electrode (cm)	Thickness (mm)	ΔT (°C)	Measured Incident Energy (MJ/m²)	Calculated Energy (MJ)
182.9	3	17.7	0.18	7.73

Observations and Notes

The estimated mass loss from the enclosure was approximately 1 799 g, and a total breach opening on all sides was approximately 1 280 cm² (bottom opening of approximately 1 110 cm², left side approximately 20 cm², right side approximately 101 cm² and a top opening of approximately 50 cm²).

3.1.5. Experiment ID: OB04

This experiment was performed on August 30, 2019. The experiment parameters are presented in Table 16. Photos of Experiment OB04 are presented in Fig. 36 through Fig. 39. Experiment OB04 used KEMA experiment circuit S04. The KEMA Experiment report identifies this experiment as 190830-7003.

Table 16. Experiment OB04 parameters.

Electrical Parameter	Target	Actual	Other
Voltage (V_{L-L})	1 000	1 063	276 (arc)
Current (A)	30 000	27 786	
Duration (ms)	1 000	1 030	
Energy (MJ)		12.328	
Other Parameters			
Electrode Length Loss cm	8.3 (Phase A)	4.8 (Phase B)	2.9 (Phase C)
Electrode Mass Loss (g)	241.0	357.5	190.5
Electrode Material	Copper		
Electrode Diameter	2.54 cm (1.0 in)		
Electrode Spacing	8.9 cm (3.5 in) on center		
Shorting Wire	2 – 24 AWG (0.51 mm diameter), single strand tinned copper		
Box Electrical Configuration	Neutral		
Generator Configuration	Neutral tied to ground via impedance		
Enclosure Breach	Bottom		
Enclosure Mass Loss (g)	110		



Fig. 36. Experiment OB04 pre-experiment (left) and post-experiment (right) copper electrodes. Phase sequence from left to right is C-B-A.



Fig. 37. Experiment OB04 enclosure breach (bottom side (left); top side (right)).



Fig. 38. Experiment OB04 electrode deflection post-experiment.

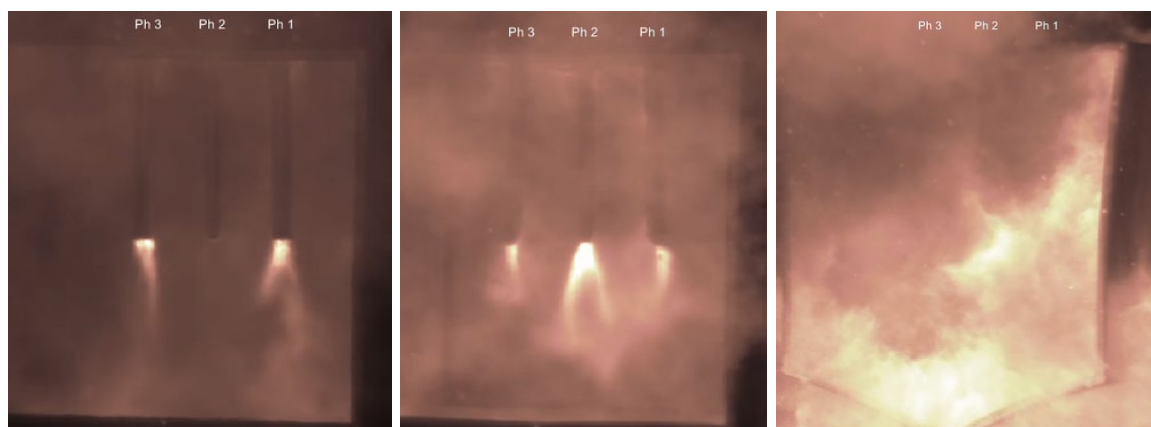


Fig. 39. Experiment OB04 visible video still shot during the arc (0.09 s (left); 0.51 s (center); 1.08 s (right)).

SNL used a plate calorimeter to measure the incident energy during the experiment, and the approximate measurements are presented in Table 17.

Table 17. Experiment OB04 plate calorimeter measurements.

Distance from Electrode (cm)	Thickness (mm)	ΔT ($^{\circ}\text{C}$)	Measured Incident Energy (MJ/m^2)	Calculated Energy (MJ)
182.9	3	10.6	0.11	4.63

Observations and Notes

The estimated mass loss from the enclosure was approximately 110 g, and a total breach opening on all sides was approximately 78 cm^2 (bottom opening of approximately 15 cm^2 and a top opening of approximately 63 cm^2).

3.1.6. Experiment ID: OB09

This experiment was performed on August 22, 2019. The experimental parameters are presented in Table 18. Photos of Experiment OB09 are presented in Fig. 40 and Fig. 41. Experiment OB09 used KEMA experiment circuit S02. The KEMA Experiment report identifies this experiment as 190822-7007.

Table 18. Experiment OB09 parameters.

Electrical Parameter	Target	Actual	Other
Voltage (V _{L-L})	1 000	1 026	297 (Arc)
Current (A)	5 000	4 794	
Duration (ms)	2 000	2 010	
Energy (MJ)		2.242	
Other Parameters			
Electrode Length Loss (cm)	6.0 (Phase A)	7.6 (Phase B)	7.1 (Phase C)
Electrode Mass Loss (g)	61.5	77.0	74.0
Electrode Material	Copper		
Electrode Diameter	1.27 cm (0.5in)		
Electrode Spacing	8.9 cm (3.5 in) on center		
Shorting Wire	2 – 24 AWG (0.51 mm diameter), single strand tinned copper		
Box Electrical Configuration	Neutral		
Generator Configuration	Neutral not grounded		
Enclosure Breach	None		



Fig. 40. Experiment OB09 pre-experiment (left) and post-experiment (right) copper electrodes. Phase sequence from left-to-right is C-B-A.

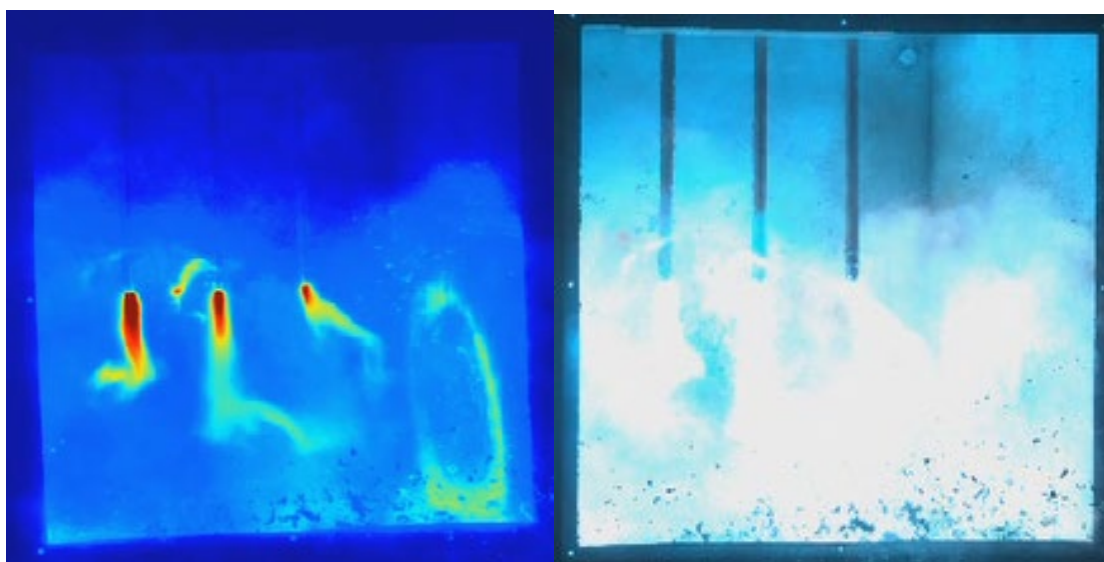


Fig. 41. Experiment OB09 thermal (left) and visible (right) video still shots during the arc ($t = 0.06$ s).

SNL used a plate calorimeter to measure the incident energy during the experiment, and the approximate measurements are presented in Table 19.

Table 19. Experiment OB09 plate calorimeter measurements.

Distance from Electrode (cm)	Thickness (mm)	ΔT (°C)	Measured Incident Energy (MJ/m ²)	Calculated Energy (MJ)
182.9	3	3.6	0.04	1.57

Observations and Notes

The steel enclosure did not breach.

3.2. Low-Voltage Experiment Results with Aluminum Electrodes

Experiments OB05 through OB08 and OB10 are presented in this subsection. All of these experiments used aluminum electrodes.

For each experiment, the following information is provided:

- Experiment specifications
- Electrode length and mass
- Photo of pre- and post-experiment configuration
- Photo of enclosure breach (if applicable)
- Voltage and current profile
- SNL Measurements (if applicable)
- Notes
- Observations

A summary of the low-voltage box experiments is presented at the end of this section (Table 30).

3.2.1. Experiment ID: OB05

This experiment was performed on August 22, 2019. The experiment parameters are presented in Table 20. Photos of Experiment OB05 are presented in Fig. 42 and Fig. 43.

Table 20. Experiment OB05 parameters.

Electrical Parameter	Target	Actual	Other
Voltage (V_{L-L})	1 000	1 027	359 (Arc)
Current (A)	1 000	1 018	
Duration (ms)	2 000	2 010	
Energy (MJ)		0.796	
Other Parameters			
Electrode Length Loss (cm)	2.4 (Phase A)	3.0 (Phase B)	3.0 (Phase C)
Electrode Mass Loss (g)		Not measured	
Electrode Material		Aluminum	
Electrode Diameter		1.27 cm (0.5 in)	
Electrode Spacing		8.9 cm (3.5 in) on center	
Shorting Wire		2 – 24 AWG (0.51 mm diameter), single strand tinned copper	
Box Electrical Configuration		Neutral	
Generator Configuration		Neutral not tied to ground	
Enclosure Breach		None	

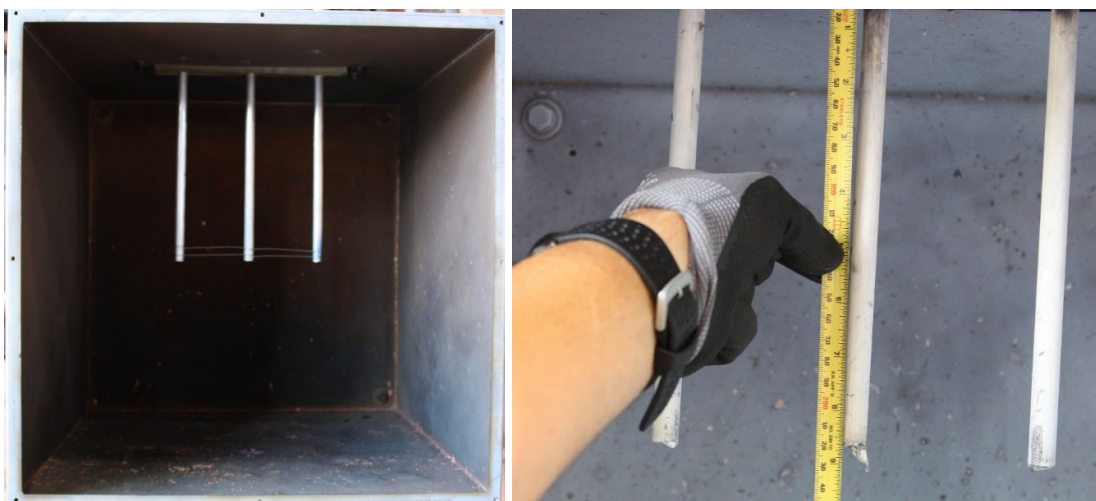


Fig. 42. Experiment OB05 pre-experiment (left) and post-experiment (right) aluminum electrodes. Phase sequence from left-to-right is C-B-A.

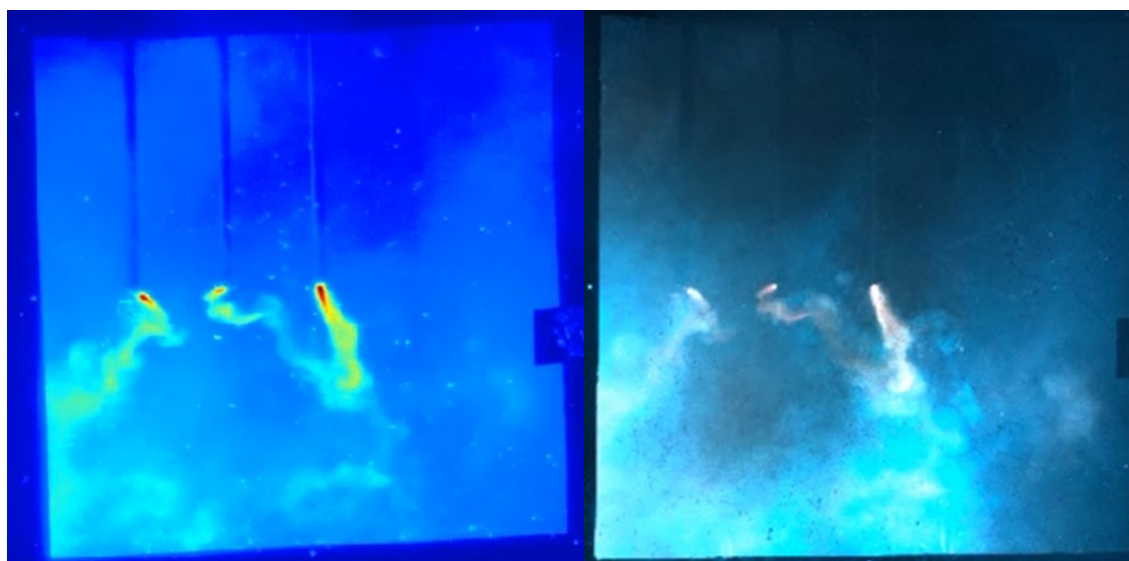


Fig. 43. Experiment OB05 thermal (left) and visible (right) video still shot during the arc ($t = 0.33\text{s}$).

SNL used a plate calorimeter to measure the incident energy during the experiment, and the approximate measurements are presented in Table 21.

Table 21. Experiment OB05 plate calorimeter measurements.

Distance from Electrode (cm)	Thickness (mm)	ΔT ($^{\circ}\text{C}$)	Measured Incident Energy (MJ/m^2)	Calculated Energy (MJ)
45.7	1	88.7	0.31	0.81

Observations and Notes

White aluminum oxide covered the electrodes and the interior of the steel enclosure. Due to the minimal mass loss of the electrodes and scale accuracy, the mass loss was not measured.

3.2.2. Experiment ID: OB06

This experiment was performed on August 23, 2019. The experiment parameters are presented in Table 22. Photos of Experiment OB06 are presented in Fig. 44 and Fig. 45.

Table 22. Experiment OB06 parameters.

Electrical Parameter	Target	Actual	Other
Voltage (V_{L-L})	1 000	1 007	424 (Arc)
Current (A)	15 000	11 959	
Duration (ms)	2 000	2 020	
Energy (MJ)		12.591	
Other Parameters			
Electrode Length Loss (cm)	10.8 (Phase A)	15.9 (Phase B)	8.3 (Phase C)
Electrode Mass Loss (g)	264.5	263.0	212.5
Electrode Material	Aluminum		
Electrode Diameter	2.54 cm (1.0 in)		
Electrode Spacing	8.9 cm (3.5 in) on center		
Shorting Wire	2 – 24 AWG (0.51 mm diameter), single strand tinned copper		
Box Electrical Configuration	Neutral		
Generator Configuration	Neutral not tied to ground		
Enclosure Breach	Bottom, both sides and top		
Enclosure Mass Loss (g)	1 670		



Fig. 44. Experiment OB06 pre-experiment (left) and post-experiment (right) aluminum electrodes. Phase sequence from left-to-right is C-B-A.



Fig. 45. Experiment OB06 enclosure breach (bottom and sides (left); rear top side (right)).

SNL used a plate calorimeter to measure the incident energy during the experiment, and the measurements are presented in Table 23.

Table 23. Experiment OB06 plate calorimeter measurements.

Distance from Electrode (cm)	Thickness (mm)	ΔT (°C)	Measured Incident Energy (MJ/m ²)	Calculated Energy (MJ)
182.9	3	27.4	0.28	11.97

The SNL spectral emission measurement was attempted, but the neutral density filter placed in front of the detector attenuated the signal to the extent that no useful spectra were collected.

Observations and Notes

The estimated mass loss from the enclosure was approximately 1 670 g, and a total breach opening on all sides was approximately 1 189 cm². (Bottom opening of approximately 1035 cm², left side approximately 40 cm², right side approximately 50 cm² and a top opening of approximately 64 cm²).

3.2.3. Experiment ID: OB07

This experiment was performed on August 23, 2019. The experiment parameters are presented in Table 24. Photos of Experiment OB07 are presented in Fig. 46 through Fig. 48.

Table 24. Experiment OB07 experiment parameters .

Electrical Parameter	Target	Actual	Other
Voltage (V _{L-L})	1 000	1 007	431 (arc)
Current (A)	15 000	12 952	
Duration (ms)	1 500	1 520	
Energy (MJ)		10.233	
Other Parameters			
Electrode Length Loss (cm)	7.0 (Phase A)	10.2 (Phase B)	5.7 (Phase C)
Electrode Mass Loss (g)	178	223	151
Electrode Material	Aluminum		
Electrode Diameter	2.54 cm (1.0 in)		
Electrode Spacing	8.9 cm (3.5 in) on center		
Shorting Wire	2 – 24 AWG (0.51 mm diameter), single strand tinned copper		
Box Electrical Configuration	Neutral		
Generator Configuration	Neutral not tied to ground		
Enclosure Breach	Bottom, both sides, and top		
Enclosure Mass Loss (g)	861		



Fig. 46. Experiment OB07 pre-experiment (left) and post-experiment (right) aluminum electrodes. Phase sequence from left-to-right is C-B-A.



Fig. 47. Experiment OB07 enclosure breach (bottom and sides (left); rear top side (right)).

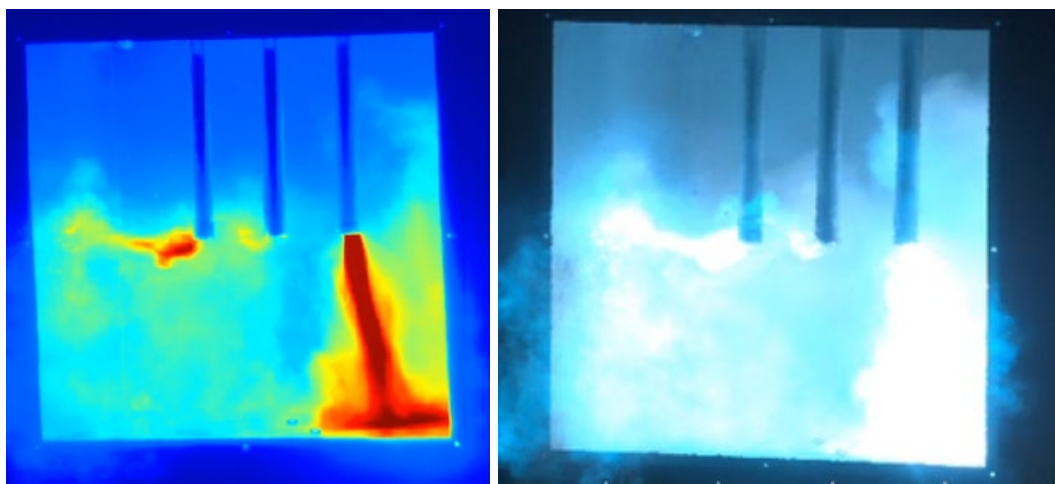


Fig. 48. Experiment OB07 thermal (left) and visible (right) video still shot during the arc ($t = 0.06$ s).

SNL used a plate calorimeter to measure the incident energy during the experiment, and the approximate measurements are presented in Table 25.

Table 25. Experiment OB07 plate calorimeter measurements.

Distance from Electrode (cm)	Thickness (mm)	ΔT ($^{\circ}\text{C}$)	Measured Incident Energy (MJ/m^2)	Calculated Energy (MJ)
182.9	3	18.7	0.19	8.17

Observations and Notes

The estimated mass loss from the enclosure was approximately 861.4 g, and a total breach opening on all sides was approximately 613 cm^2 (bottom opening of approximately 549 cm^2 , left side approximately 6 cm^2 , right side approximately 19 cm^2 , and a top opening of approximately 39 cm^2).

3.2.4. Experiment ID: OB08

This experiment was performed on August 23, 2019. The experiment parameters are presented in Table 26. Photos of Experiment OB08 are presented in Fig. 49 and Fig. 50. A photo of the post-experiment aluminum electrodes with a comparative electrode at the bottom is shown in Fig. 51.

Table 26. Experiment OB08 parameters.

Electrical Parameter	Target	Actual	Other
Voltage (V_{L-L})	1 000	1 062	748 (arc)
Current (A)	30 000	24 870	
Duration (ms)	1 000	1 020	
Energy (MJ)		19.57	
Other Parameters			
Electrode Length Loss (cm)	0.8 (Phase A)	0.8 (Phase B)	0.8 (Phase C)
Electrode Mass Loss (g)	210.0	216.0	170.5
Electrode Material	Aluminum		
Electrode Diameter	2.54 cm (1.0 in)		
Electrode Spacing	8.9 cm (3.5 in) on center		
Shorting Wire	2 – 24 AWG (0.51 mm diameter), single strand tinned copper		
Box Electrical Configuration	Neutral		
Generator Configuration	Neutral not tied to ground		
Enclosure Breach	Yes		
Enclosure Mass Loss (g)	72		



Fig. 49. Experiment OB08 pre-experiment (left) and post-experiment (right) aluminum electrodes. Phase sequence from left-to-right is C-B-A. Note the center electrode was ejected free from the box during the experiment.



Fig. 50. Experiment OB08 enclosure breach (bottom and sides (left); rear top (right)).



Fig. 51. Experiment OB08 aluminum electrodes post-experiment (top three, bottom electrode is from another experiment and included for comparison).

SNL used a plate calorimeter to measure the incident energy during the experiment, and the approximate measurements are presented in Table 27.

Table 27. Experiment OB08 plate calorimeter measurements.

Distance from Electrode (cm)	Thickness (mm)	ΔT ($^{\circ}C$)	Measured Incident Energy (MJ/m^2)	Calculated Energy (MJ)
182.9	3	37.1	0.39	16.2

Observations and Notes

The steel enclosure was breached. The Phase B aluminum electrode was ejected from the enclosure. The Phase A and C electrodes were deflected towards the steel box sides. All aluminum electrodes broke during the experiment near the thin cross-sectional area at the rod holder. There is evidence from the thermal damage and examination of the rod top halves that arcing was occurring between the rods above the box for some time. The change in the electrical current and voltage waveform just prior to 0.6 s provided an indication of when the failure might have occurred.

The estimated mass loss from the enclosure was approximately 72 g, and a total breach opening on all sides was approximately 51 cm². (bottom opening of approximately 40 cm² and a top opening of approximately 11 cm²).

3.2.5. Experiment ID: OB10

This experiment was performed on August 22, 2019. The experiment parameters are presented in Table 28. Photos of Experiment OB10 are presented in Fig. 52 and Fig. 53.

Table 28. Experiment OB10 parameters.

Electrical Parameter	Target	Actual	Other
Voltage (V_{L-L})	1 000	1 028	381 (arc)
Current (A)	5 000	4 869	
Duration (ms)	2 000	2 010	
Energy (MJ)		4.118	
Other Parameters			
Electrode Length Loss (cm)	9.8 (Phase A)	10.0 (Phase B)	5.4 (Phase C)
Electrode Mass Loss (g)	61	60	54
Electrode Material	Aluminum		
Electrode Diameter	1.27 cm (0.5 in)		
Electrode Spacing	8.9 cm (3.5 in) on center		
Shorting Wire	2 – 24 AWG (0.51 mm diameter), single strand tinned copper		
Box Electrical Configuration	Neutral		
Generator Configuration	Neutral tied to ground via impedance		
Enclosure Breach	None		



Fig. 52. Experiment OB10 pre-experiment (left) and post-experiment (right) aluminum electrodes. Phase sequence from left-to-right is C-B-A.

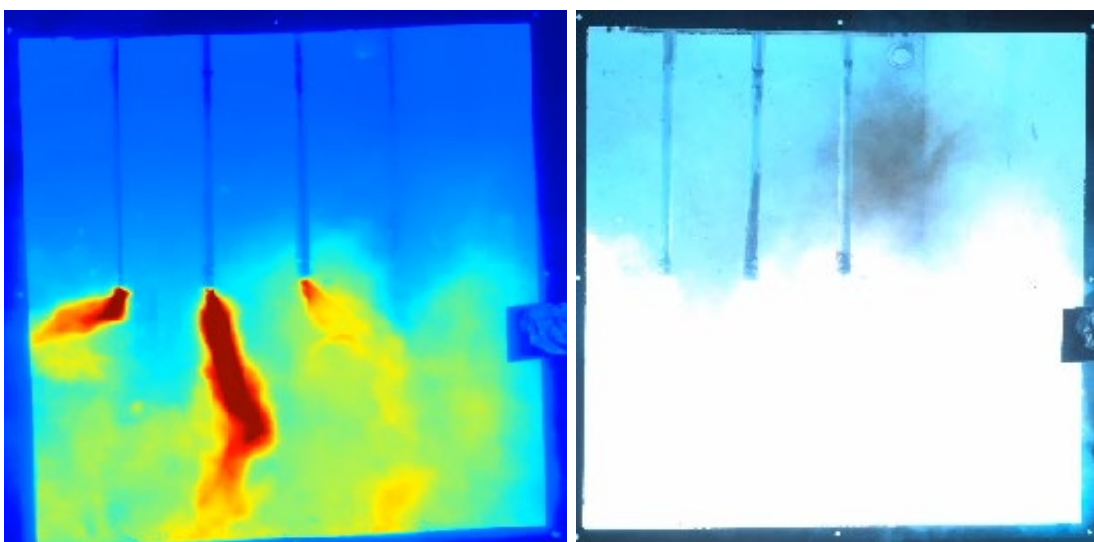


Fig. 53. Experiment OB10 thermal (left) and visible (right) video still shot during arc ($t = 0.06s$).

SNL used a plate calorimeter to measure the incident energy during the experiment, and the approximate measurements are presented in Table 29.

Table 29. Experiment OB10 plate calorimeter measurements.

Distance from Electrode (cm)	Thickness (mm)	ΔT ($^{\circ}C$)	Measured Incident Energy (MJ/m^2)	Calculated Energy (MJ)
45.7	1	423.4	1.47	3.85

Observations and Notes

The aluminum electrodes were reused from Experiment OB05. The electrodes were shifted down following Experiment OB05 to ensure the bottom of the electrodes were at the center of the box.

3.3. Summary of Low-Voltage Box Experiments

Eleven low-voltage box experiments were performed at four different current levels and durations (Table 30). The total electrical energy ranged from approximately 0.2 MJ to 20.2 MJ. Significant deflection of the electrodes was noted in the 30 kA experiments, and those results should be used with caution.

With regard to mass loss, the aluminum electrodes experienced approximately 72 % more mass loss than the copper electrodes when normalized to experiment arc energy. Given that the density of aluminum is slightly less than 1/3 that of copper (2.70 g/cm³ versus 8.96 g/cm³), aluminum electrodes lost almost twice (approximately 1.93 times) as much volume as copper for a given arc energy.

During these open box experiments, measurement devices recorded both the electrical energy (voltage and current) and calorimeter heat rise (ΔT in degrees C) of 1 mm (0.04 in) or 3 mm (0.12 in) nominally thick black copper plate calorimeters, located an approximate distance of 46 cm (18 in) or 183 cm (72 in) in front of the open boxes. To compare relative evolved energy collected on the calorimeters to electrical energy input, the equivalent radiated energy (radiated area \times real heat flux \times time) indicated by the calorimeter was calculated and compared to the actual electrical energy (in MJ).

The evolved calorimeter energy in Table 31 and Fig. 54 was calculated as described in Section 2.4.4.1. This calculation assumes 100 % absorption of incident radiation on the black copper calorimeter plates and either uniform arc radiation during the 1 s to 3 s arc duration or similar spatial radiation for the aluminum and copper arcs. Given measured ΔT values of approximately 3.6 °C to 423 °C (38.5 °F to 793 °F) and an expected thermocouple uncertainty of ± 1.2 °C (2.2 °F), the data presented in Fig. 54 shows a significant difference in radiated energy as a function of metal electrode composition.

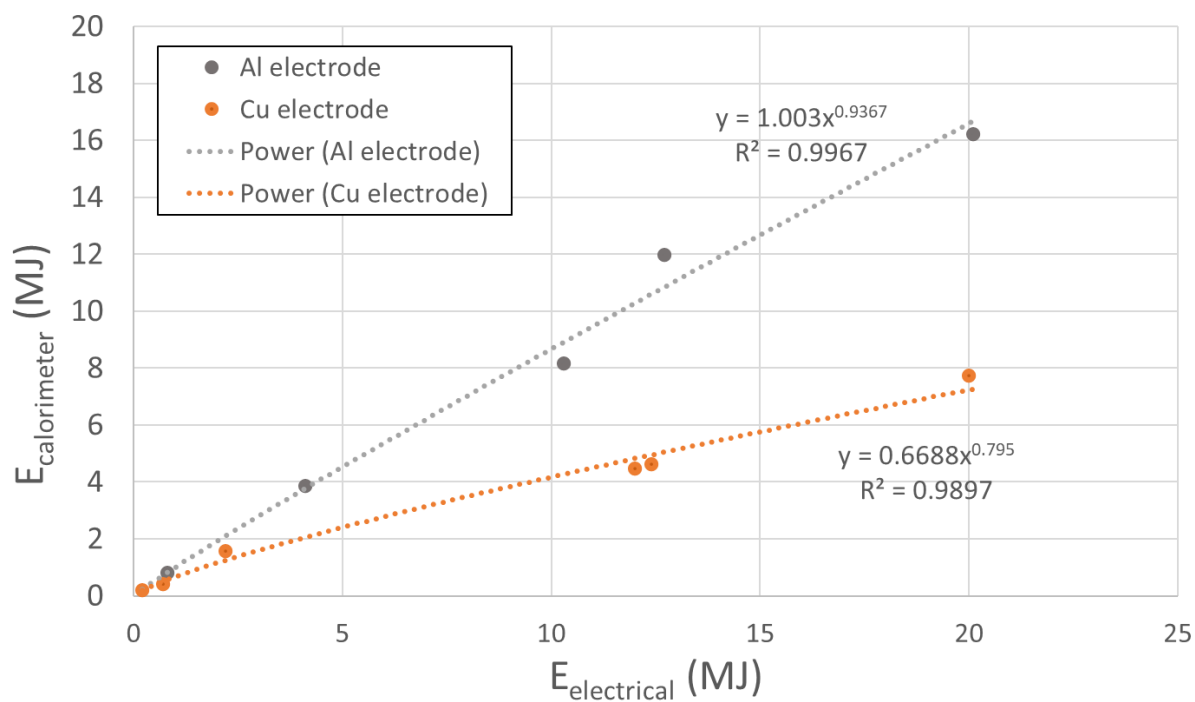


Fig. 54. Comparison of actual electrical energy input and calculated calorimeter energy with power law fits indicated by dashed lines for aluminum (Al) and copper (Cu) electrodes.

Table 30. Summary of low-voltage box experiments.

Experiment			Rod Material		Rod Diameter (cm)		System Voltage (kV)			Current (kA)		Arc Duration (s)		Energy (MJ)	Notes
#	Seq	Date	Al	Cu	1.3	2.5	Target	Actual	Arc	Target	Actual	Target	Actual	Actual	
OB01(a)	1	Aug 22		X	X		1.00	1.03	0.35	1.00	1.05	2.00	2.01	0.2	
OB01(b)	2	Aug 22		X	X		1.00	1.03	0.31	1.00	1.03	2.00	2.02	0.7	
OB02	9	Aug 30		X		X	1.00	1.01	0.27	15.00	14.02	2.00	2.02	12.0	
OB03	10	Aug 30		X		X	1.00	1.01	0.31	15.00	13.80	3.00	3.03	20.0	Duration changed from 4 seconds based on results from OB06, 07, and 02
OB04	11	Aug 30		X		X	1.00	1.06	0.28	30.00	27.79	1.00	1.03	12.4	
OB05	3	Aug 22	X		X		1.00	1.03	0.36	1.00	1.02	2.00	2.01	0.8	
OB06	6	Aug 23	X			X	1.00	1.01	0.42	15.00	11.96	2.00	2.02	12.7	
OB07	7	Aug 23	X			X	1.00	1.01	0.43	15.00	12.95	1.50	1.52	10.3	Duration changed from 4 seconds based on results from OB06
OB08	8	Aug 23	X			X	1.00	1.06	0.43	30.00	24.87	1.00	1.02	20.1	Phase 'B' electrode ejected, arcing outside box
OB09	5	Aug 22		X	X		1.00	1.03	0.30	5.00	4.79	2.00	2.01	2.2	Phase A voltage waveform not reported.
OB10	4	Aug 22	X		X		1.00	1.03	0.38	5.00	4.87	2.00	2.01	4.1	

Table 31. Low-voltage box experiment comparison of measured electrical energy and calculated energy from calorimeter heat rise.

Experiment			Rod Material		Electrical Energy	Plate Calorimeter Calculated Energy	Plate Calorimeter Thickness	Distance	Plate calorimeter ΔT
#	Seq	Date	Al	Cu	(MJ)	(MJ)	(mm)	(cm)	(°C)
OB01(a)	1	Aug 22		X	0.2	0.197	1	46	21.6
OB01(b)	2	Aug 22		X	0.7	0.410	1	46	45.1
OB02	9	Aug 30		X	12.0	4.456	3	183	10.2
OB03	10	Aug 30		X	20.0	7.733	3	183	17.7
OB04	11	Aug 30		X	12.4	4.631	3	183	10.6
OB05	3	Aug 22	X		0.8	0.807	1	46	88.7
OB06	6	Aug 23	X		12.7	11.970	3	183	27.4
OB07	7	Aug 23	X		10.3	8.170	3	183	18.7
OB08	8	Aug 23	X		20.1	16.208	3	183	37.1
OB09	5	Aug 22		X	2.2	1.573	3	183	3.6
OB10	4	Aug 22	X		4.1	3.854	1	46	423.4

4. Medium-Voltage Experiment Results

KEMA performed calibration runs to ensure that the power circuits selected met the experimental program needs. The calibrations were measured at a shorting bus within the laboratory's facility, and the actual experiment conditions were slightly different because of the additional circuit length to the open box and that of the open box. The resulting calibration experiments are presented in Table 32 with detail provided in the KEMA experiment report (Appendix C).

Table 32. Medium-voltage circuit calibration.

Voltage (V)	Symmetrical Current (kA)	Current Peak (kA)	Circuit
6 900	15.3	42.9	190916-9002
6 900	30.6	86.5	190916-9004

The calibration experiments were performed for about 10 cycles to ensure stabilization of the waveform. The duration of the arc during the actual experiments was determined by the ability to maintain the arc within the enclosure and the breaking of the circuit by the laboratory's protective device(s). Provided that the arc did not prematurely extinguish prior to the desired arc time, the laboratory ensured that the arc duration parameter was met by automatically triggering their protective devices to open at the specified duration. Because there was a delay in the opening of the circuit (breaker opening time), the actual durations were longer than the desired durations. Table 33 present the experimental parameter variations planned for this series of experiments.

Table 33. Medium-voltage experiments planned nominal parameters.

Experiment #	Rod Material		Bus size (cm)		System Voltage (kV)	Current (kA)	Duration (s)
	Al	Cu	7.6	10.2			
OBMV1	X			X	6.9	15.0	2
OBMV2	X			X	6.9	30.0	1
OBMV3	X			X	6.9	15.0	5
OBMV4		X	X		6.9	15.0	5
OBMV5		X	X		6.9	30.0	2

The following provides a quick summary of the experimental configuration and results for each medium-voltage open box experiment. The opportunity arose to perform medium-voltage open box experiments because the medium-voltage bus duct experiments were not performed. The final experiment configurations were based on the availability of materials (enclosure and bus bars), and the parameters were chosen to allow for comparison between medium-voltage experiments and between medium-voltage and low-voltage experiments.

Changes to the open box experimental durations were made based on observations and model predictions.

For each experiment, the following information is provided:

- Experiment specifications
- Electrode length and mass
- Photo of pre- and post-experiment configuration
- Photo of enclosure breach (if applicable)
- Photo of bus bars post-experiment
- Voltage and current profile
- SNL Measurements (if applicable)
- Notes
- Observations

A summary of the medium-voltage box experiments is presented at the end of this section (Table 46).

4.1. Medium-Voltage Experiment Results with Copper Electrodes

Two experiments were performed at medium-voltage in the box configuration with copper electrodes. These were Experiments OBMV04 and OBMV05. The results from these experiments are presented next.

4.1.1. Experiment ID: OBMV04

This experiment was performed on September 17, 2019. The experiment parameters are presented in Table 34. Photos of Experiment OBMV04 are presented in Fig. 55 through Fig. 57.

Table 34. Experiment OBMV04 parameters.

Electrical Parameter	Target	Actual	Other
Voltage (V _{L-L})	6 900	6 915	543 (arc)
Current (A)	15 000	14 330	
Duration (ms)	5 000	5 080	
Energy (MJ)		51.8	
Other Parameters			
Electrode Length Loss (cm)	12.4 (Phase A)	12.1 Phase B)	12.1 (Phase C)
Electrode Mass Loss (g)	1 066.0	1 104.0	1 082.0
Electrode Material	Copper		
Electrode Dimensions	1.27 cm (0.5 in) x 7.6 cm (3.0 in)		
Electrode Spacing	13 cm (5 in) on center		
Shorting Wire	2 – 24 AWG (0.51 mm diameter), single strand tinned copper		
Box Electrical Configuration	Neutral		
Generator Configuration	Neutral tied to ground via impedance		
Enclosure Breach	Sides, bottom, back		
Additional Cladding	Back	Sides	Bottom
Add. Cladding Thickness (cm)	0.29	0.18	0.18
Enclosure Mass Loss (g)		12 444	



Fig. 55. Experiment OBMV04 pre-experiment (left) and post-experiment (right) copper electrodes. Phase sequence from left to right is C-B-A.



Fig. 56. Experiment OBMV04 enclosure breach (Left-to-right: Right side, back side, left side).

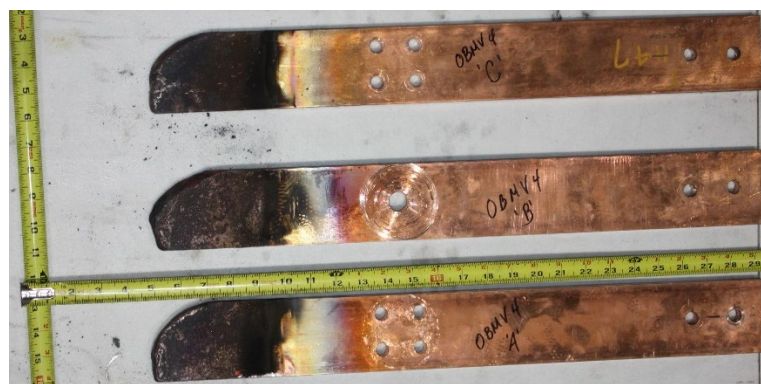


Fig. 57. Experiment OBMV04 copper electrode remanence post-experiment.

A combination of thermal measurement devices including a plate thermometer, ASTM Slug Calorimeters, and thermal capacitance slugs (T_{cap}) were used in this experiment as described in Section 2.4.7. The approximate measured data is presented in Table 35.

Table 35. Experiment OBMV04 thermal measurements.

Location	Instrument (ID)	Max Heat Flux (kW/m²) ± 1 kW/m² or ± 5%	Average Heat Flux During Arc (kW/m²) ± 1 kW/m² or ± 5%
Vertical	Plate Thermometer (2)	1 627	478
Location	Instrument (ID)	Total Incident Energy (kJ/m²) ± 2.4 kJ/m² or ± 5%	Average Heat Flux During Arc (kW/m²) ± 1.5 kW/m² or ± 2.9%
Vertical	T_{cap} (1)	1 926	255
Horizontal	T_{cap} (3)	4 569	346
Horizontal	T_{cap} (4)	5 850	296
Location	Instrument (ID)	Total Incident Energy (kJ/m²) ± 18 kJ/m² or ± 4%	Time to Max Temperature (s) ± 3%
Vertical	ASTM (A)	1 137	6
Horizontal	ASTM (B)	2 575	8

Breakdown experiments: Prior to the HEAF, median breakdown voltage was approximately 14 kV, resulting in a breakdown field of approximately 28 kV/cm consistent with typical air breakdown strength of 25 kV/cm to 30 kV/cm. The breakdown voltage was also measured during the 5 s HEAF and was observed to decrease to approximately 12.3 kV, or approximately 24 kV/cm with subsequent breakdowns occurring as low as approximately 6.3 kV to 10 kV (12.6 kV/cm to 20 kV/cm). Again, this reduced holdoff strength appears real but does not approach typical bus bar design electrical fields of 0.7 kV/cm to 1 kV/cm and would not be expected to result in propagating breakdown into nearby switchgear at these dielectric holdoff values.

Air conductivity measurements were taken during this experiment. A significant change in air conductance were observed at approximately 4.27 m (14 ft) from the open box during the HEAF experiment. Air conductance values in the range of approximately 1.6×10^{-5} S to 9×10^{-5} S were recorded; for the 0.5 cm (0.2 in) gap and 3.2 cm (1.25 in) radius sensor. This resulted in a conductivity of approximately 0.16 μ S/cm to 9 μ S/cm or 0.016 mS/m to 0.09 mS/m, similar to the conductivity of deionized water.

No EMI fields were detected above the ambient interference level trigger from this arc fault.

Observations and Notes

The estimated mass loss from the enclosure was approximately 12 444 g, and a total breach opening on all sides was approximately 2 796 cm² (bottom opening of approximately 1 224 cm², left side approximately 946 cm², and right side approximately 626 cm²).

Burn through was observed on both sides and bottom through all layers of cladding. The back side only had the internal cladding consumed.

4.1.2. Experiment ID: OBMV05

This experiment was performed on September 16, 2019. The experimental parameters are presented in Table 36. Photos of Experiment OBMV05 are presented in Fig. 58 and Fig. 59.

Table 36. Experiment OBMV05 parameters.

Electrical Parameter	Target	Actual	Other	
Voltage (V _{L-L})	6 900	6 917	405 (arc)	
Current (A)	30 000	28 642		
Duration (ms)	2 000	2 320		
Energy (MJ)		43.5		
Other Parameters				
Electrode Length Loss (cm)	13.0 (Phase A)	12.7 (Phase B)	12.1 (Phase C)	
Electrode Mass Loss (g)	1 009.5	1 142.0	1 064.0	
Electrode Material	Copper			
Electrode Diameter	1.27 cm (0.5 in) x 7.6 cm (3.0 in)			
Electrode Spacing	13 cm (5 in) on center			
Shorting Wire	2 – 24 AWG (0.51 mm diameter), single strand tinned copper			
Box Electrical Configuration	Neutral			
Generator Configuration	Neutral tied to ground via impedance			
Enclosure Breach	Side and top			
Additional Cladding	Back	Left	Right	Bottom
Add. Cladding Thickness (cm)	0.29	0.18	0.29	0.18
Enclosure Mass Loss (g)	5 666			



Fig. 58. Experiment OBMV05 pre-experiment (top) and post-experiment (bottom, left-to-right, left side from outside, front, right side from outside). Phase sequence from left to right is C-B-A.

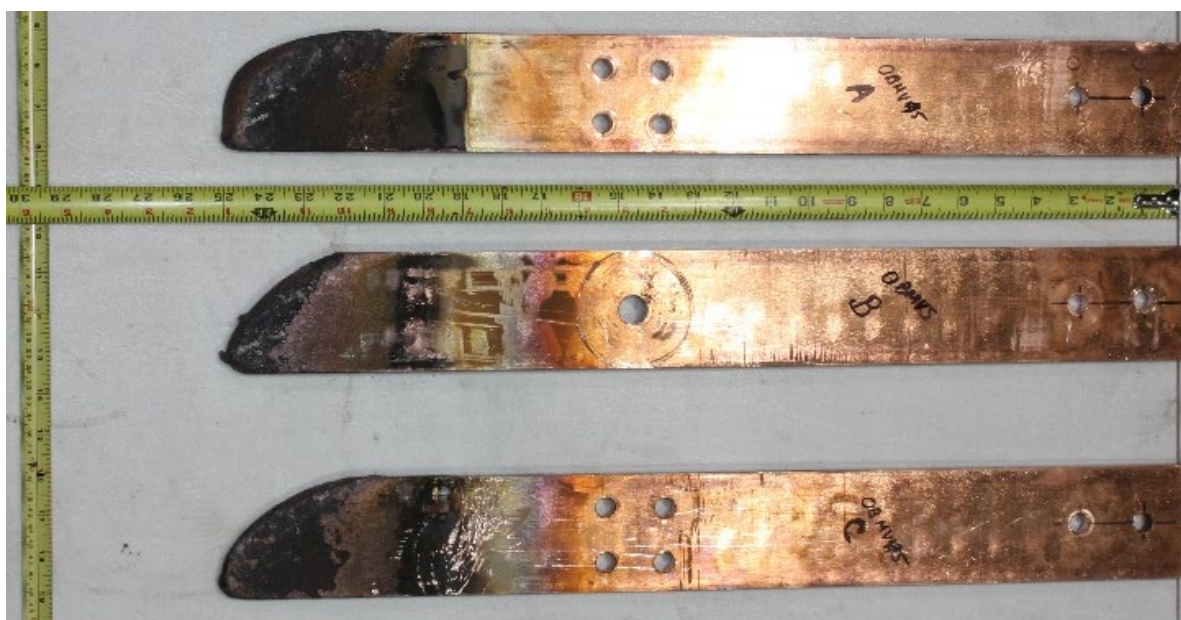


Fig. 59. Experiment OBMV05 copper electrodes post-experiment.

A combination of thermal measurement devices including a plate thermometer, ASTM Slug Calorimeters, and thermal capacitance slugs (T_{cap}) were used in this experiment as described in Section 2.4.7. The approximate measured data is presented in Table 37.

Table 37. Experiment OBMV05 thermal measurements.

Location	Instrument (ID)	Max Heat Flux (kW/m ²) ± 1 kW/m ² or ± 5%	Average Heat Flux During Arc (kW/m ²) ± 1 kW/m ² or ± 5%
Vertical	Plate Thermometer (2)	3 636	1 486
Location	Instrument (ID)	Total Incident Energy (kJ/m ²) ± 2.4 kJ/m ² or ± 5%	Average Heat Flux During Arc (kW/m ²) ± 1.5 kW/m ² or ± 2.9%
Vertical	T_{cap} (1)	2 816	723
Horizontal	T_{cap} (3)	1 215	97
Horizontal	T_{cap} (4)	1 161	74
Location	Instrument (ID)	Total Energy (kJ/m ²) ±18 kJ/m ² or ± 4%	Time (s) to Max Temperature ± 3%
Vertical	ASTM (A)	1 974	4
Horizontal	ASTM (B)	602	34

Breakdown Testing: Prior to the HEAF, the median breakdown voltage was approximately 13.1 kV, resulting in a breakdown field of approximately 26 kV/cm consistent with typical air breakdown strength of 25 kV/cm to 30 kV/cm. Breakdown voltage was also measured during the 2 s, 30 kA HEAF and was observed to decrease to as low as approximately 3.5 kV to 6.5 kV (8 kV/cm to 13 kV/cm) for 3 s, before recovering to greater than approximately 10 kV. Again, this significantly reduced holdoff strength appears real but did not approach typical bus bar design electrical fields of approximately 0.7 kV/cm to 1 kV/cm and would not be expected to result in propagating breakdown into nearby switchgear at these dielectric holdoff values.

Air conductivity measurements: During this large arc fault, large changes in air conductance were observed over the first second of the HEAF. Air conductance values as low as approximately 3.6×10^{-3} S were recorded for the 0.5 cm (0.2 in) gap and 3.2 cm (1.25 in) radius sensor. This resulted in a conductivity of approximately 115 μ S/cm or 0.011 S/m, similar to the conductivity of drinking water.

Ultimately damage (melting of the aluminum electrodes) occurred to the pie pan sensor, which was approximately 1.8 m (6.0 ft) from the front of the open box. Subsequent air

conductivity experiments were conducted at approximately 3.0 m (10.0 ft) and 4.3 m (14 ft) distances using duplicate devices.

EMI measurements: No EMI fields were detected above the ambient interference level trigger from this arc fault.

Observations and Notes

The steel enclosure breached on both sides and at the top around the bar mounting block. The bottom was not breached but was deflected approximately 9.4 cm (3.7 in) at center of the front face opening.

The estimated mass loss from the enclosure was approximately 5 666 g, and a total breach opening on all sides of approximately 711 cm² (bottom opening of approximately 13 cm², left side approximately 351 cm², right side approximately 98 cm², and a top opening of approximately 249 cm²).

4.2. Medium-Voltage Experiment Results with Aluminum Electrodes

Four experiments were performed at medium-voltage in the box configuration with aluminum electrodes. These were Experiments OBMV01 through OBMV03 and OBMV06. The results from these experiments are presented next.

4.2.1. Experiment ID: OBMV01

This experiment was performed on September 18, 2019. The experiment parameters are presented in Table 38. Photos of Experiment OBMV01 are presented in Fig. 60 and Fig. 61.

Table 38. Experiment OBMV01 parameters.

Electrical Parameter	Target	Actual	Other
Voltage (V_{L-L})	6 900	6 914	543 (arc)
Current (A)	15 000	14 280	
Duration (ms)	2 000	3 180	
Energy (MJ)		37.5	
Other Parameters			
Electrode Length Loss (cm)	10.8 (Phase A)	12.1 (Phase B)	10.5 (Phase C)
Electrode Mass Loss (g)	412.5	477.0	434.0
Electrode Material	Aluminum		
Electrode Dimensions	10.2 cm (4.0 in) x 1.27 cm (0.5 in)		
Electrode Spacing	13 cm (5 in) on center		
Shorting Wire	2 – 24 AWG (0.51 mm diameter), single strand tinned copper		
Box Electrical Configuration	Neutral		
Generator Configuration	Neutral tied to ground via impedance		
Enclosure Breach	Excessive		
Additional Cladding	None		
Enclosure Mass Loss (g)	10 168		



Fig. 60. Experiment OBMV01 pre-experiment (top) and post-experiment (left side (bottom left), back (bottom center), right side (bottom right)). Phase sequence from left to right is C-B-A.



Fig. 61. Experiment OBMV01 aluminum electrode post-experiment.

A combination of thermal measurement devices including a plate thermometer, ASTM Slug Calorimeters, and thermal capacitance slugs (T_{cap}) were used in this experiment as described in Section 2.4.7. The approximate measured data is presented in Table 39.

Table 39. Experiment OBMV01 thermal measurements

Location	Instrument (ID)	Max Heat Flux (kW/m²) ± 1 kW/m² or ± 5%	Average Heat Flux During Arc (kW/m²) ± 1 kW/m² or ± 5%	Notes
Vertical	Plate Thermometer (2)	414	250	
Location	Instrument (ID)	Total Incident Energy (kJ/m²) ± 2.4 kJ/m² or ± 5%	Average Heat Flux During Arc (kW/m²) ± 1.5 kW/m² or ± 2.9%	Notes
Vertical	T_{cap} (1)	1 038	160	
Horizontal	T_{cap} (3)	7 000	1 357	
Horizontal	T_{cap} (4)	5 500	936	
Location	Instrument (ID)	Total Energy (kJ/m²) ± 18 kJ/m² or ± 4%	Time (s) to Max Temperature ± 3%	Notes
Vertical	ASTM (A)	749	6	
Horizontal	ASTM (B)	No Data	No Data	Exposure exceeded device range

Air breakdown experiments were not conducted during experiment OBMV01.

During this arc fault experiment, changes in air conductance were observed at approximately 4.27 m (14 ft) distance from open box. A minimum air conductance value of approximately 1.15×10^{-4} S and several events of approximately 1.6×10^{-5} S were recorded with an uncertainty of 9×10^{-6} S for the 0.5 mm (0.02 in) gap and 3.2 cm (1.25 in) radius sensor. This resulted in a maximum conductivity of approximately 1 μ S/cm or 0.1 mS/m, similar to the conductivity of drinking water. Results from this test are presented in Fig. 62.

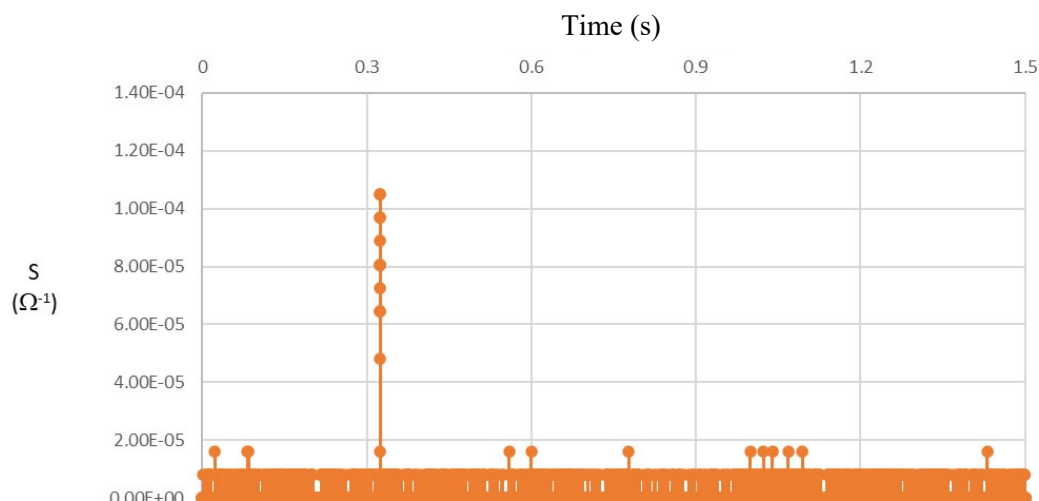


Fig. 62. Air conductivity measurement during OBMV01.

No EMI fields were detected above the ambient interference level trigger from this arc fault.

Observations and Notes

The laboratories timer experienced a failure, and the experiment lasted for 3 180 ms versus the planned 2 000 ms. This resulted in an experiment that was 59 % longer than planned. As such more of the enclosure was consumed than estimated during the experiment planning phase which supported the use of a single clad box. The additional duration resulted in little of the box remaining after the experiment and limited the usability of the results to evaluate enclosure burn through. However, conductor material loss and all other instrumentation worked as planned and provided usable data. Additional measures were taken by the laboratory to ensure that the timer failure did not occur in subsequent experiments. The experiment was repeated as OBMV06.

4.2.2. Experiment ID: OBMV02

This experiment was performed on September 17, 2019. The experiment parameters are presented in Table 40. Photos of experiment OBMV02 are presented in Fig. 63 through Fig. 65.

Table 40. Experiment OBMV02 parameters.

Electrical Parameter	Target	Actual	Other
Voltage (V_{L-L})	6 900	6 915	468 (arc)
Current (A)	30 000	29 143	
Duration (ms)	1 000	1 120	
Energy (MJ)		21.42	
Electrode Length Loss (cm)	5.7 (Phase A)	5.7 (Phase B)	7.0 (Phase C)
Electrode Mass Loss (g)	319.5	333.5	291.5
Other Parameters			
Electrode Material	Aluminum		
Electrode Dimensions	10.2 cm (4.0 in) x 1.27 cm (0.5 in)		
Electrode Spacing	13 cm (5 in) on center		
Shorting Wire	2 – 24 AWG (0.51 mm diameter), single strand tinned copper		
Box Electrical Configuration	Neutral		
Generator Configuration	Neutral tied to ground via impedance		
Enclosure Breach	No		
Additional Cladding	Back	Sides	Bottom
Add. Cladding Thickness (cm)	0.18	0.18	0.18
Enclosure Mass Loss (g)	982 (cladding only)		



Fig. 63. Experiment OBMV02 pre-experiment (left) and post-experiment (right) aluminum electrodes. Phase sequence from left to right is C-B-A.



Fig. 64. Experiment OBMV2 enclosure breach (Left-to-right: left side, bottom side, right side).



Fig. 65. Experiment OBMV02 aluminum electrodes post-experiment.

A combination of thermal measurement devices including a plate thermometer, ASTM Slug Calorimeters, and thermal capacitance slugs (T_{cap}) were used in this experiment as described in Section 2.4.7. The approximate measured data is presented in Table 41.

Table 41. Experiment OBMV02 thermal measurements.

Location	Instrument (ID)	Max Heat Flux (kW/m ²) ± 1 kW/m ² or ± 5%	Average Heat Flux During Arc (kW/m ²) ± 1 kW/m ² or ± 5%	Notes
Vertical	Plate Thermometer (2)	3 817	1 835	
Location	Instrument (ID)	Total Incident Energy (kJ/m ²) ± 2.4 kJ/m ² or ± 5%	Average Heat Flux During Arc (kW/m ²) ± 1.5 kW/m ² or ± 2.9%	Notes
Vertical	T_{cap} (1)	2 182	1 477	
Horizontal	T_{cap} (3)	532	286	
Horizontal	T_{cap} (4)	531	317	
Location	Instrument (ID)	Total Incident Energy (kJ/m ²) ± 18 kJ/m ² or ± 4%	Time (s) to Max Temperature ± 3%	Notes
Vertical	ASTM (A)	2 149	2	
Horizontal	ASTM (B)	No Data	No Data	Sensor non-functional

High-voltage breakdown experiments were conducted prior to and during the arc fault experiment. Prior to the HEAF experiment, median breakdown voltage was measured at approximately 15.1 kV and shown in Fig. 66, consistent with typical, air breakdown strength of approximately 25 kV/cm to 30 kV/cm. Breakdown voltage was measured during the HEAF and was observed to decrease to approximately 11.6 kV or approximately 23 kV/cm as shown in Fig. 67. This decrease, while notable, does not approach typical bus bar electrical fields of approximately 0.7 kV/cm to 1 kV/cm and would not be expected to result in propagating breakdown into nearby switchgear at these dielectric holdoff values.

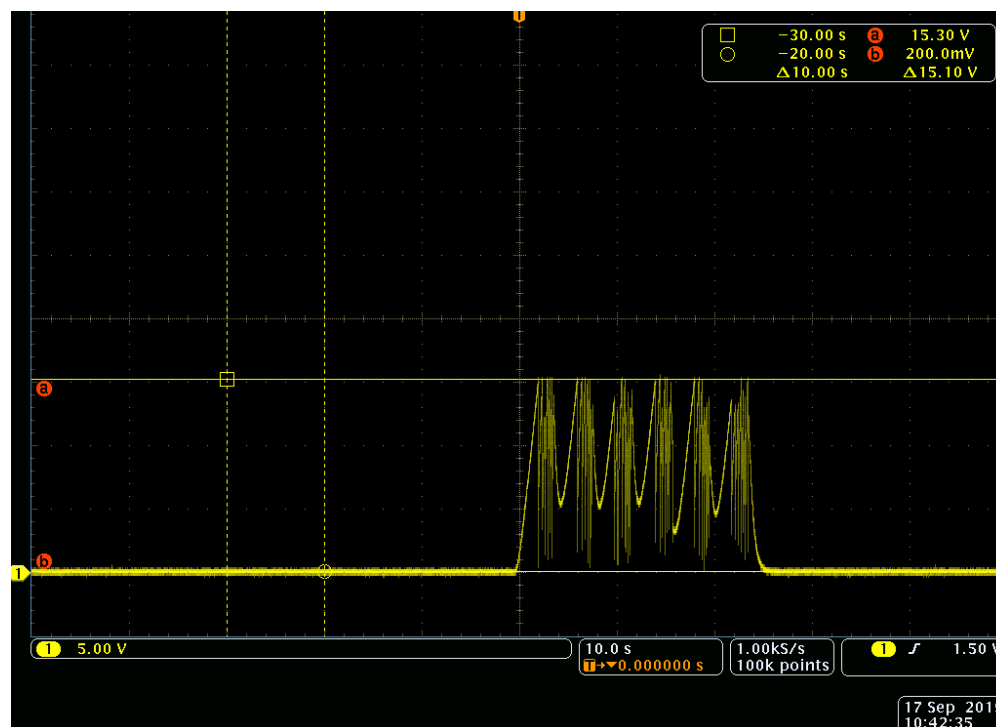


Fig. 66. Breakdown experiment prior to Experiment OBMV02.

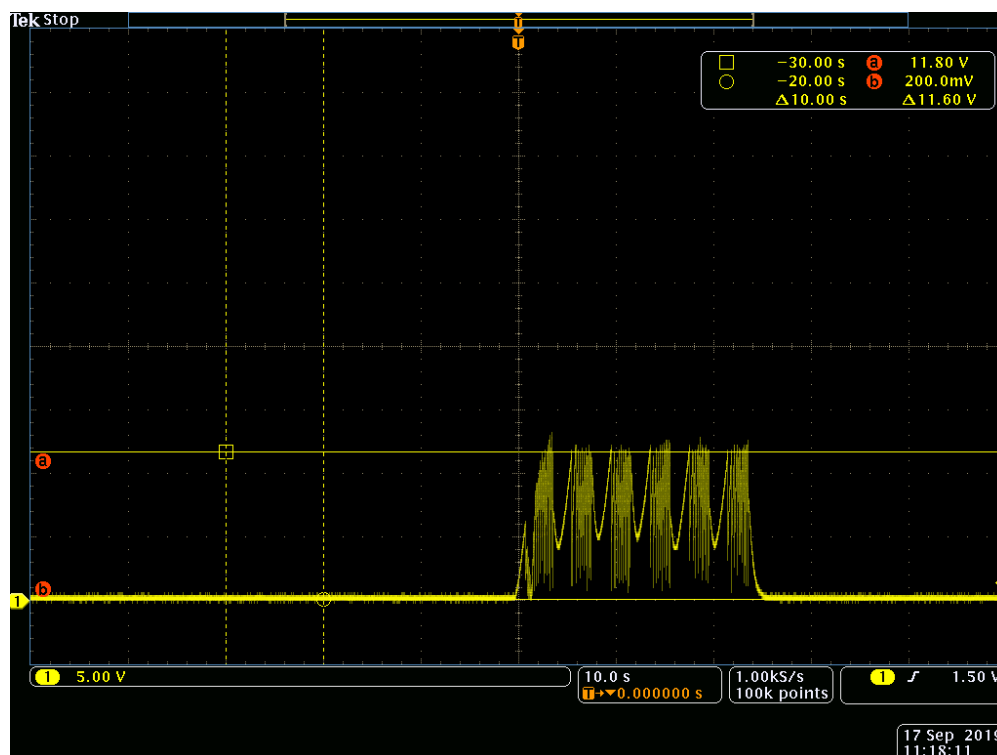


Fig. 67. Breakdown experiment during Experiment OBMV02.

During this arc fault experiment, changes in air conductance were observed at approximately 3 m (10 ft) from the open box. Air conductance values as low as approximately 6×10^{-4} S were recorded with an uncertainty of 9×10^{-9} S for the 0.5mm (0.02 in) gap and 3.2 cm (1.25 in) radius sensor. These results are presented in Fig. 68 and represent a conductivity of approximately 6 μ S/cm or 0.6 mS/m, similar to the conductivity of drinking water.

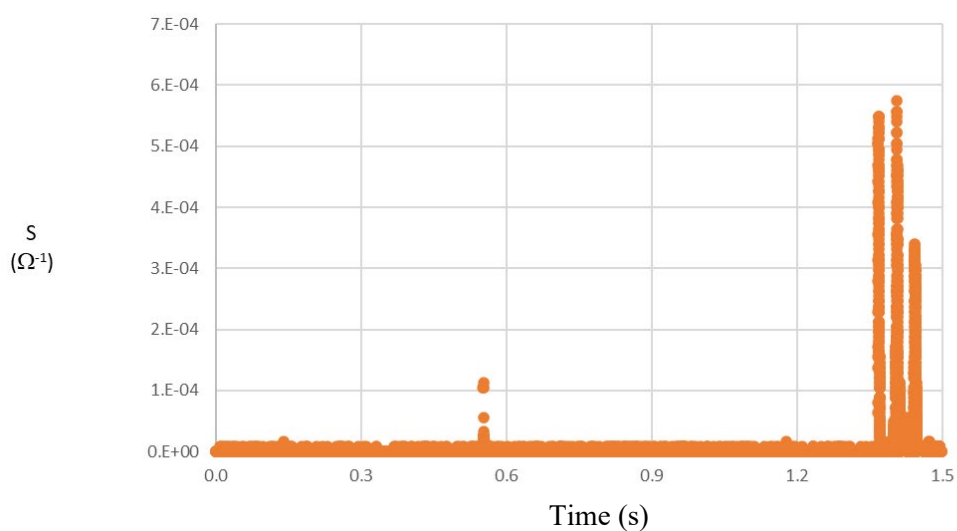


Fig. 68. Air conductance measurements during experiment OBMV02.

No EMI fields were detected above the ambient interference level trigger from this arc fault.

Observations and Notes

There was no breach of the outer layer of the box enclosure, only a breach in the inner cladding. The estimated mass loss from the enclosure internal cladding was approximately 982.2 g, and a total breach opening on all sides of approximately 699 cm² (bottom opening of approximately 71 cm², left side approximately 334 cm², and right side approximately 294 cm²).

4.2.3. Experiment ID: OBMV03

This experiment was performed on September 18, 2019. The experimental parameters are presented in Table 42. Photos of Experiment OBMV03 are presented in Fig. 69 through Fig. 71.

Table 42. Experiment OBMV03 parameters.

Electrical Parameter	Target	Actual	Other	
Voltage (V _{L-L})	6 900	6 918	475 (arc)	
Current (A)	15 000	14 370		
Duration (ms)	5 000	5 050		
Energy (MJ)		55.7		
Electrode Length Loss (cm)	21.6 (Phase A)	22.2 Phase B)	22.2 (Phase C)	
Electrode Mass Loss (g)	765.5	779.5	751.0	
Other Parameters				
Electrode Material	Aluminum			
Electrode Dimensions	10.2 cm (4.0 in) x 1.27 cm (0.5 in)			
Electrode Spacing	13 cm (5 in) on center			
Shorting Wire	2 – 24 AWG (0.51 mm diameter), single strand tinned copper			
Box Electrical Configuration	Neutral			
Generator Configuration	Neutral tied to ground via impedance			
Enclosure Breach	Bottom, Sides, Top, Back (partial)			
Additional Cladding	Back	Left	Right	Bottom
Add. Cladding Thickness (cm)	0.29	0.18	0.29	0.18
Enclosure Mass Loss (g)	17483			



Fig. 69. Experiment OBMV03 pre-experiment (left) and post-experiment (right) aluminum electrodes. Phase sequence from left to right is C-B-A.



Fig. 70. Experiment OBMV03 enclosure breach (left-to-right: Left side, back side, right side, top).



Fig. 71. Experiment OBMV03 aluminum electrode post-experiment.

A combination of thermal measurement devices including a plate thermometer, ASTM Slug Calorimeters, and thermal capacitance slugs (T_{cap}) were used in this experiment as described in Section 2.4.7. The approximate measured data is presented in Table 43.

Table 43. Experiment OBMV03 thermal measurements.

Location	Instrument (ID)	Max Heat Flux (kW/m ²) ± 1 kW/m ² or ± 5%	Average Heat Flux During Arc (kW/m ²) ± 1 kW/m ² or ± 5%	Notes
Vertical	Plate Thermometer (2)	716	369	
Location	Instrument (ID)	Total Incident Energy (kJ/m ²) ± 2.4 kJ/m ² or ± 5%	Average Heat Flux During Arc (kW/m ²) ± 1.5 kW/m ² or ± 2.9%	Notes
Vertical	T _{cap} (1)	2 327	351	
Horizontal	T _{cap} (3)	8 385	1 032	
Horizontal	T _{cap} (4)	12 441	965	
Location	Instrument (ID)	Total Incident Energy (kJ/m ²) ± 18 kJ/m ² or ± 4%	Time (s) to Max Temperature ± 3%	Notes
Vertical	ASTM (A)	1 457	9	
Horizontal	ASTM (B)	No Data	No Data	Exposure exceeded device range

Prior to the HEAF, the median breakdown voltage was approximately 15 kV, consistent with typical air breakdown strength of approximately 25 kV/cm to 30 kV/cm. Breakdown voltage was also measured during the HEAF experiment and was observed to decrease to as low as approximately 8.3 kV or approximately 16 kV/cm. Again, this decrease does not approach typical bus bar design electrical fields of approximately 0.7 kV/cm to 1 kV/cm and would not be expected to result in propagating breakdown into nearby switchgear at these dielectric holdoff values.

Air conductance values in the range of approximately 0.8×10^{-4} S to 6×10^{-4} S were recorded for the 0.5 mm (0.02 in) gap and 3.2 cm (1.25 in) radius sensor. This resulted in a conductivity of approximately 0.8 μ S/cm to 6 μ S/cm or 0.6 mS/m, similar to the conductivity of drinking water. The results from this test are presented in Fig. 72.

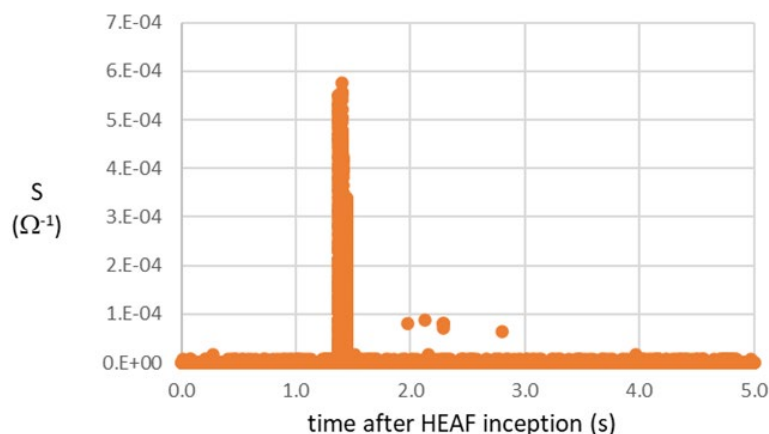


Fig. 72. Experiment OBMV03 air conductance measurement.

Observations and Notes

The box burned through all sides except the back. The bottom of the box was completely consumed with large holes on both sides. The top behind the GPO3 insulative red board also experienced burn through.

The estimated mass loss from the enclosure was approximately 17 483 g, and a total breach opening on all sides of approximately 4 183 cm² (bottom was completely gone approximately 2 080 cm², left side approximately 1 309 cm², right side approximately 684 cm² and top openings of approximately 112 cm²).

4.2.4. Experiment ID: OBMV06

This experiment was performed on September 18, 2019. The experiment parameters are presented in Table 44. Photos of Experiment OBMV06 are presented in Fig. 73 through Fig. 75.

Table 44. Experiment OBMV06 parameters.

Electrical Parameter	Target	Actual	Other
Voltage (V_{L-L})	6 900	6 913	493 (arc)
Current (A)	15 000	14 596	
Duration (ms)	2 000	2 050	
Energy (MJ)		22.72	
Other Parameters			
Electrode Length Loss (cm)	8.6 (Phase A)	8.9 (Phase B)	7.6 (Phase C)
Electrode Mass Loss (g)	252.0	252.0	223.0
Electrode Material	Aluminum		
Electrode Dimensions	7.6 cm (3.0 in) x 1.27 cm (0.5 in)		
Electrode Spacing	13 cm (5 in) on center		
Shorting Wire	2 – 24 AWG (0.51 mm diameter), single strand tinned copper		
Box Electrical Configuration	Neutral		
Generator Configuration	Neutral tied to ground via impedance		
Enclosure Breach	Bottom, sides, and back		
Additional Cladding	None		
Enclosure Mass Loss (g)	5 763		



Fig. 73. Experiment OBMV06 pre-experiment (left) and post-experiment (right) aluminum electrodes. Phase sequence from left to right is C-B-A.



Fig. 74. Experiment OBMV6 enclosure breach (Left-to-right: left side, back side, bottom side, and right side).

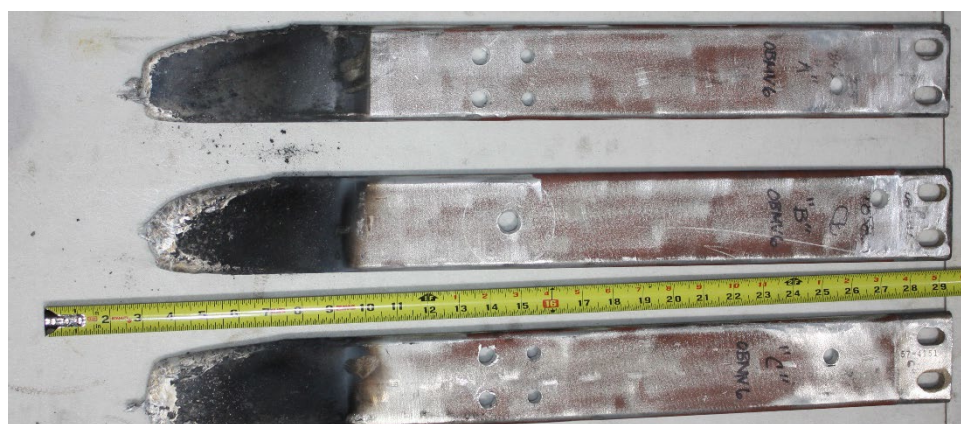


Fig. 75. Experiment OBMV06 aluminum electrodes post-experiment.

A combination of thermal measurement devices including a plate thermometer, ASTM Slug Calorimeters, and thermal capacitance slugs (T_{cap}) were used in this experiment as described in Section 2.4.7. The approximate measured data is presented in Table 45.

Table 45. Experiment OBMV06 thermal measurements.

Location	Instrument (ID)	Max Heat Flux (kW/m ²) ± 1 kW/m ² or ± 5%	Average Heat Flux During Arc (kW/m ²) ± 1 kW/m ² or ± 5%	Notes
Vertical	Plate Thermometer (2)	445	236	
Location	Instrument (ID)	Total Incident Energy (kJ/m ²) ± 2.4 kJ/m ² or ± 5%	Average Heat Flux During Arc (kW/m ²) ± 1.5 kW/m ² or ± 2.9%	Notes
Vertical	T_{cap} (1)	649	166	
Horizontal	T_{cap} (3)	2 893	849	
Horizontal	T_{cap} (4)	3 805	820	
Location	Instrument (ID)	Total Incident Energy (kJ/m ²) ± 18 kJ/m ² or ± 4%	Time (s) to Max Temperature ± 3%	Notes
Vertical	ASTM (A)	471	8	
Horizontal	ASTM (B)	2 157	4	

High-voltage breakdown experiments were conducted prior to and during the OBMV06 experiment. Prior to the HEAF, median breakdown voltage was approximately 14.3 kV, consistent with typical air breakdown strength of approximately 25 kV/cm to 30 kV/cm. Breakdown voltage was also measured during the HEAF and was observed to decrease to as low as approximately 11 kV or approximately 22 kV/cm. This decrease does not approach typical bus bar electrical fields of approximately 0.7 kV/cm to 1 kV/cm and would not be expected to result in propagating breakdown into nearby switchgear at these dielectric holdoff values.

Air conductance experiments resulted in levels below minimum experiments resolution (conductance less than 1×10^{-6} S).

Observations and Notes

The box sides were single clad. Due to the failure in Experiment OBMV01 and the experiment schedule, the nominal 10 cm (4 in) by 1.3 cm (0.5 in) aluminum bus bar electrodes used in OBMV01 through OBMV03 were not available. The options were to use

two nominal 10 cm (4 in) by 0.6 cm (0.25 in) bars per phase or 7.6 cm (3 in) by 1.3 cm (0.5 in) bars. The latter was selected to ensure homogeneity of the electrode and to eliminate variations that the double bus bar per phase might have introduced.

4.3. Summary of Medium-Voltage Open Box Experiments

Six medium-voltage box experiments were performed at two different current levels and 3 different durations. The total arc energy among the experiments ranged from approximately 22 MJ to 59 MJ. The experiment results are summarized below in Table 46. A summary of the total incident energy measured by the slug calorimeters (copper and tungsten) are presented in Table 47.

Table 46. Summary of medium-voltage open box experiment results.

Experiment	Rod Material		Nominal Bar Diameter (cm)		System Voltage (kV) $\pm 3\%$			Current (kA) $\pm 3\%$		Arc Duration (s) $\pm 3\%$		Energy (MJ) $\pm 3\%$	Notes
#	Al	Cu	7.6	10.0	Target	Actual	Arc	Target	Actual	Target	Actual	Actual	
OBMV1	X			X	6.9	6.9	0.314	15	14.3	2.00	3.18	37.5	Lab timer failure. Experiment repeated as OBMV06
OBMV2	X			X	6.9	6.9	0.270	30	29.1	1.00	1.12	21.4	
OBMV3	X			X	6.9	6.9	0.274	15	14.4	5.00	5.05	55.7	
OBMV4		X	X		6.9	6.9	0.264	15	14.3	5.00	5.08	51.8	
OBMV5		X	X		6.9	6.9	0.234	30	28.6	2.00	2.32	43.5	
OBMV6	X		X		6.9	6.9	0.285	15	14.6	2.00	2.05	22.7	

Table 47. Medium-voltage box experiment summary of thermal measurements.

Experiment #	Rod Material		Electrical Energy $\pm 3\%$	Array	Distance (m)	ASTM (Copper) Slug	T _{cap} (Tungsten) Slug
	Al	Cu	(MJ)			Max. Total Incident Energy (MJ/m ²) ± 0.018 MJ/m ² or $\pm 4\%$	Max. Total Incident Energy (MJ/m ²) ± 0.002 MJ/m ² or $\pm 5\%$
OBMV01	X		37.5	Horizontal	0.84	Exceeded range	7.000
				Vertical	1.65	0.749	1.038
OBMV02	X		21.4	Horizontal	0.84	No data	0.532
				Vertical	1.65	2.149	2.182
OBMV03	X		55.7	Horizontal	0.84	Exceeded range	12.441
				Vertical	1.65	1.457	2.327
OBMV04		X	51.8	Horizontal	0.84	2.575	5.585
				Vertical	1.65	1.137	1.926
OBMV05		X	43.5	Horizontal	0.84	0.602	1.215
				Vertical	1.65	1.974	2.816
OBMV06	X		22.7	Horizontal	0.84	2.157	3.805
				Vertical	1.65	0.471	0.649

5. Summary and Conclusion

This section provides a brief summary and conclusions made from the series of experiments documented in this report.

5.1. Summary

A series of seventeen (17) arcing fault experiments were performed in an open box configuration. Each experiment consisted of a three-phase arcing fault initiated and sustained with aluminum or copper electrodes within the cubical box with one side open to the environment. The magnitude of the arc current and duration was varied at a nominal system voltage of either 1 000V or 6 900V. Electrical parameters are summarized in Table 48. Numerous measurements were made to characterize the environment surrounding the open box, including external heat flux, external incident energy, electric field strength, air conductivity, optical emission spectrum, and mass loss. Photometric equipment was deployed to capture the event using a combination of devices to characterize the thermal environment, and event timing.

Table 48. Summary of low-voltage and medium-voltage experiment parameters.

Experiment #	Nominal Voltage (kV)	Current (kA)	Arc Duration (s)	Energy (MJ)	Mass loss (g)	
					Enclosure	Electrodes
OB01(a)	1.00	1.05	2.01	0.201	None	24.5
OB01(b)	1.00	1.03	2.02	0.736	None	
OB02	1.00	14.02	2.02	11.989	386	762.5
OB03	1.00	13.80	3.03	19.886	1 799	1 327.5
OB04	1.00	27.79	1.03	12.328	110	789.0
OB05	1.00	1.02	2.01	0.796	None	See OB10
OB06	1.00	11.96	2.02	12.591	1,670	740.0
OB07	1.00	12.95	1.52	10.233	861	552.0
OB08	1.00	24.87	1.02	19.570	72*	596.5*
OB09	1.00	4.79	2.01	2.242	None	212.5
OB10	1.00	4.87	2.01	4.118	None	175.0
OBMV01	6.9	14.3	3.18	37.5	10 168	1 323.5
OBMV02	6.9	29.1	1.12	21.4	982	944.5
OBMV03	6.9	14.4	5.05	55.7	17 483	2 296.0
OBMV04	6.9	14.3	5.08	51.8	12 444	3 252.0
OBMV05	6.9	28.6	2.32	43.5	5 666	3 215.5
OBMV06	6.9	14.6	2.05	22.7	5 763	727.0

* electrode failure

5.2. Conclusions

This series of experiments provide valuable information related to the characteristics of the electrical arc and potential hazards, including:

- Thermal energy measurements which provide direct comparison between aluminum and copper electrodes. Low-voltage results are shown in Section 3.3.
- Mass loss data was collected for the electrodes and the steel enclosure. This information can be subsequently used to evaluate or develop prediction models to support hazard modeling.
 - For the electrodes, more mass was lost for copper electrodes than aluminum when normalized to an equivalent electrical experimental energy.
 - For the steel enclosure, more steel mass was lost during the aluminum electrode experiments versus the copper electrode experiments when normalized to an equivalent electrical experimental energy.
- Air conductivity and breakdown strength measurements were made during a number of experiments. For the experimental conditions and locations investigated, the results indicated that HEAF byproduct dispersed into the air causing equipment arc over was unlikely at the measurement locations. This conclusion may not hold for locations closer to the source.
- Surface conductivity measurements of HEAF byproduct surface deposition showed a decrease in resistance compared to pre-experimental conditions. For the experimental conditions and locations investigated, the result indicated that an impact on plant safety equipment is not likely. The impact of surface deposition, however, is highly dependent on the design, configuration, location, and sensitivity of the equipment.
- For the experimental conditions and locations investigated, the electromagnetic interference measurements showed that the EMI signature was small and not likely to impact sensitive plant equipment.

Acknowledgments

Funding for this work was provided by the U.S. Nuclear Regulatory Commission, Office of Research. This report was developed jointly between the National Institute of Standards and Technology (NIST), Sandia National Laboratories, and the U.S. Nuclear Regulatory Commission.

References

- [1] NRC RIL 2021-10, NIST TN 2188, SNL SAND2021-12049 R, Report on High Energy Arcing Fault Experiments, Experimental Results from Medium Voltage Electrical Enclosures, U.S. Nuclear Regulatory Commission, Washington, DC, National Institute of Standards and Technology, Gaithersburg, MD, Sandia National Laboratories, Albuquerque, NM, November 2021.
- [2] NRC Information Notice 2017-04: High Energy Arcing Faults in Electrical Equipment Containing Aluminum Components, US NRC, Washington, DC, August 2017.
- [3] OECD Fire Project – Topical Report No. 1, Analysis of High Energy Arcing Faults (HEAF) Fire Events, Nuclear Energy Agency Committee on the Safety of Nuclear Installations, Organization for Economic Cooperation and Development, June 2013.
- [4] EPRI/NRC-RES Fire PRA Methodology for Nuclear Power Facilities, Volume 2: Detailed Methodology. Electric Power Research Institute (EPRI), Palo Alto, CA, and U.S. Nuclear Regulatory Commission, Office of Nuclear Regulatory Research (RES), Rockville, MD: 2005, EPRI TR-1011989 and NUREG/CR-6850.
- [5] Fire Probabilistic Risk Assessment Methods Enhancements: Supplement 1 to NUREG/CR-6850 and EPRI 1011989, EPRI, Palo Alto, CA, and NRC, Washington, DC.: December 2009.
- [6] NEA HEAF Project – TOPICAL REPORT No. 1, Experimental Results from the International High Energy Arcing Fault (HEAF) Research Program – Phase 1 Experiments 2014 to 2016, Nuclear Energy Agency Committee on The Safety of Nuclear Installations, 2017
- [7] Memorandum from Mark Henry Salley, to Thomas H. Boyce, Regarding submittal of possible generic issue concerning the damage caused by high energy arc faults in electrical equipment containing aluminum components, ADAMS Accession No. ML16126A096, May 2016.
- [8] Memorandum from Joseph Giitter to Michael F. Weber, regarding Results of Generic Issue Review Panel Screening Evaluation for Proposed Generic Issue PRE-GI-018, ‘High Energy Arcing Faults involving Aluminum,’ ADAMS Accession No. ML16349A027, July 15, 2017.
- [9] Memorandum from Michael Franovich and Michael Cheok to Raymond V. Furstenau, regarding Assessment Plan for Pre-GI-018, Proposed Generic Issue on High Energy Arc Faults Involving Aluminum, ADAMS Accession No. ML18172A189, August 22, 2018.
- [10] An International Phenomena Identification and Ranking Table (PIRT) Expert Elicitation Exercise for High Energy Arcing Faults (HEAFs), US NRC, Washington, DC, NUREG-2218, January 2018.
- [11] Memorandum from Raymond V. Fustenau to Andrea D. Veil, regarding Closure of Proposed Generic Issue Pre-GI-018, ‘High-Energy Arc Faults Involving Aluminum,’ ADAMS Accession No. ML21237A360, August 31, 2021.
- [12] K. Armijo and P. Clem, et. al., “Electrical Arc Fault Particle Size Characterization,” Sandia Report SAND 2019-11145, September 2019.
- [13] Tambakuchi, A., et. al., *NRC HEAF Tests, Imaging and Measurement Methodology Report*, SAND2021-12086 R, Sandia National Laboratories, September 2018.
- [14] Lafarge, T. and Possolo, A, "The NIST Uncertainty Machine," NCLSI Measure J. Meas. Sci., Vol. 10, No. 3, pp.20-27, September 2015.

- [15] SAND202-5747 C, Characterization of DC Arc-Plasmas Generated by High-Voltage Photovoltaic Power Systems; Winters, Caroline, Cruz-Cabrera, Alvaro Augusto, Armijo, Kenneth Miguel, Sandia National Laboratories, June 2020.
- [16] RIL 2021-09, SAND2021-11327, HEAF Cable Fragility at the Solar Furnace at the National Solar Thermal Test Facility, Experimental Results, U.S. Nuclear Regulatory Commission, Washington, DC, Sandia National Laboratories, Albuquerque, NM, September 2021.
- [17] Putorti, A., Melly, M., Bareham, S., and Praydis Jr., J., "Characterizing the Thermal Effects of High Energy Arc Faults." 23rd International Conference on Structural Mechanics in Reactor Technology (SMiRT 23) – 14th International Post-Conference Seminar on "FIRE SAFETY IN NUCLEAR POWER PLANTS AND INSTALLATIONS," Salford, UK, August 17-18, 2015, <http://www.grs.de/en/publications/grs-a-3845>.
- [18] Ingason, H. and Wickstrom, U., "Measuring incident radiant heat flux using the plate thermometer," *Fire Safety Journal*, Vol. 42, No. 2, 2007, pp. 161-166.
- [19] Taylor, B.N. and Kuyatt, C.E., "Guidelines for evaluating and expressing the uncertainty of NIST measurement results," NIST Technical Note 1297, National Institute of Standards and Technology, Gaithersburg, MD, USA, 1994.
- [20] Joint Committee for Guides in Metrology. Evaluation of measurement data – Guide to the expression of uncertainty in measurement, Sèvres, France: International Bureau of Weights and Measures (BIPM), URL www.bipm.org/en/publications/guides/gum.html, BIPM, IEC, IFCC, ILAC, ISO, IUPAC, IUPAP and OIML, JCGM 100:2008, GUM 1995 with minor corrections (2008).
- [21] Joint Committee for Guides in Metrology. International vocabulary of metrology – Basic and general concepts and associated terms (VIM), Sèvres, France: International Bureau of Weights and Measures (BIPM), 3rd ed., URL www.bipm.org/en/publications/guides/vim.html, BIPM, IEC, IFCC, ILAC, ISO, IUPAC, IUPAP and OIML, JCGM 200:2012 (2008 version with minor corrections) (2012).
- [22] ASTM (1993), *Manual on the Use of Thermocouples in Temperature Measurement*, ASTM Manual Series: MNL12, Revision of Special Publication (STP) 470B, 4th ed., ASTM International, West Conshohocken, PA, 1993, United States.
- [23] McGrattan, K., Hostikka, S., McDermott, R., Floyd, J., Weinschenk, C., Overholt, K., Fire Dynamics Simulator, Technical Reference Guide. National Institute of Standards and Technology, Gaithersburg, MD, USA, and VTT Technical Research Centre of Finland, Espoo, Finland, sixth edition, September 2013. Vol. 1: Mathematical Model; Vol. 2: Verification Guide; Vol. 3: Validation Guide; Vol. 4: Configuration Management Plan.
- [24] ASTM Standard F1959 / F1959M-14, 2014, "Standard Experiment Method for Determining the Arc Rating of Materials for Clothing," ASTM International, West Conshohocken, PA, 2014.
- [25] ASTM Standard E457-08, "Standard Test Method for Measuring Heat-Transfer Rate Using a Thermal Capacitance (Slug) Calorimeter," ASTM International, West Conshohocken, PA, 2008.
- [26] Prodyn Technologies Electric Field Sensors, D-Dot Free Field-Radial Output Data Sheet, <https://www.prodyntech.com/wp-content/uploads/2021/01/AD-Series-Free-Field-D-Dot-Data-Sheet.jpg>, Albuquerque, NM, site accessed November 2021.
- [27] MIL-STD-461G, 11 December 2015 Department of Defense Interface Standard Requirements for the Control of Electromagnetic Interference Characteristics of

Subsystems and Equipment, Table XI RS103 limits p. 145 and Figure RS105-1 RS 105 limit for all applications p. 155.

- [28] EPRI TR-102323, Revision 3, Guidelines for Electromagnetic Interference Testing of Power Plant Equipment, <https://www.osti.gov/servlets/purl/837279>, Electric Power Research Institute, Palo Alto, CA, November 2004.
- [29] Tektronix Mixed Domain Oscilloscopes, MDO4000C Series Datasheet, Tektronix, Beaverton, OR, <https://www.tek.com> site accessed November 2021.
- [30] NFPA 70, National Electric Code, 2020 Edition, National Fire Protection Association, Quincy, MA, 2020.
- [31] ASTM D2477, Standard Test Method for Dielectric Breakdown Voltage and Dielectric Strength of Insulating Gases at Commercial Power Frequencies, ASTM International, West Conshohocken, PA, 2020.
- [32] IEEE 1584, Guide for Performing Arc-Flash Hazard Calculations, Institute of Electrical and Electronic Engineers, New York, NY, 2018.

Appendix A: Engineering Drawings

This appendix provides detailed drawings and information on the experiment facility, experiment object, and instrumentation.

A.1 Experimental Facility

Drawings of the facility are presented in Fig. 76 through Fig. 81.

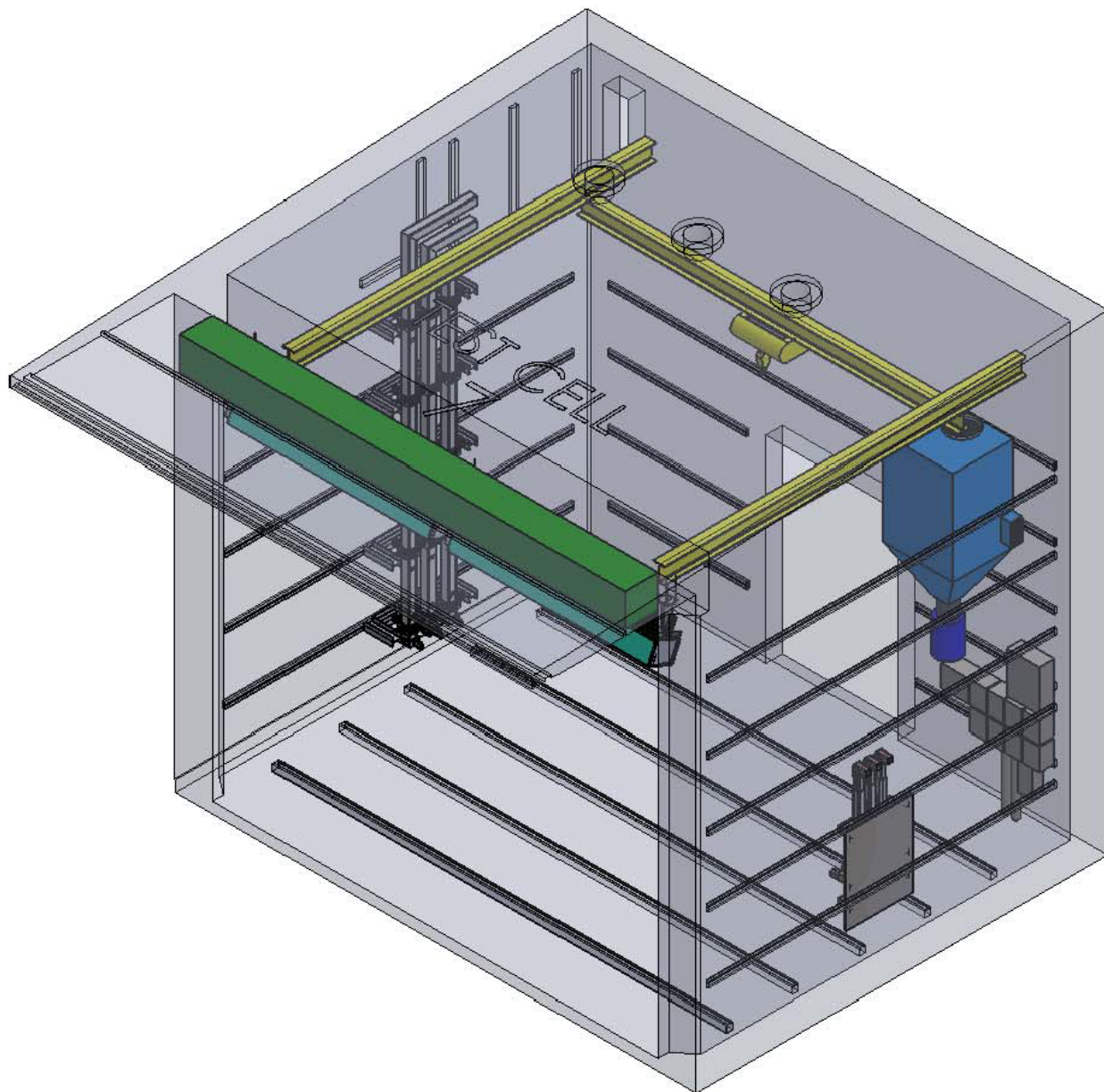


Fig. 76. Isometric drawing of Test Cell #7.

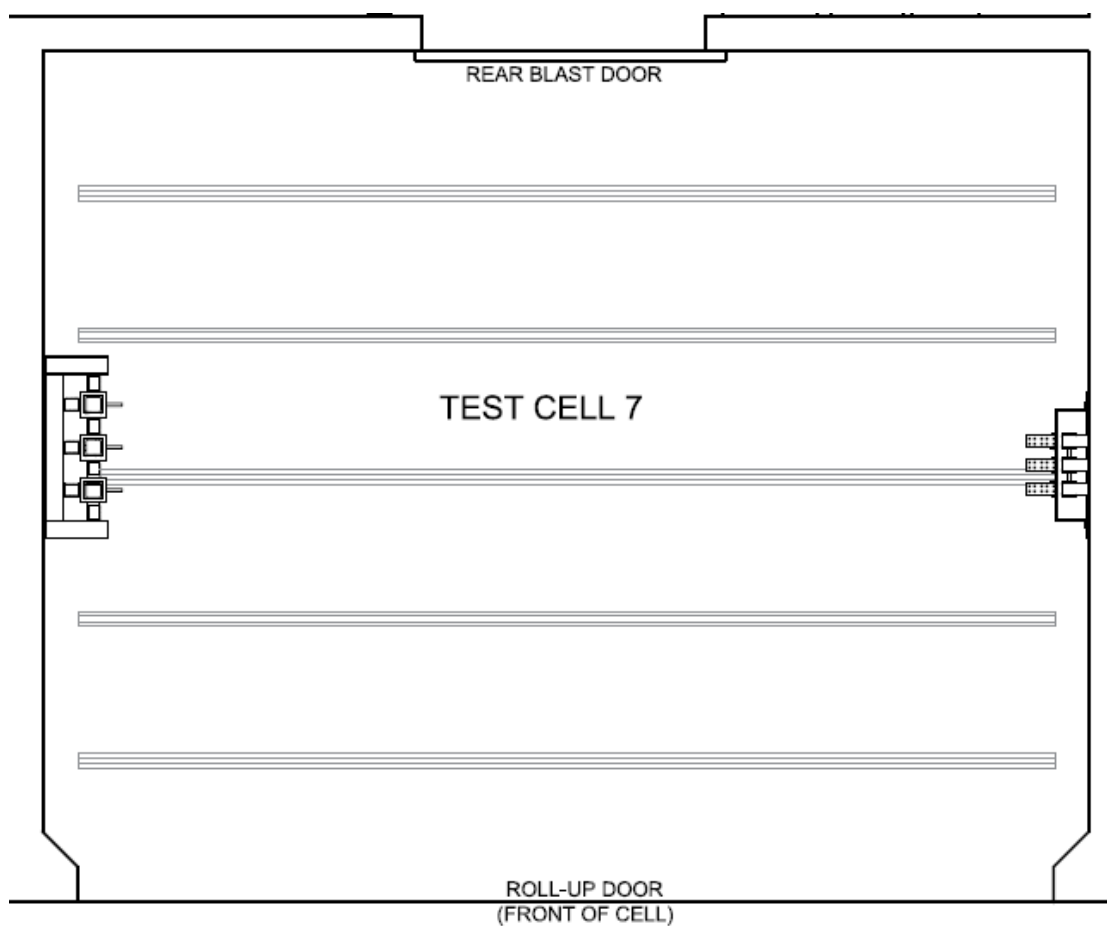


Fig. 77. Plan view of Experiment Cell #7.
Low-voltage power connections located on right side of drawing.

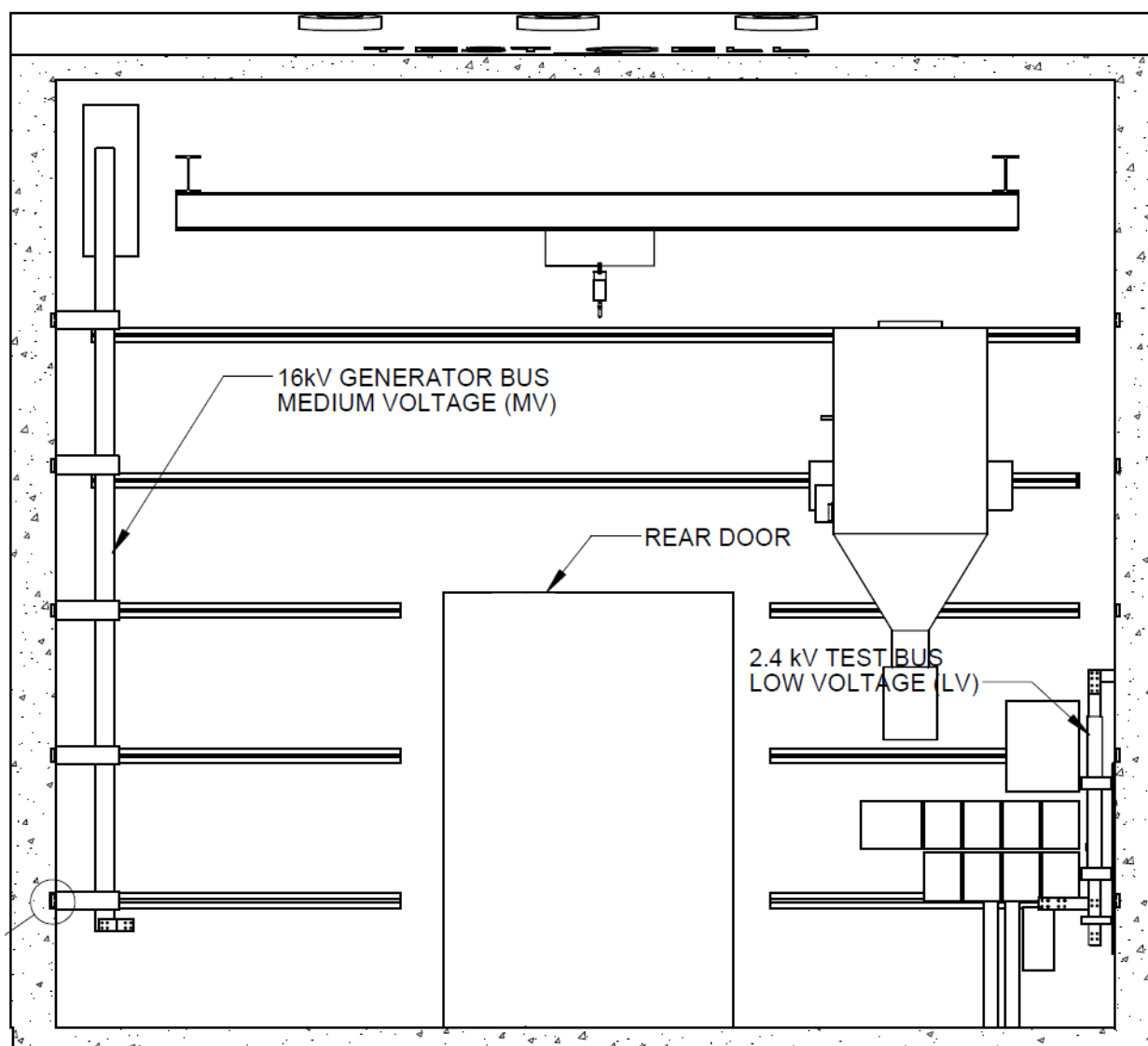


Fig. 78. Elevation view of Test Cell #7.
Low-voltage power connections located on right side of drawing.

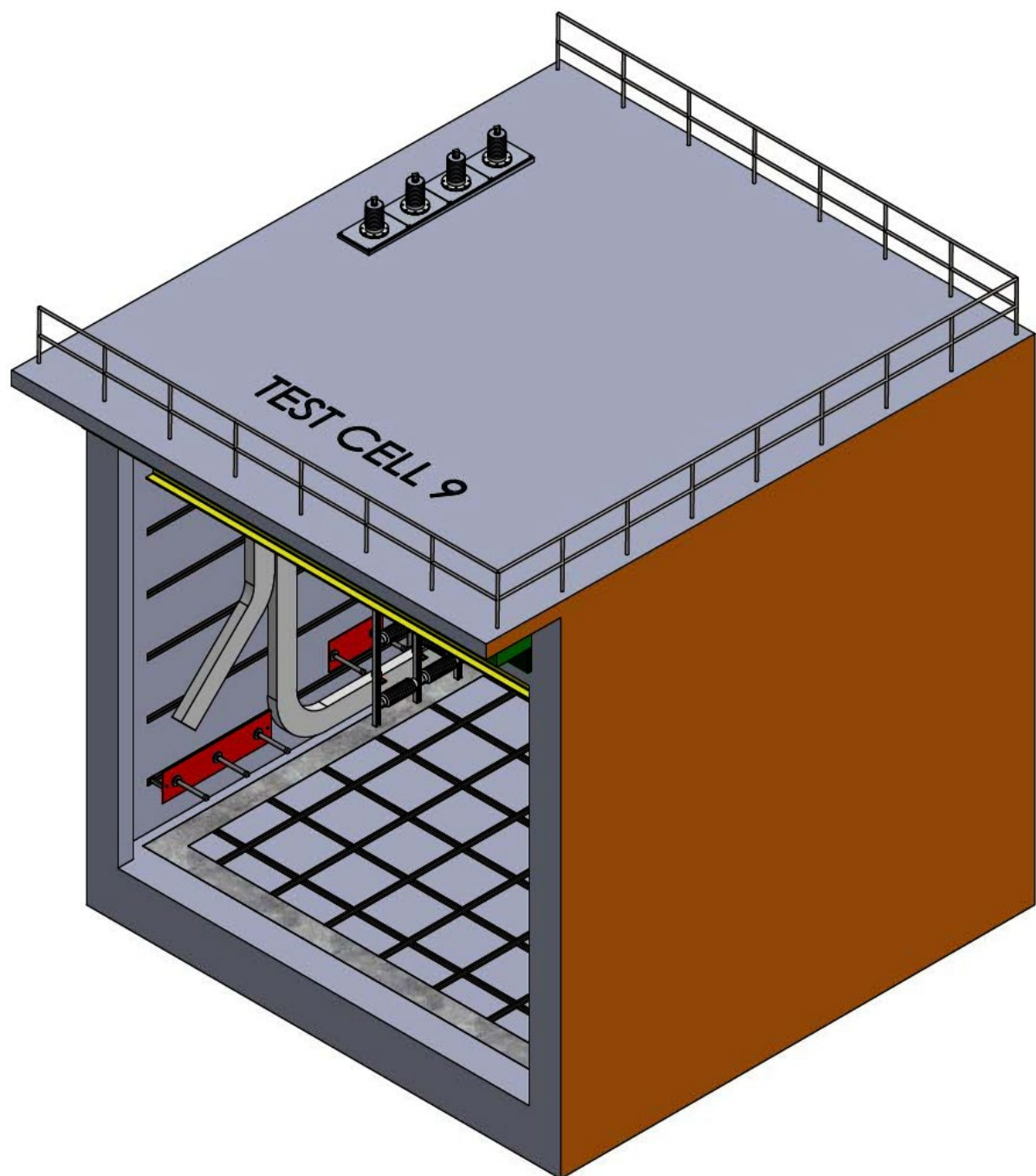


Fig. 79. Isometric drawing of Test Cell #9.

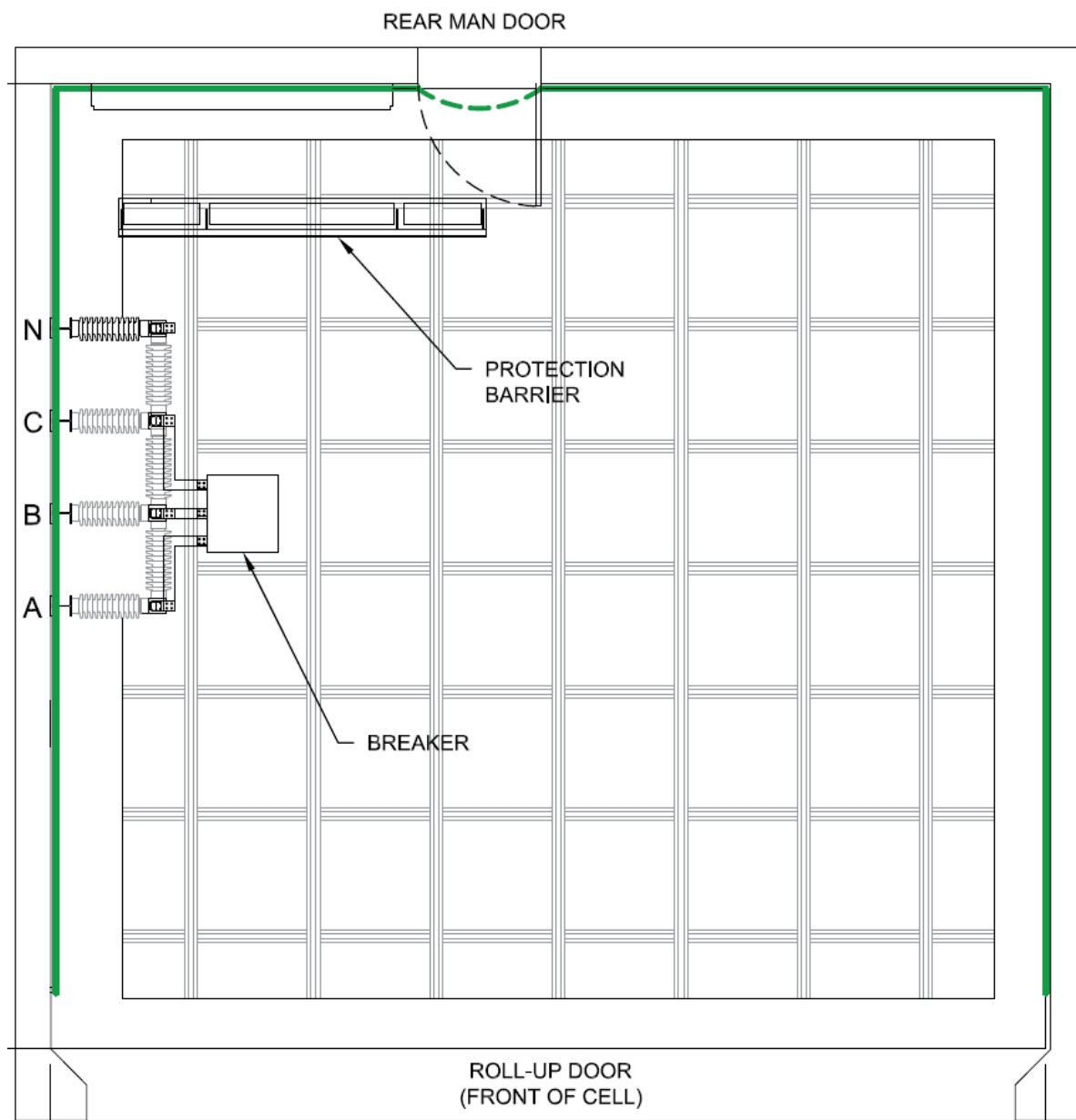


Fig. 80. Plan view of Test Cell #9.

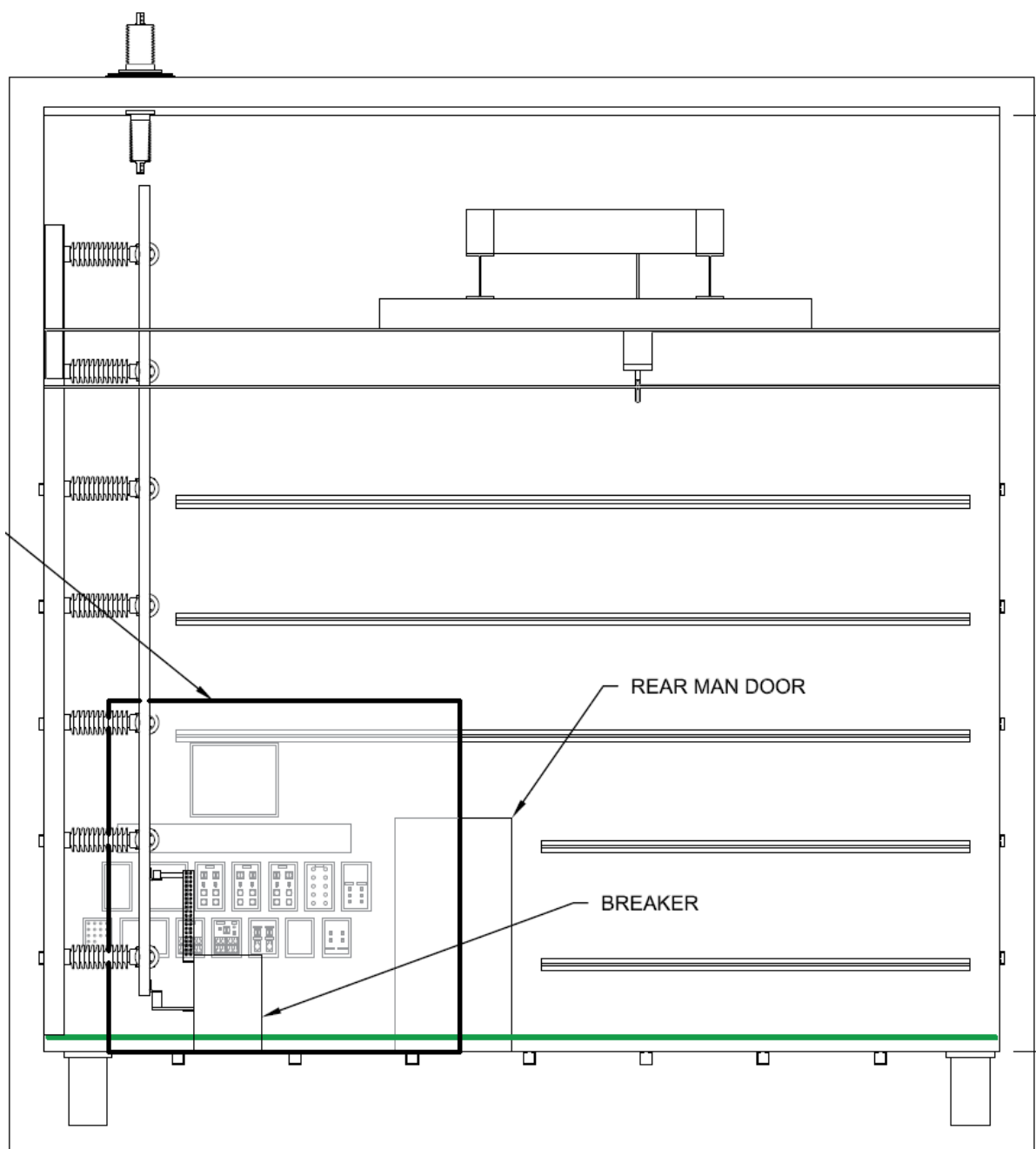


Fig. 81. Elevation view of Test Cell #9. Breaker shown in drawing is part of KEMA protection system and is not the open box.

A.2 Support Drawings

SNL manufactured three phase electrode holders for the low-voltage box experiments. The drawing of this component is presented below.

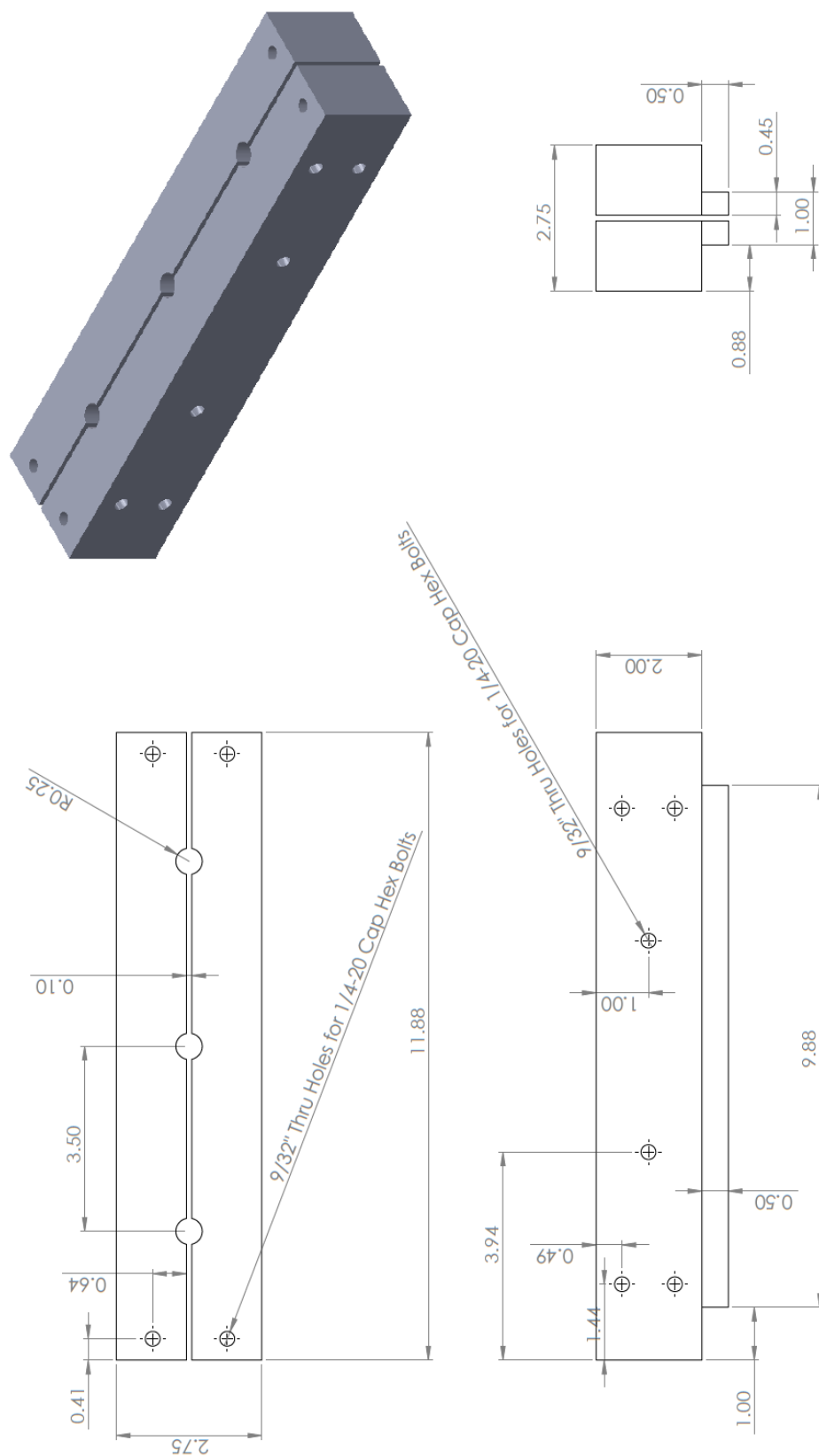


Fig. 82. Electrode holder used in open box experiments. All nominal dimensions shown in inches.

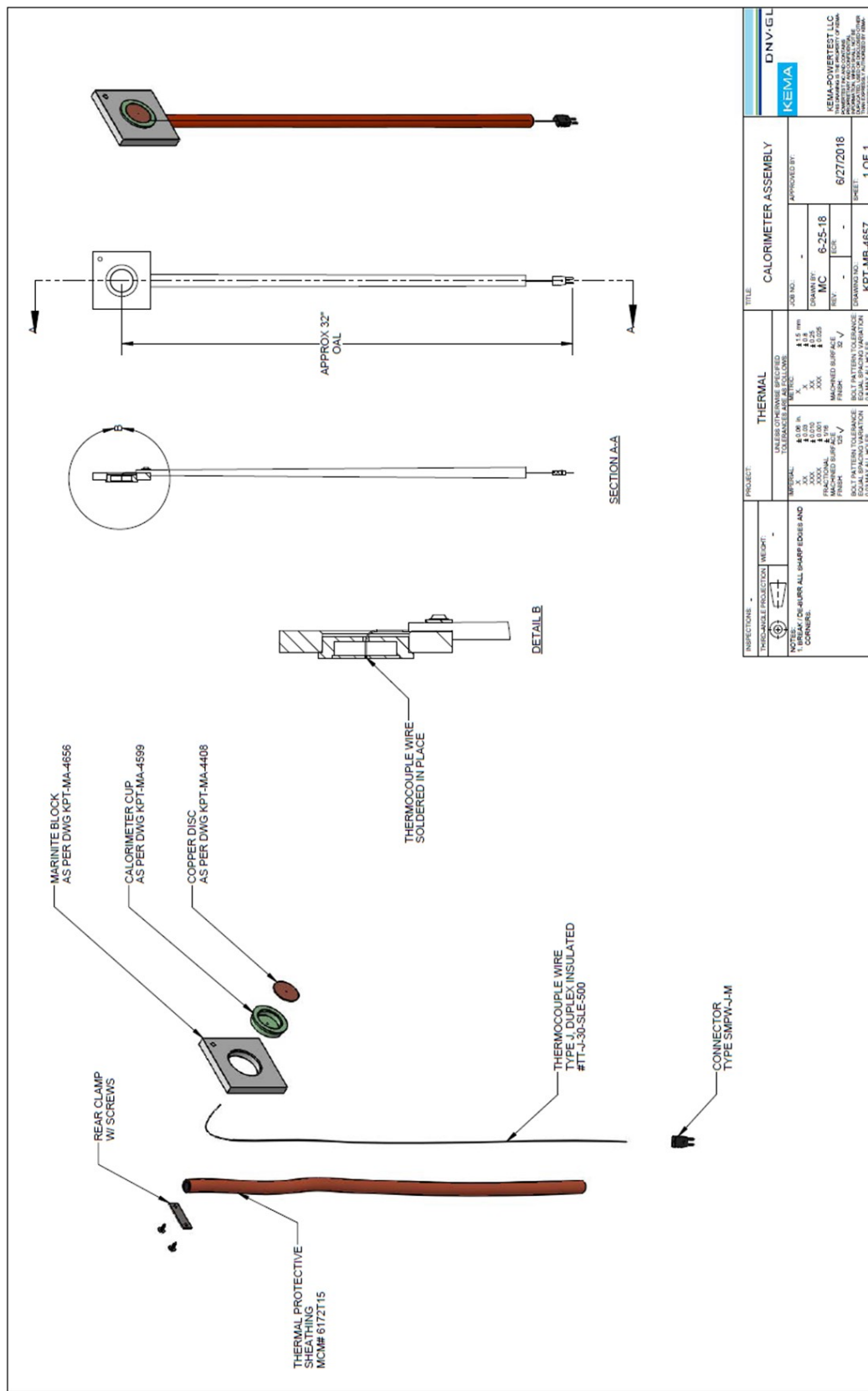


Fig. 83. Drawing KPT-MB-4657, ASTM Calorimeter Assembly.

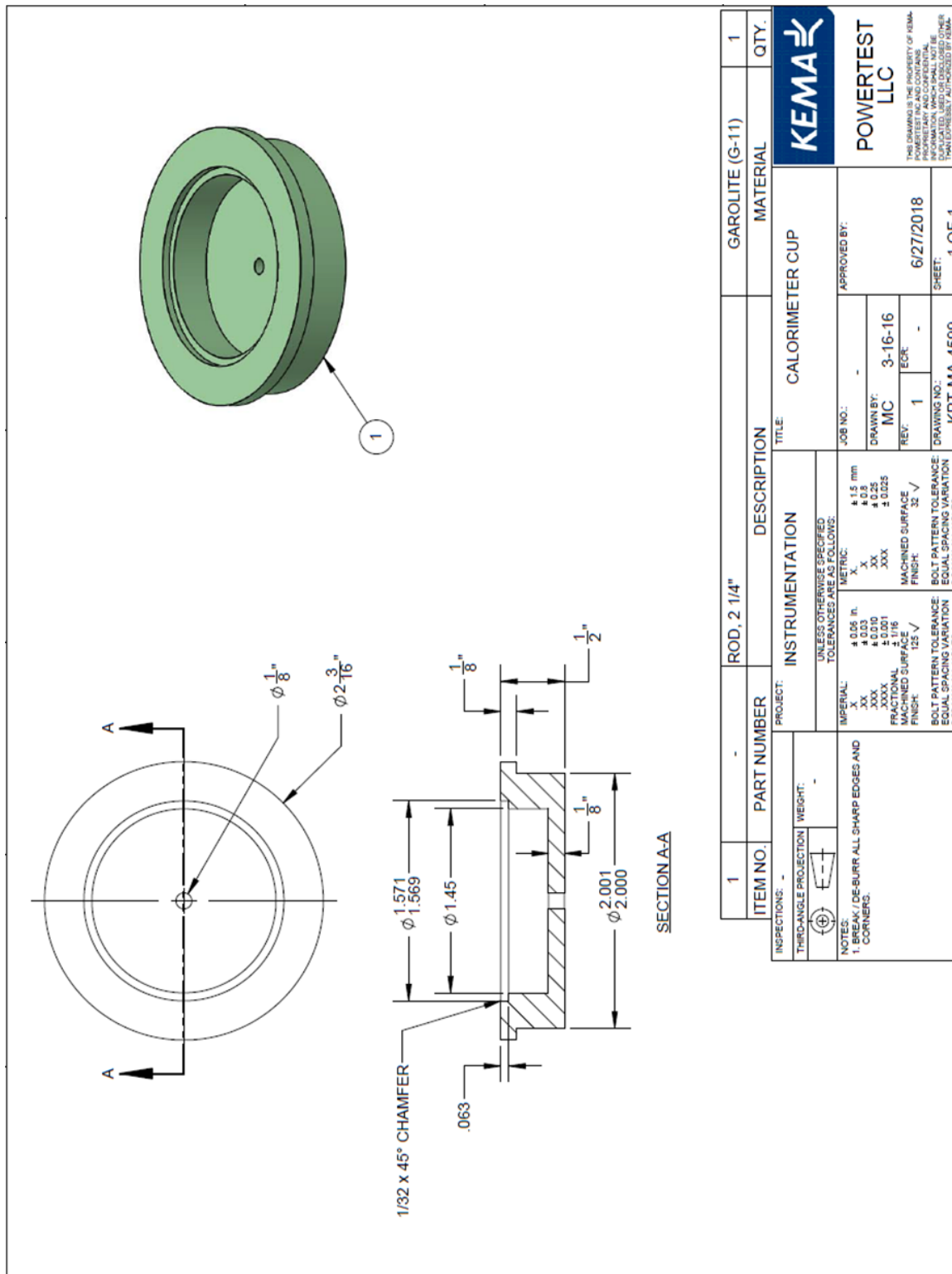


Fig. 84. Drawing KPT-MA-4599, ASTM Calorimeter Cup.

Appendix B: Measurement Plots

This appendix provides presents plots of the various measurement made during the experimental series.

B.1 Spectroscopy

B.1.1 Experiment OB01(a)

SNL used the spectrometer during this experiment. The iris was opened to 3 mm without the use of any optical density filter in place. During the experiment, the spectral features saturated the detectors. The detector was positioned to focus immediately below the center copper electrode tip (Phase B). The spectrum from this experiment is presented in Fig. 85 , with many emitting materials contributing to the signal. There was no direct characterization of the material within the box, so species and concentration were unknown. It is also important to note this data has not been processed to consider the effects of detector efficiency or non-linearity, neither has a background been subtracted to try and remove the broad band, graybody emission. Due to the saturation, no temperature inference was attempted.

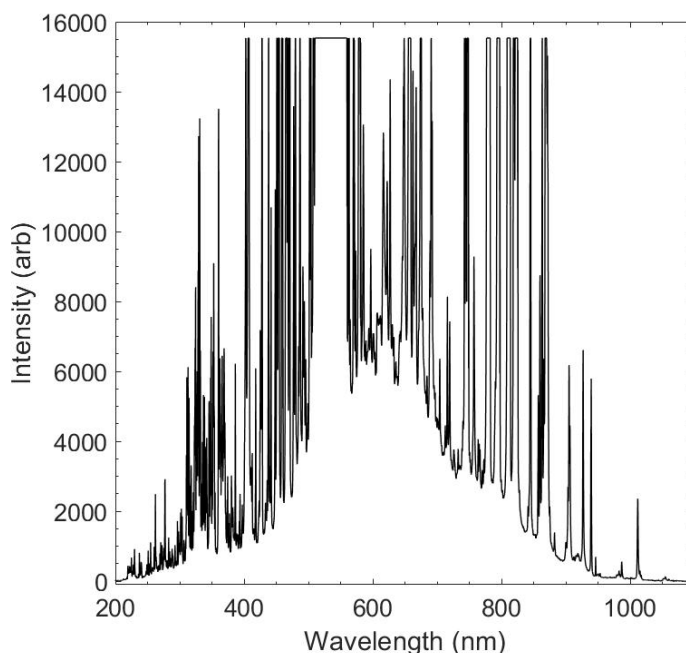


Fig. 85. Spectrum from Experiment OB01(a).

B.1.2 Experiment OB01(b)

SNL used the spectrometer during this experiment. The iris was opened to 1 mm without the use of any optical density filter in place. The detector was positioned to look immediately below the center copper electrode tip. Spectral features saturated the detector at early times. By the middle of the experiment, the spectrometer was recording features that could be analyzed, and weak

features were present at the end of the experiment. The spectrum from this experiment is presented in Fig. 86 and Fig. 87.

In both the left and right spectra of Fig. 87, two copper transitions at approximately 793.3 nm and 809.3 nm were visible and isolated. These transitions were identified as temperature sensitive in previous work. However, in order to accurately infer temperature, two additional lines at 570 nm and 578.2 nm must be resolved as well. Unfortunately, as seen in all spectra that region experienced significant interference from additional species emission. Therefore, no temperature inference was attempted, and the spectra presented had no data processing for detector non-linearity, efficiency, or background subtraction.

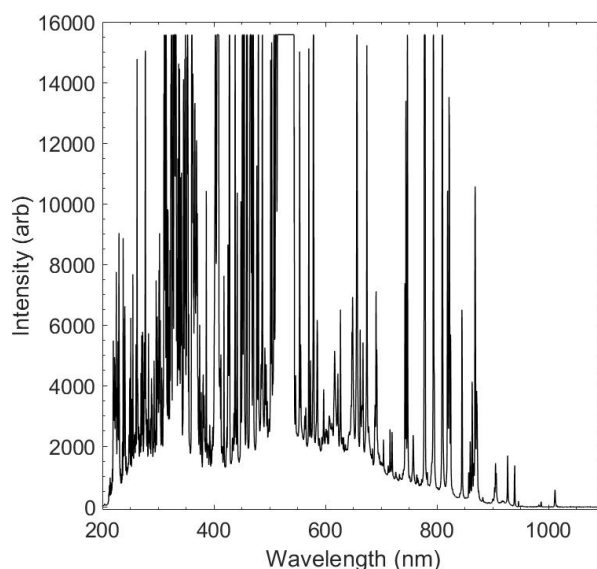


Fig. 86. Spectrum from Experiment OB01(b), early.

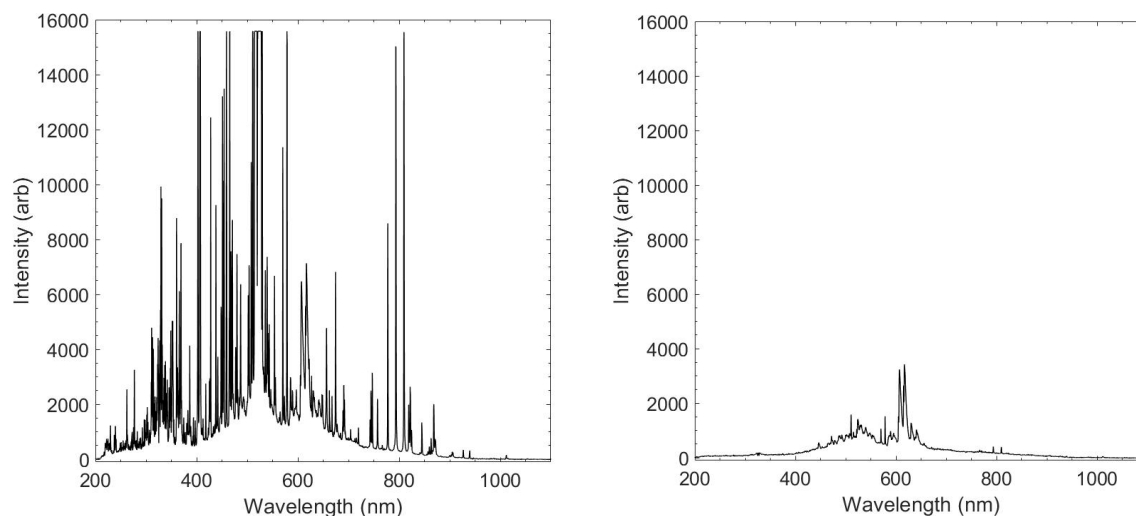


Fig. 87. Spectrum from Experiment OB01(b), mid-experiment (left) and late (right).

B.1.3 Experiment OB02

No spectroscopy used during this experiment.

B.1.4 Experiment OB03

No spectroscopy used during this experiment.

B.1.5 Experiment OB04

No spectroscopy used during this experiment.

B.1.6 Experiment OB05

SNL used the spectrometer during this experiment. The iris was opened to 1 mm, and a 0.3 neutral density optical filter was in place. The detector was positioned to focus immediately below the center electrode tip (Phase B). Spectra contained high baseline emission as well as spectral features (Fig. 88).

Unlike the prior spectra in Experiments OB01a and OB01b, this spectrum contains emission from aluminum and reacting aluminum compounds. The sharp and narrow spectral features, like that at approximately 400 nm, are indicative of atomic emission, but broader manifolds of emission, like those from approximately 450 nm to 575 nm, are likely generated by molecular emission. These may be reacting aluminum molecules and radicals. With proper analysis, accounting for detector efficiency, nonlinearity, and background, these manifolds could be fit for temperature and compared to atomic aluminum emission from the plasma. However, that processing development was out of the scope of this project.

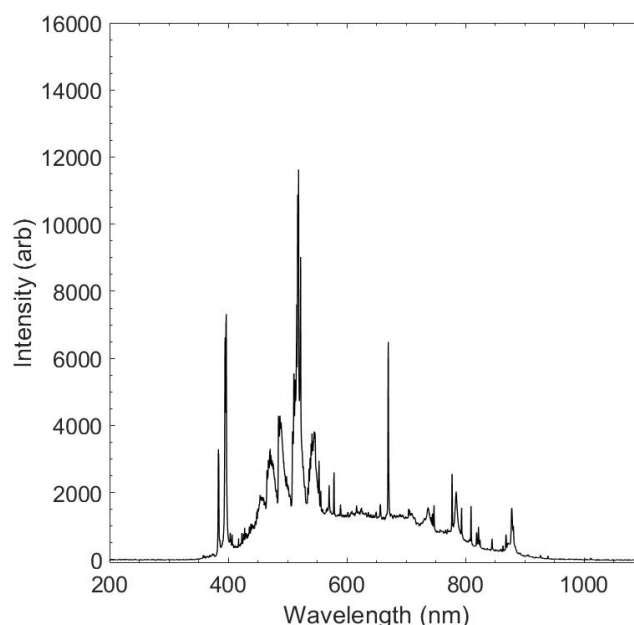


Fig. 88. Experiment OB05 spectra.

B.1.7 Experiment OB06

No spectroscopy used during this experiment.

B.1.8 Experiment OB07

SNL used the spectrometer during this experiment. The iris was opened to 1 mm with a 0.6 neutral density filter in place. The detector was positioned to focus approximately 7.6 cm (3 in) below the center copper electrode tip (Phase B). The spectrum from this experiment is presented in Fig. 89. Initial spectra contained metallic features (Fig. 89 top) before transitioning to broadband emission (Fig. 89 bottom left and bottom right).

The optical emission spectroscopy can be used to infer temperatures from the arc and from the surrounding environment. For this experiment, the spectrometer measurement volume was placed 3 inches below the central aluminum electrode to collect 'non-metallic' spectra. A 0.6 neutral density filter was placed in front of the spectrometer. The broadband, graybody emission can be assumed to follow a black body curve. The curve can be calibrated using a black body source and the same geometry as the experiment. If possible, it is a best practice to calibrate the experiment in-situ, which was not possible for this series. The data in Fig. 89 were not corrected for detector nonlinearity, efficiency, or background for the case of the top spectrum.

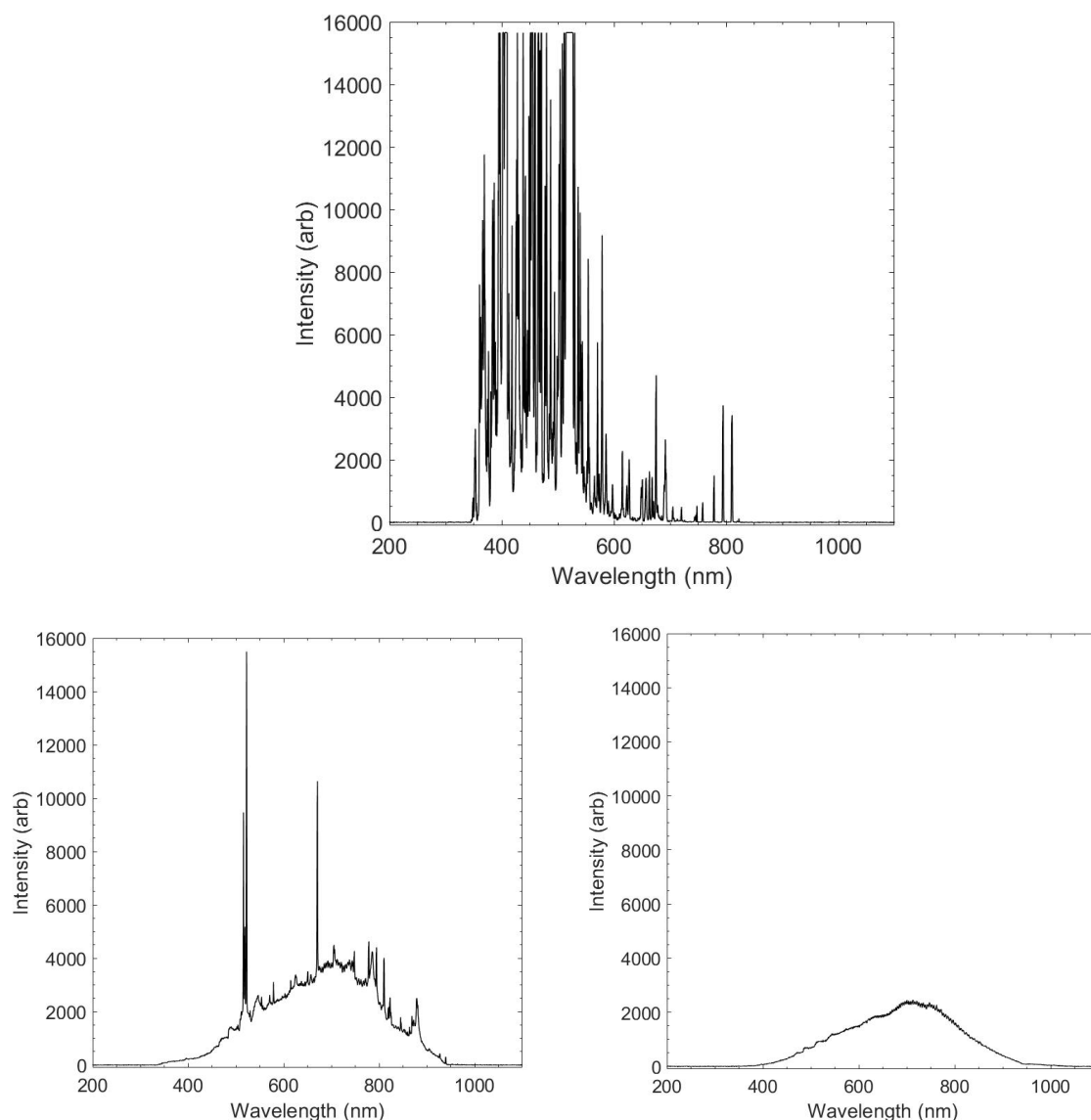


Fig. 89. Experiment OB07 spectral profiles, an early profile with spectral features (top), transition spectral features (bottom left), and a broadband emission spectrum (bottom right).

B.1.9 Experiment OB08

SNL used the spectrometer during this experiment. The iris was opened to 1 mm with a 0.6 neutral density filter in place. The detector was positioned to focus approximately 7.6 cm (3 in) below the center copper electrode tip (Phase B). This was to capture ‘non-metallic’ arc profiles. Broadband profiles varied throughout the experiments. The spectrum from this experiment is presented in Fig. 90.

These three spectra contained a few weak spectral features, but they were dominated by graybody emission. Because the material generated by the arc or from the surrounding environment was

never characterized, the exact radiators were unknown. These spectra were likely dominated by smoke particulate matter.

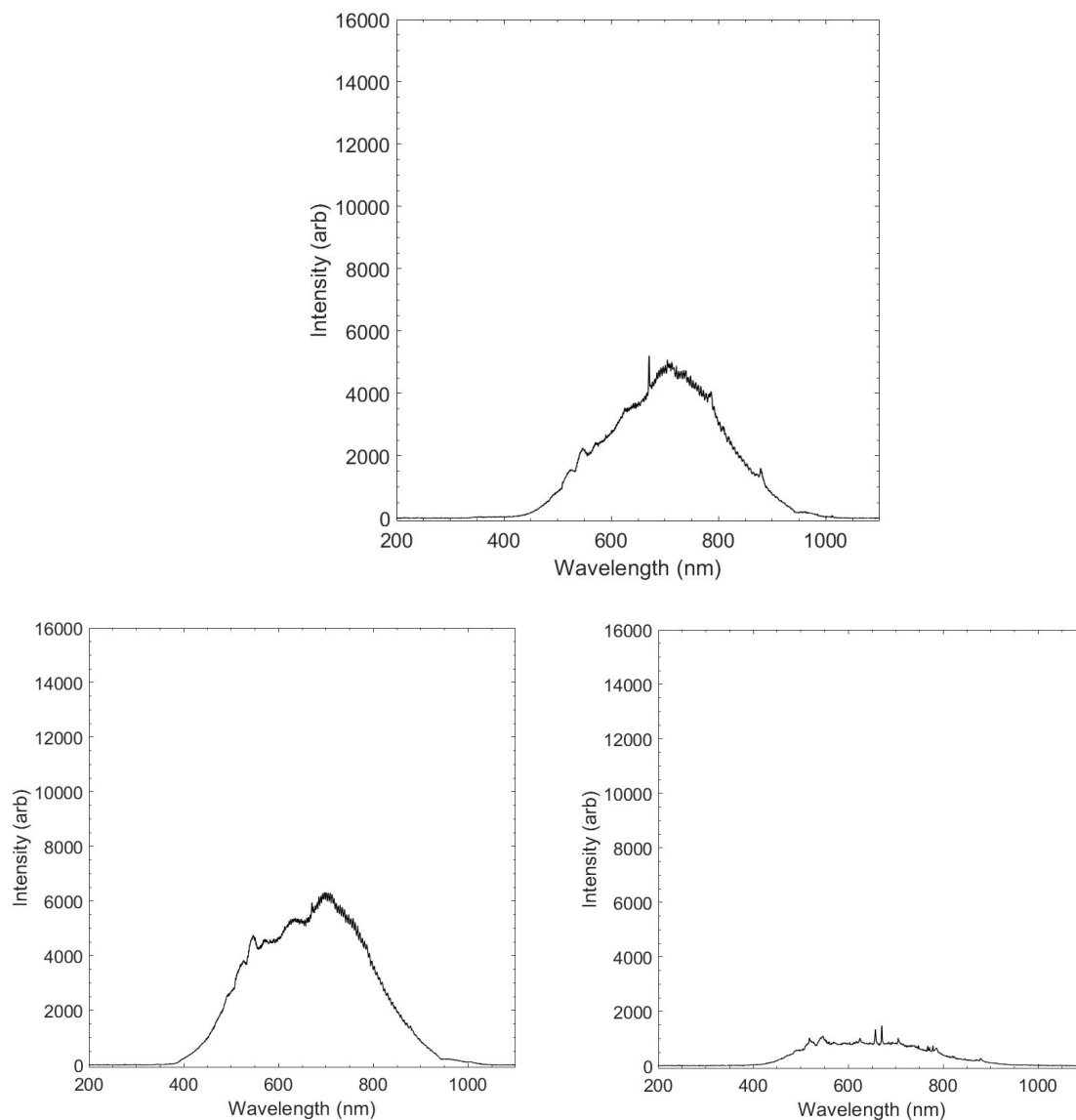


Fig. 90. Experiment OB08 spectra showing an early profile with spectral features (top), transition spectral features (bottom left), and broadband emission spectra (bottom right).

B.1.10 Experiment OB09

SNL used the spectrometer during this experiment. The iris was opened to 3 mm with the use of a 0.3 neutral density filter. The detector was positioned to focus immediately below the center copper electrode tip (Phase B). The spectra contained strong metallic features, and the intensity varied throughout the experiment. The spectra from this experiment are presented in Fig. 91.

The spectrum on the left is from the beginning of the experiment, and the spectrum on the right is near the end of the experiment. The intensity of the features decreased, likely due to the arc decay. Metallic copper features at approximately 793.3 nm and 809.3 nm were visible in both spectra. They dominated the later-time spectrum, Fig. 91 (right).

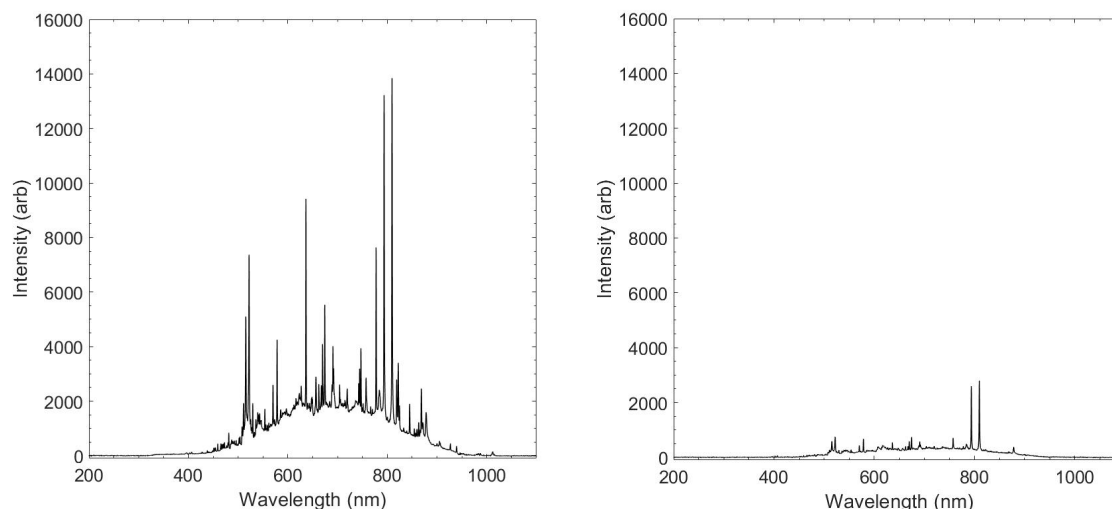


Fig. 91. Experiment OB09 spectra at the beginning of the experiment (left) and near the end (right).

B.1.11 Experiment OB10

SNL used the spectrometer during this experiment. The iris was opened to 1 mm with a 0.6 neutral density optical density filter in place. The first several spectra saturated the detector before the signal level decreased to a resolvable level. The signal level continued to decrease over the experiment. The detector was positioned to focus immediately below the center aluminum electrode tip (Phase B). The spectrum from this experiment is presented in Fig. 92.

The spectra intensity decreased for both the spectral features and the graybody emission throughout the experiment. These spectra had both atomic and molecular features, indicating emission from both metallic and reacting aluminum.

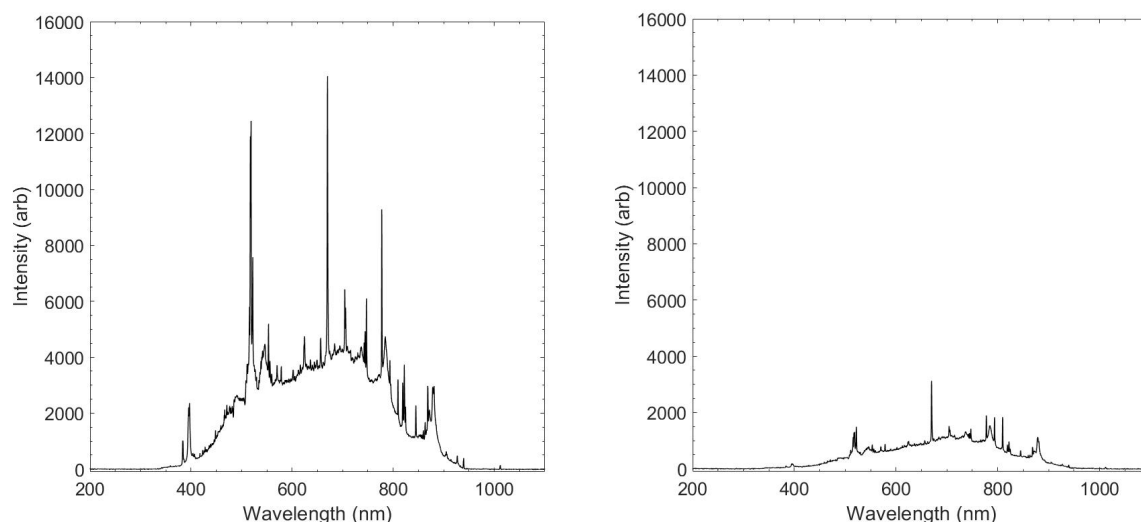


Fig. 92. Experiment OB10 spectra an early profile (left) and a late profile (right).

B.1.12 Experiment OBMV01

SNL used the spectrometer during this experiment. The spectrum from this experiment is presented in Fig. 93.

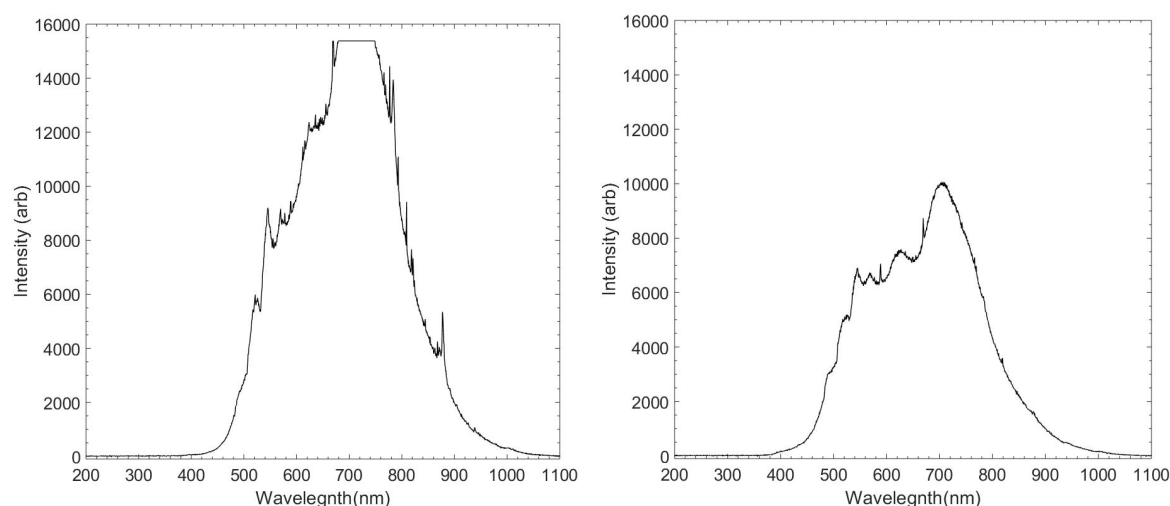


Fig. 93. Experiment OBMV01 spectrum from early in the experiment (left) and later in the experiment (right).

B.1.13 Experiment OBMV02

SNL used the spectrometer during this experiment. The spectrum from this experiment is presented in Fig. 94.

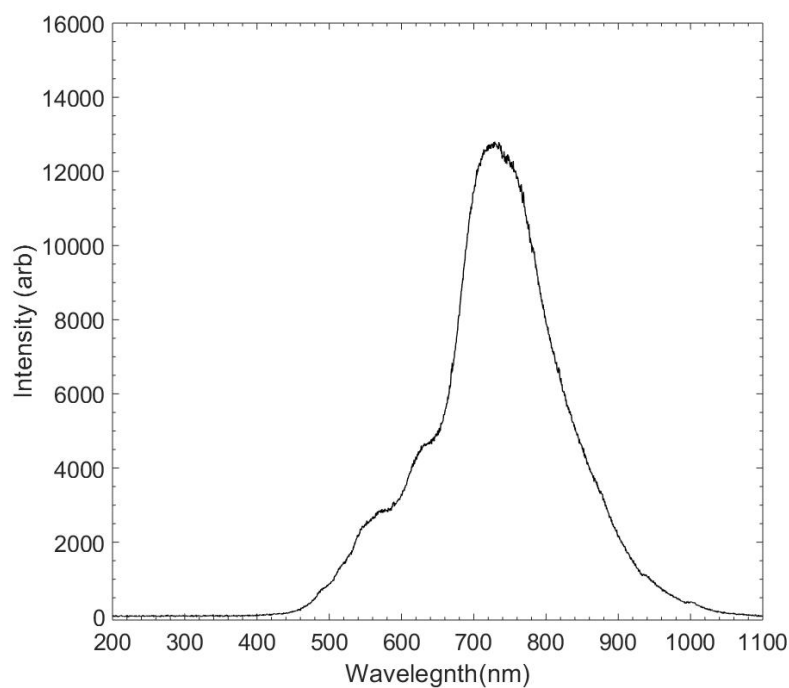


Fig. 94. Spectrum from Experiment OBMV02.

B.1.14 Experiment OBMV03

SNL used the spectrometer during this experiment. The spectrum from this experiment is presented in Fig. 95.

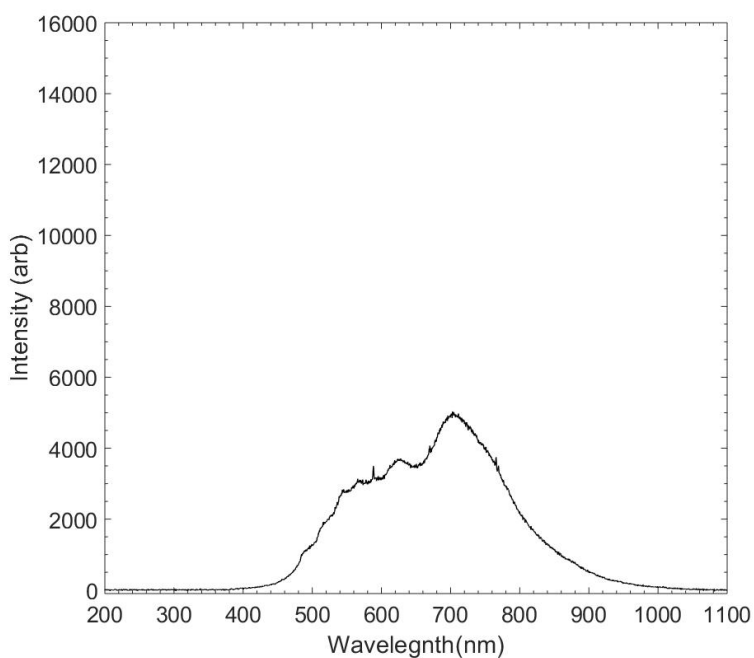


Fig. 95. Spectrum from Experiment OBMV03.

B.1.15 Experiment OBMV04

No spectroscopy used during this experiment.

B.1.16 Experiment OBMV05

SNL used the spectrometer during this experiment. The iris was opened to 1 mm without the use of any optical density filter in place. The detector was positioned to focus immediately below the center copper electrode tip (Phase B). The spectrum from this experiment is presented in Fig. 96.

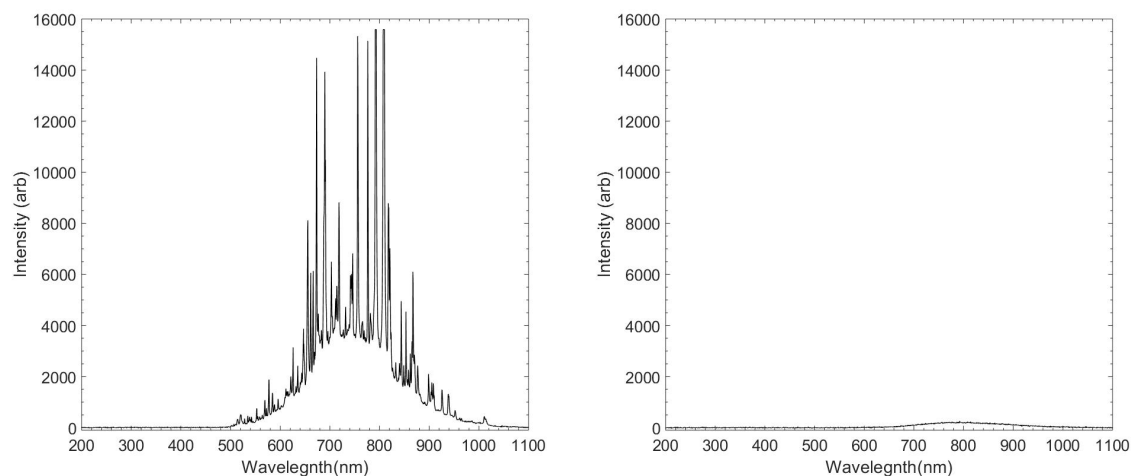


Fig. 96. Experiment OBMV05 spectrum early in the experiment (left) and later in the experiment (right).

B.1.17 Experiment OBMV06

No spectroscopy used during this experiment.

B.2 Electrical

B.2.1 Experiment OB01(a)

The electrical measurements are presented in Fig. 97 and Fig. 98.

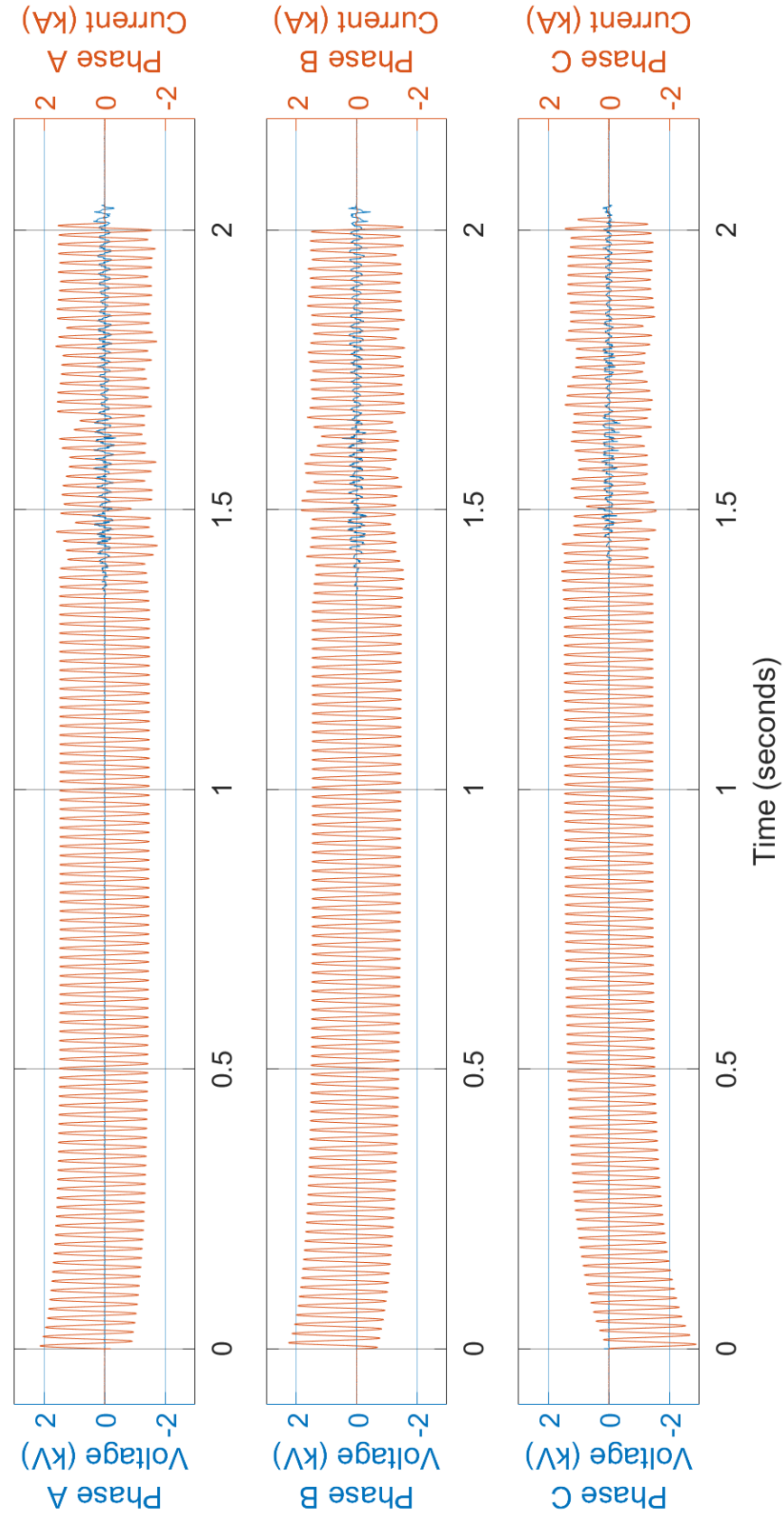


Fig. 97. Voltage and current measurements for Experiment OB01(a).

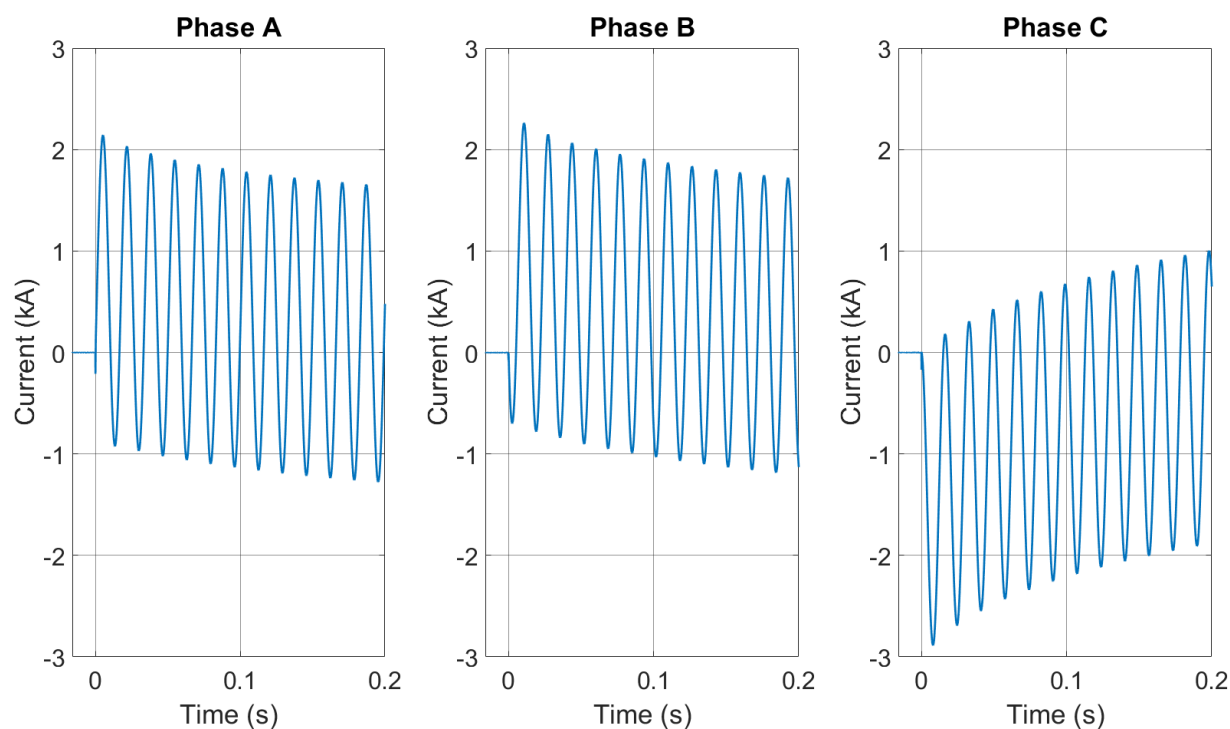


Fig. 98. Transient current profiles for Experiment OB01(a).

B.2.2 Experiment OB01(b)

Electrical measurements are presented in Fig. 99 and Fig. 100. It should be noted that the raw data file for Phase C had a voltage divider in place and that signal needed to be multiplied by 2. This only affected the Phase C voltage, and the waveforms presented below have been corrected.

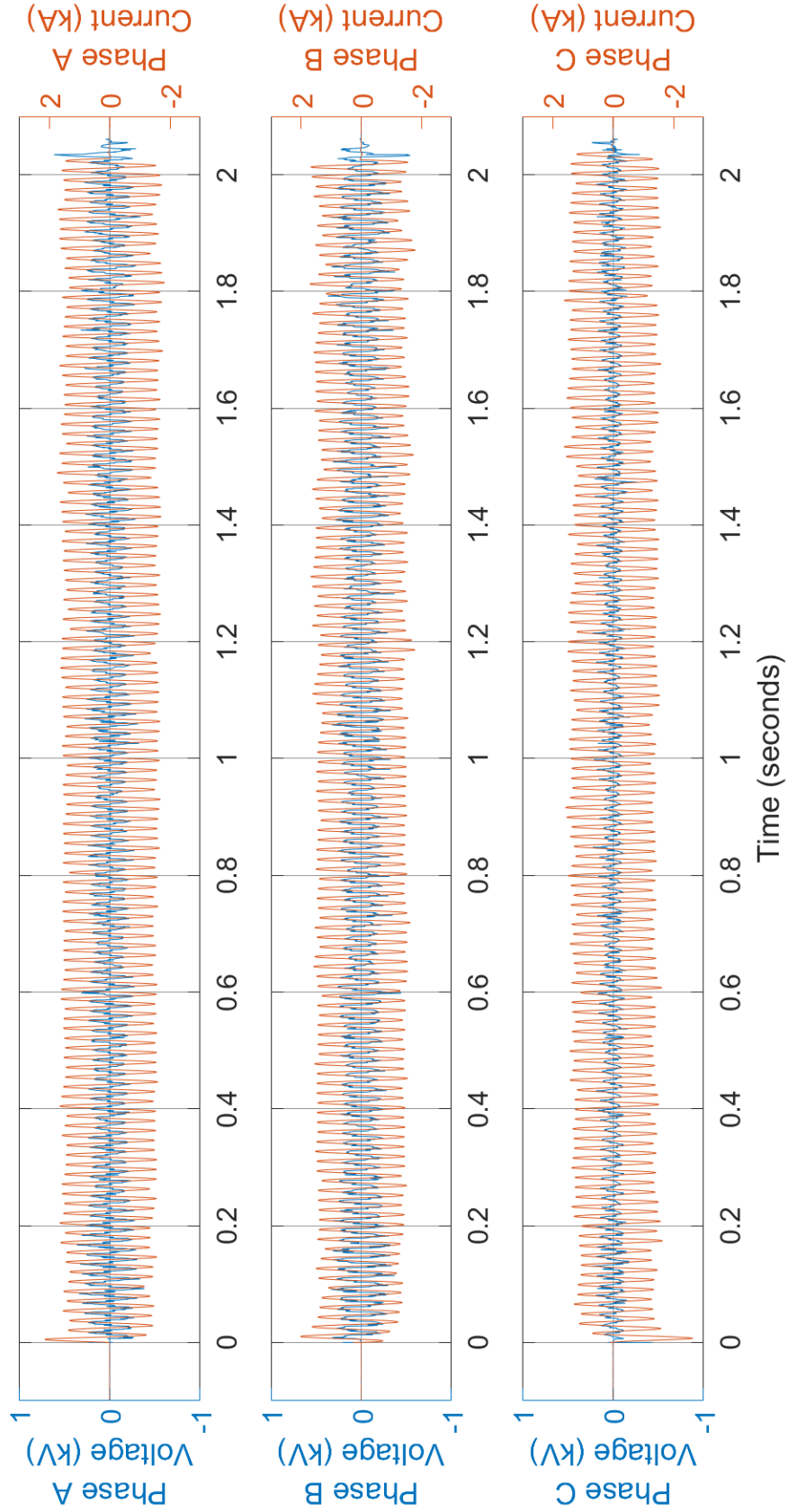


Fig. 99. Voltage and current measurements for Experiment OB01(b).

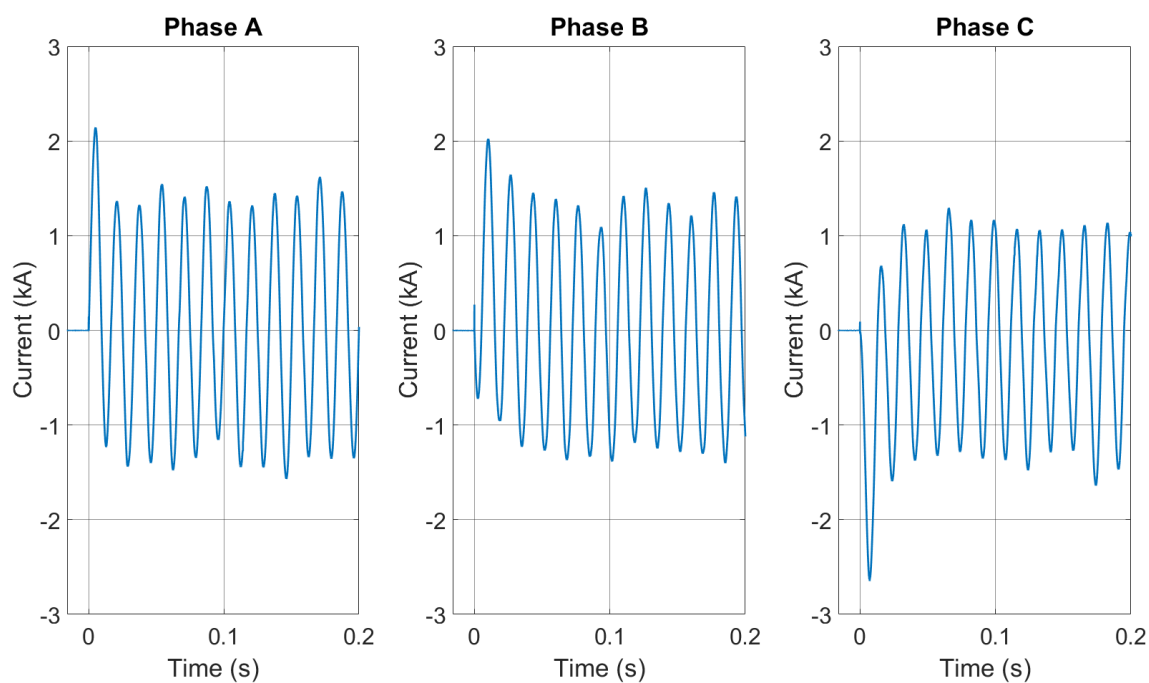


Fig. 100. Transient current profiles for Experiment OB01(b).

B.2.3 Experiment OB02

Electrical measurements are presented in Fig. 101 and Fig. 102.

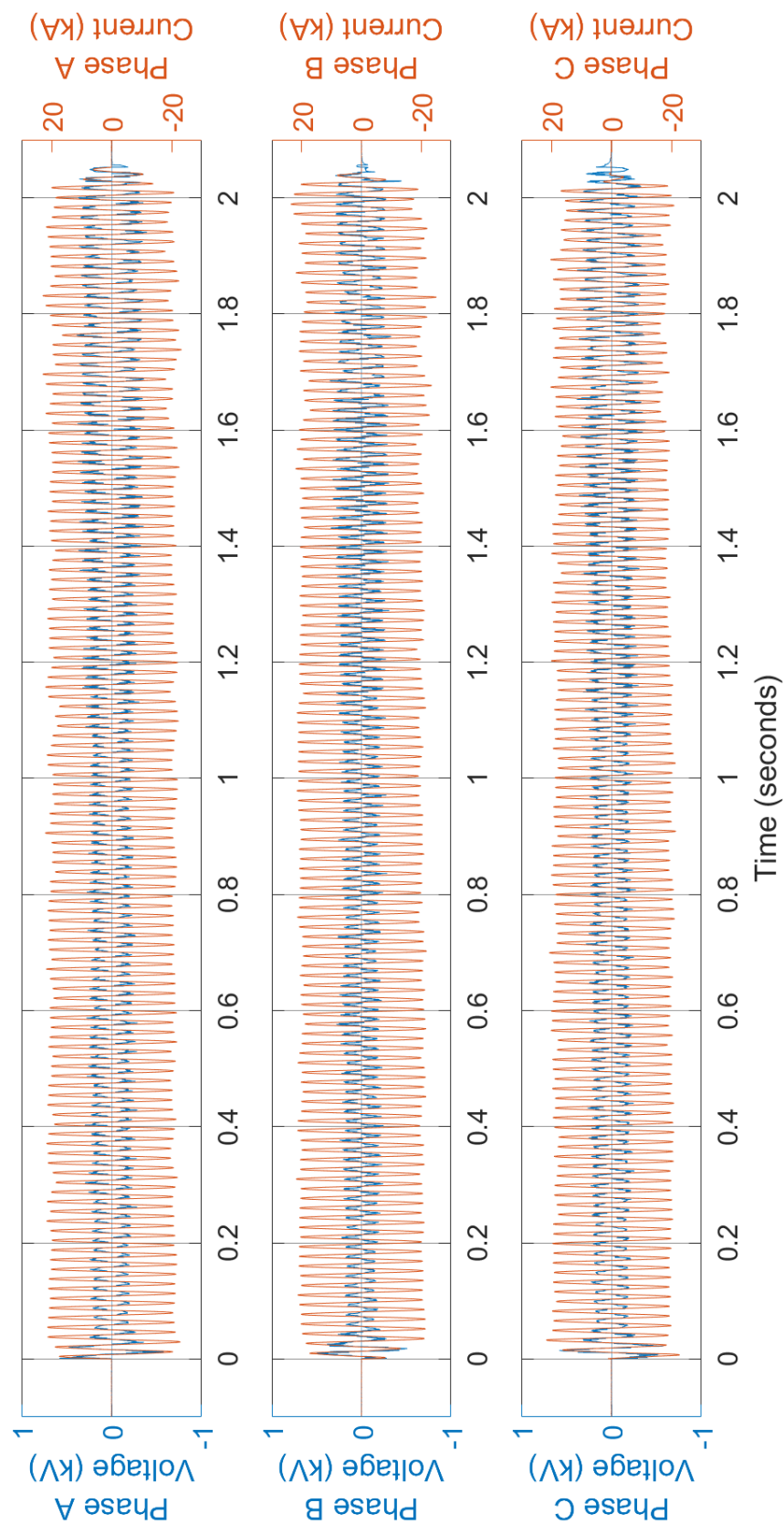


Fig. 101. Experiment OB02 voltage and current measurements.

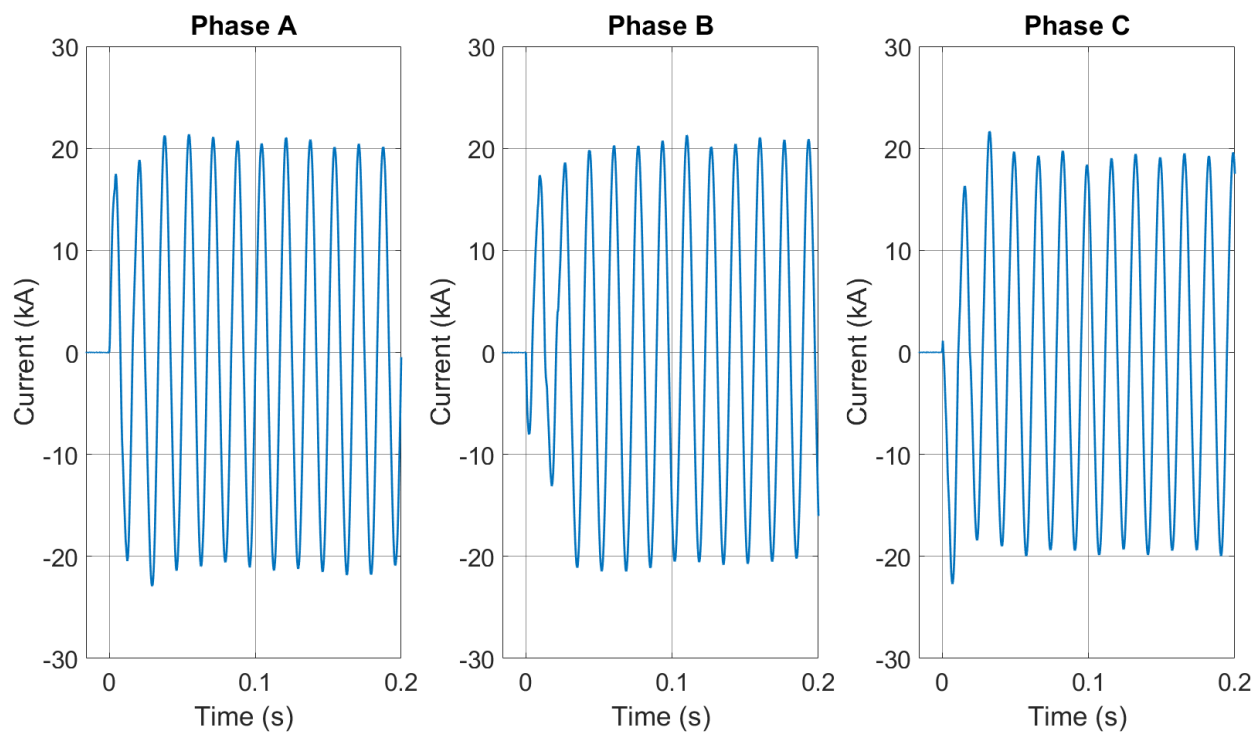


Fig. 102. Experiment OB02 transient current profiles.

B.2.4 Experiment OB03

Electrical measurements are presented in Fig. 103 and Fig. 104.

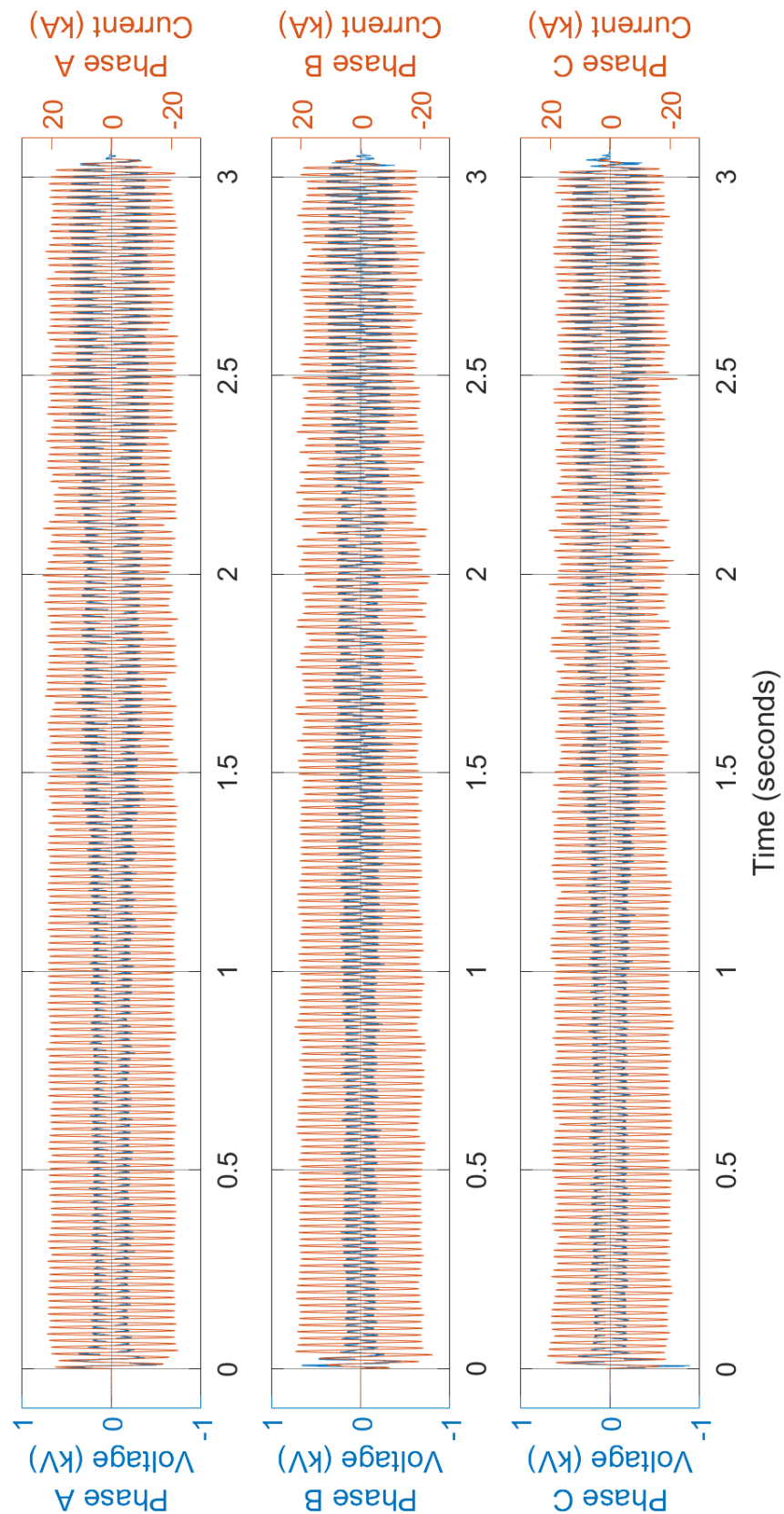


Fig. 103. Experiment OB03 voltage and current measurements.

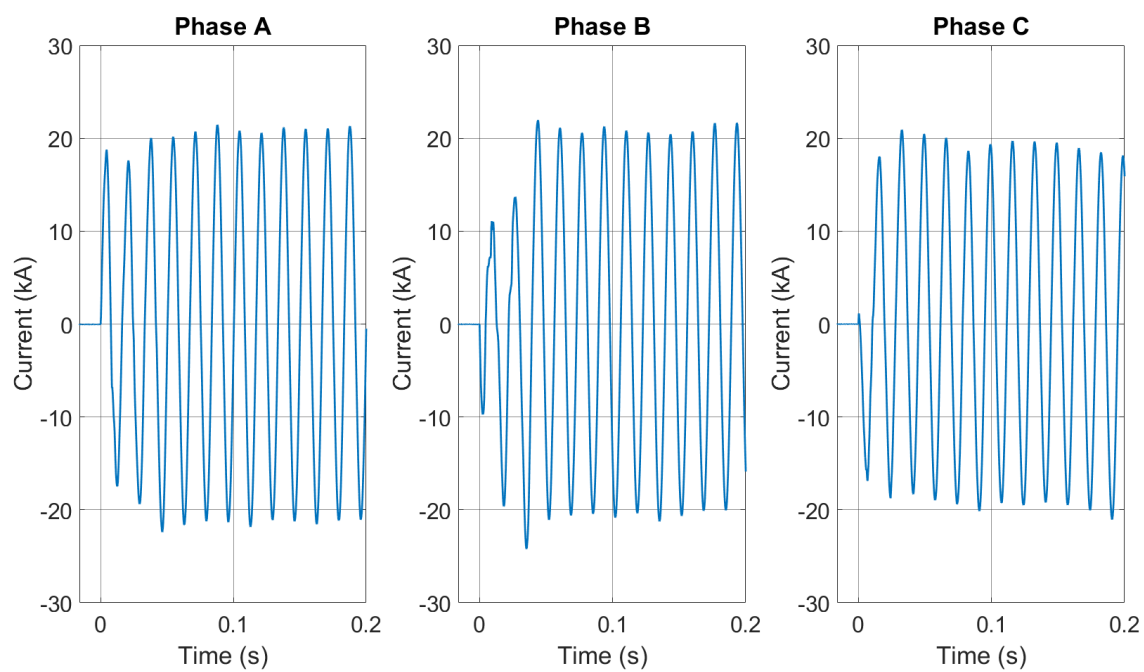


Fig. 104. Experiment OB03 transient current profiles.

B.2.5 Experiment OB04

Electrical measurements are presented in Fig. 105 and Fig. 106.

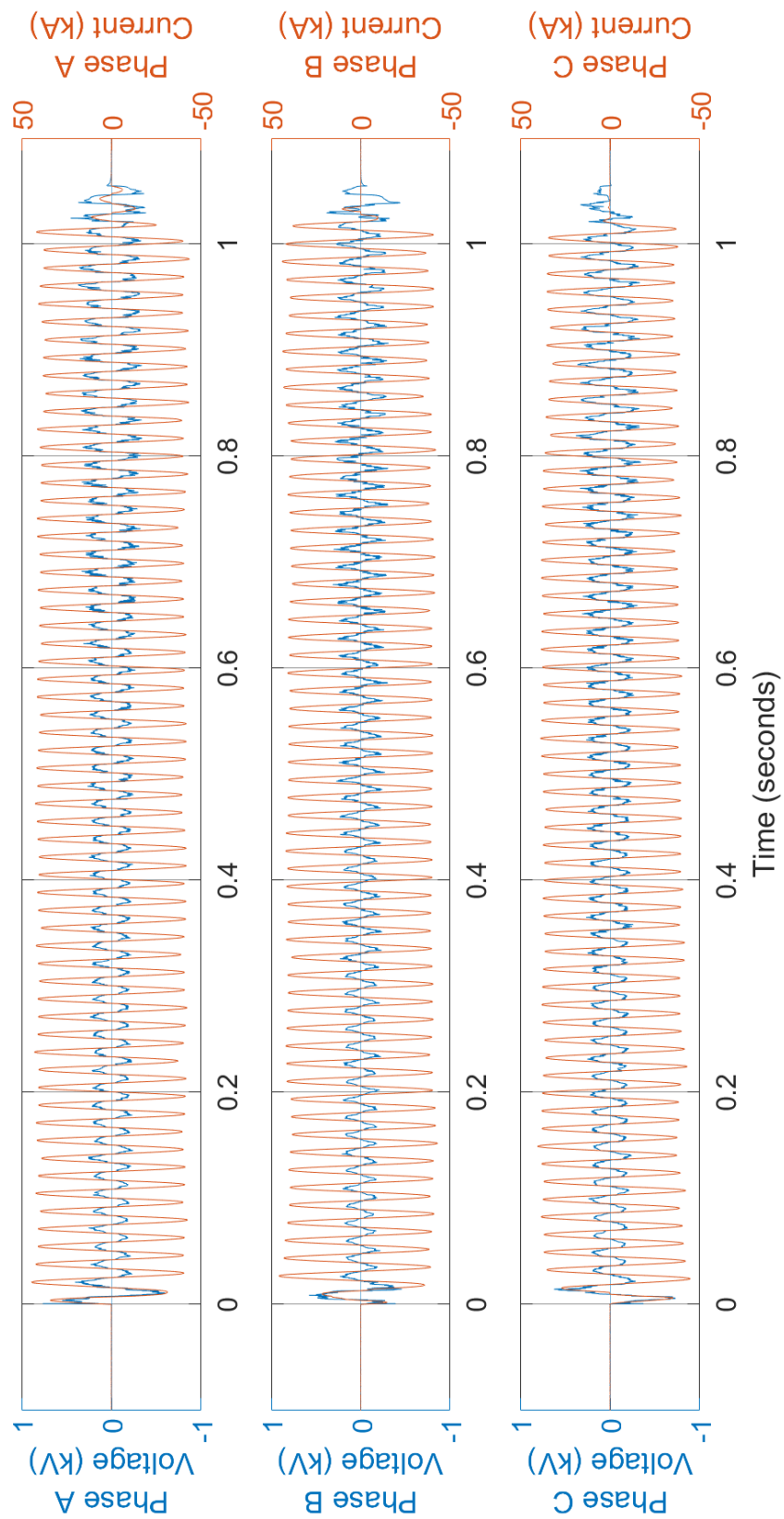


Fig. 105. Experiment OB04 voltage and current measurements.

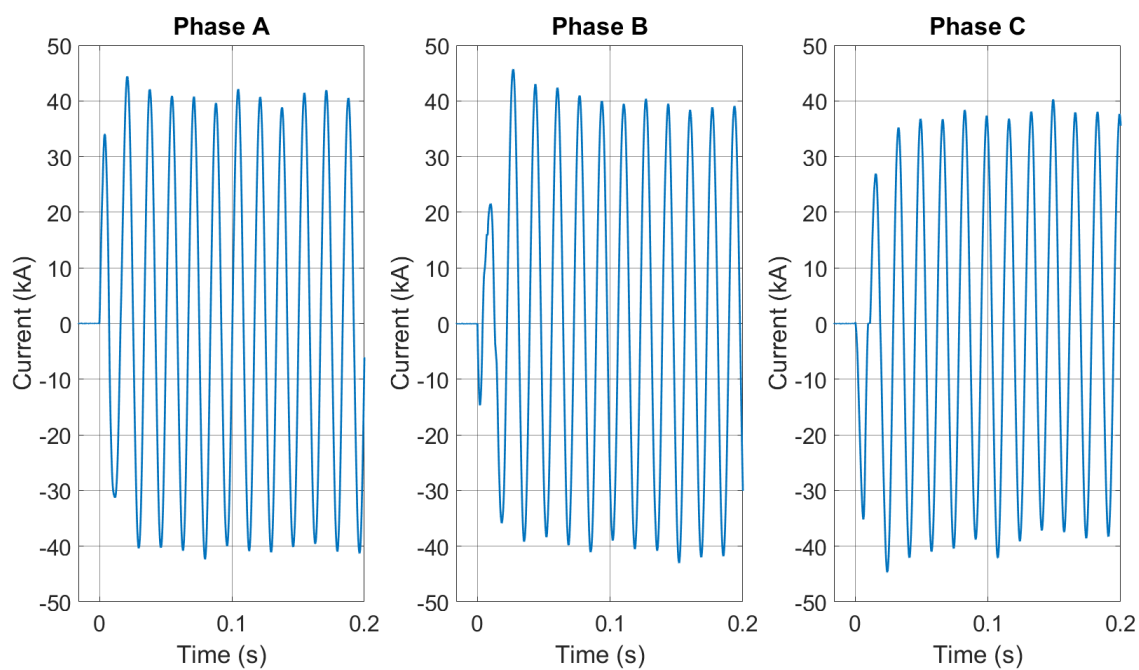


Fig. 106. Experiment OB04 transient current profiles.

B.2.6 Experiment OB05

Electrical measurements are presented in Fig. 107 and Fig. 108.

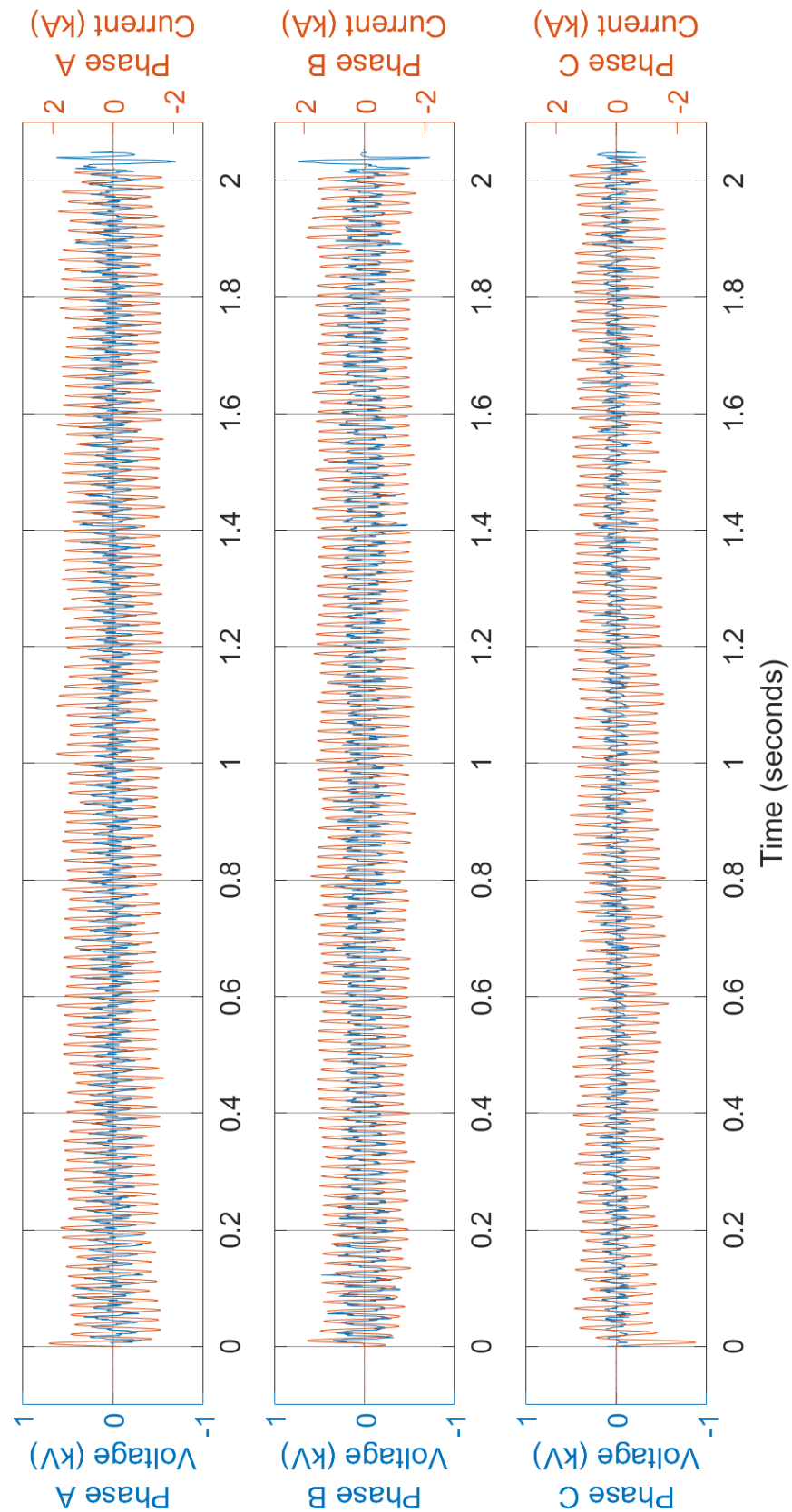


Fig. 107. Experiment OB05 voltage and current measurements.

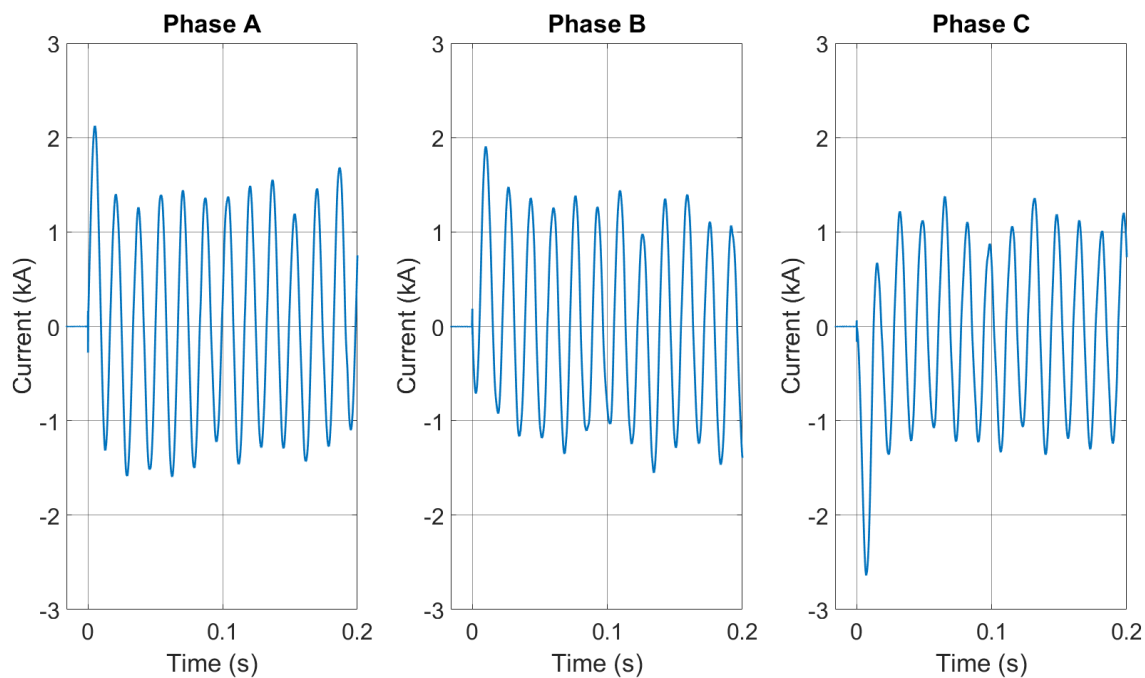


Fig. 108. Experiment OB05 transient current profiles.

B.2.7 Experiment OB06

Electrical measurements are presented in Fig. 109 and Fig. 110.

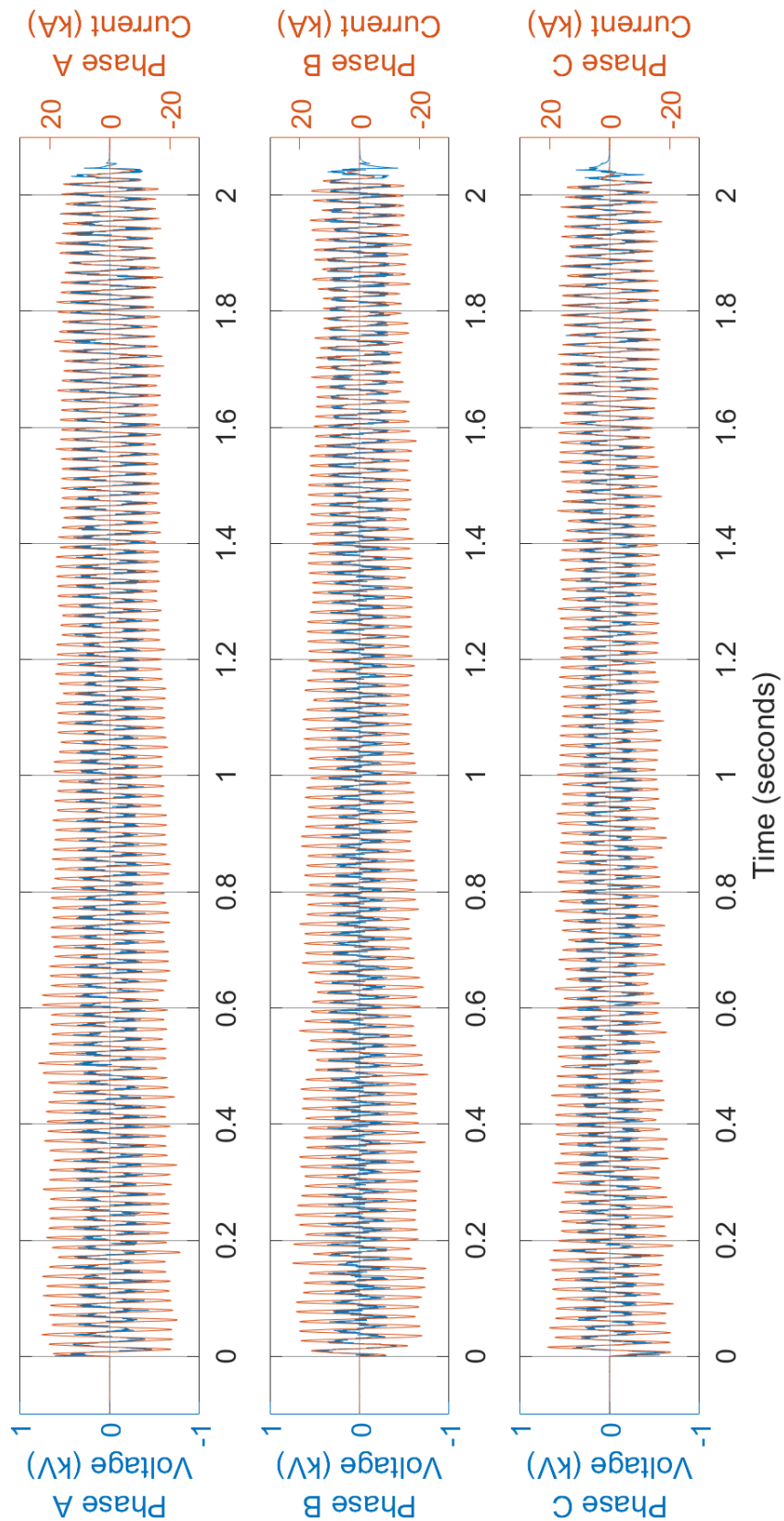


Fig. 109. Experiment OB06 voltage and current measurements.

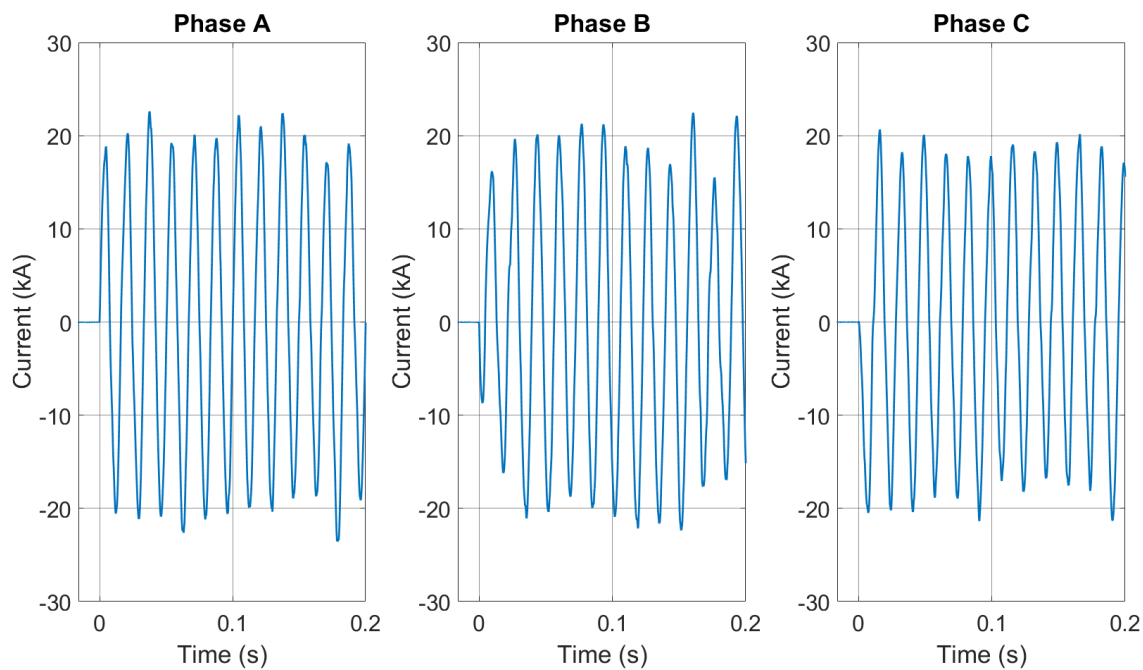


Fig. 110. Experiment OB06 transient current profiles.

B.2.8 Experiment OB07

Electrical measurements are presented in Fig. 111 through Fig. 112.

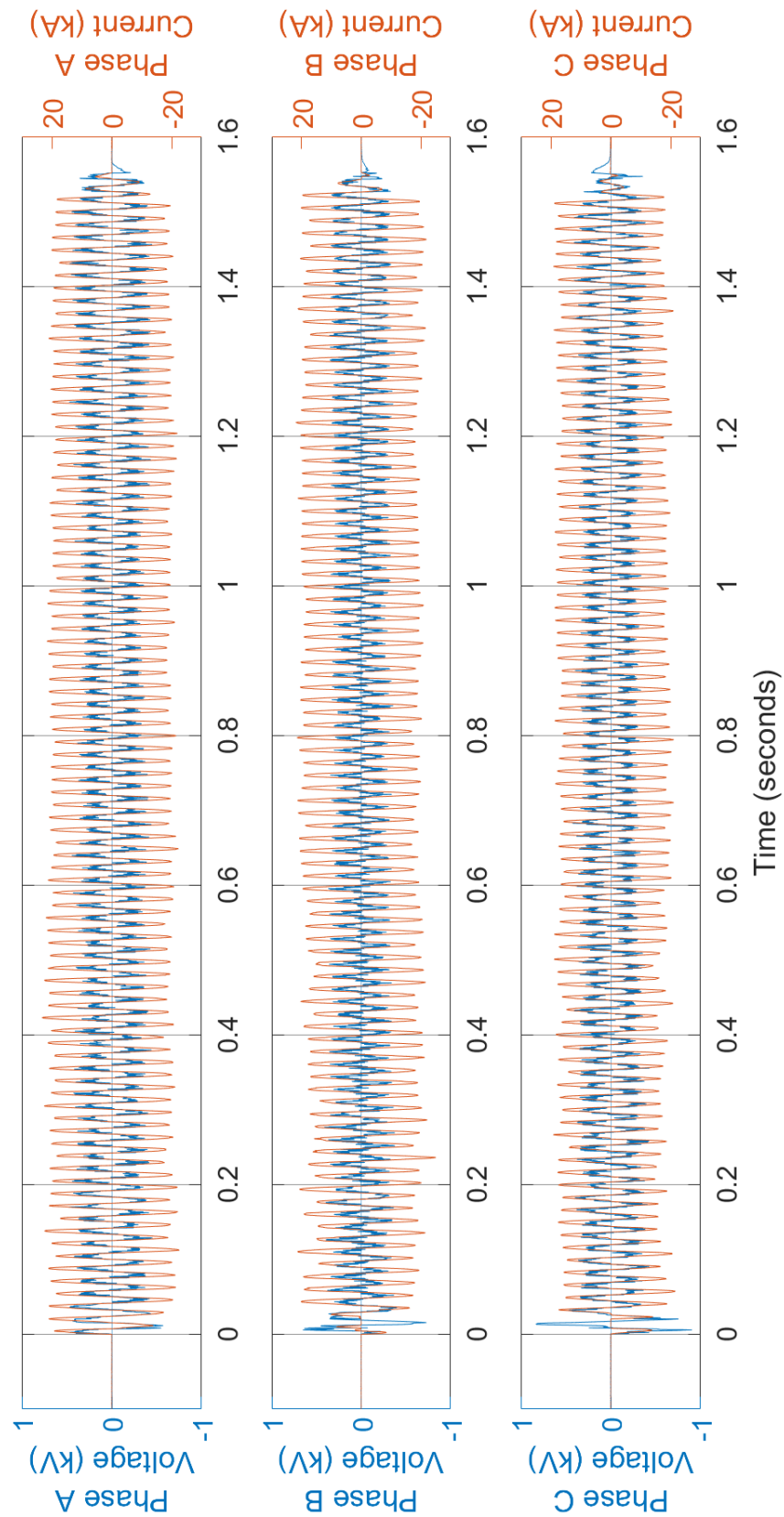


Fig. 111. Experiment OB07 voltage and current measurements.

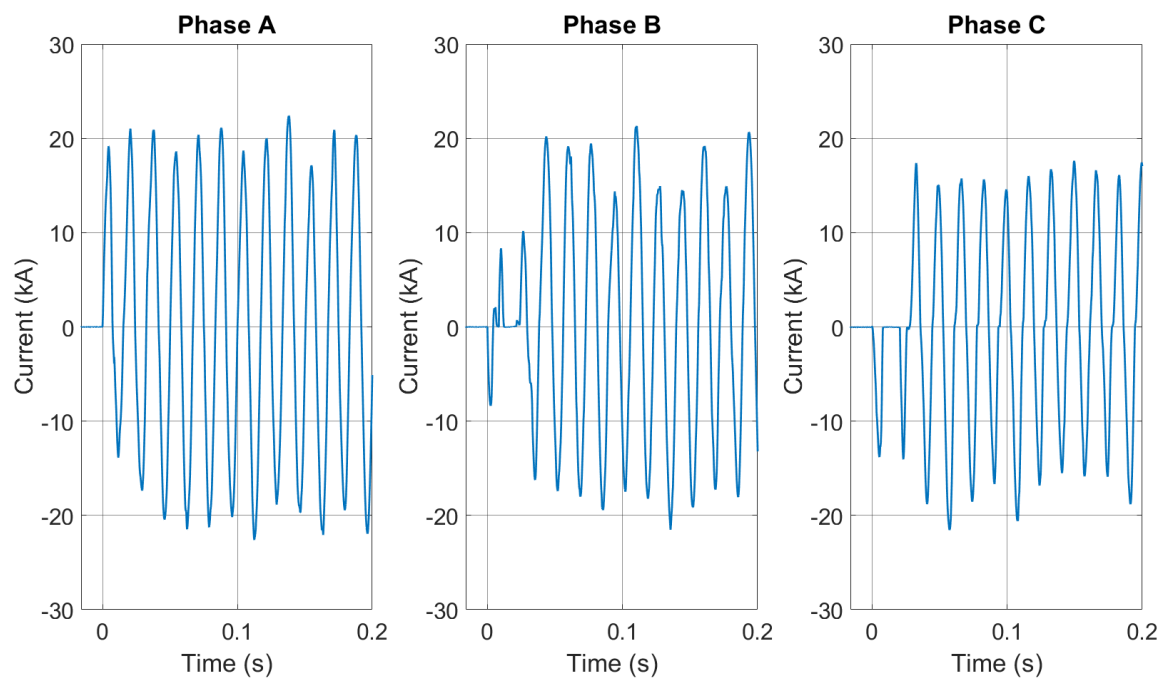


Fig. 112. Experiment OB07 transient current profiles.

B.2.9 Experiment OB08

The electrical measurements are presented in Fig. 113 and Fig. 114.

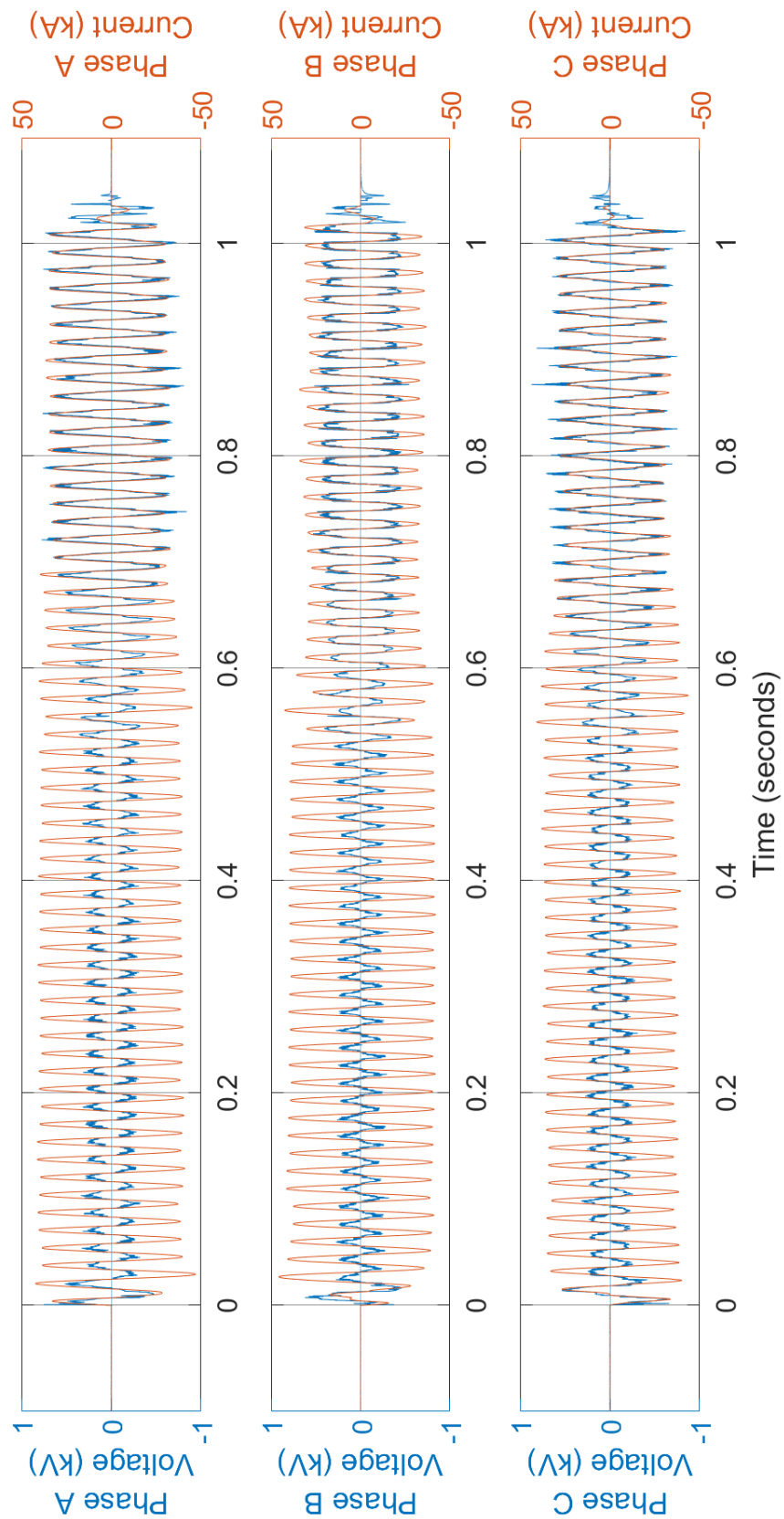


Fig. 113. Experiment OB08 voltage and current measurements.

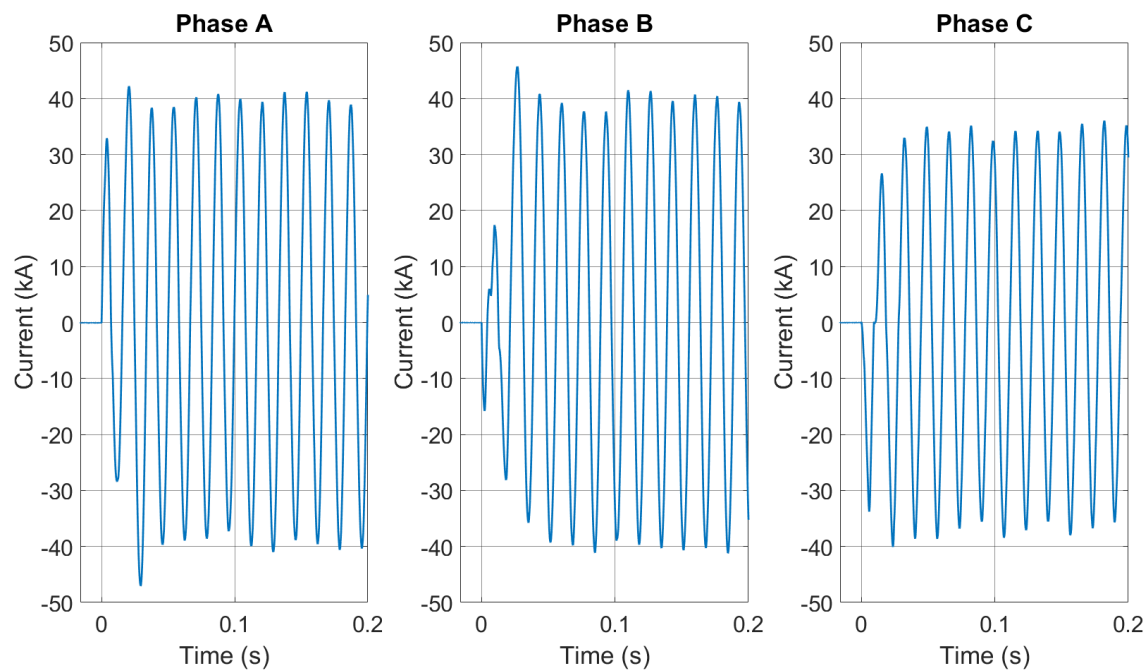


Fig. 114. Experiment OB08 transient current profiles.

B.2.10 Experiment OB09

Electrical measurements are presented in Fig. 115 and Fig. 116.

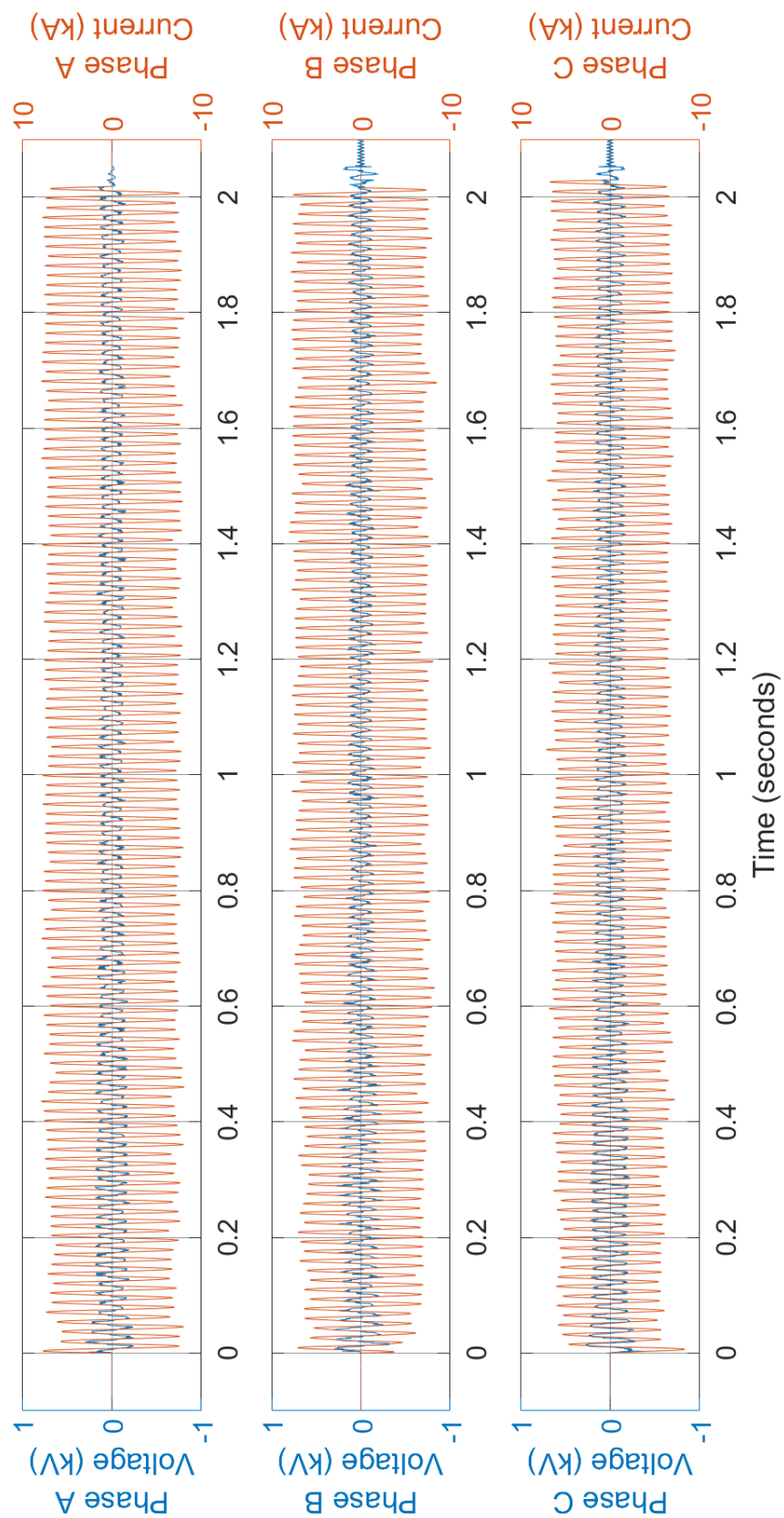


Fig. 115. Experiment OB09 voltage and current measurements.

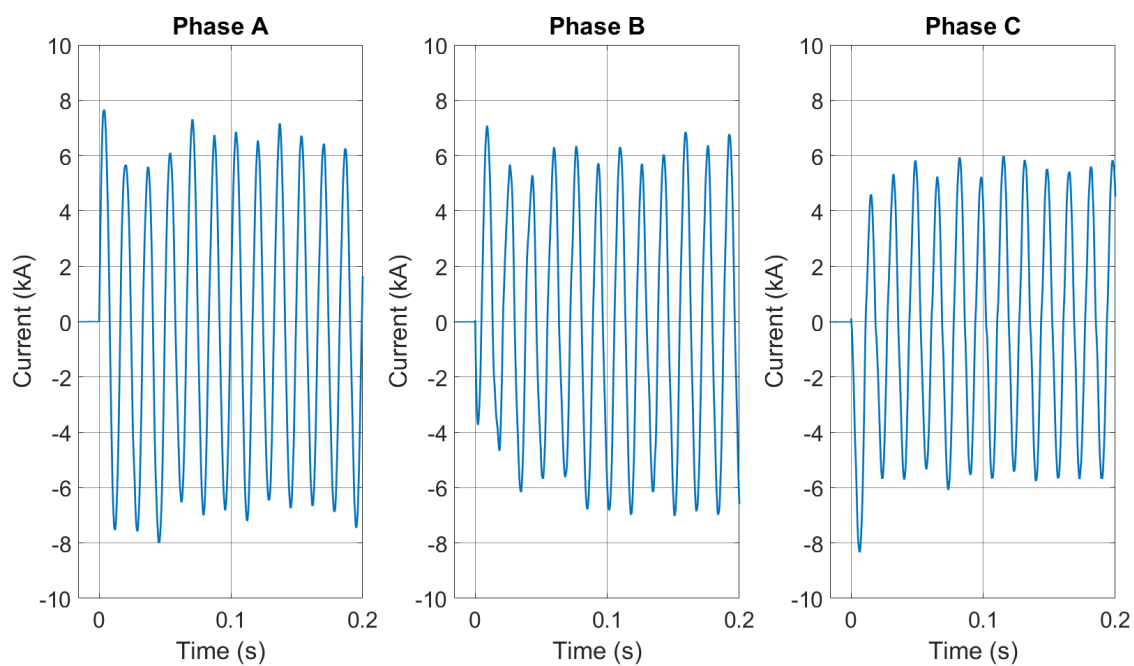


Fig. 116. Experiment OB09 transient current profiles.

B.2.11 Experiment OB10

Electrical measurements are presented in Fig. 117 and Fig. 118.

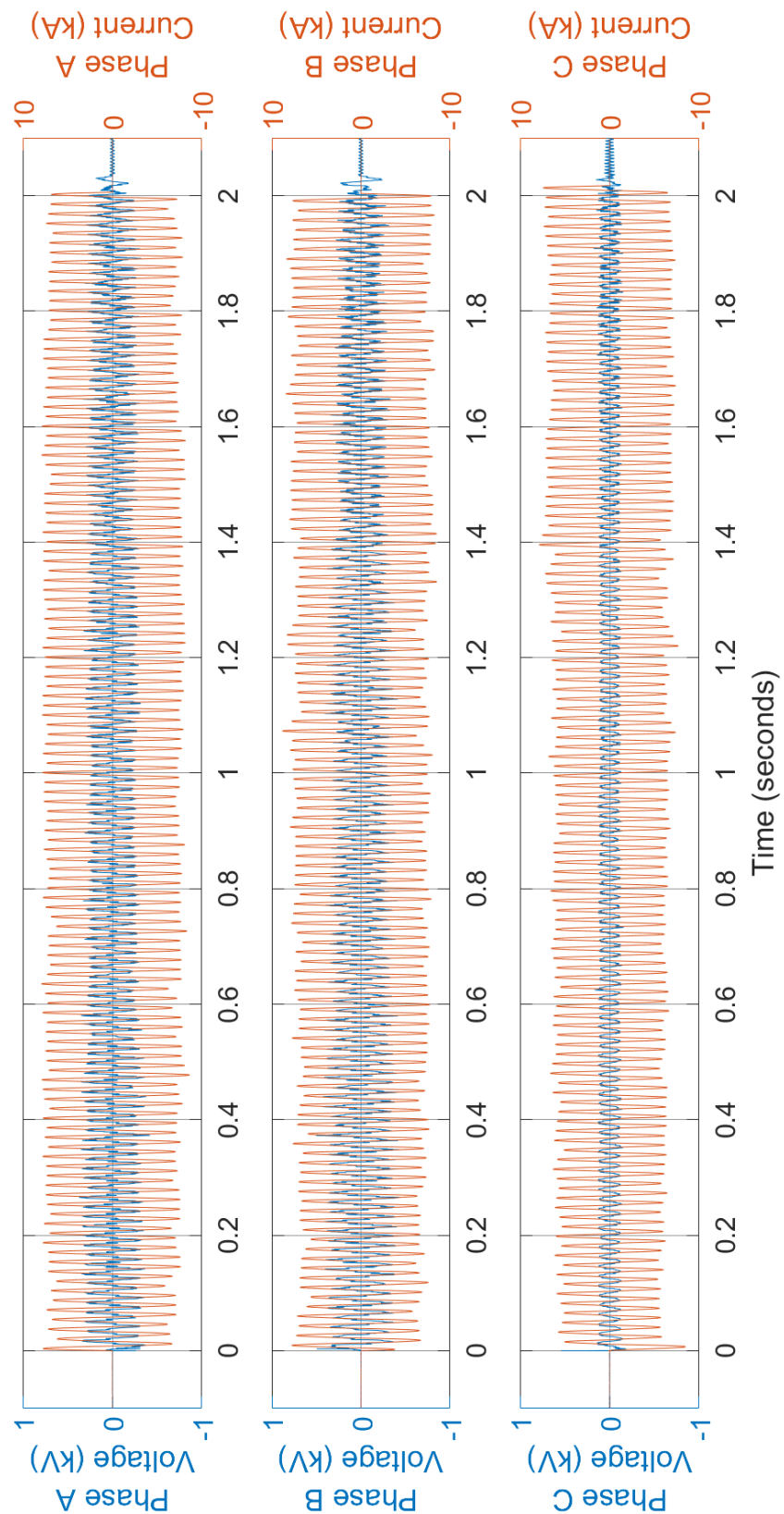


Fig. 117. Experiment OB10 voltage and current measurements.

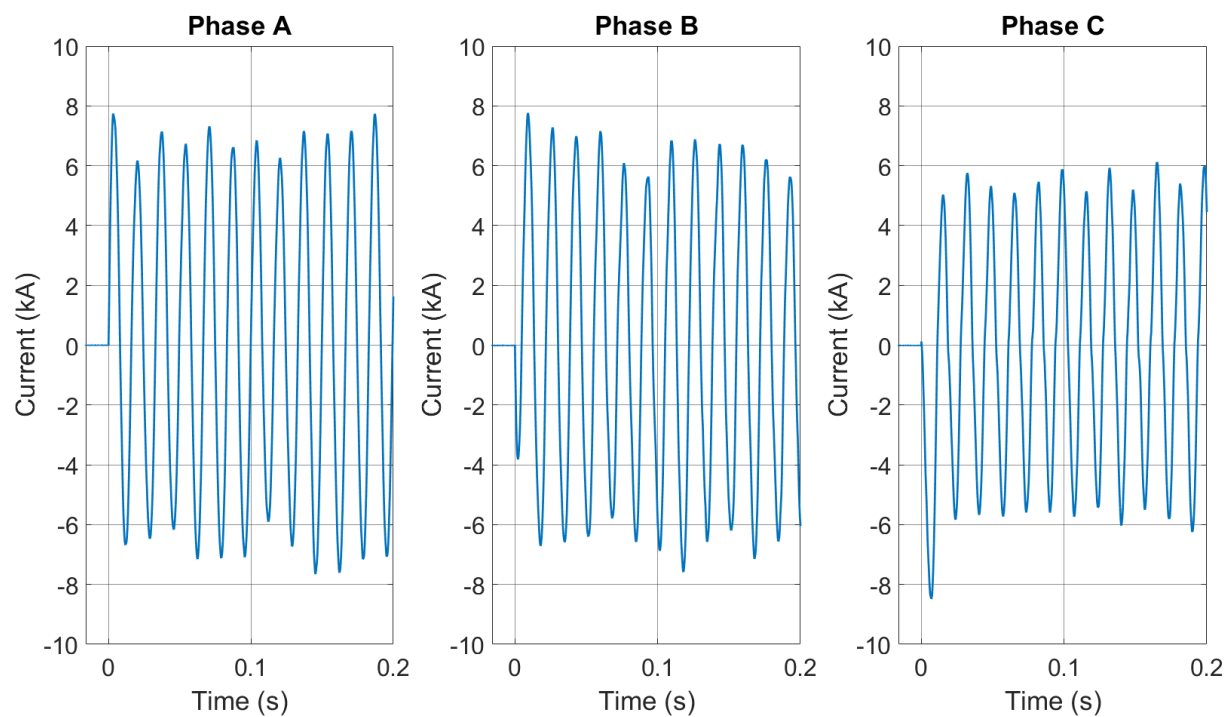


Fig. 118. Experiment OB10 transient current profiles.

B.2.12 Experiment OBMV01

Electrical measurements are presented in Fig. 119 through Fig. 121.

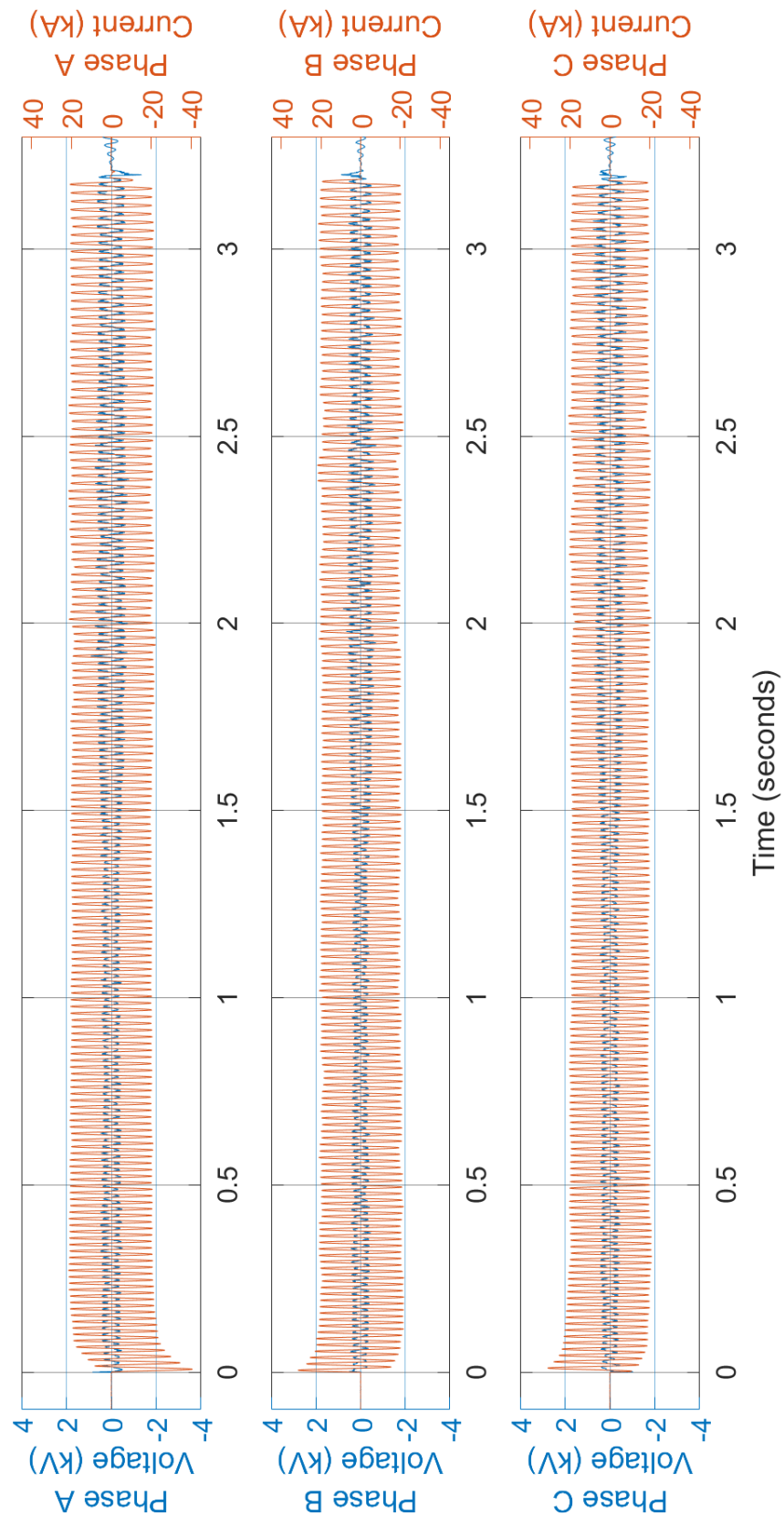


Fig. 119. Experiment OBMV01 voltage and current measurements.

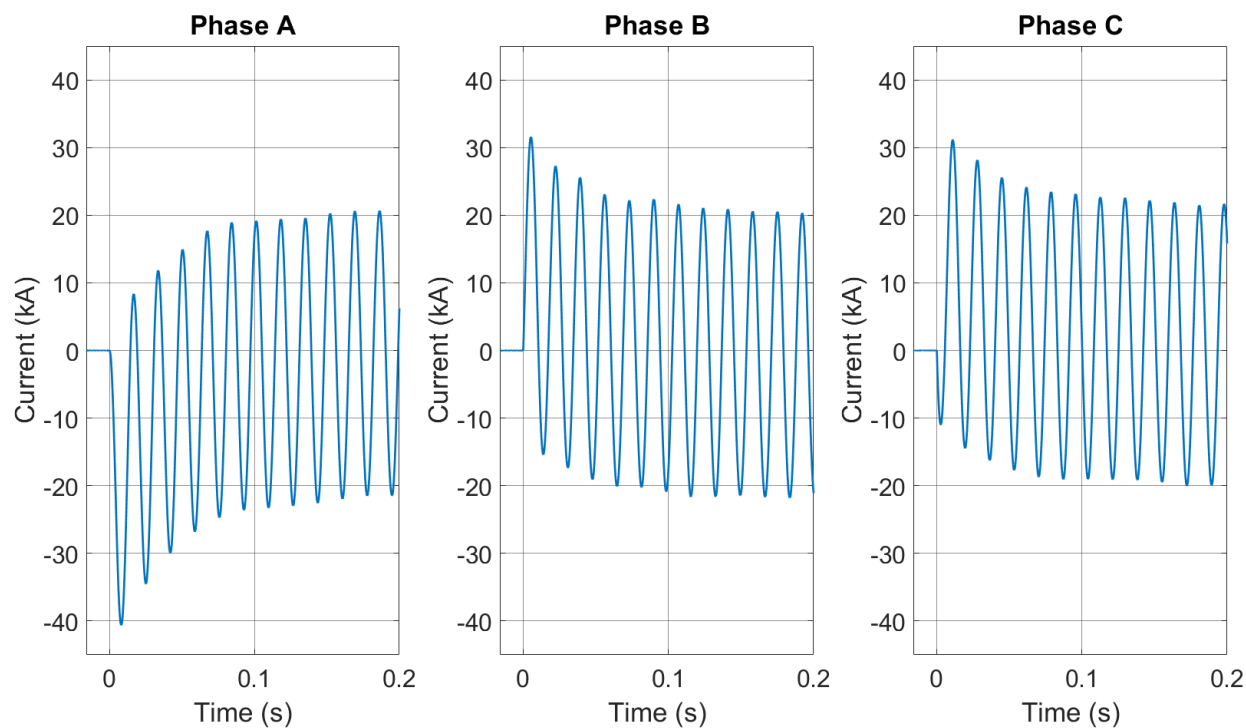


Fig. 120. Experiment OBMV01 transient current profiles.

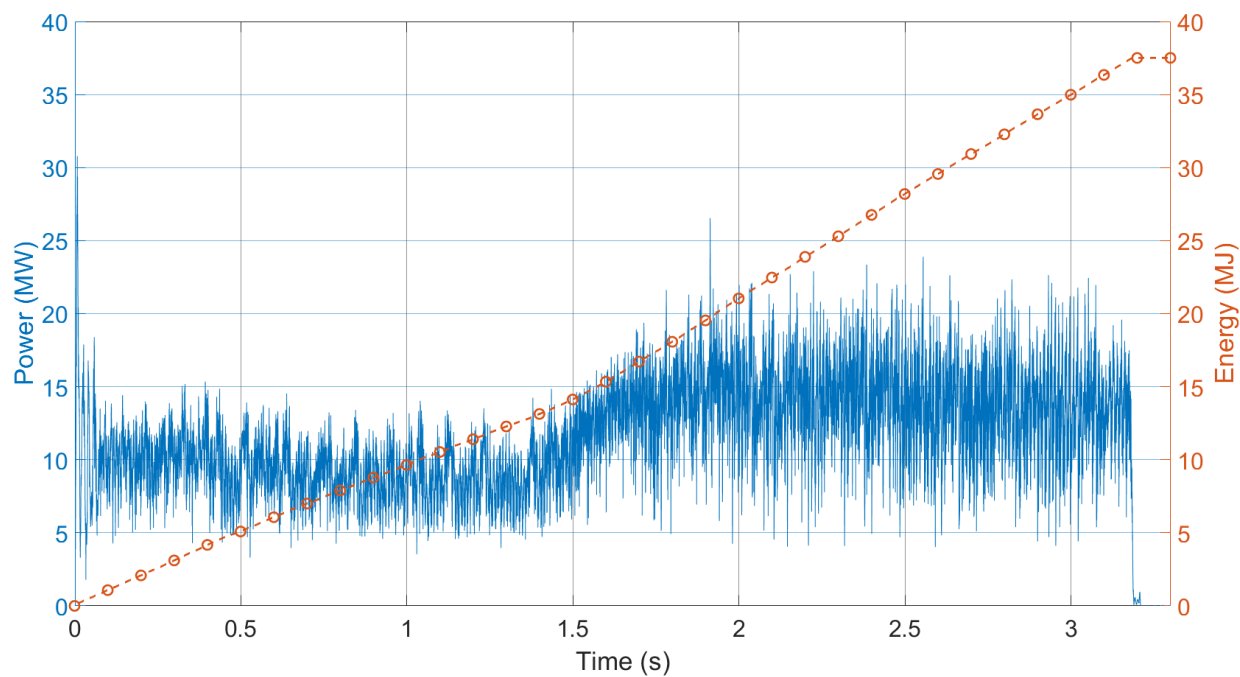


Fig. 121. Experiment OBMV01 power and energy profiles.

B.2.13 Experiment OBMV02

Electrical measurements are presented in Fig. 122 through Fig. 124.

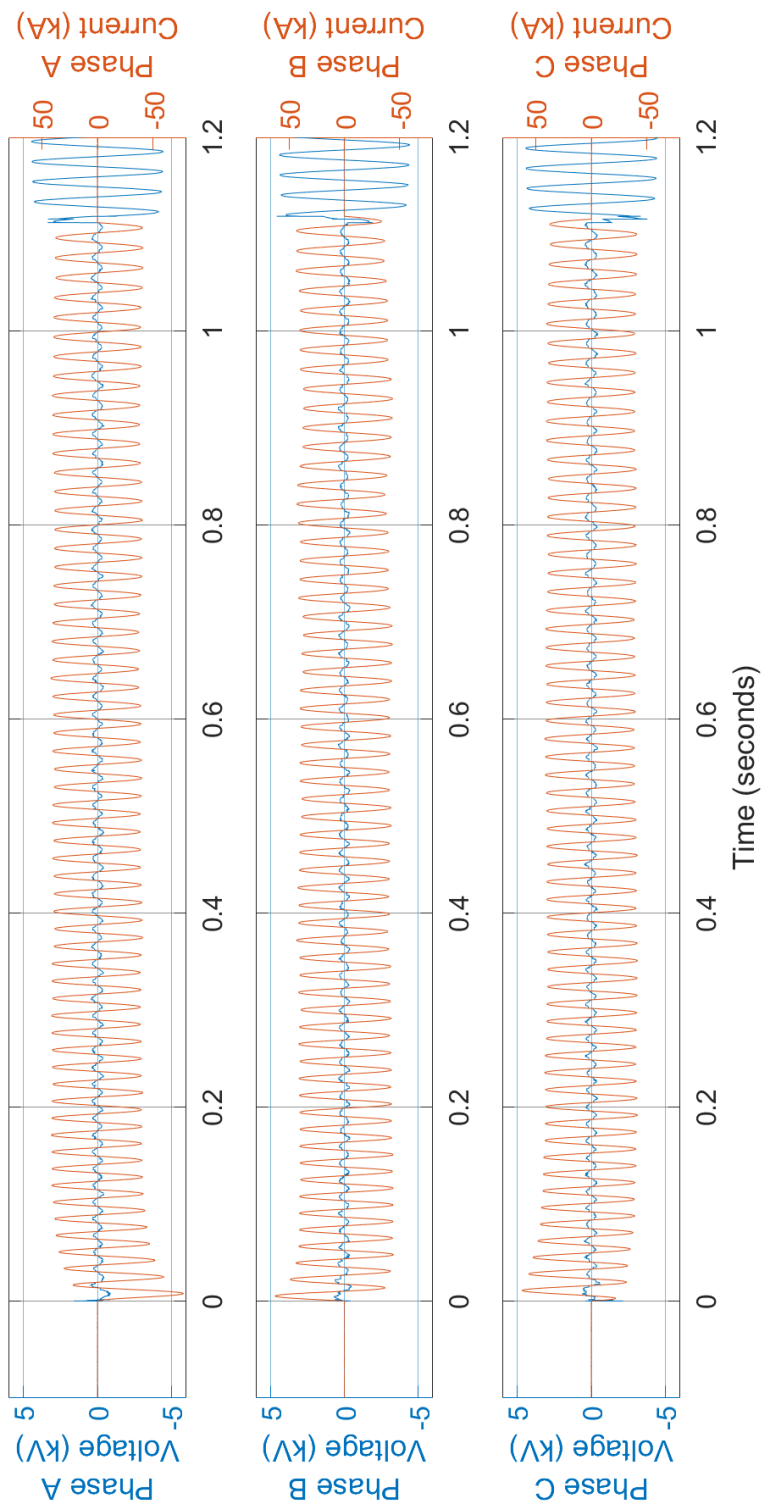


Fig. 122. Experiment OBMV02 voltage and current measurements.

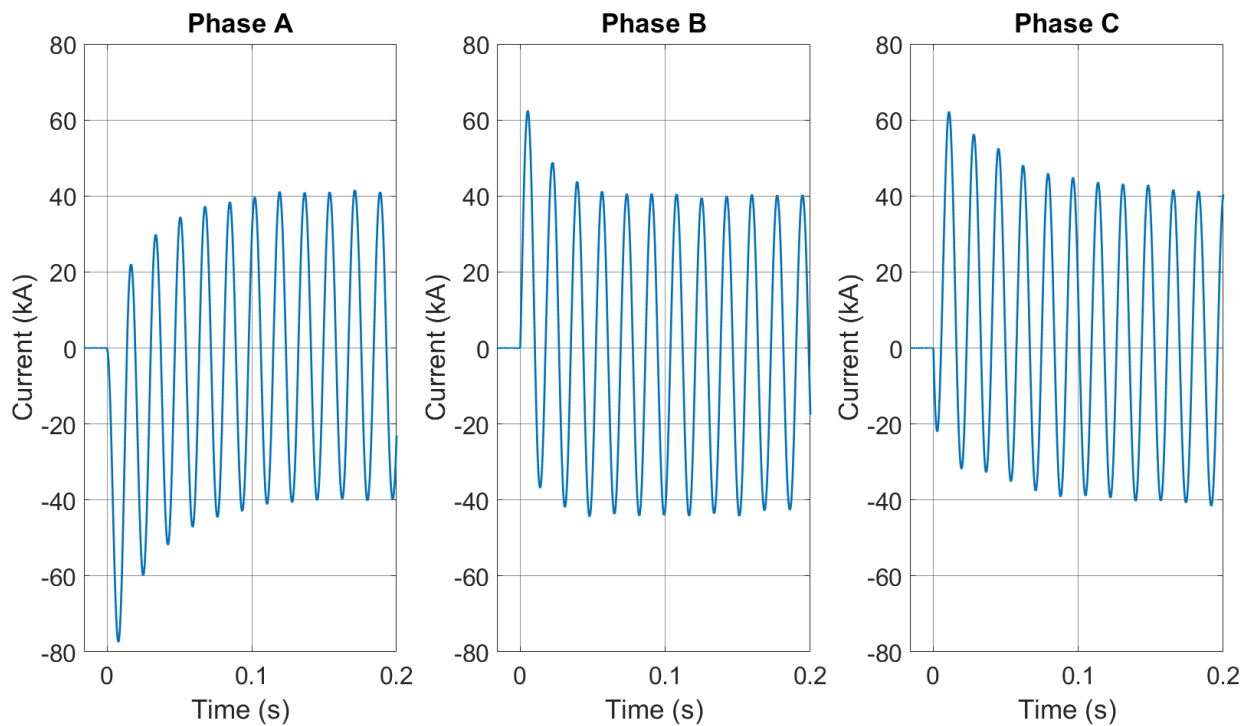


Fig. 123. Experiment OBMV02 transient current profiles.

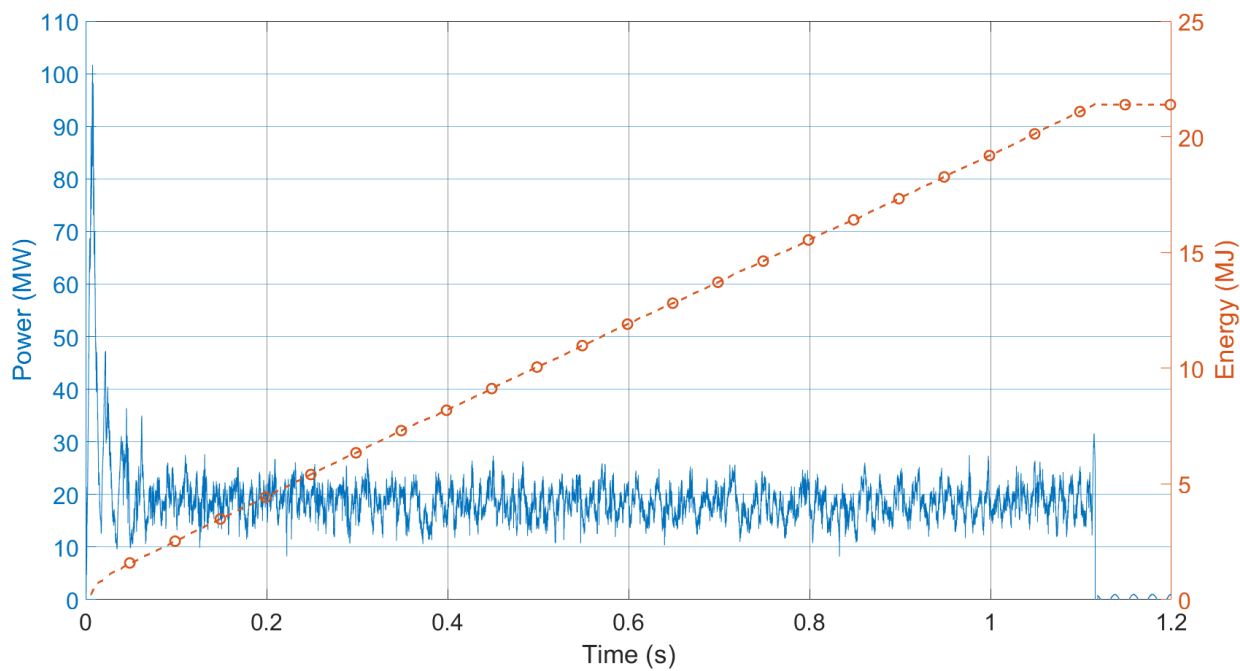


Fig. 124. Experiment OBMV02 power and energy profiles.

B.2.14 Experiment OBMV03

Electrical measurements are presented in Fig. 125 through Fig. 127.

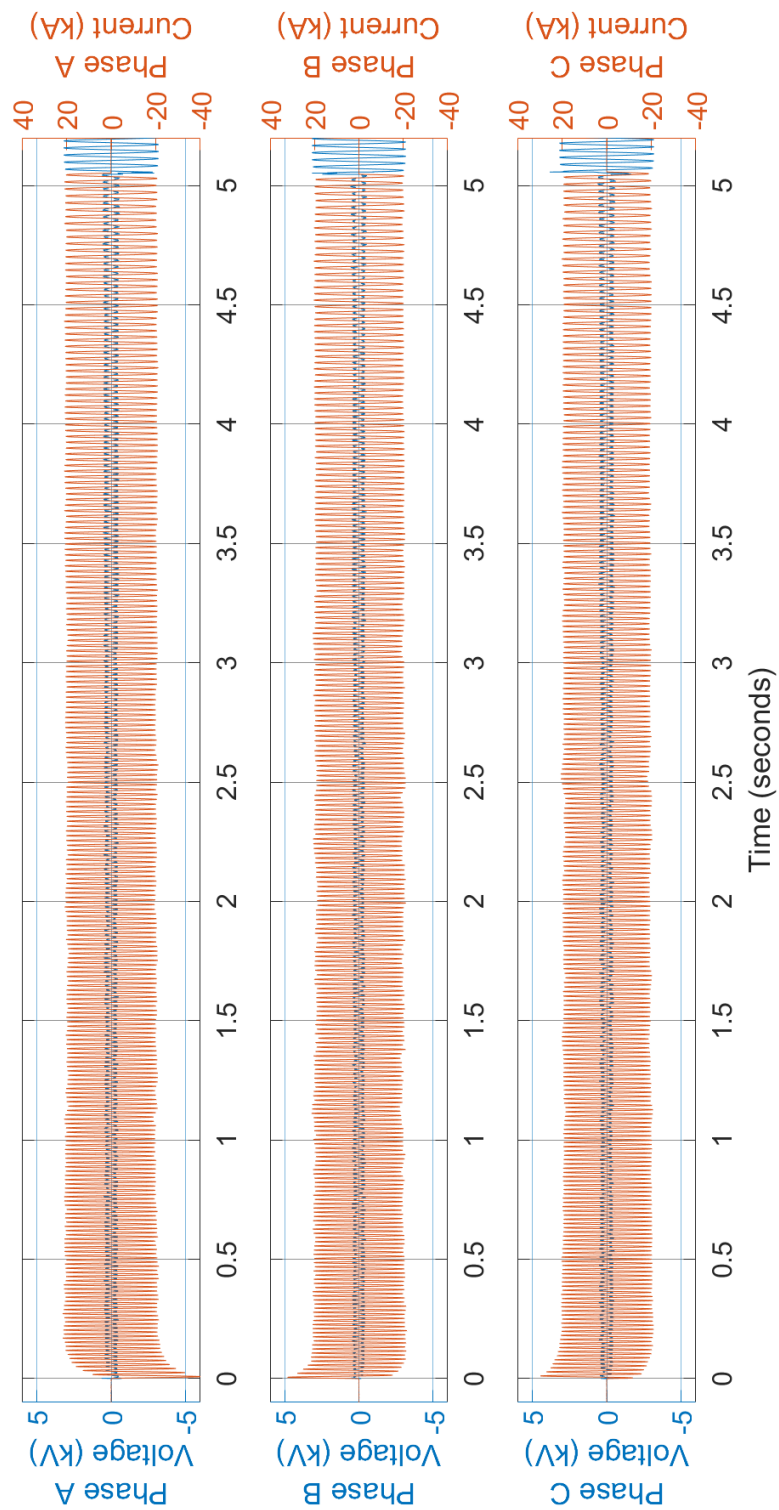


Fig. 125. Experiment OBMV03 voltage and current measurements.

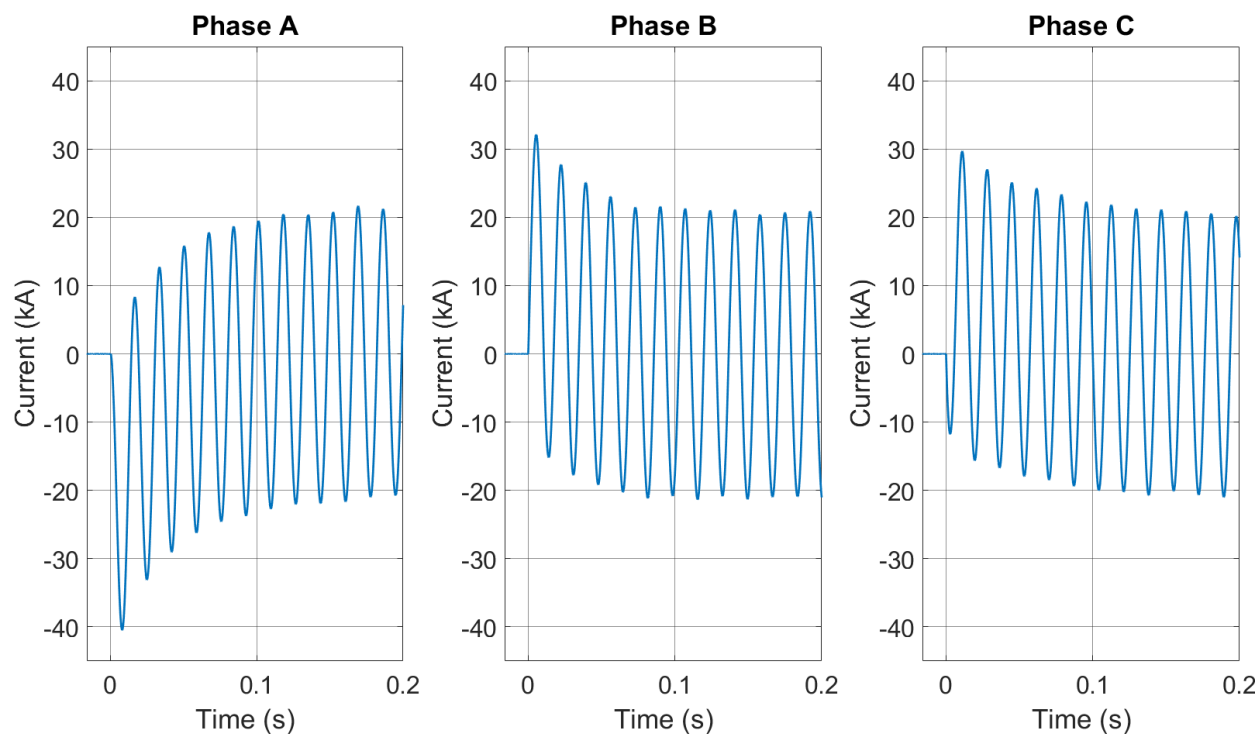


Fig. 126. Experiment OBMV03 transient current profiles.

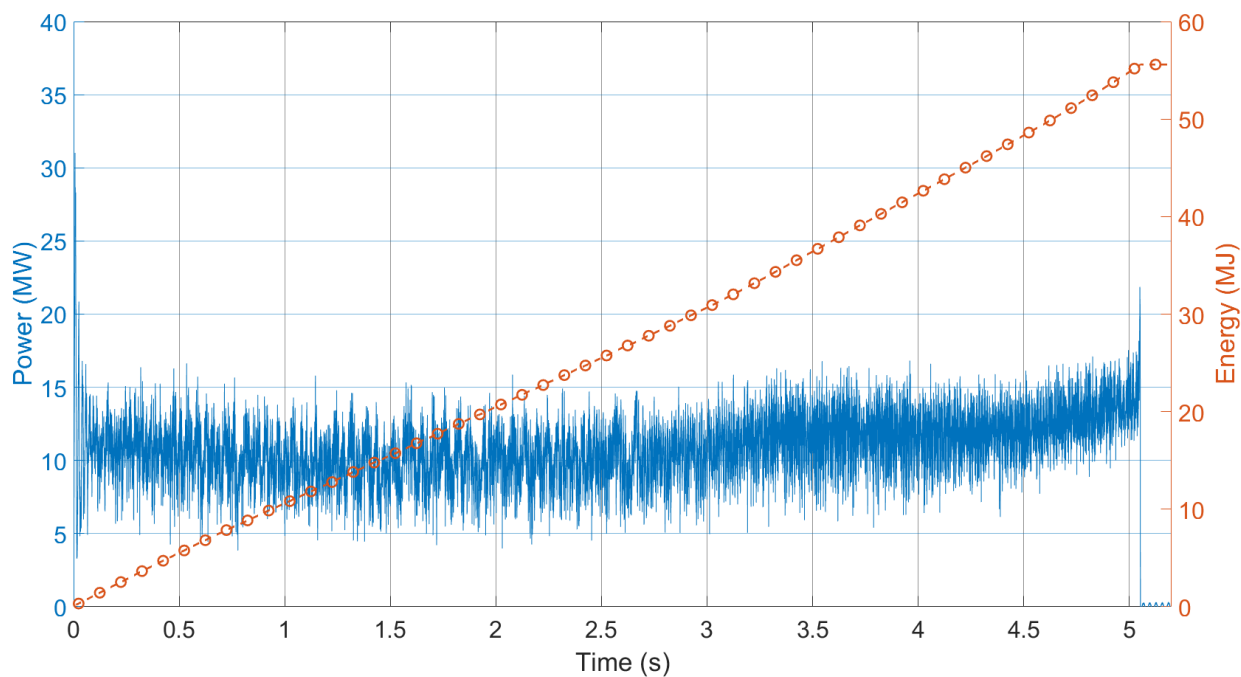


Fig. 127. Experiment OBMV03 power and energy profiles.

B.2.15 Experiment OBMV04

Electrical measurements are presented in Fig. 128 through Fig. 130.

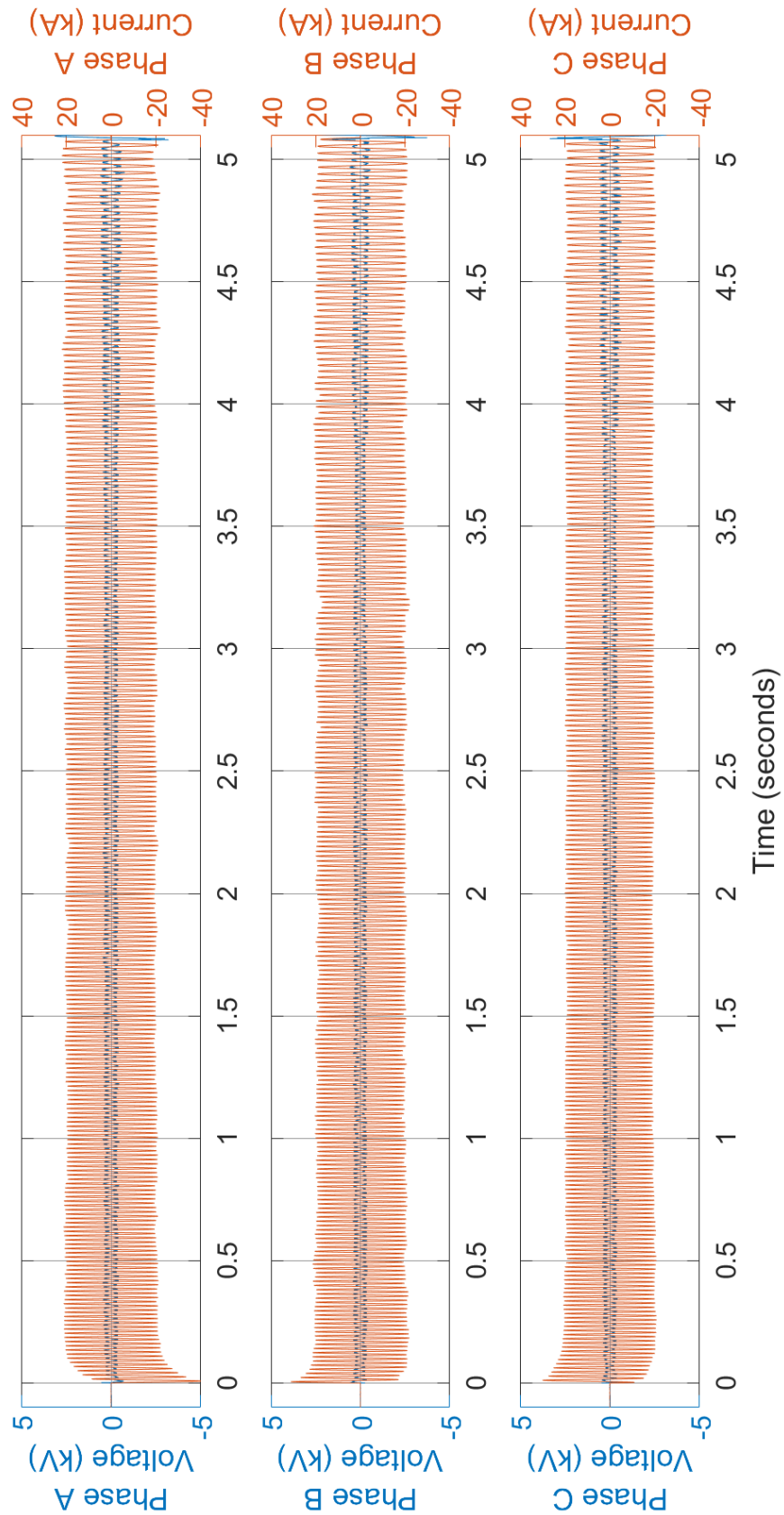


Fig. 128. Experiment OBMV04 voltage and current measurements.

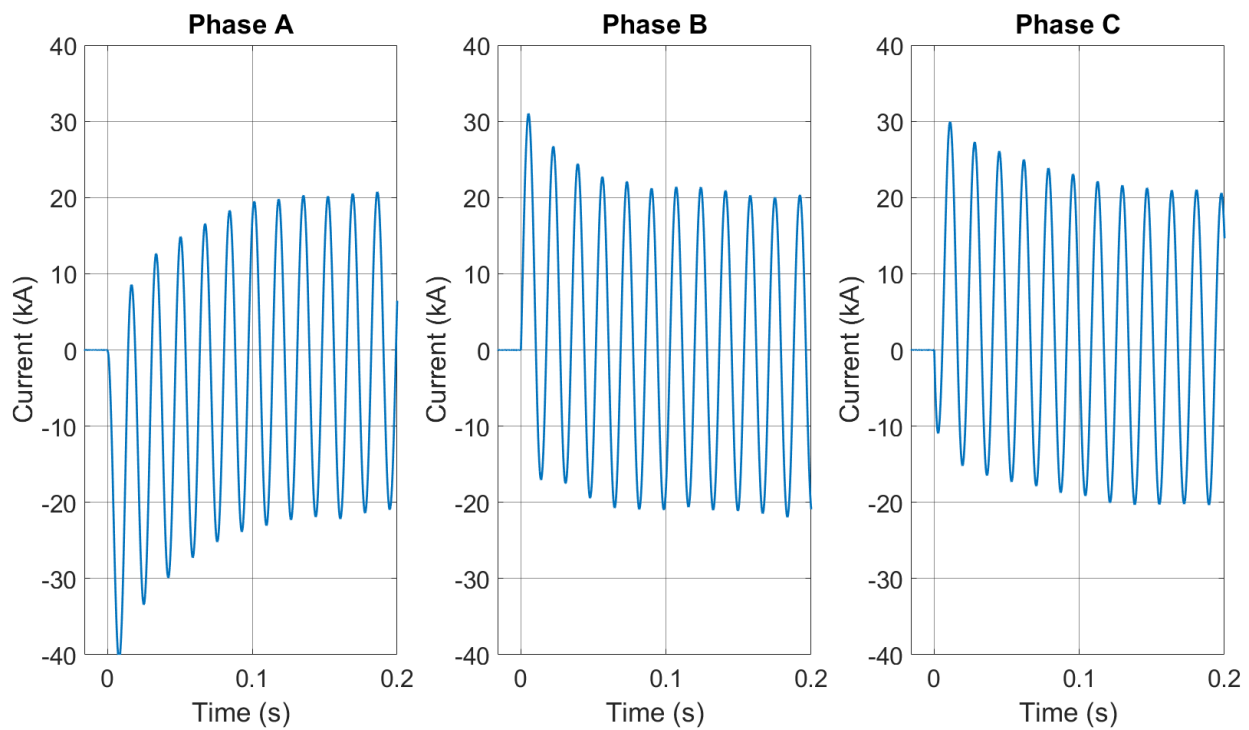


Fig. 129. Experiment OBMV04 transient current profiles.

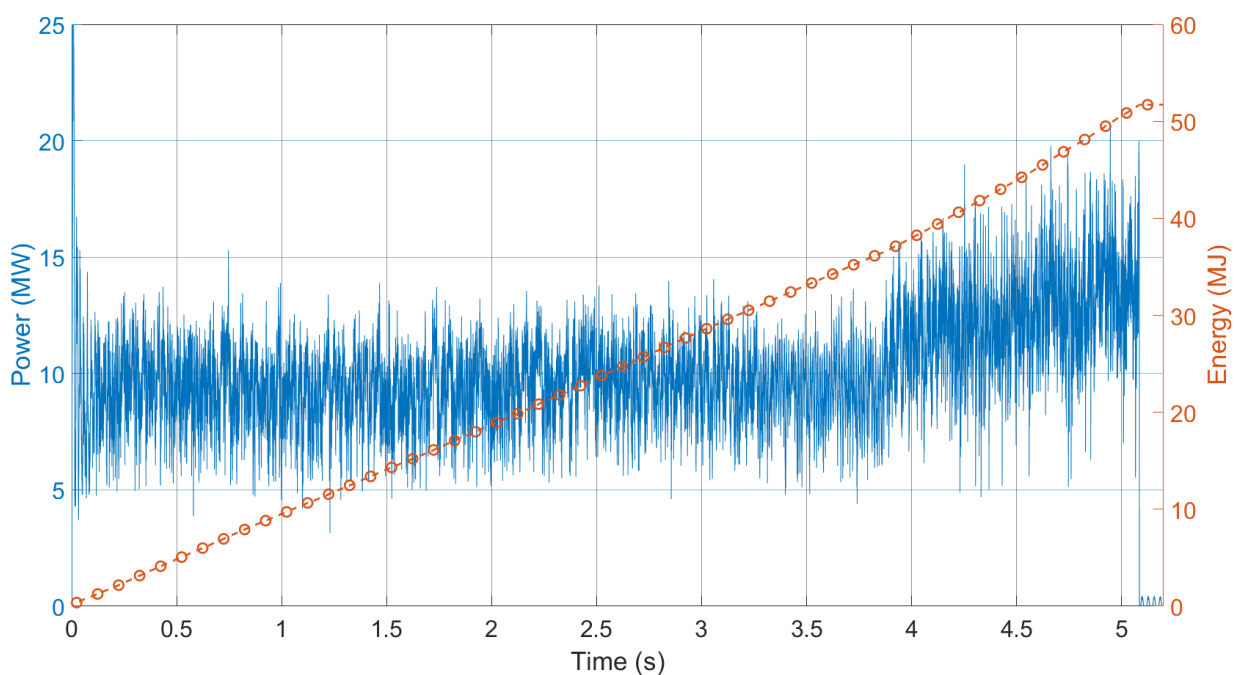


Fig. 130. Experiment OBMV04 power and energy profiles.

B.2.16 Experiment OBMV05

Electrical measurements are presented in Fig. 131 through Fig. 133.

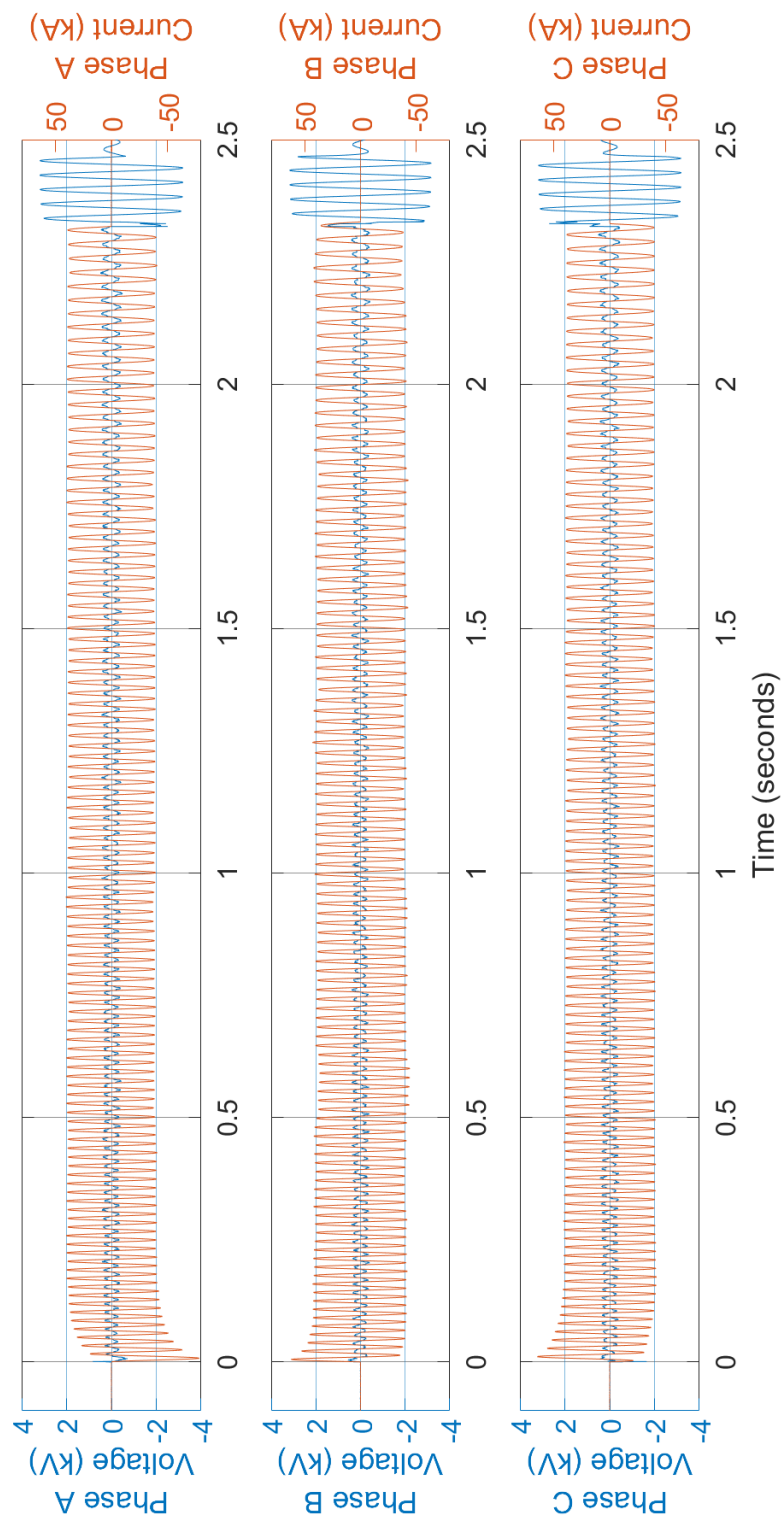


Fig. 131. Experiment OBMV05 voltage and current measurements.

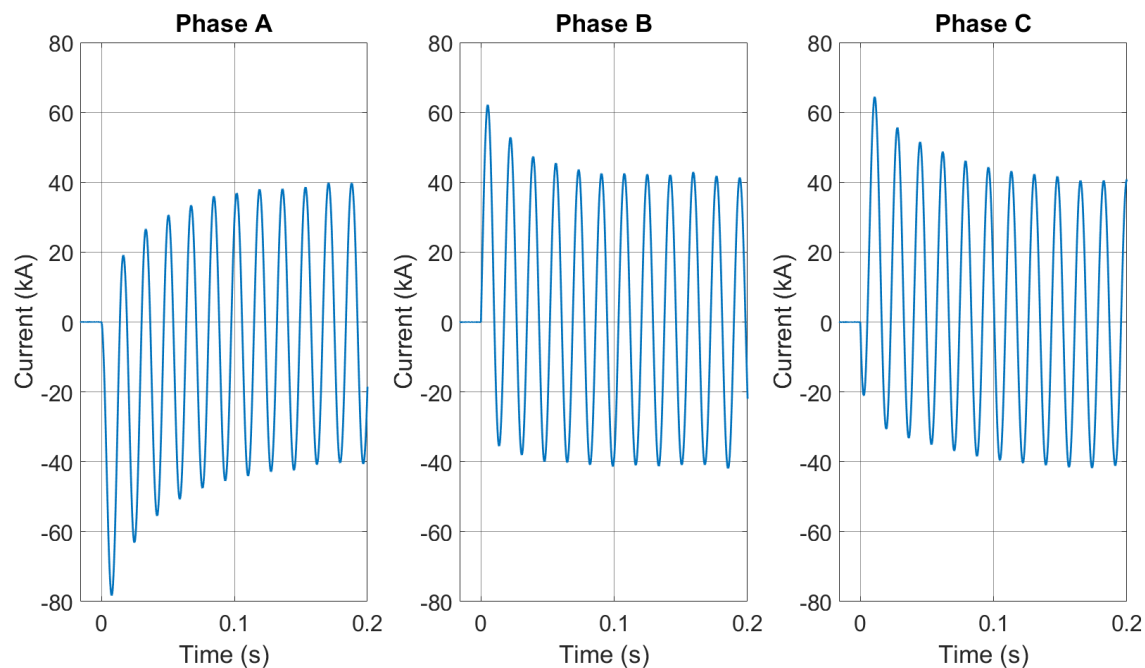


Fig. 132. Experiment OBMV05 transient current profiles.

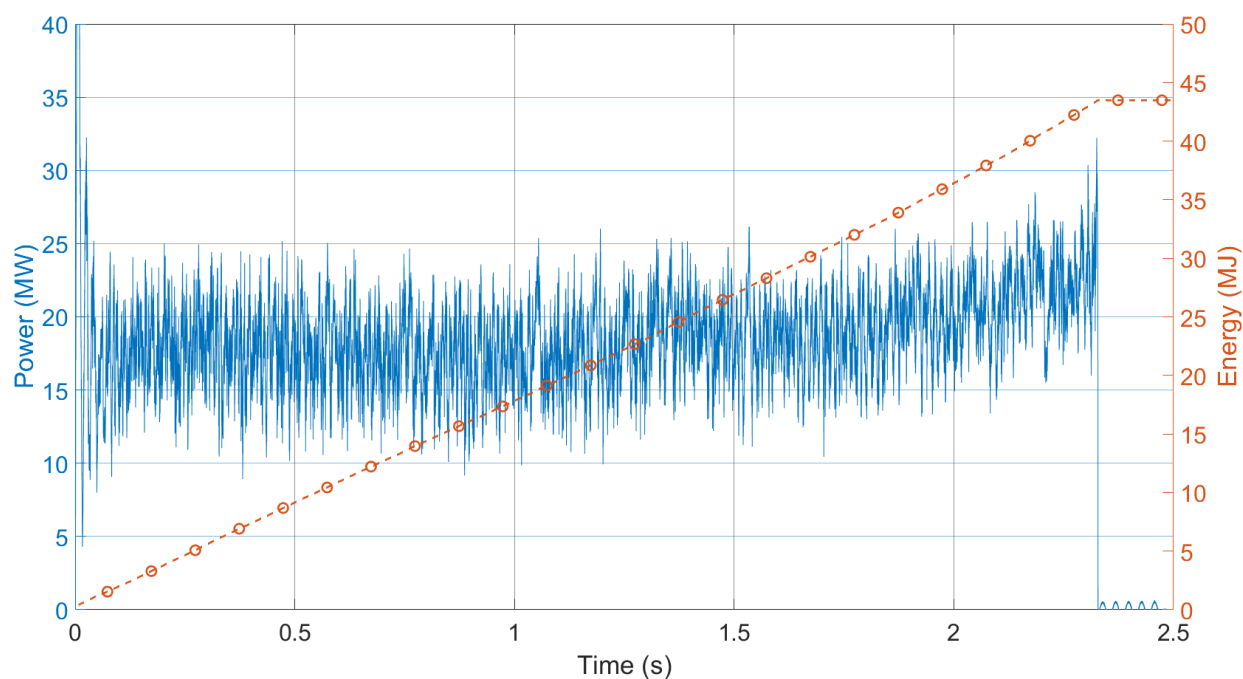


Fig. 133. Experiment OBMV05 power and energy profiles.

B.2.17 Experiment OBMV06

Electrical measurements are presented in Fig. 134 through Fig. 136.

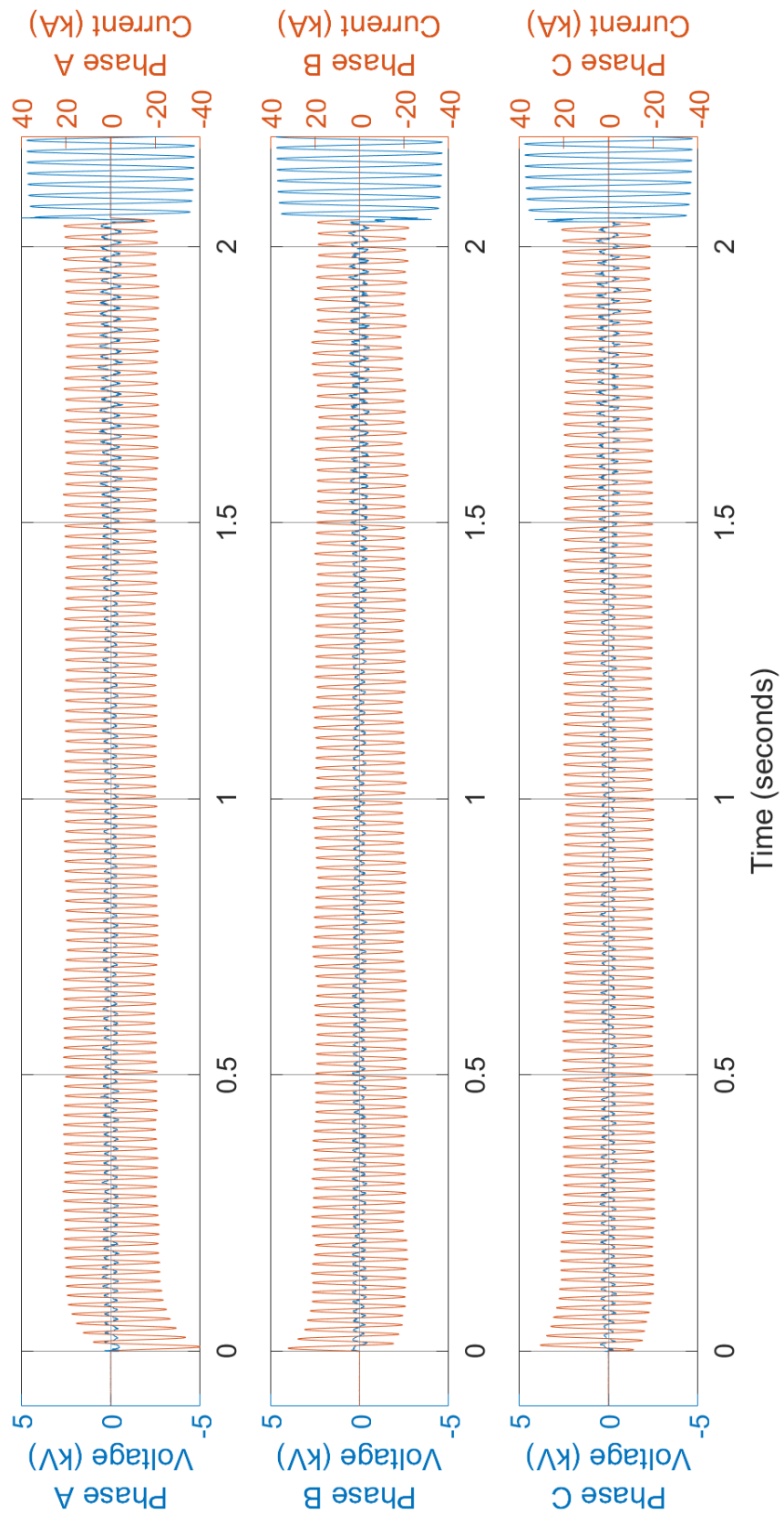


Fig. 134. Experiment OBMV06 voltage and current measurements.

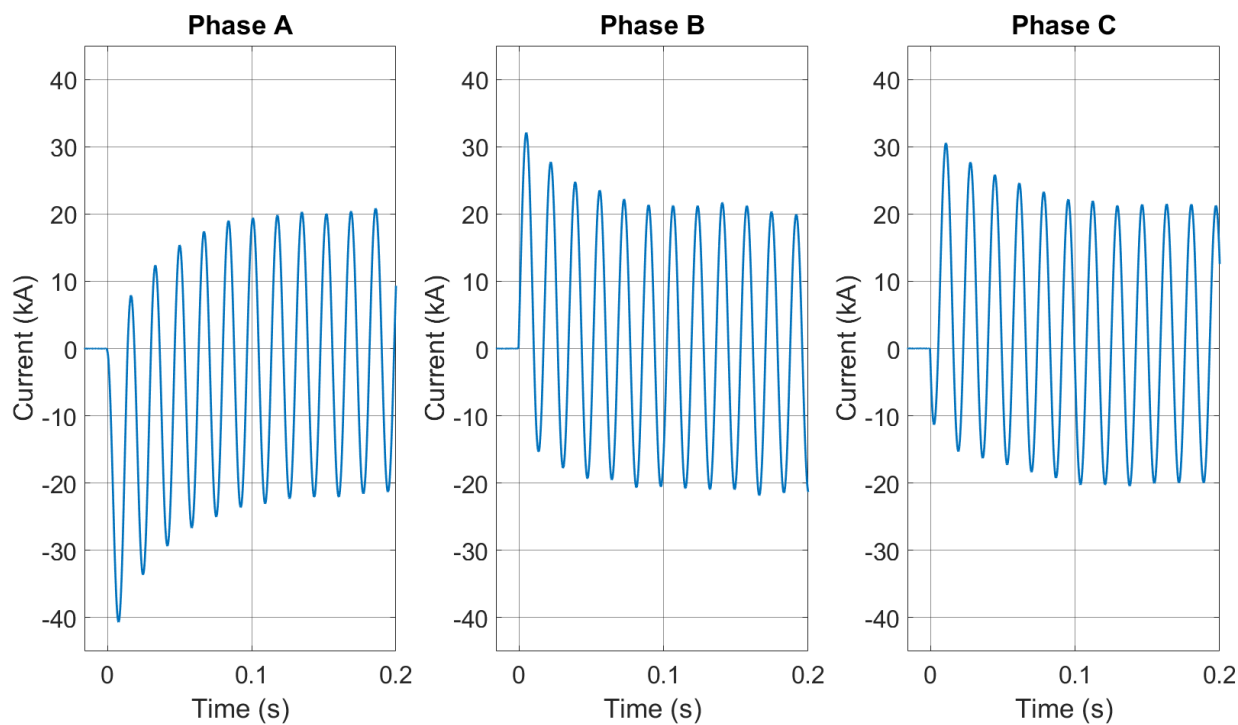


Fig. 135. Experiment OBMV06 transient current profiles.

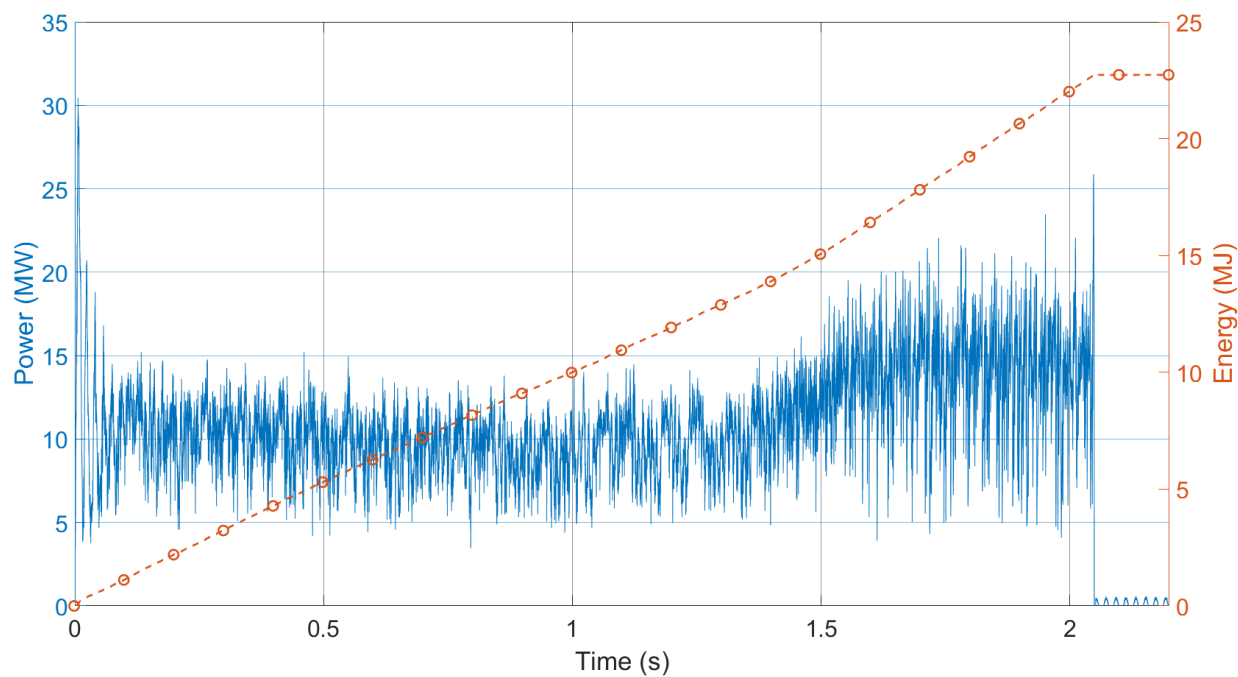


Fig. 136. Experiment OBMV06 power and energy profiles.

Appendix C: KEMA Experiment Report

This appendix provides a copy of KEMA experiment report.

KEMA TEST REPORT

24512323

Object Medium & Low Voltage Switchgear

Type High Energy Arc Fault (HEAF) **Serial No.** N/A

Various V, rms – Various kA, rms – 60 Hz

Client U.S. Nuclear Regulatory Commission
Washington, DC, USA

Tested by KEMA-Powertest LLC,
4379 County Line Road
Chalfont, PA 18914, USA

Date of tests 22, 23, 26, 27, 28, 29 and 30 August 2019 and 16, 17 and 18 September 2019

Test specification The arc fault tests have been carried out in accordance with client's instructions.

This report applies only to the object tested. The responsibility for conformity of any object having the same type references as that tested rests with the Manufacturer.

This report consists of 356 pages in total.

KEMA Powertest, LLC



Frank Cielo
Head of Department, Operations
KEMA Laboratories

INFORMATION SHEET

1 KEMA Type Test Certificate

A KEMA Type Test Certificate contains a record of a series of (type) tests carried out in accordance with a recognized standard. The object tested has fulfilled the requirements of this standard and the relevant ratings assigned by the manufacturer are endorsed by DNV GL. In addition, the object's technical drawings have been verified and the condition of the object after the tests is assessed and recorded. The Certificate contains the essential drawings and a description of the object tested. A KEMA Type Test Certificate signifies that the object meets all the requirements of the named subclauses of the standard. It can be identified by gold-embossed lettering on the cover and a gold seal on its front sheet.

The Certificate is applicable to the object tested only. DNV GL is responsible for the validity and the contents of the Certificate. The responsibility for conformity of any object having the same type references as the one tested rests with the manufacturer.

Detailed rules on types of certification are given in DNV GL's Certification procedure applicable to KEMA Laboratories.

2 KEMA Report of Performance

A KEMA Report of Performance is issued when an object has successfully completed and passed a subset (but not all) of test programmes in accordance with a recognized standard. In addition, the object's technical drawings have been verified and the condition of the object after the tests is assessed and recorded. The report is applicable to the object tested only. A KEMA Report of Performance signifies that the object meets the requirements of the named subclauses of the standard. It can be identified by silver-embossed lettering on the cover and a silver seal on its front sheet.

The sentence on the front sheet of a KEMA Report of Performance will state that the tests have been carried out in accordance with The object has complied with the relevant requirements.

3 KEMA Test Report

A KEMA Test Report is issued in all other cases. Reasons for issuing a KEMA Test Report could be:

- Tests were performed according to the client's instructions.
- Tests were performed only partially according to the standard.
- No technical drawings were submitted for verification and/or no assessment of the condition of the object after the tests was performed.
- The object failed one or more of the performed tests.

The KEMA Test Report can be identified by the grey-embossed lettering on the cover and grey seal on its front sheet.

In case the number of tests, the test procedure and the test parameters are based on a recognized standard and related to the ratings assigned by the manufacturer, the following sentence will appear on the front sheet. The tests have been carried out in accordance with the client's instructions. Test procedure and test parameters were based on If the object does not pass the tests such behaviour will be mentioned on the front sheet. Verification of the drawings (if submitted) and assessment of the condition after the tests is only done on client's request.

When the tests, test procedure and/or test parameters are not in accordance with a recognized standard, the front sheet will state the tests have been carried out in accordance with client's instructions.

4 Official and uncontrolled test documents

The official test documents of DNV GL are issued in bound form. Uncontrolled copies may be provided as a digital file for convenience of reproduction by the client. The copyright has to be respected at all times.

5 Accreditation of KEMA Laboratories

The KEMA Laboratories of DNV GL are accredited in accordance with ISO/IEC 17025 by the respective national accreditation bodies. KEMA Laboratories Arnhem, the Netherlands, is accredited by RvA under nos. L020, L218, K006 and K009. KEMA Laboratories Chalfont, United States, is accredited by A2LA under no. 0553.01. KEMA Laboratories Prague, the Czech Republic, is accredited by CAI as testing laboratory no. 1035.

TABLE OF CONTENTS

1	Identification of the object tested	9
1.1	Ratings/characteristics of the object tested	9
1.2	Description of the object tested	9
2	General Information	10
2.1	The tests were witnessed by	10
2.2	The tests were carried out under responsibility of	10
2.3	Accuracy of measurement	11
2.4	Notes	11
3	Legend	12
4	Checking the prospective current.....	13
4.1	Condition before test	13
4.2	Test results and oscillograms	14
5	Open Box Test # 1 (OB01(A)) - 1000 V, 1 kA	17
5.1	Condition before test	17
5.2	Test circuit S01	18
5.3	Test results and oscillograms	19
5.4	Condition / inspection after test	21
6	Open Box Test # 2 (OB01(B)) - 1000 V, 1 kA	22
6.1	Condition before test	22
6.2	Test circuit S01	23
6.3	Test results and oscillograms	24
6.4	Condition / inspection after test	26
7	Open Box Test # 3 (OB05) - 1000 V, 1 kA	27
7.1	Condition before test	27
7.2	Test circuit S01	28
7.3	Test results and oscillograms	29
7.4	Condition / inspection after test	31
8	Open Box Test # 4 (OB10) - 1000 V, 5 kA	32
8.1	Condition before test	32
8.2	Test circuit S02	33
8.3	Test results and oscillograms	34
8.4	Condition / inspection after test	36
9	Open Box Test # 5 (OB09) - 1000 V, 5 kA	37
9.1	Condition before test	37
9.2	Test circuit S02	38

9.3	Test results and oscillograms	39
9.4	Condition / inspection after test	41
10	Checking the prospective current.....	42
10.1	Condition before test	42
10.2	Test results and oscillograms	43
11	Open Box Test # 6 (OB06) - 1000 V, 15 kA.....	46
11.1	Condition before test	46
11.2	Test circuit S03	47
11.3	Test results and oscillograms	48
11.4	Condition / inspection after test	50
12	Open Box Test # 7 (OB07) - 1000 V, 15 kA.....	51
12.1	Condition before test	51
12.2	Test circuit S03	52
12.3	Test results and oscillograms	53
12.4	Condition / inspection after test	55
13	Open Box Test # 8 (OB08) - 1000 V, 30 kA.....	56
13.1	Condition before test	56
13.2	Test circuit S04	57
13.3	Test results and oscillograms	58
13.4	Condition / inspection after test	60
14	Open Box Test # 9 (OB11) - Single Phase Investigation.....	61
14.1	Condition before test	61
14.2	Test circuit S05	62
14.3	Test results and oscillograms	63
14.4	Condition / inspection after test	65
15	Checking the prospective current.....	66
15.1	Condition before test	66
15.2	Test results and oscillograms	67
16	Sample 2-13 (A) - 480 V, 13.5 kA	70
16.1	Condition before test	70
16.2	Test circuit S06	71
16.3	Test results and oscillograms	72
16.4	Condition / inspection after test	74
17	Sample 2-13 (B) - 600 V, 13.5 kA	75
17.1	Condition before test	75
17.2	Test circuit S07	76
17.3	Test results and oscillograms	77

17.4	Condition / inspection after test	79
18	Sample 2-13 (C) - 600 V, 13.5 kA	80
18.1	Condition before test	80
18.2	Test circuit S07	81
18.3	Test results and oscillograms	82
18.4	Condition / inspection after test	84
19	Sample 2-13 (D) - 600 V, 13.5 kA	85
19.1	Condition before test	85
19.2	Test circuit S07	86
19.3	Test results and oscillograms	87
19.4	Condition / inspection after test	89
20	Sample 2-13 (E) - 600 V, 13.5 kA.....	90
20.1	Condition before test	90
20.2	Test circuit S07	91
20.3	Test results and oscillograms	92
20.4	Condition / inspection after test	94
21	Sample 2-13 (F) - 480 V, 13.5 kA.....	95
21.1	Condition before test	95
21.2	Test circuit S06	96
21.3	Test results and oscillograms	97
21.4	Condition / inspection after test	99
22	Sample 2-13 (G) - 600 V, 13.5 kA	100
22.1	Condition before test	100
22.2	Test circuit S07	101
22.3	Test results and oscillograms	102
22.4	Condition / inspection after test	104
23	Checking the prospective current.....	105
23.1	Condition before test	105
23.2	Test results and oscillograms	106
24	Sample 2-18 (A) - 480 V, 25 kA	111
24.1	Condition before test	111
24.2	Test circuit S09	112
24.3	Test results and oscillograms	113
24.4	Condition / inspection after test	115
25	Sample 2-18 (B) - 600 V, 25 kA	116
25.1	Condition before test	116
25.2	Test circuit S08	117



25.3	Test results and oscillograms	118
25.4	Condition / inspection after test	120
26	Open Box Test # 10 (OB02) - 1000 V, 15 kA.....	121
26.1	Condition before test	121
26.2	Test circuit S03	122
26.3	Test results and oscillograms	123
26.4	Condition / inspection after test	125
27	Open Box Test # 11 (OB03) - 1000 V, 15 kA.....	126
27.1	Condition before test	126
27.2	Test circuit S03	127
27.3	Test results and oscillograms	128
27.4	Condition / inspection after test	130
28	Open Box Test # 12 (OB04) - 1000 V, 30 kA.....	131
28.1	Condition before test	131
28.2	Test circuit S04	132
28.3	Test results and oscillograms	133
28.4	Condition / inspection after test	135
29	Open Box Test # 13 (OB16) - Single Phase Investigation	136
29.1	Condition before test	136
29.2	Test circuit S05	137
29.3	Test results and oscillograms	138
29.4	Condition / inspection after test	140
30	Open Box Test # 14 (OB12(A)) - Single Phase Investigation.....	141
30.1	Condition before test	141
30.2	Test circuit S05	142
30.3	Test results and oscillograms	143
30.4	Condition / inspection after test	145
31	Open Box Test # 15 (OB15) - Single Phase Investigation	146
31.1	Condition before test	146
31.2	Test circuit S05	147
31.3	Test results and oscillograms	148
31.4	Condition / inspection after test	150
32	Open Box Test # 16 (OB14) - Single Phase Investigation	151
32.1	Condition before test	151
32.2	Test circuit S05	152
32.3	Test results and oscillograms	153
32.4	Condition / inspection after test	155



33	Open Box Test # 17 (OB12(B) & OB12(C)) - Single Phase Investigation	156
33.1	Condition before test	156
33.2	Test circuit S05	157
33.3	Test results and oscillograms	158
33.4	Condition / inspection after test	161
34	Open Box Test # 18 - 480 V, 13.5 kA.....	162
34.1	Condition before test	162
34.2	Test circuit S06	163
34.3	Test results and oscillograms	164
34.4	Condition / inspection after test	166
35	Checking the prospective current.....	167
35.1	Condition before test	167
35.2	Test results and oscillograms	168
36	OBMV # 5	173
36.1	Condition before test	173
36.2	Test circuit S11	174
36.3	Test results and oscillograms	175
36.4	Condition / inspection after test	177
37	OBMV # 2	178
37.1	Condition before test	178
37.2	Test circuit S11	179
37.3	Test results and oscillograms	180
37.4	Condition / inspection after test	182
38	OBMV # 4	183
38.1	Condition before test	183
38.2	Test circuit S10	184
38.3	Test results and oscillograms	185
38.4	Condition / inspection after test	187
39	OBMV # 1	188
39.1	Condition before test	188
39.2	Test circuit S10	189
39.3	Test results and oscillograms	190
39.4	Condition / inspection after test	192
40	OBMV # 3	193
40.1	Condition before test	193
40.2	Test circuit S10	194
40.3	Test results and oscillograms	195



40.4	Condition / inspection after test	197
41	OBMV # 6	198
41.1	Condition before test	198
41.2	Test circuit S10	199
41.3	Test results and oscillograms	200
41.4	Condition / inspection after test	202
42	Attachments	203
	1. Calorimeter Data Records [15 PAGES]	
	2. Instrumentation Information Sheets [2 PAGES]	
	3. Photographs (269) [135 PAGES]	
	End of Document [1 PAGE]	

1 IDENTIFICATION OF THE OBJECT TESTED

1.1 Ratings/characteristics of the object tested

Voltage	Various V
Number of phases	3
Frequency	60 Hz
Short-circuit current	Various kA

1.2 Description of the object tested

Low and Medium Voltage Box Tests, High Energy Arcing Faults
Low Voltage Switchgear, High Energy Arcing Faults

2 GENERAL INFORMATION

2.1 The tests were witnessed by

Name	Company
Christopher Brown	National Institute of Standards and Technology (NIST)
Michael Selepak	
Anthony Putorti	
Scott Bareham	
Andre Thompson	
Philip Deardorff	
Benny Lee	BSI Electrical Contractors Montgomeryville, PA, USA
John Jones	
Robert Taylor	
Jeff McKnight	
Byron Demostehnous	Sandia National Laboratories Albuquerque, NM, USA
Kenneth Armijo	
James Taylor	
Alvaro Augusto Cruz-Cabrera	
Chris Lafleur	
Raina Weaver	
Scott Sanborn	
Austin Glover	
Paul Clem	
Ray Martinez	
Caroline Winters	
Nick Melly	U.S. Nuclear Regulatory Commission Washington, DC, USA
Kenneth Hamburger	
Kenn Miller	
Gabriel Taylor	
Thomas Koshy	
Ken Fleischer	Electric Power Research Institute
Marko Randelovic	

2.2 The tests were carried out under responsibility of

Name	Company
Joe Duffy	KEMA-Powertest LLC, Chalfont, PA, USA

2.3 Accuracy of measurement

The guaranteed uncertainty in the figures mentioned, taking into account the total measuring system, is less than 3%, unless mentioned otherwise. Measurement uncertainty can be verified by reviewing the instrument calibration records. The instruments used are calibrated on a regular basis and are traceable to the National Institute of Standards and Technology.

2.4 Notes

-

3 LEGEND

Phase indications

If more than one phase is recorded on oscillogram, the phases are indicated by the digits 1, 2 and 3. These phases 1, 2 and 3 correspond to the phase values in the columns of the accompanying table, respectively from left to right.

Explanation of the letter symbols and abbreviations on the oscillograms

pu	Per unit (the reference length of one unit is represented by the black bar on the oscillogram)
I1TO	Current through test object
I2TO	Current through test object
I3TO	Current through test object
Ineut	Neutral current
PT # 1	Pressure transducer # 1
PT # 2	Pressure transducer # 2
PT # 3	Pressure transducer # 3
PT # 4	Pressure transducer # 4
TRIG	Trigger signal transient recorder
U1TO	Voltage across test object
U2TO	Voltage across test object
U3TO	Voltage across test object

4 CHECKING THE PROSPECTIVE CURRENT

Standard and date

Standard	Client's instructions
Test date	22 August 2019

4.1 Condition before test

Shorting bar connected at station terminals directly prior to test device.

4.2 Test results and oscillograms

Overview of test numbers

190822-7001, 7002

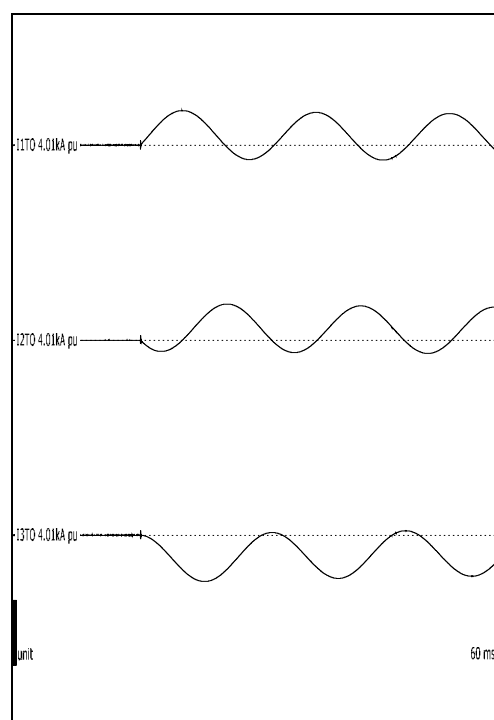
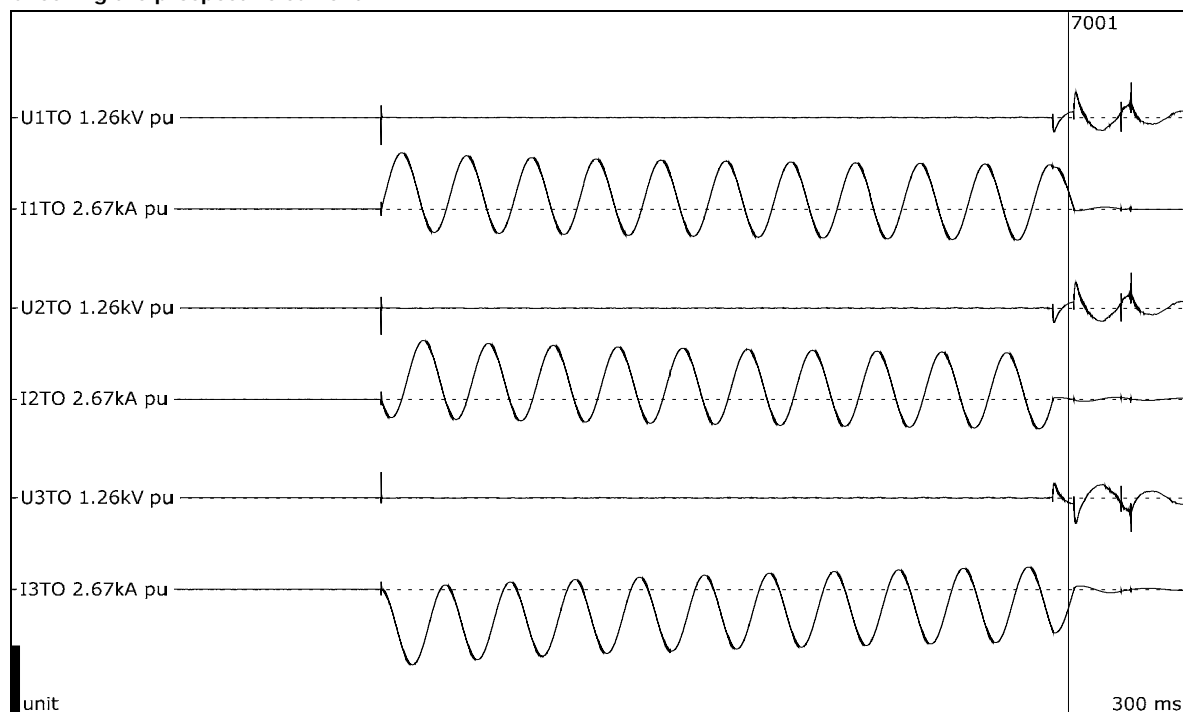
Remarks

Prospective circuit parameters calibrated in this test duty:

190822-7001: 1000 V, 1040 A, 2860 A peak.

190822-7002: 1000 V, 5053 A, 14.9 kA peak.

Checking the prospective current

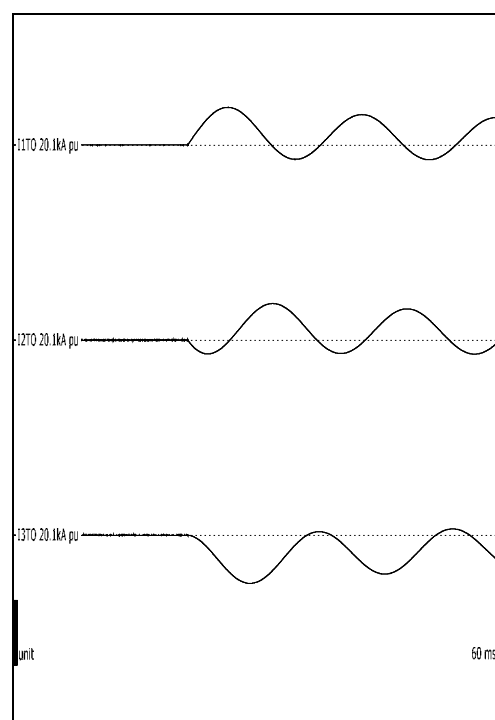
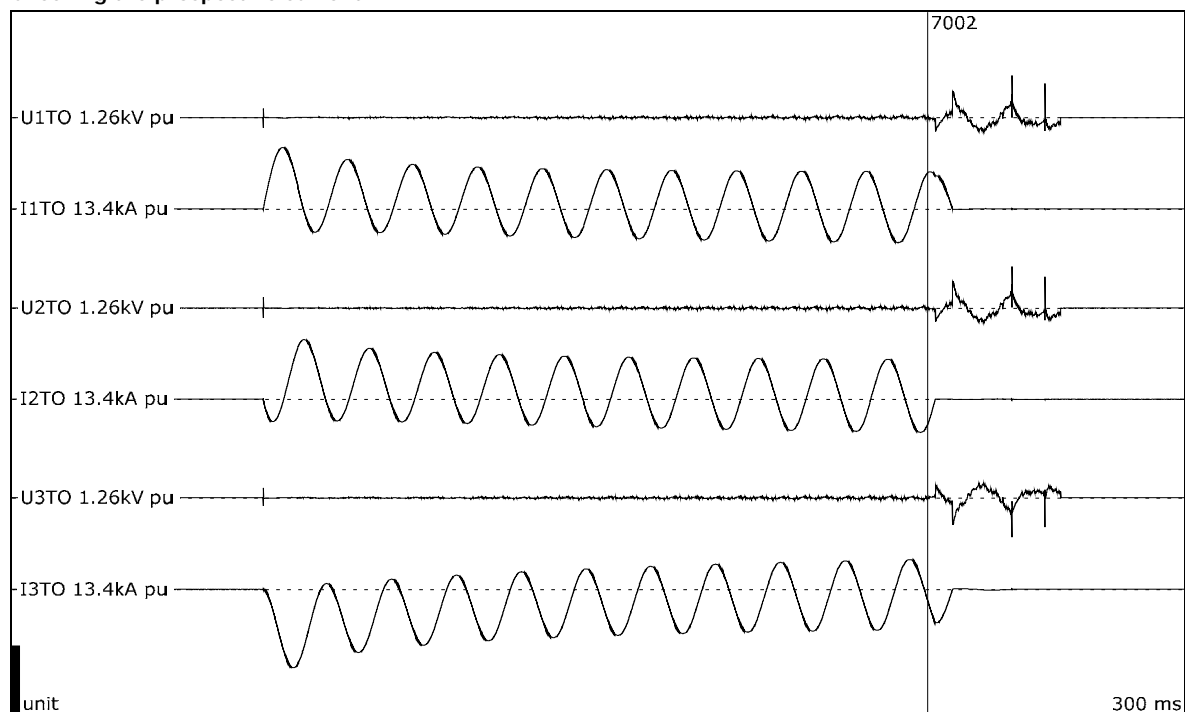


Test number: 190822-7001

Phase		A	B	C
Current	kA _{peak}	2.13	2.23	-2.86
Current, a.c. component	kA _{RMS}	1.04	1.04	1.04
Current, a.c. component, three-phase average	kA _{RMS}	1.04		
Duration, current	s	0.176	0.176	0.175

Observations: No visible disturbance.

Checking the prospective current



Test number: 190822-7002

Phase		A	B	C
Current	kA _{peak}	11.6	11.3	-14.9
Current, a.c. component	kA _{RMS}	4.89	5.15	5.12
Current, a.c. component, three-phase average	kA _{RMS}	5.05		
Duration, current	s	0.170	0.170	0.169

Observations: No visible disturbance.

5 OPEN BOX TEST # 1 (OB01(A)) - 1000 V, 1 KA

Standard and date

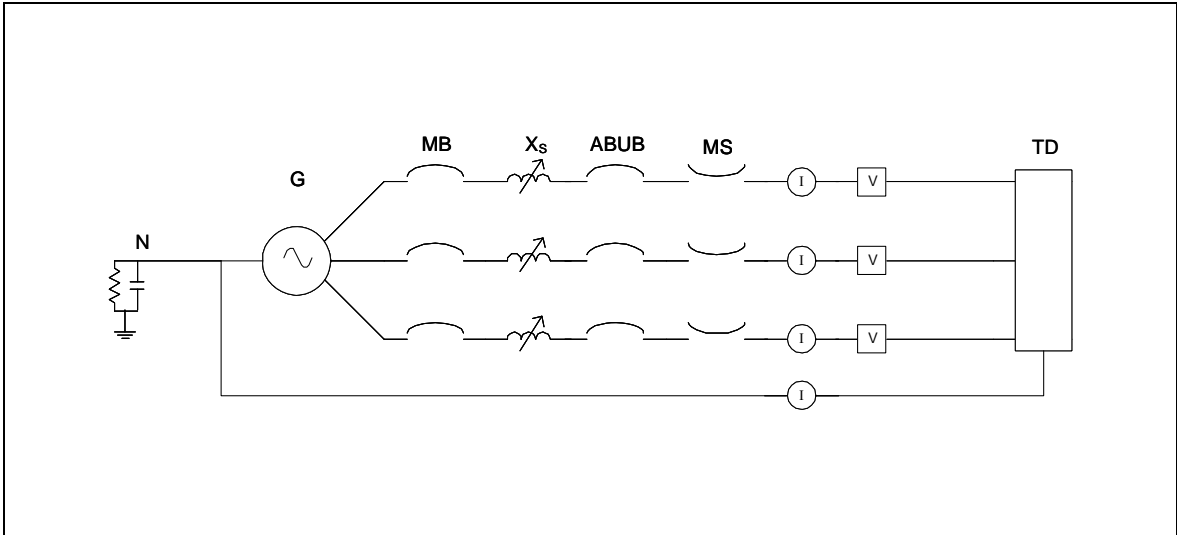
Standard	Client's instructions
Test date	22 August 2019

5.1 Condition before test

Test device new. Arc to be initiated by #10 AWG stranded wire. Arc wire connected to 1/2" diameter copper rods. Test duration is 2 seconds.



5.2 Test circuit S01



G	= Generator	ABUB	= Aux. Breaker	R	= Resistance
N	= Neutral	XFMR	= Transformer	C	= Capacitance
MB	= Main Breaker	TD	= Test Device	V	= Voltage Measurement
MS	= Make Switch	X	= Inductance	I	= Current Measurement

Supply		
Power	MVA	1.801
Frequency	Hz	60
Phase(s)		3
Voltage	V	1000
Sym. Current	kA	1.040
Peak current	kA	2.86
Impedance	Ω	0.5551

Remarks: -

5.3 Test results and oscillograms

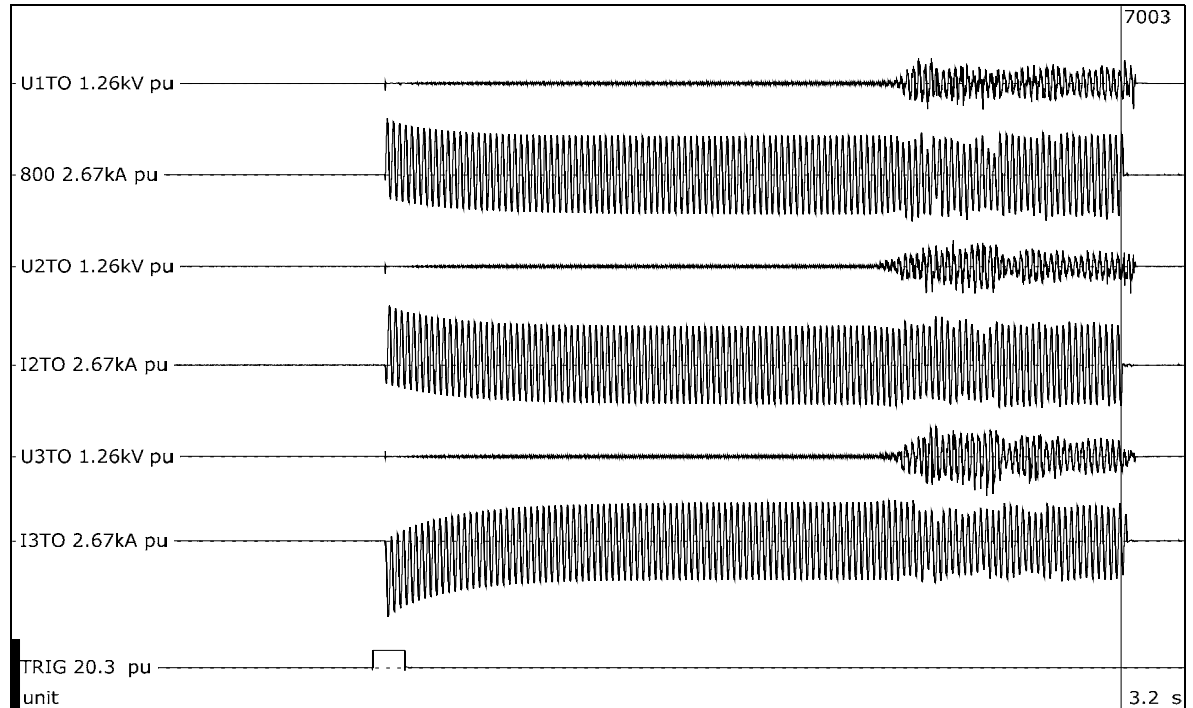
Overview of test numbers

190822-7003

Remarks

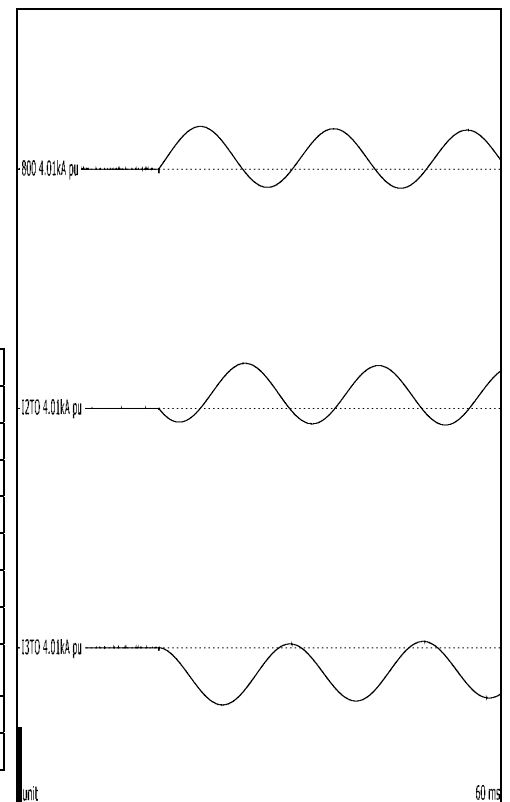
-

Open Box Test # 1 (OB01) - 1000 V, 1 kA



Test number: 190822-7003

Phase		A	B	C
Applied voltage, phase-to-ground	V _{RMS}	577	577	577
Applied voltage, phase-to-phase	V _{RMS}	999		
Making current	kA _{peak}	2.14	2.26	-2.89
Current, a.c. component, beginning	A _{RMS}	1064	1061	1050
Current, a.c. component, middle	A _{RMS}	1052	1049	1039
Current, a.c. component, end	A _{RMS}	1119	1006	985
Current, a.c. component, average	A _{RMS}	1042	1048	1009
Current, a.c. component, three-phase average	A _{RMS}	1033		
Duration	s	2.01	2.01	2.01
Arc energy	kJ	66.7	106	27.9



Observations: Emission of flames and gas observed. Arc wire took approximately 1.35 seconds to melt and initiate the arc.

5.4 Condition / inspection after test

Box lightly damaged, another arc test can be performed with this sample.

6 OPEN BOX TEST # 2 (OB01(B)) - 1000 V, 1 KA

Standard and date

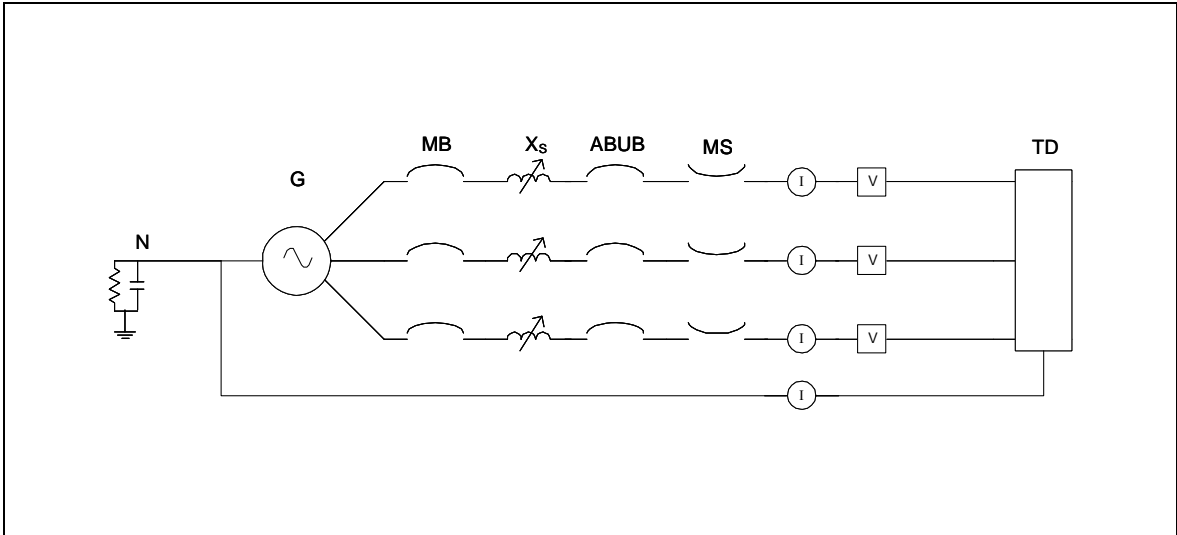
Standard	Client's instructions
Test date	22 August 2019

6.1 Condition before test

Test device previously subjected to arc test at 1000 V, 1 kA. Arc to be initiated by #24 AWG wire. Arc wire connected to 1/2" diameter copper rods. Test duration is 2 seconds.



6.2 Test circuit S01



G	= Generator	ABUB	= Aux. Breaker	R	= Resistance
N	= Neutral	XFMR	= Transformer	C	= Capacitance
MB	= Main Breaker	TD	= Test Device	V	= Voltage Measurement
MS	= Make Switch	X	= Inductance	I	= Current Measurement

Supply		
Power	MVA	1.801
Frequency	Hz	60
Phase(s)		3
Voltage	V	1000
Sym. Current	kA	1.040
Peak current	kA	2.86
Impedance	Ω	0.5551

Remarks: -

6.3 Test results and oscillograms

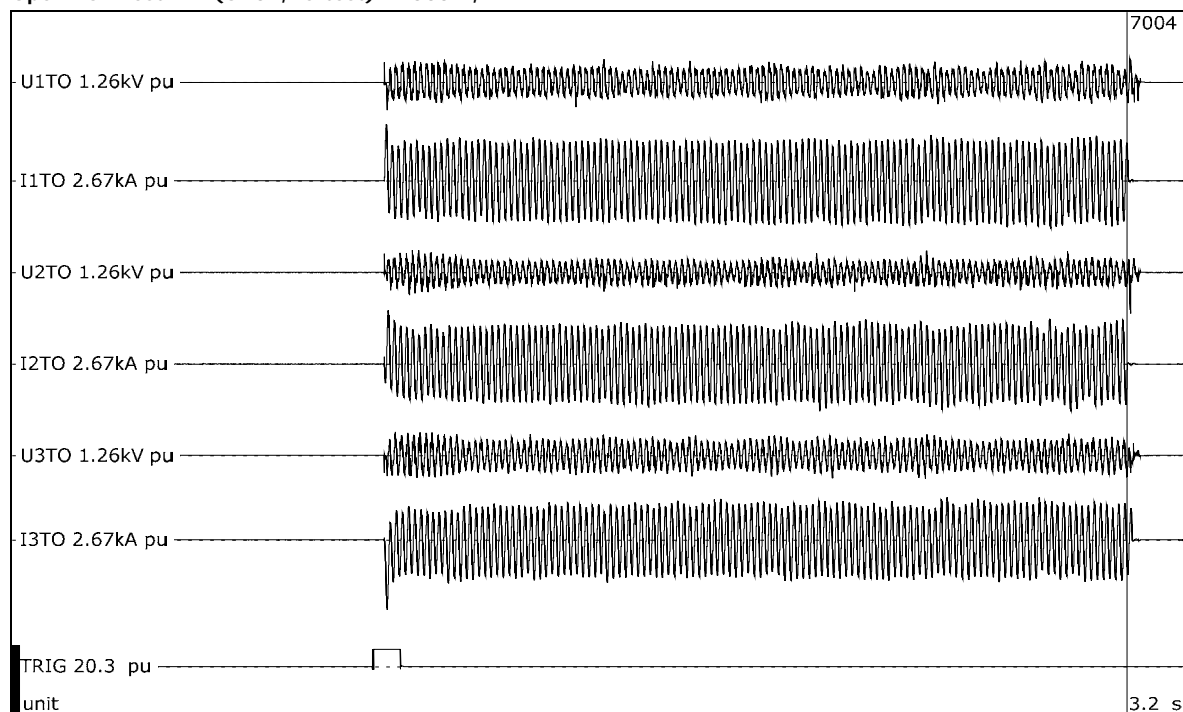
Overview of test numbers

190822-7004

Remarks

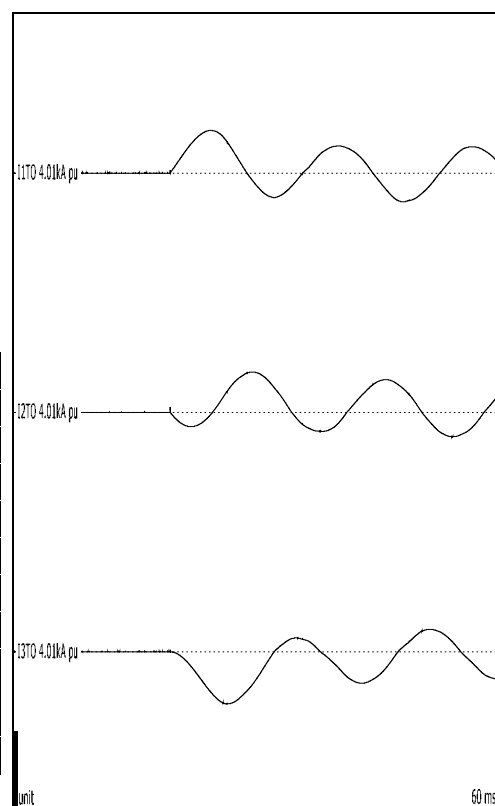
-

Open Box Test # 2 (OB01, re-test) - 1000 V, 1 kA



Test number: 190822-7004

Phase		A	B	C
Applied voltage, phase-to-ground	V _{RMS}	577	577	577
Applied voltage, phase-to-phase	V _{RMS}	999		
Making current	kA _{peak}	2.14	2.02	-2.63
Current, a.c. component, beginning	A _{RMS}	1056	1009	985
Current, a.c. component, middle	A _{RMS}	1124	1035	1015
Current, a.c. component, end	A _{RMS}	1128	1011	974
Current, a.c. component, average	A _{RMS}	1083	1030	985
Current, a.c. component, three-phase average	A _{RMS}	1033		
Duration	s	2.02	2.02	2.02
Arc energy	kJ	248	289	199



Observations: Emission of flames and gas observed.

6.4 Condition / inspection after test

Box slightly more damaged than previous arc test. End of copper conductors melted slightly.

7 OPEN BOX TEST # 3 (OB05) - 1000 V, 1 KA

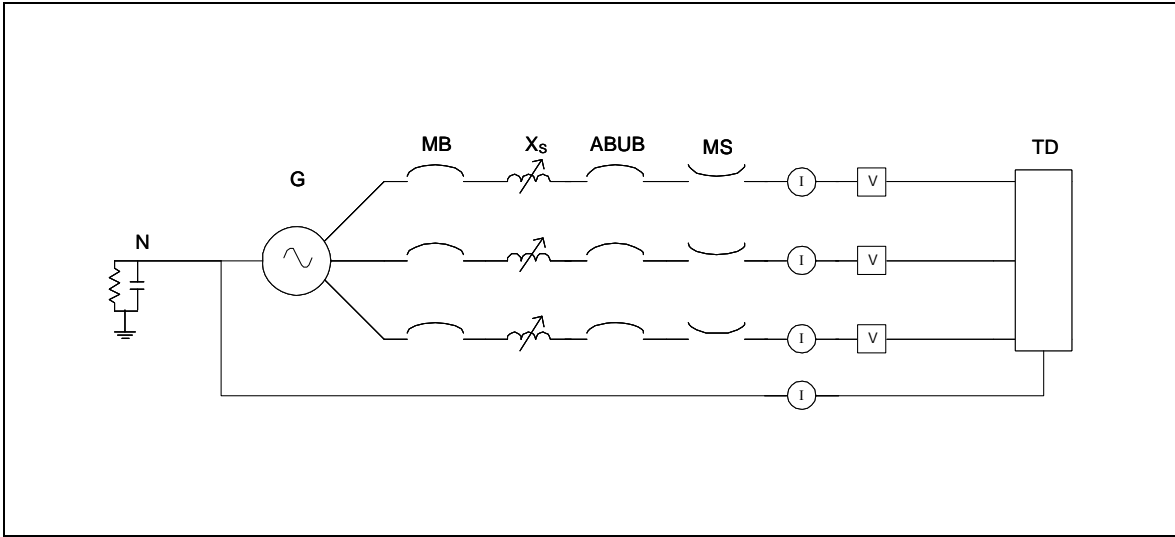
Standard and date

Standard	Client's instructions
Test date	22 August 2019

7.1 Condition before test

Test device previously subjected to two arc tests at 1000 V, 1 kA. Arc to be initiated by #24 AWG wire. Arc wire connected to 1/2" diameter aluminum rods. Test duration is 2 seconds.

7.2 Test circuit S01



G	= Generator	ABUB	= Aux. Breaker	R	= Resistance
N	= Neutral	XFMR	= Transformer	C	= Capacitance
MB	= Main Breaker	TD	= Test Device	V	= Voltage Measurement
MS	= Make Switch	X	= Inductance	I	= Current Measurement

Supply		
Power	MVA	1.801
Frequency	Hz	60
Phase(s)		3
Voltage	V	1000
Sym. Current	kA	1.040
Peak current	kA	2.86
Impedance	Ω	0.5551

Remarks: -

7.3 Test results and oscillograms

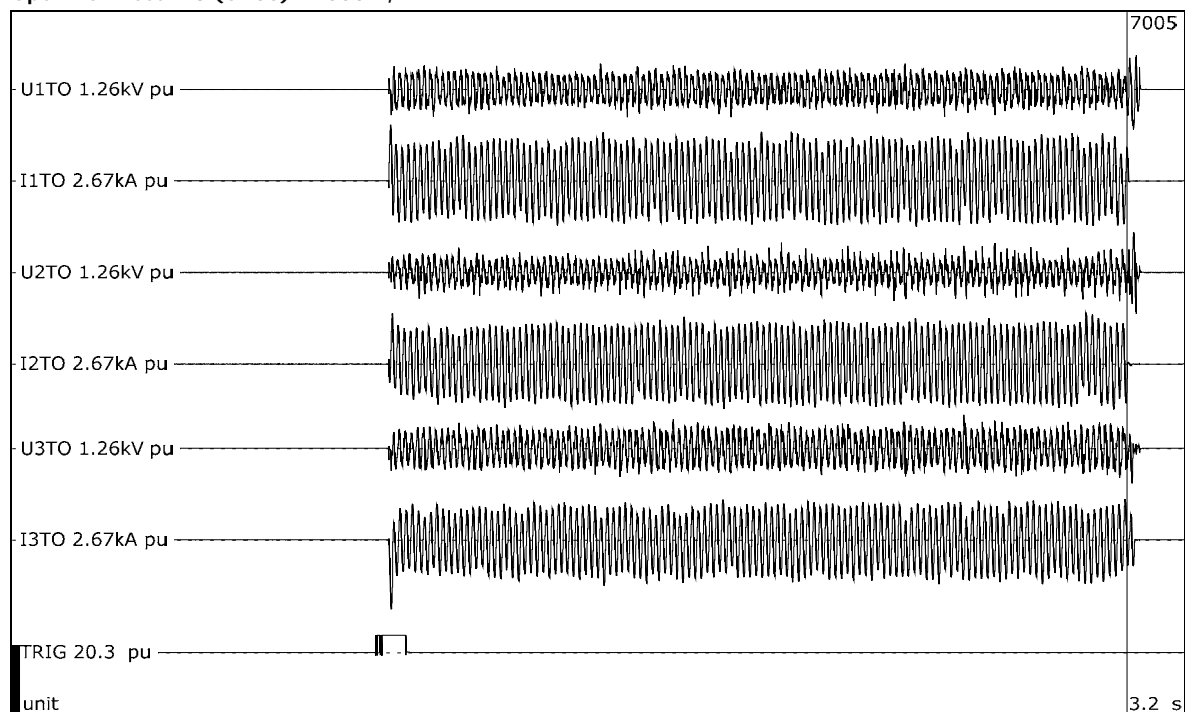
Overview of test numbers

190822-7005

Remarks

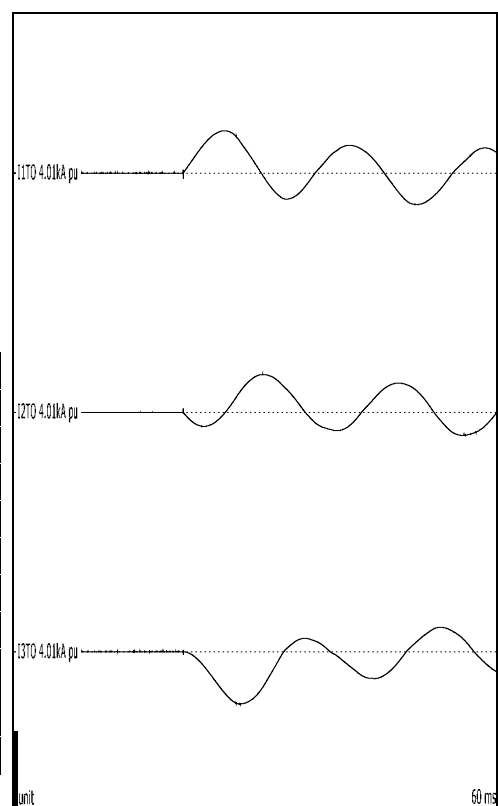
-

Open Box Test # 3 (OB05) - 1000 V, 1 kA



Test number: 190822-7005

Phase		A	B	C
Applied voltage, phase-to-ground	V _{RMS}	577	577	577
Applied voltage, phase-to-phase	V _{RMS}	999		
Making current	kA _{peak}	2.12	1.91	-2.63
Current, a.c. component, beginning	A _{RMS}	1088	958	949
Current, a.c. component, middle	A _{RMS}	1173	1064	963
Current, a.c. component, end	A _{RMS}	1000	1075	943
Current, a.c. component, average	A _{RMS}	1080	1031	942
Current, a.c. component, three-phase average	A _{RMS}	1018		
Duration	s	2.01	2.01	2.01
Arc energy	kJ	262	329	205



Observations: Emission of flames and gas observed.

7.4 Condition / inspection after test

Box covered in ash, but still able to withstand another arc test. Aluminum rods discolored to a slightly white color.

8 OPEN BOX TEST # 4 (OB10) - 1000 V, 5 KA

Standard and date

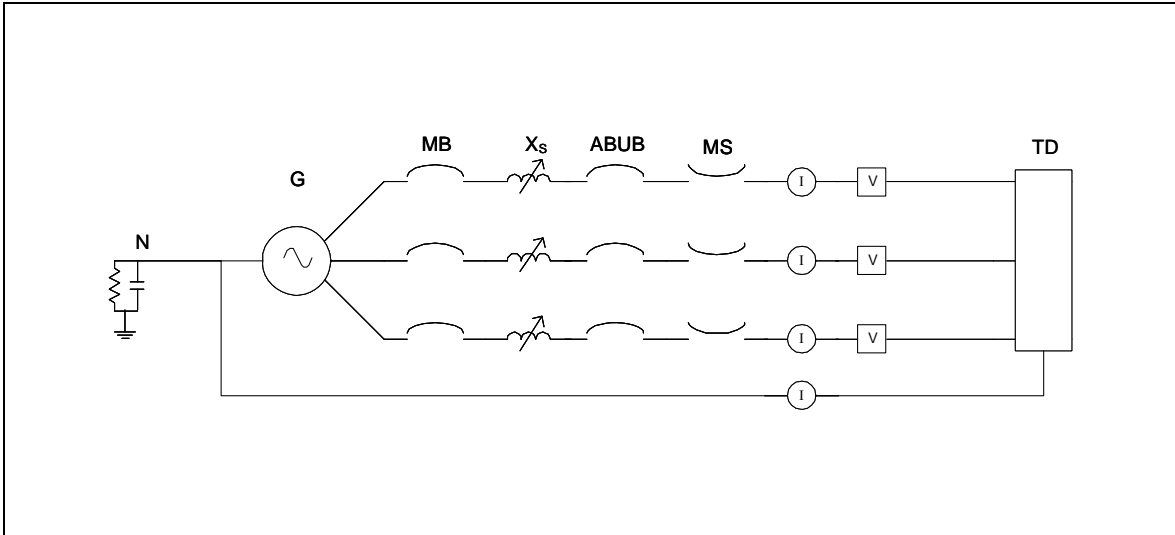
Standard	Client's instructions
Test date	22 August 2019

8.1 Condition before test

Test device previously subjected to three arc tests at 1000 V, 1 kA. Arc to be initiated by #24 AWG wire. Arc wire connected to 1/2" diameter aluminum rods. Test duration is 2 seconds.



8.2 Test circuit S02



G	= Generator	ABUB	= Aux. Breaker	R	= Resistance
N	= Neutral	XFMR	= Transformer	C	= Capacitance
MB	= Main Breaker	TD	= Test Device	V	= Voltage Measurement
MS	= Make Switch	X	= Inductance	I	= Current Measurement

Supply		
Power	MVA	8.75
Frequency	Hz	60
Phase(s)		3
Voltage	V	1000
Sym. Current	kA	5.053
Peak current	kA	14.9
Impedance	Ω	0.114

Remarks: -

8.3 Test results and oscillograms

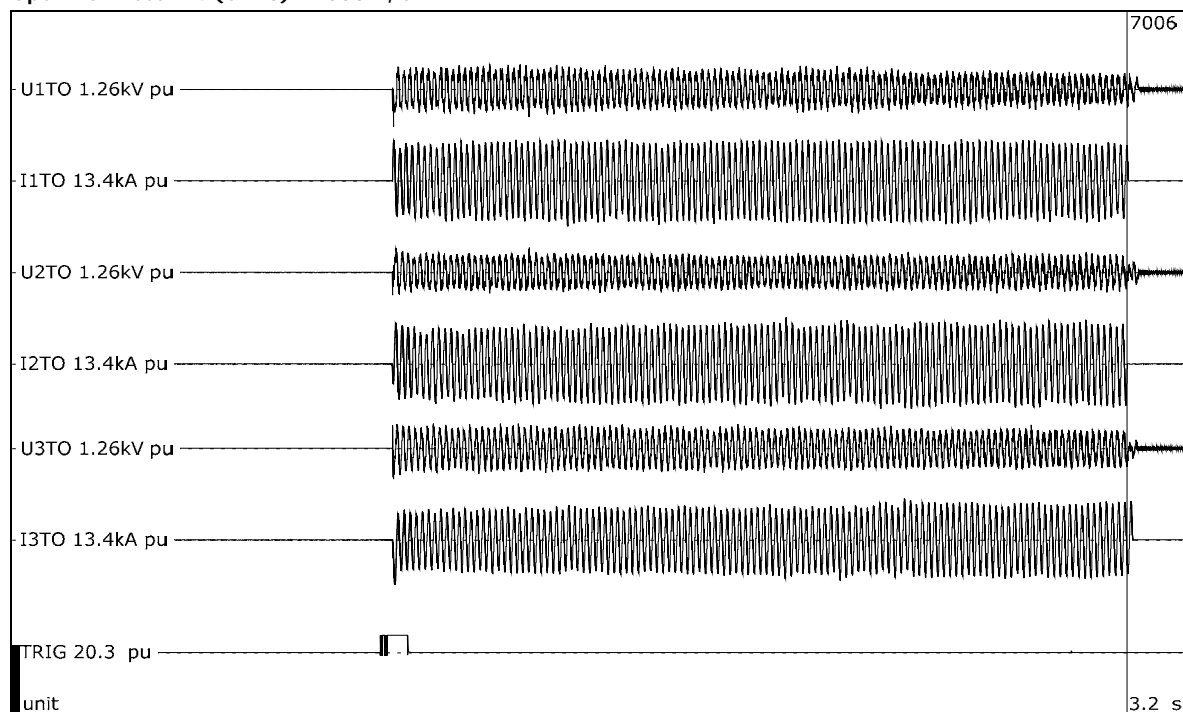
Overview of test numbers

190822-7006

Remarks

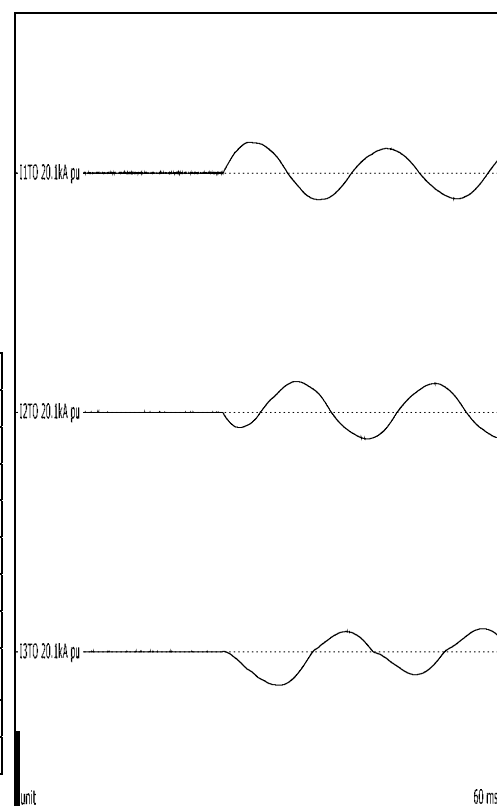
-

Open Box Test # 4 (OB10) - 1000 V, 5 kA



Test number: 190822-7006

Phase		A	B	C
Applied voltage, phase-to-ground	V _{RMS}	577	577	577
Applied voltage, phase-to-phase	V _{RMS}	999		
Making current	kA _{peak}	7.73	7.76	-8.47
Current, a.c. component, beginning	A _{RMS}	4812	4548	4309
Current, a.c. component, middle	A _{RMS}	5190	5297	4487
Current, a.c. component, end	A _{RMS}	5041	5559	4936
Current, a.c. component, average	A _{RMS}	5193	5081	4499
Current, a.c. component, three-phase average	A _{RMS}	4924		
Duration	s	2.00	2.00	2.00
Arc energy	kJ	1190	1960	968



Observations: Emission of flames and gas observed.

8.4 Condition / inspection after test

Interior and sides of the exterior of the box were heavily burned. Box will be replaced for next test.

9 OPEN BOX TEST # 5 (OB09) - 1000 V, 5 KA

Standard and date

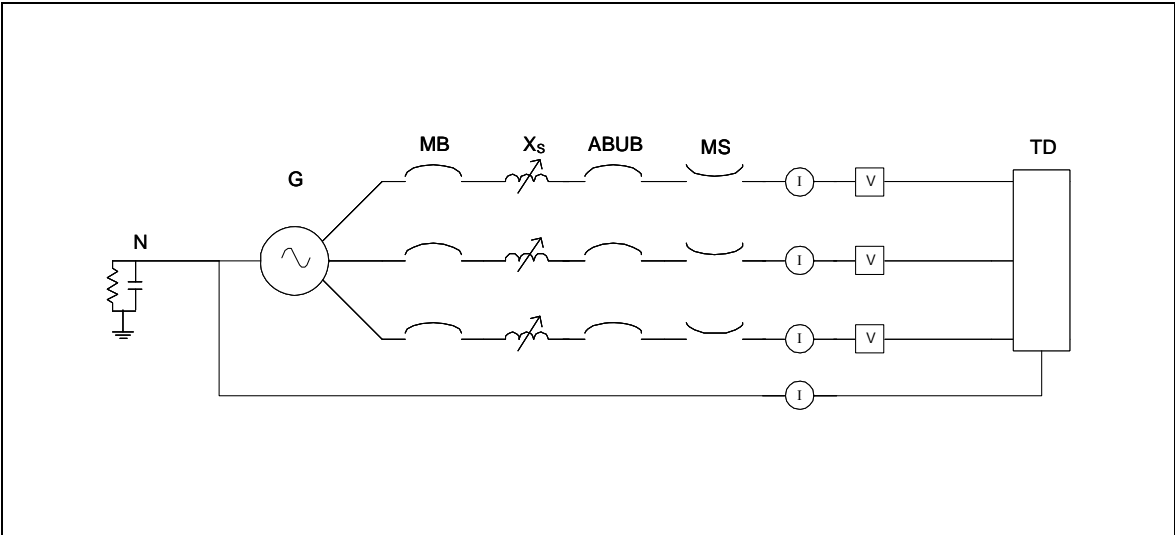
Standard	Client's instructions
Test date	22 August 2019

9.1 Condition before test

Test device new. Arc to be initiated by #24 AWG wire. Arc wire connected to 1/2" diameter copper rods. Test duration is 2 seconds.



9.2 Test circuit S02



G	= Generator	ABUB	= Aux. Breaker	R	= Resistance
N	= Neutral	XFMR	= Transformer	C	= Capacitance
MB	= Main Breaker	TD	= Test Device	V	= Voltage Measurement
MS	= Make Switch	X	= Inductance	I	= Current Measurement

Supply		
Power	MVA	8.75
Frequency	Hz	60
Phase(s)		3
Voltage	V	1000
Sym. Current	kA	5.053
Peak current	kA	14.9
Impedance	Ω	0.114

Remarks: -

9.3 Test results and oscillograms

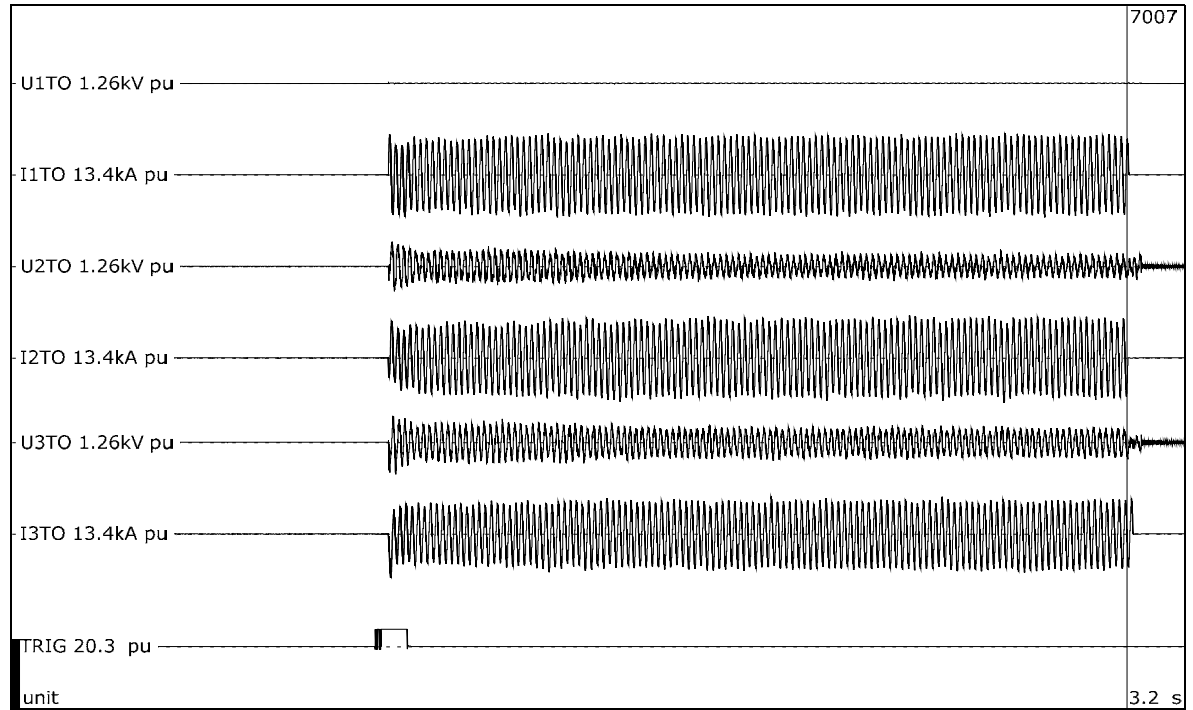
Overview of test numbers

190822-7007

Remarks

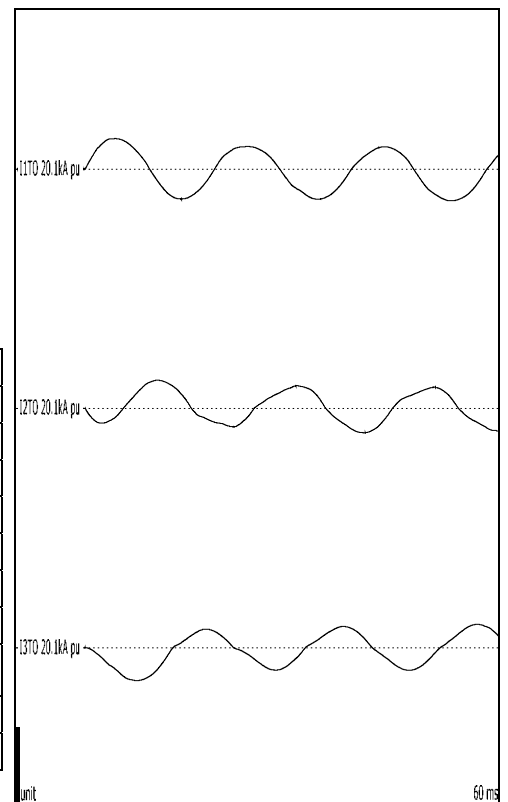
-

Open Box Test # 5 (OB09) - 1000 V, 5 kA



Test number: 190822-7007

Phase		A	B	C
Applied voltage, phase-to-ground	V _{RMS}	577	577	577
Applied voltage, phase-to-phase	V _{RMS}	999		
Making current	kA _{peak}	7.64	7.07	-8.32
Current, a.c. component, beginning	A _{RMS}	5011	3955	4100
Current, a.c. component, middle	A _{RMS}	5140	5170	4313
Current, a.c. component, end	A _{RMS}	5296	5113	4494
Current, a.c. component, average	A _{RMS}	5179	4869	4370
Current, a.c. component, three-phase average	A _{RMS}	4806		
Duration	s	2.01	2.01	2.01
Arc energy	kJ	21.7	1401	819



Observations: Emission of flames and gas observed.

9.4 Condition / inspection after test

Interior and sides of the exterior of the box were heavily burned. Box will be replaced for next test.

10 CHECKING THE PROSPECTIVE CURRENT

Standard and date

Standard	Client's instructions
Test date	23 August 2019

10.1 Condition before test

Shorting bar connected at station terminals directly prior to test device.

10.2 Test results and oscillograms

Overview of test numbers

190823-7001, 7002

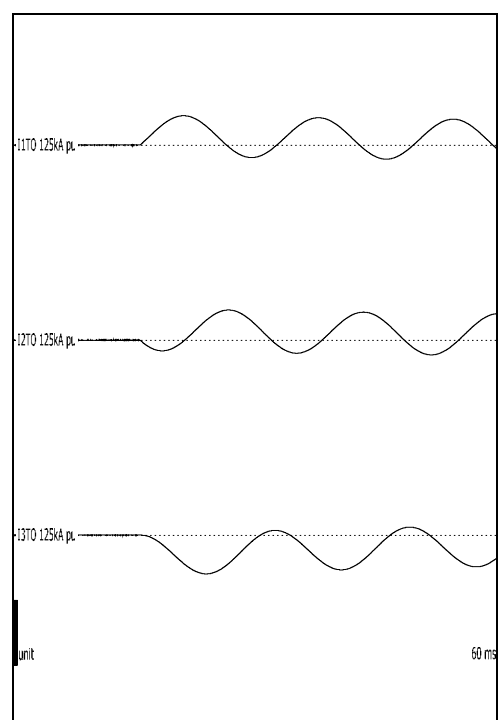
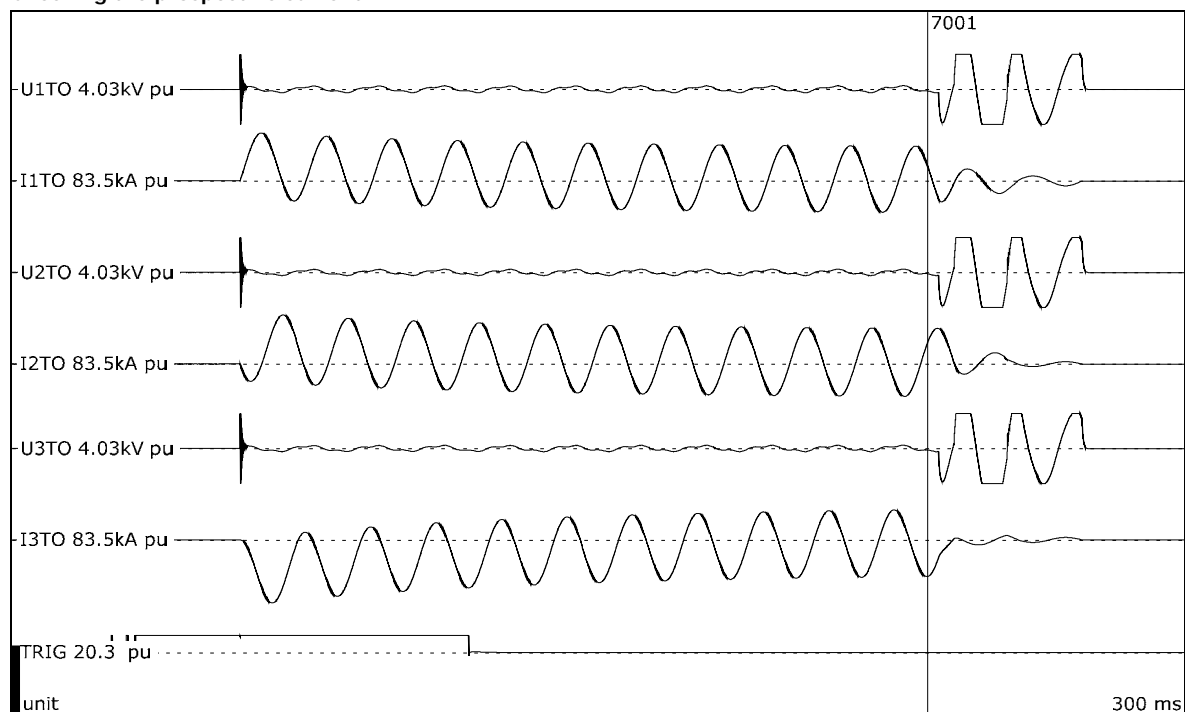
Remarks

Prospective circuit parameters calibrated in this test duty:

190823-7001: 1064 V, 30 kA, 79.1 kA peak.

190823-7002: 1009 V, 15 kA, 40.4 kA peak.

Checking the prospective current

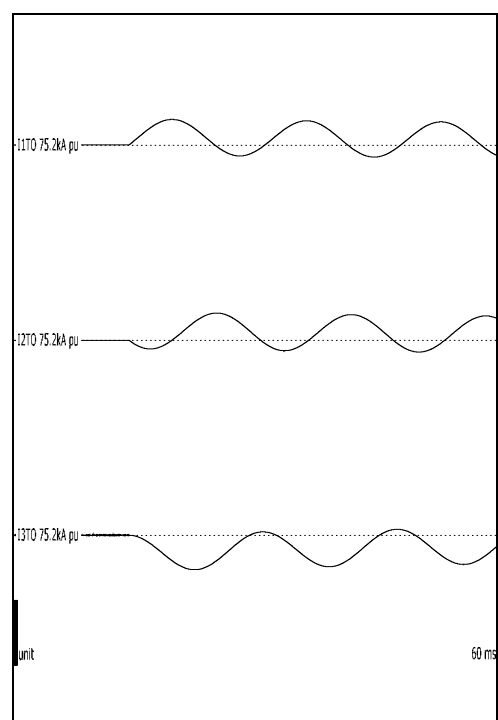
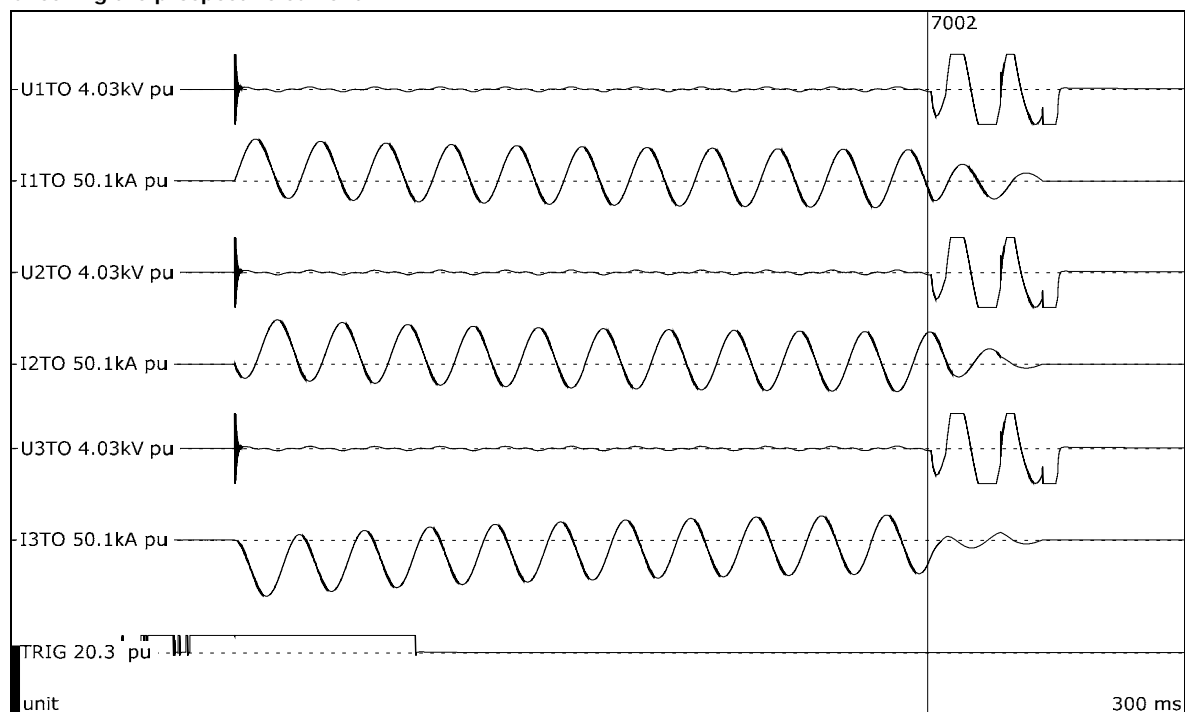


Test number: 190823-7001

Phase		A	B	C
Current	kA _{peak}	56.6	58.1	-74.6
Current, a.c. component	kA _{RMS}	27.8	28.7	28.1
Current, a.c. component, three-phase average	kA _{RMS}	28.2		
Duration, current	s	0.176	0.176	0.175

Observations: No visible disturbance.

Checking the prospective current



Test number: 190823-7002

Phase		A	B	C
Current	kA _{peak}	29.7	31.3	-40.0
Current, a.c. component	kA _{RMS}	14.6	15.1	14.9
Current, a.c. component, three-phase average	kA _{RMS}	14.9		
Duration, current	s	0.177	0.177	0.176

Observations: No visible disturbance.

11 OPEN BOX TEST # 6 (OB06) - 1000 V, 15 KA

Standard and date

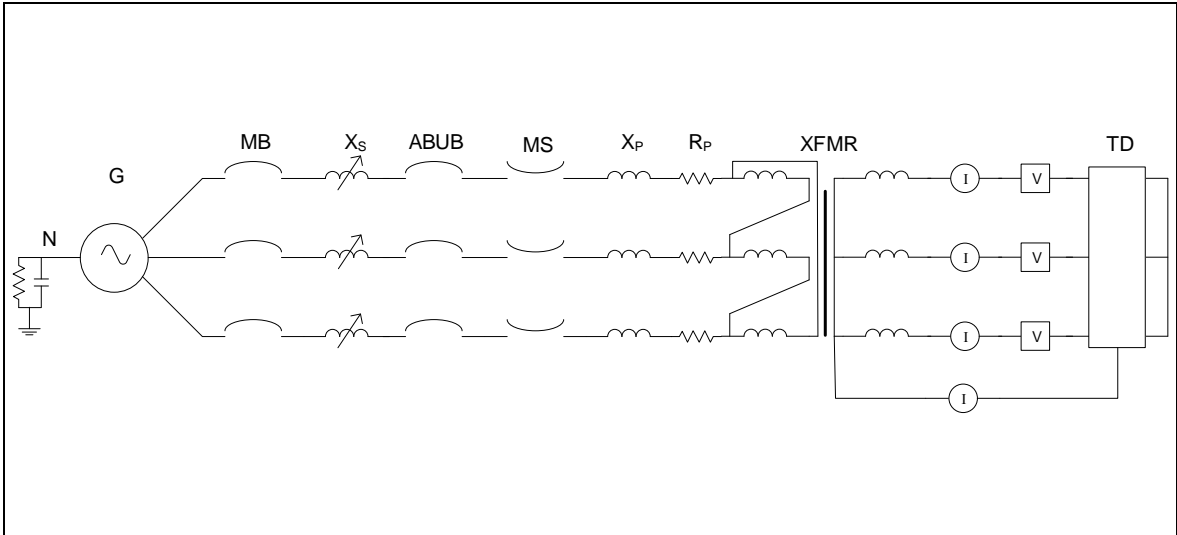
Standard	Client's instructions
Test date	23 August 2019

11.1 Condition before test

Test device new. Arc to be initiated by #24 AWG wire. Arc wire connected to 1" diameter aluminum rods. Test duration is 2 seconds.



11.2 Test circuit S03



G	= Generator	ABUB	= Aux. Breaker	R	= Resistance
N	= Neutral	XFMR	= Transformer	C	= Capacitance
MB	= Main Breaker	TD	= Test Device	V	= Voltage Measurement
MS	= Make Switch	X	= Inductance	I	= Current Measurement

Supply		
Power	MVA	26.2
Frequency	Hz	60
Phase(s)		3
Voltage	V	1009
Sym. Current	kA	15
Peak current	kA	40.4
Impedance	Ω	0.014

Remarks: -

11.3 Test results and oscillograms

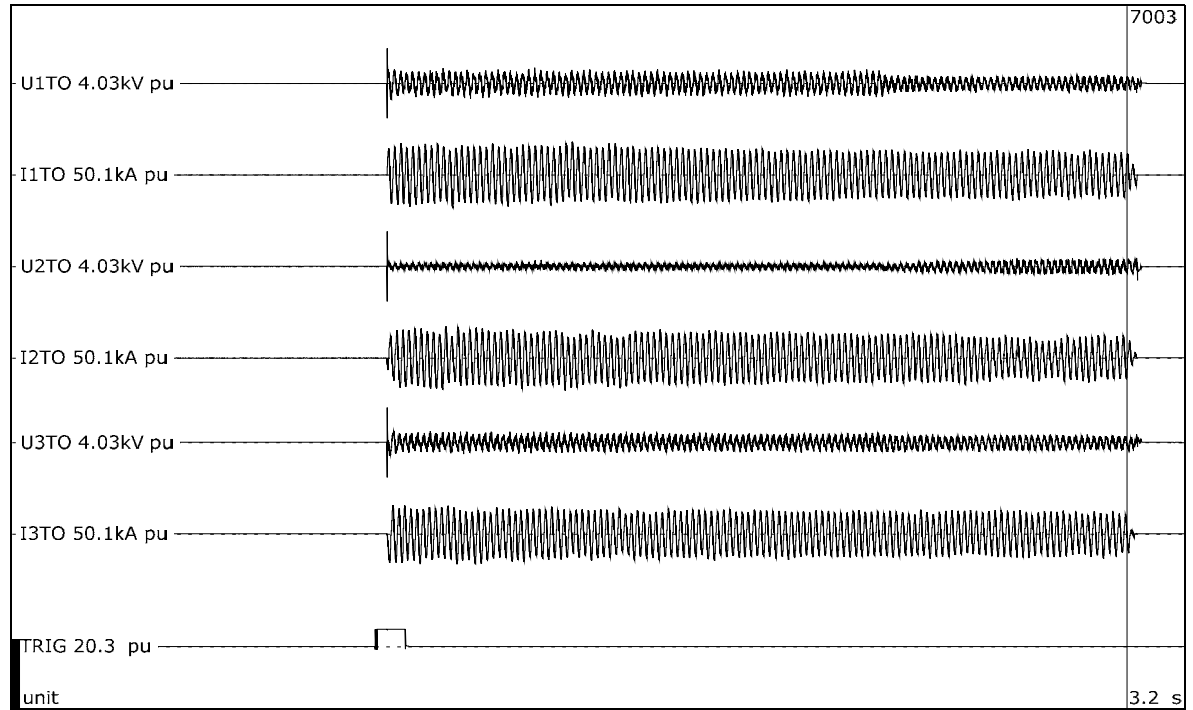
Overview of test numbers

190823-7003

Remarks

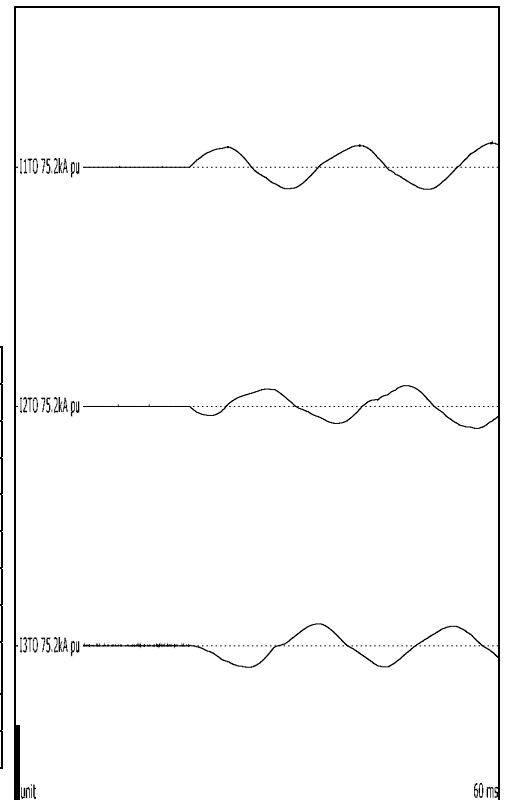
-

Open Box Test # 6 (OB06) - 1000 V, 15 kA



Test number: 190823-7003

Phase		A	B	C
Applied voltage, phase-to-ground	V _{RMS}	583	583	583
Applied voltage, phase-to-phase	V _{RMS}	1010		
Making current	kA _{peak}	-21.1	19.6	20.6
Current, a.c. component, beginning	kA _{RMS}	14.1	9.95	14.5
Current, a.c. component, middle	kA _{RMS}	12.8	12.6	11.4
Current, a.c. component, end	kA _{RMS}	11.3	9.74	10.1
Current, a.c. component, average	kA _{RMS}	13.1	12.1	12.1
Current, a.c. component, three-phase average	kA _{RMS}	12.4		
Duration	s	2.02	2.02	2.02
Arc energy	kJ	7434	483	4674



Observations: Emission of flames and gas observed.

11.4 Condition / inspection after test

Bottom of box burned completely through. Sides of box heavily burned, but not burned through completely.

12 OPEN BOX TEST # 7 (OB07) - 1000 V, 15 KA

Standard and date

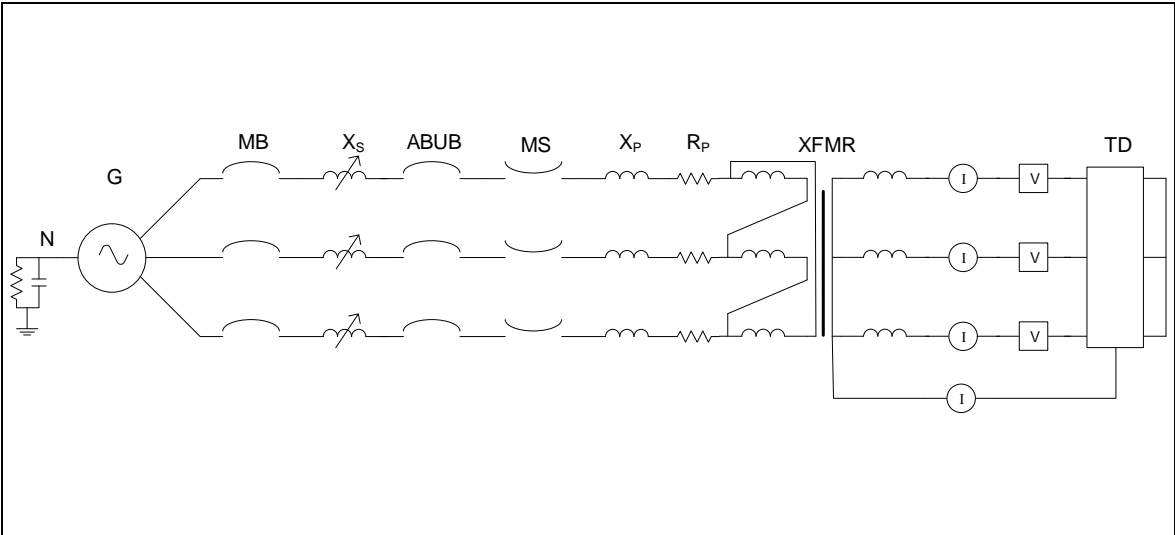
Standard	Client's instructions
Test date	23 August 2019

12.1 Condition before test

Test device new. Arc to be initiated by #24 AWG wire. Arc wire connected to 1" diameter aluminum rods. Test duration is 1.5 seconds.



12.2 Test circuit S03



G	= Generator	ABUB	= Aux. Breaker	R	= Resistance
N	= Neutral	XFMR	= Transformer	C	= Capacitance
MB	= Main Breaker	TD	= Test Device	V	= Voltage Measurement
MS	= Make Switch	X	= Inductance	I	= Current Measurement

Supply		
Power	MVA	26.2
Frequency	Hz	60
Phase(s)		3
Voltage	V	1009
Sym. Current	kA	15
Peak current	kA	40.4
Impedance	Ω	0.014

Remarks: -

12.3 Test results and oscillograms

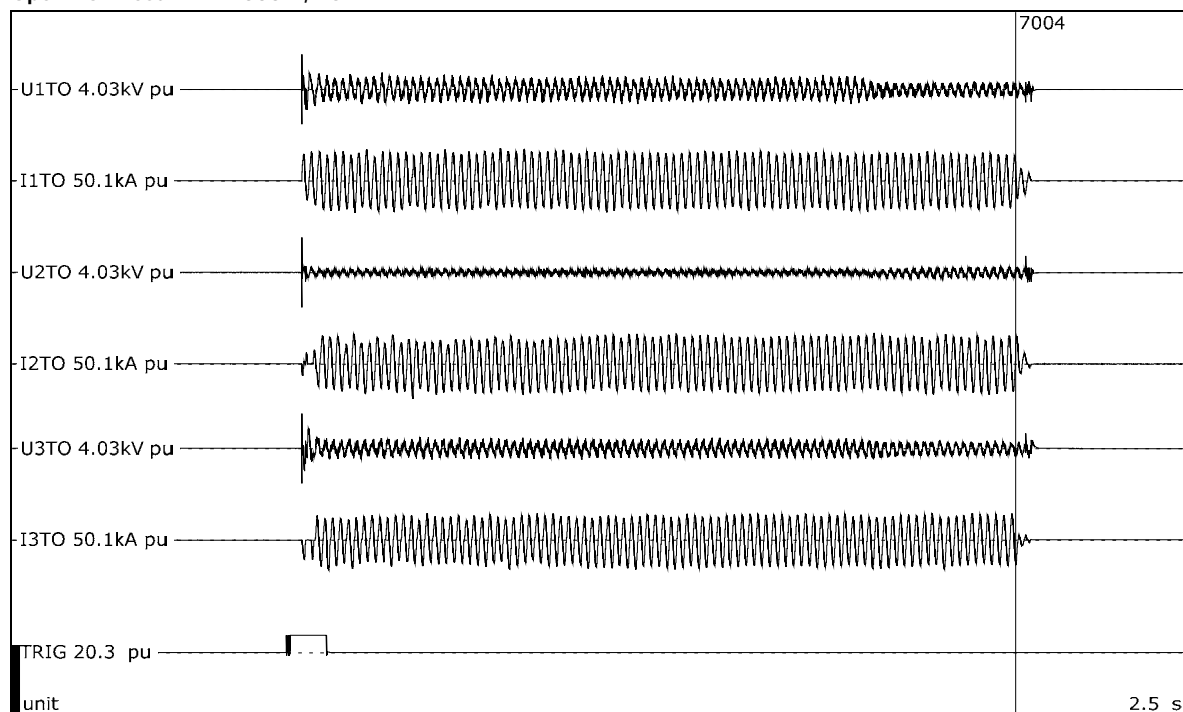
Overview of test numbers

190823-7004

Remarks

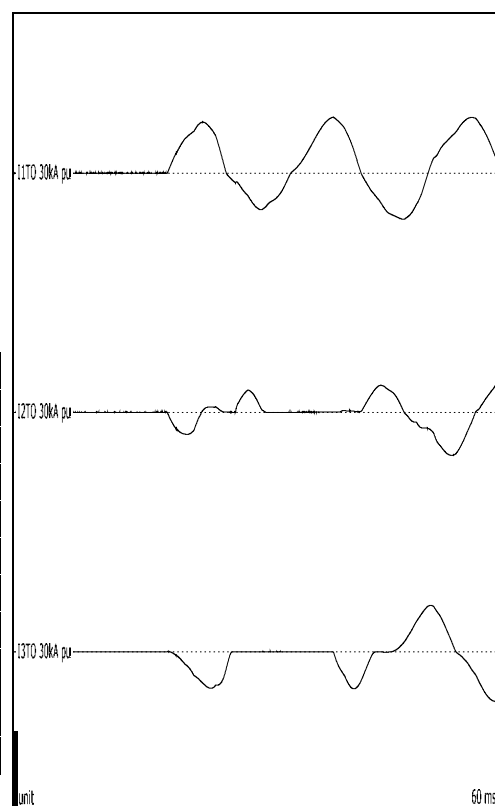
-

Open Box Test # 7 - 1000 V, 15 kA



Test number: 190823-7004

Phase		A	B	C
Applied voltage, phase-to-ground	V _{RMS}	583	583	583
Applied voltage, phase-to-phase	V _{RMS}	1010		
Making current	kA _{peak}	20.9	10.2	17.4
Current, a.c. component, beginning	kA _{RMS}	14.5	13.0	12.6
Current, a.c. component, middle	kA _{RMS}	13.9	14.0	13.0
Current, a.c. component, end	kA _{RMS}	13.6	14.6	12.7
Current, a.c. component, average	kA _{RMS}	13.9	12.3	11.8
Current, a.c. component, three-phase average	kA _{RMS}	12.6		
Duration	s	1.52	1.52	1.52
Arc energy	kJ	6460	118	3655



Observations: Emission of flames and gas observed. Arc extinguished for approximately 12 ms on B & C phases before re-igniting. After this period, the arc was sustained on B & C phases for the remainder of the test.

12.4 Condition / inspection after test

Bottom of box burned completely through. Sides of box heavily burned, but not burned through completely. There were two small holes on the side of the box towards the bottom of the box.

13 OPEN BOX TEST # 8 (OB08) - 1000 V, 30 KA

Standard and date

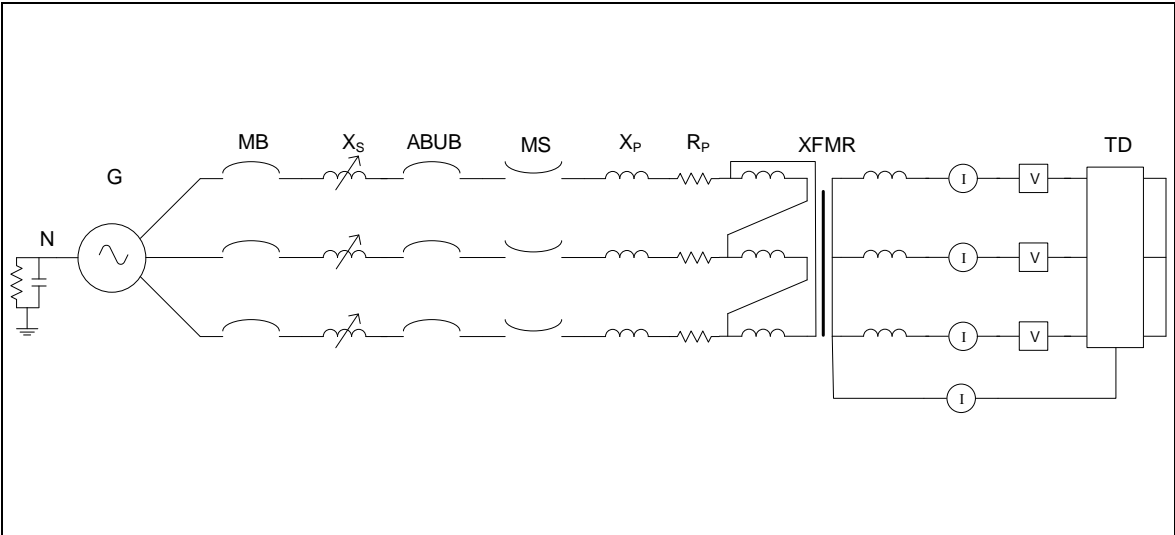
Standard	Client's instructions
Test date	23 August 2019

13.1 Condition before test

Test device new. Arc to be initiated by #24 AWG wire. Arc wire connected to 1" diameter aluminum rods. Test duration is 1 second.



13.2 Test circuit S04



G	= Generator	ABUB	= Aux. Breaker	R	= Resistance
N	= Neutral	XFMR	= Transformer	C	= Capacitance
MB	= Main Breaker	TD	= Test Device	V	= Voltage Measurement
MS	= Make Switch	X	= Inductance	I	= Current Measurement

Supply		
Power	MVA	55.3
Frequency	Hz	60
Phase(s)		3
Voltage	V	1064
Sym. Current	kA	30
Peak current	kA	79.1
Impedance	Ω	0.020

Remarks: -

13.3 Test results and oscillograms

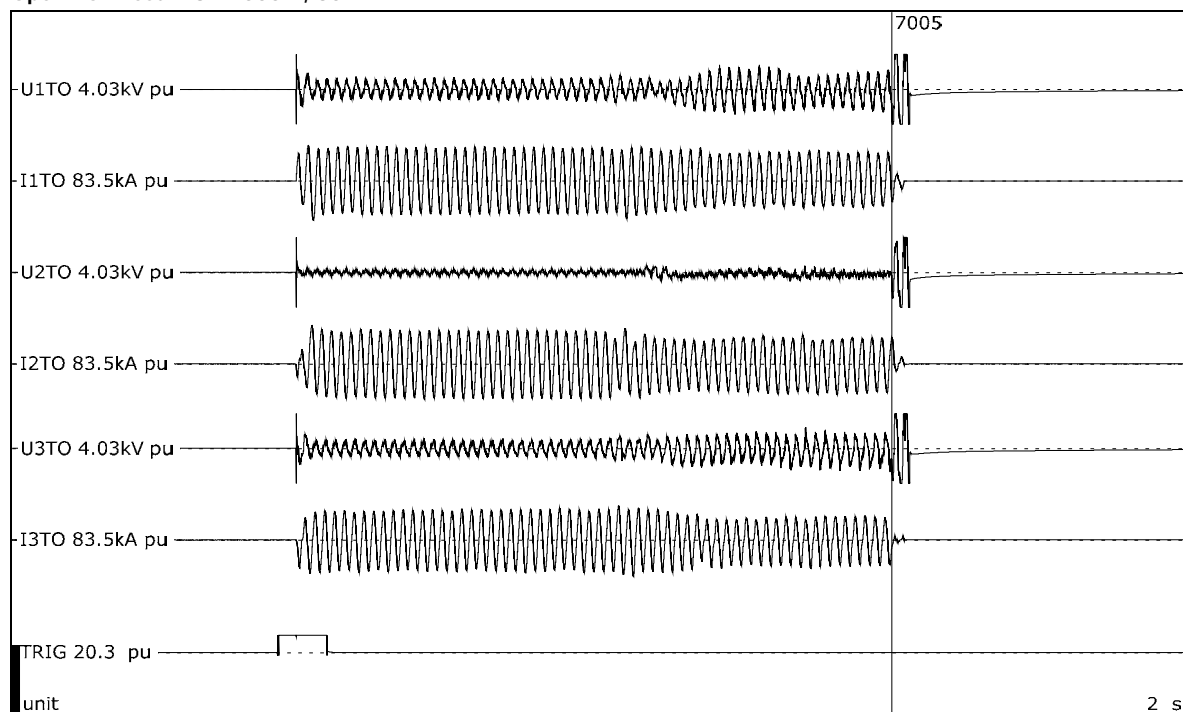
Overview of test numbers

190823-7005

Remarks

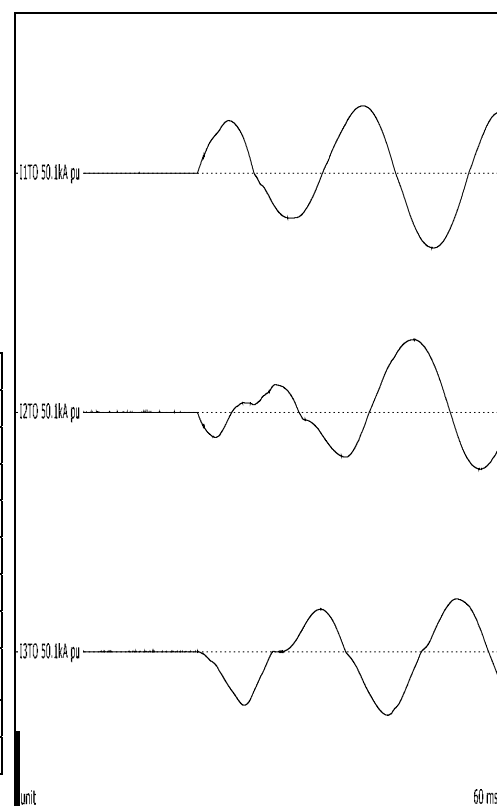
-

Open Box Test # 8 - 1000 V, 30 kA



Test number: 190823-7005

Phase		A	B	C
Applied voltage, phase-to-ground	V _{RMS}	614	614	614
Applied voltage, phase-to-phase	V _{RMS}	1063		
Making current	kA _{peak}	-47.0	45.7	-40.1
Current, a.c. component, beginning	kA _{RMS}	28.8	28.0	26.0
Current, a.c. component, middle	kA _{RMS}	27.7	28.1	26.2
Current, a.c. component, end	kA _{RMS}	23.5	23.3	20.6
Current, a.c. component, average	kA _{RMS}	26.1	24.8	23.9
Current, a.c. component, three-phase average	kA _{RMS}	24.9		
Duration	s	1.01	1.01	1.01
Arc energy	MJ	10.5	1.17	7.90



Observations: Emission of flames and gas observed.

13.4 Condition / inspection after test

Small hole burned through bottom of box. Sides of box burned, but not completely through. B-phase aluminum rod ejected from the box. A and C phase rods were bent away from one another. Aluminum rods broke apart.

14 OPEN BOX TEST # 9 (OB11) - SINGLE PHASE INVESTIGATION

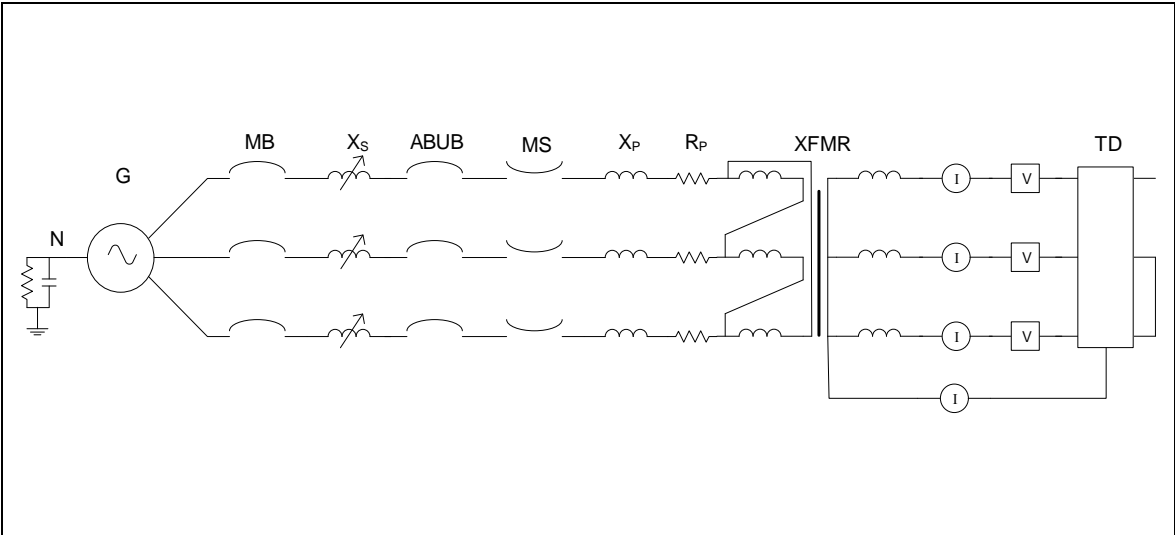
Standard and date

Standard	Client's instructions
Test date	23 August 2019

14.1 Condition before test

Test box previously subject to arc tests on 8/23. Aluminum rods new. Arc to be initiated by #24 AWG wire. Arc wire connected to 1" diameter aluminum rods on B & C phase only. Test duration is 100 milliseconds. Purpose of the test is to measure how long it takes for arc to propagate to third phase.

14.2 Test circuit S05



G	= Generator	ABUB	= Aux. Breaker	R	= Resistance
N	= Neutral	XFMR	= Transformer	C	= Capacitance
MB	= Main Breaker	TD	= Test Device	V	= Voltage Measurement
MS	= Make Switch	X	= Inductance	I	= Current Measurement

Supply		
Power	MVA	26.2
Frequency	Hz	60
Phase(s)		3
Voltage	V	1009
Sym. Current	kA	15
Peak current	kA	40.4
Impedance	Ω	0.014

Remarks: Test conducted with arc wire only between two phases. Supply table above shows the available 3-phase circuit when arc propagated from 1-phase arc to 3-phase arc.

14.3 Test results and oscillograms

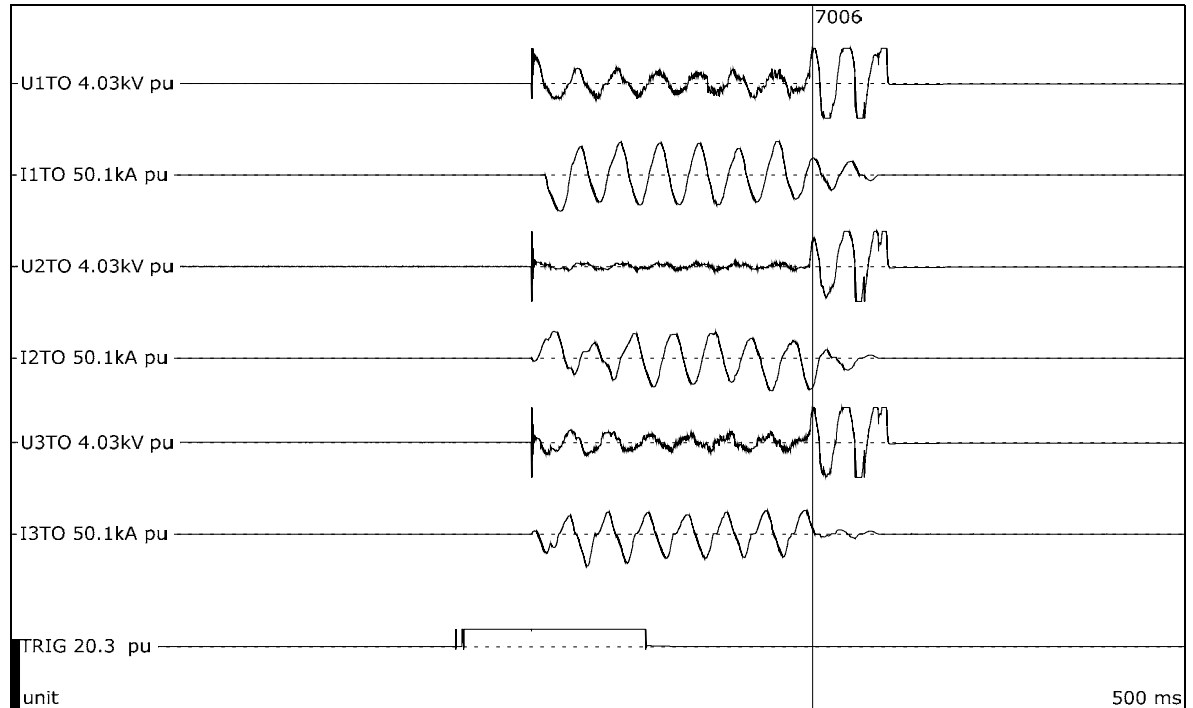
Overview of test numbers

190823-7006

Remarks

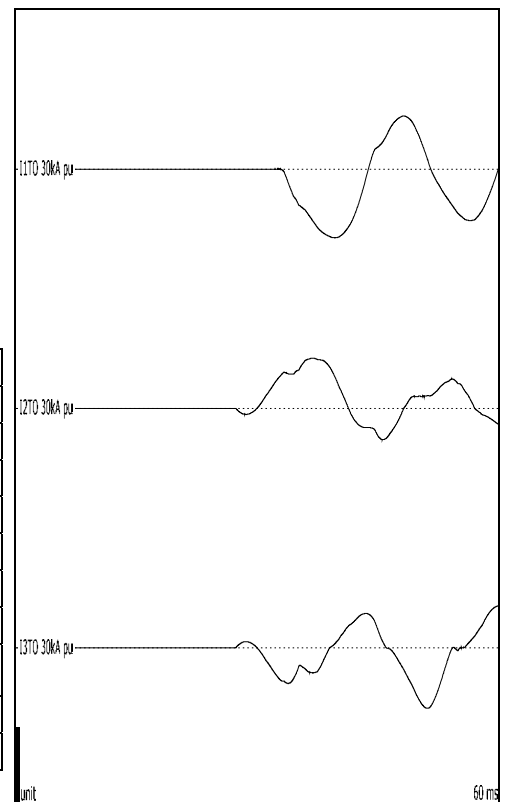
-

Open Box Test # 9 - Single Phase Investigation



Test number: 190823-7006

Phase		A	B	C
Applied voltage, phase-to-ground	V _{RMS}	583	583	583
Applied voltage, phase-to-phase	V _{RMS}	1010		
Making current	kA _{peak}	-25.9	18.8	-22.9
Current, a.c. component, beginning	kA _{RMS}	15.1	9.44	11.2
Current, a.c. component, middle	kA _{RMS}	15.4	12.7	11.2
Current, a.c. component, end	kA _{RMS}	15.4	2.82	11.2
Current, a.c. component, average	kA _{RMS}	15.2	11.7	11.9
Current, a.c. component, three-phase average	kA _{RMS}	12.9		
Duration	s	0.114	0.120	0.117
Arc energy	kJ	758	73.0	334



Observations: Emission of flames and gas observed. Arc propagated to A-phase rod in approximately 6 ms.

14.4 Condition / inspection after test

Minimal damage to test box observed.

15 CHECKING THE PROSPECTIVE CURRENT

Standard and date

Standard	Client's instructions
Test date	26 August 2019

15.1 Condition before test

Shorting bar connected at station terminals directly prior to test device.

15.2 Test results and oscillograms

Overview of test numbers

190826-7001, 7002

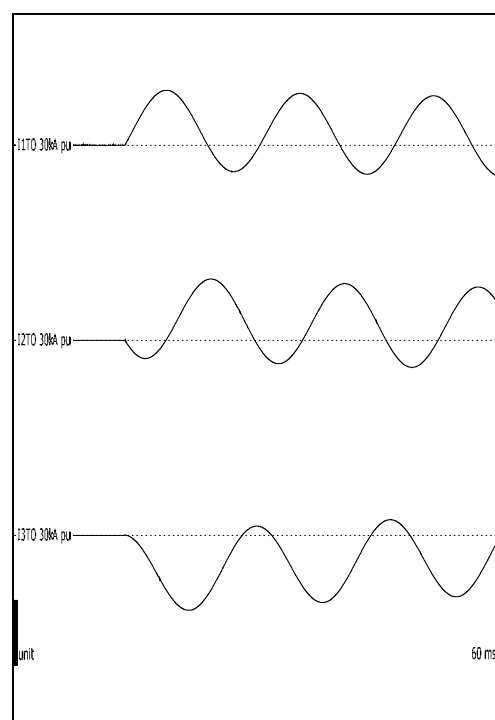
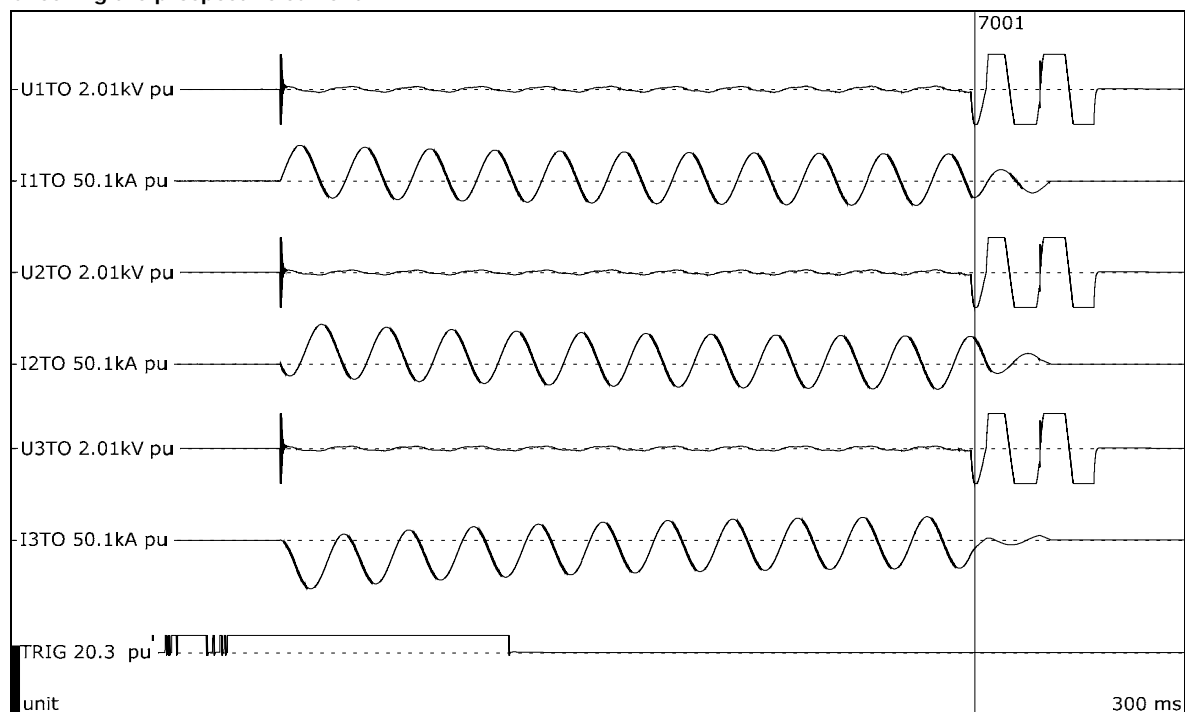
Remarks

Prospective circuit parameters calibrated in this test duty:

190826-7001: 616 V, 13.5 kA, 35.6 kA peak.

190826-7002: 489 V, 13.5 kA, 35.5 kA peak.

Checking the prospective current

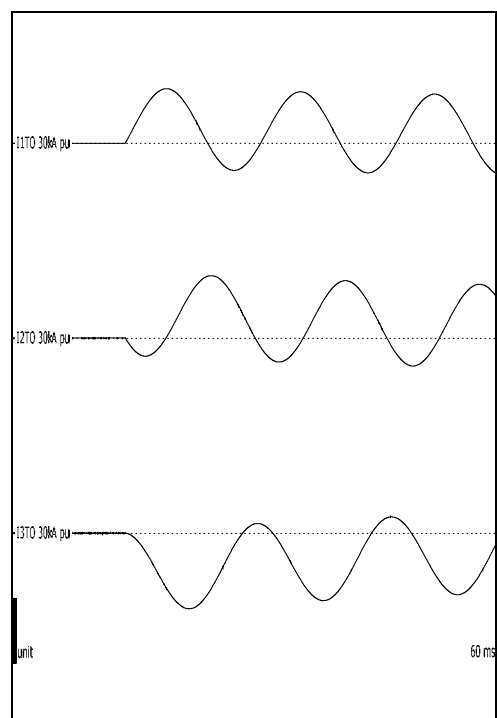
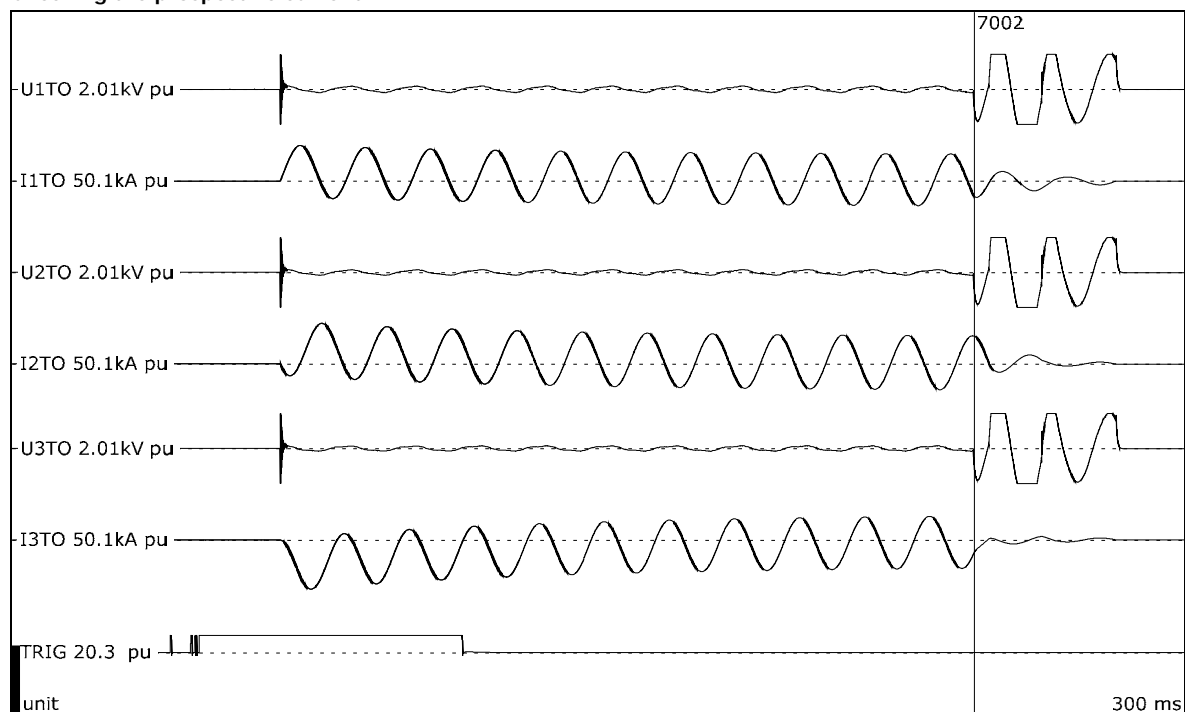


Test number: 190826-7001

Phase		A	B	C
Current	kA _{peak}	25.3	28.2	-34.7
Current, a.c. component	kA _{RMS}	13.0	13.4	13.0
Current, a.c. component, three-phase average	kA _{RMS}	13.1		
Duration, current	s	0.177	0.177	0.177

Observations: No visible disturbance.

Checking the prospective current



Test number: 190826-7002

Phase		A	B	C
Current	kA _{peak}	25.1	28.9	-34.9
Current, a.c. component	kA _{RMS}	13.0	13.6	13.2
Current, a.c. component, three-phase average	kA _{RMS}	13.3		
Duration, current	s	0.177	0.177	0.176

Observations: No visible disturbance.

16 SAMPLE 2-13 (A) - 480 V, 13.5 KA

Standard and date

Standard	Client's instructions
Test date	26 August 2019

16.1 Condition before test

Switchgear new. Arc to be initiated by #10 AWG stranded wire.

Pressure transducers # 1 & 2 located on right side of switchgear (when facing the front of the gear).

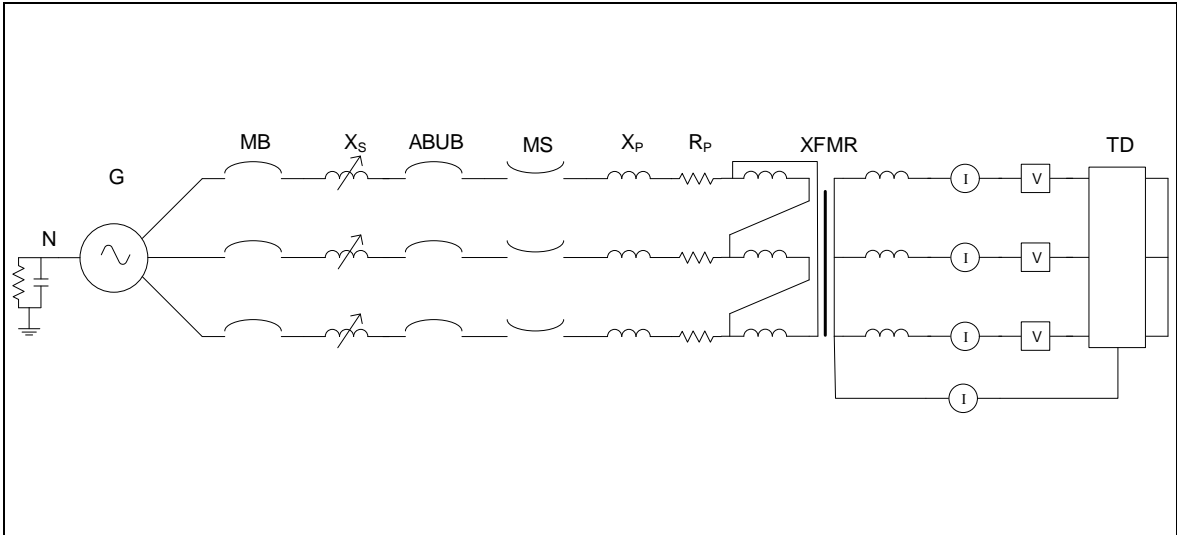
Pressure transducers # 3 & 4 located on left side of switchgear (when facing the front of the gear).

Pressure transducers # 1 & 3 are 0-50 PSI transducers.

Pressure transducers # 2 & 4 are 0-30 PSI transducers.



16.2 Test circuit S06



G	= Generator	ABUB	= Aux. Breaker	R	= Resistance
N	= Neutral	XFMR	= Transformer	C	= Capacitance
MB	= Main Breaker	TD	= Test Device	V	= Voltage Measurement
MS	= Make Switch	X	= Inductance	I	= Current Measurement

Supply		
Power	MVA	11.4
Frequency	Hz	60
Phase(s)		3
Voltage	V	489
Sym. Current	kA	13.5
Peak current	kA	35.5
Impedance	Ω	0.021

Remarks: -

16.3 Test results and oscillograms

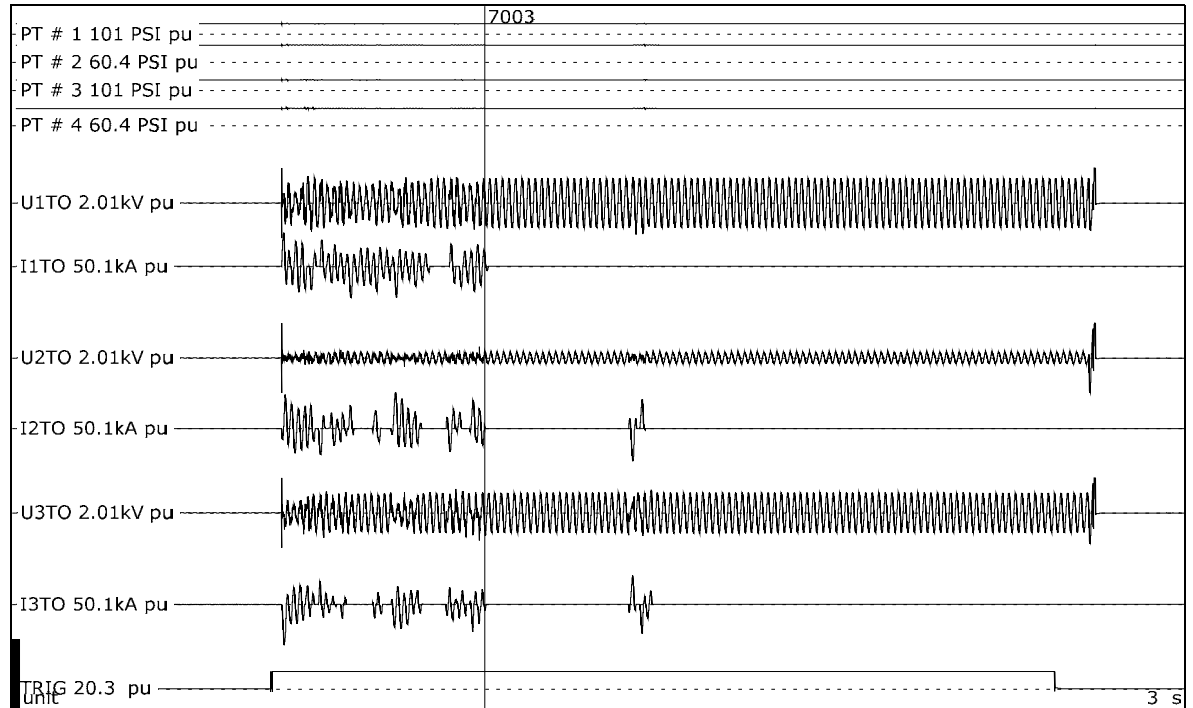
Overview of test numbers

190826-7003

Remarks

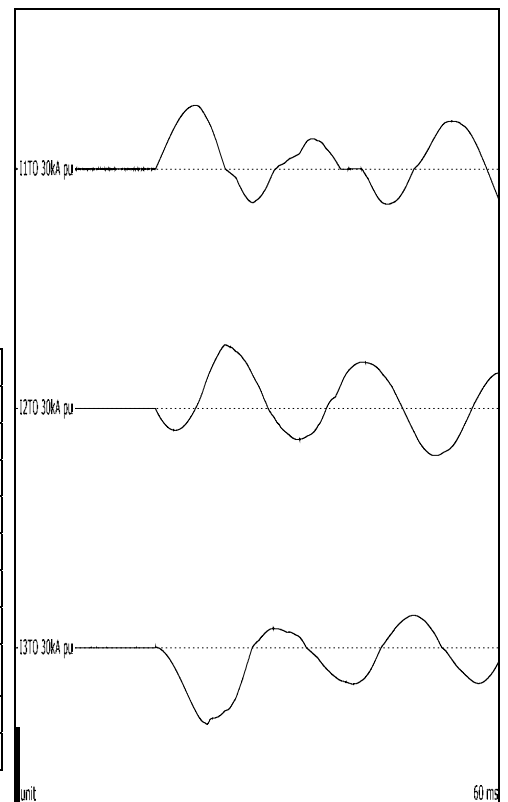
Voltage traces for this test duty appear uneven on the oscillographs. This is due to the fact that station voltage dividers are referenced to ground. The test was conducted with the neutral of the wye transformer floating, so the station voltage dividers do not have a solid reference.

Sample 2-13 (A) - 480 V, 13.5 kA



Test number: 190826-7003

Phase		A	B	C
Applied voltage, phase-to-ground	V _{RMS}	282	282	282
Applied voltage, phase-to-phase	V _{RMS}	488		
Making current	kA _{peak}	24.0	23.8	-28.7
Current, a.c. component, beginning	kA _{RMS}	10.7	11.9	10.2
Current, a.c. component, middle	kA _{RMS}	7.52	9.15	5.89
Current, a.c. component, end	kA _{RMS}	7.98	4.04	5.44
Current, a.c. component, average	kA _{RMS}	8.78	9.35	7.71
Current, a.c. component, three-phase average	kA _{RMS}	8.61		
Duration	s	0.519	0.519	0.519
Arc energy	kJ	1122	28.9	554



Observations: Emission of flames and gas observed.

16.4 Condition / inspection after test

Switchgear sustained minimal damage. Arc self-extinguished.

17 SAMPLE 2-13 (B) - 600 V, 13.5 KA

Standard and date

Standard	Client's instructions
Test date	27 August 2019

17.1 Condition before test

Switchgear previously subjected to arc test at 480 V, 13.5 kA. Arc to be initiated by two #10 AWG stranded wires.

Pressure transducers # 1 & 2 located on right side of switchgear (when facing the front of the gear).

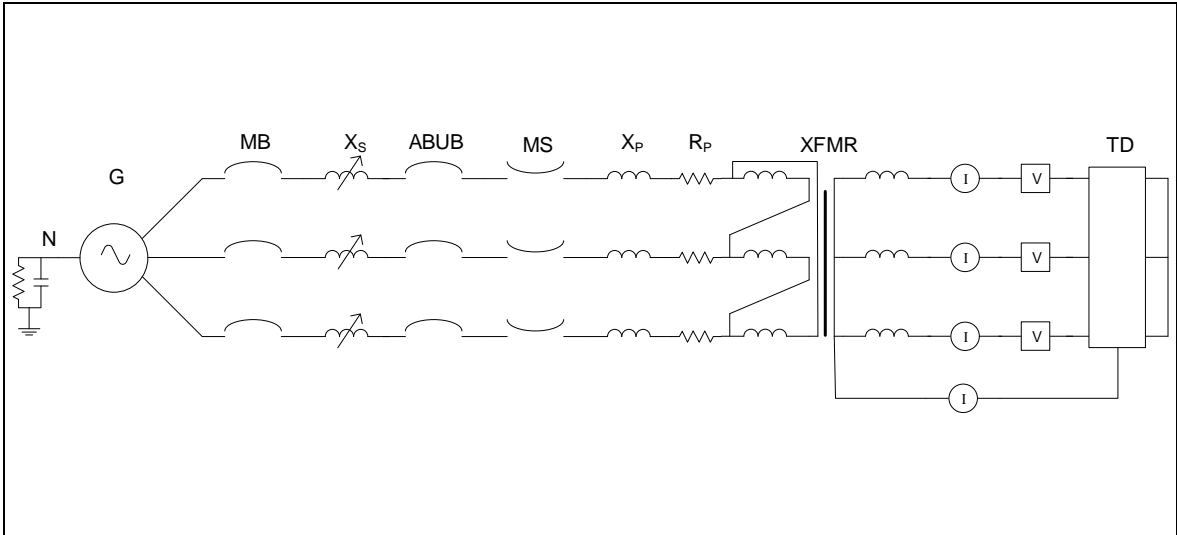
Pressure transducers # 3 & 4 located on left side of switchgear (when facing the front of the gear).

Pressure transducers # 1 & 3 are 0-50 PSI transducers.

Pressure transducers # 2 & 4 are 0-30 PSI transducers.



17.2 Test circuit S07



G	= Generator	ABUB	= Aux. Breaker	R	= Resistance
N	= Neutral	XFMR	= Transformer	C	= Capacitance
MB	= Main Breaker	TD	= Test Device	V	= Voltage Measurement
MS	= Make Switch	X	= Inductance	I	= Current Measurement

Supply		
Power	MVA	14.4
Frequency	Hz	60
Phase(s)		3
Voltage	V	616
Sym. Current	kA	13.5
Peak current	kA	35.6
Impedance	Ω	0.026

Remarks: -

17.3 Test results and oscillograms

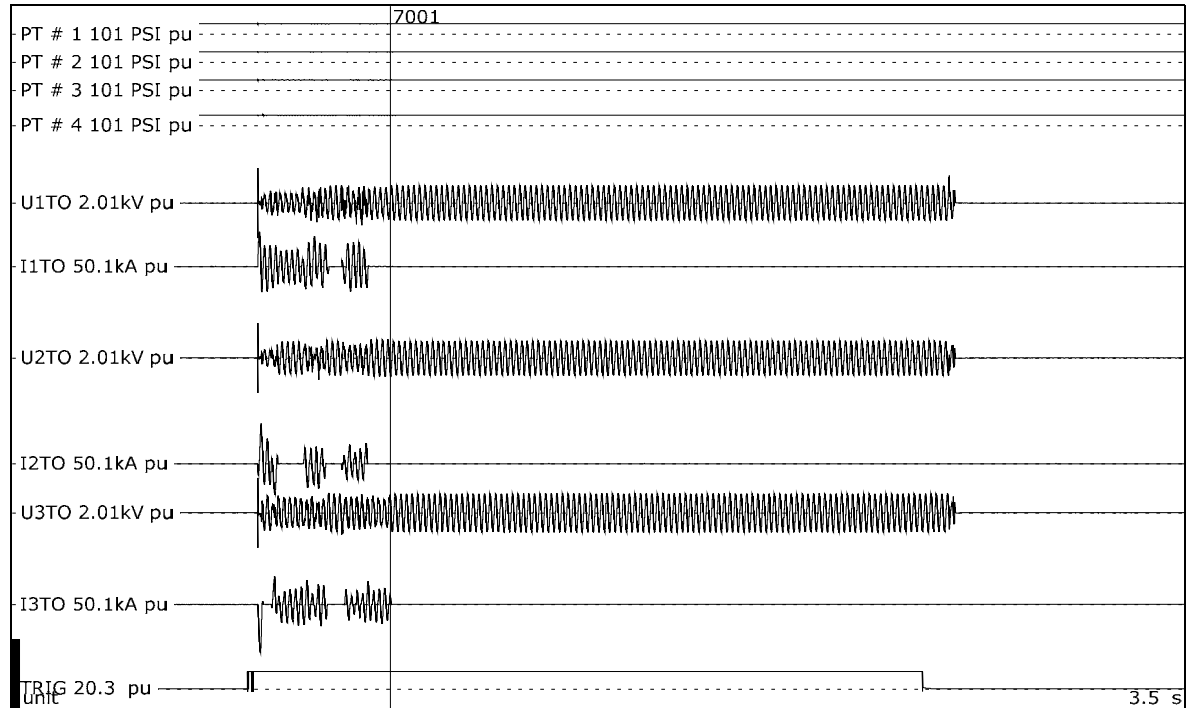
Overview of test numbers

190827-7001

Remarks

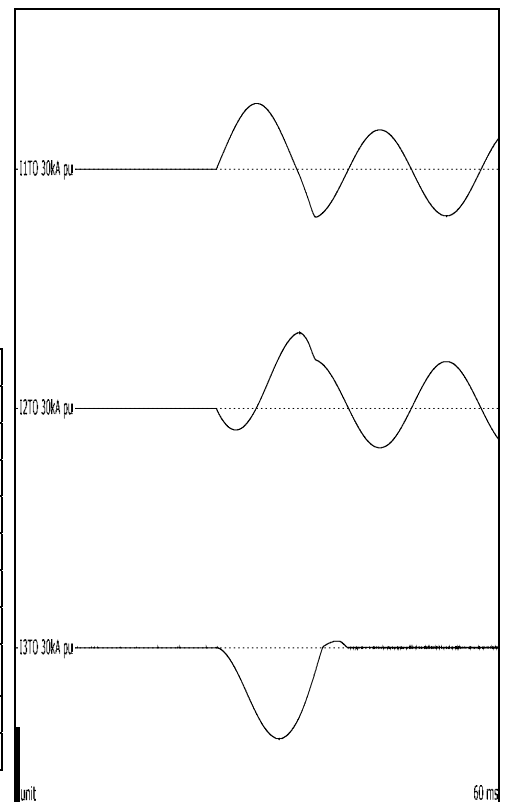
-

Sample 2-13 (B) - 600 V, 13.5 kA



Test number: 190827-7001

Phase		A	B	C
Applied voltage, phase-to-ground	V _{RMS}	356	356	356
Applied voltage, phase-to-phase	V _{RMS}	617		
Making current	kA _{peak}	24.7	28.5	-34.3
Current, a.c. component, beginning	kA _{RMS}	13.4	14.0	2.05
Current, a.c. component, middle	kA _{RMS}	8.76	7.33	6.74
Current, a.c. component, end	kA _{RMS}	0.000	0.000	7.95
Current, a.c. component, average	kA _{RMS}	9.91	9.46	8.27
Current, a.c. component, three-phase average	kA _{RMS}	9.22		
Duration	s	0.332	0.332	0.396
Arc energy	kJ	562	216	596



Observations: Emission of flames and gas observed.

17.4 Condition / inspection after test

Switchgear sustained minimal damage. Arc self-extinguished.

18 SAMPLE 2-13 (C) - 600 V, 13.5 KA

Standard and date

Standard	Client's instructions
Test date	27 August 2019

18.1 Condition before test

Switchgear in same condition as after trial 190827-7001. Arc to be initiated by two #10 AWG stranded wires. Additional grounding plate added to gear to attempt to sustain the arc.

Pressure transducers # 1 & 2 located on right side of switchgear (when facing the front of the gear).

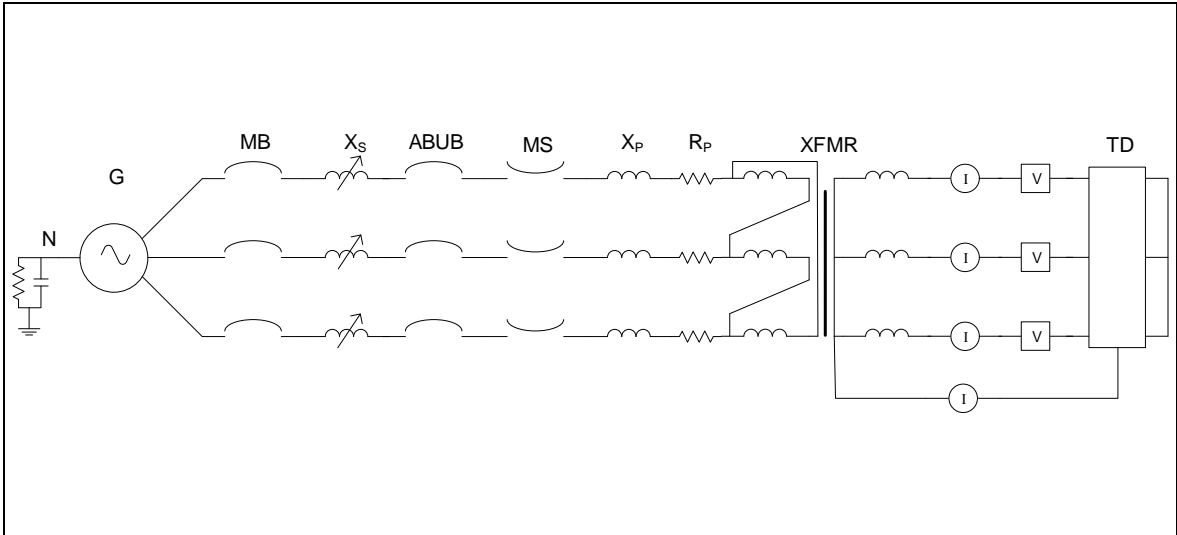
Pressure transducers # 3 & 4 located on left side of switchgear (when facing the front of the gear).

Pressure transducers # 1 & 3 are 0-50 PSI transducers.

Pressure transducers # 2 & 4 are 0-30 PSI transducers.



18.2 Test circuit S07



G	= Generator	ABUB	= Aux. Breaker	R	= Resistance
N	= Neutral	XFMR	= Transformer	C	= Capacitance
MB	= Main Breaker	TD	= Test Device	V	= Voltage Measurement
MS	= Make Switch	X	= Inductance	I	= Current Measurement

Supply		
Power	MVA	14.4
Frequency	Hz	60
Phase(s)		3
Voltage	V	616
Sym. Current	kA	13.5
Peak current	kA	35.6
Impedance	Ω	0.026

Remarks: -

18.3 Test results and oscillograms

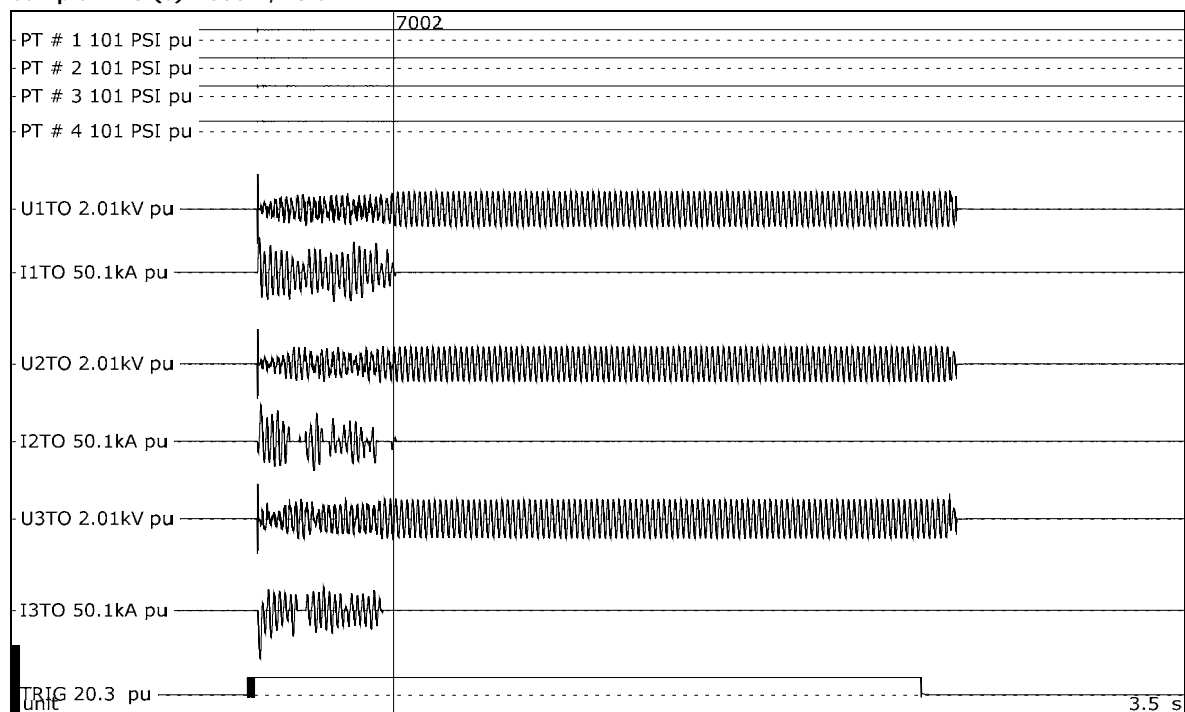
Overview of test numbers

190827-7002

Remarks

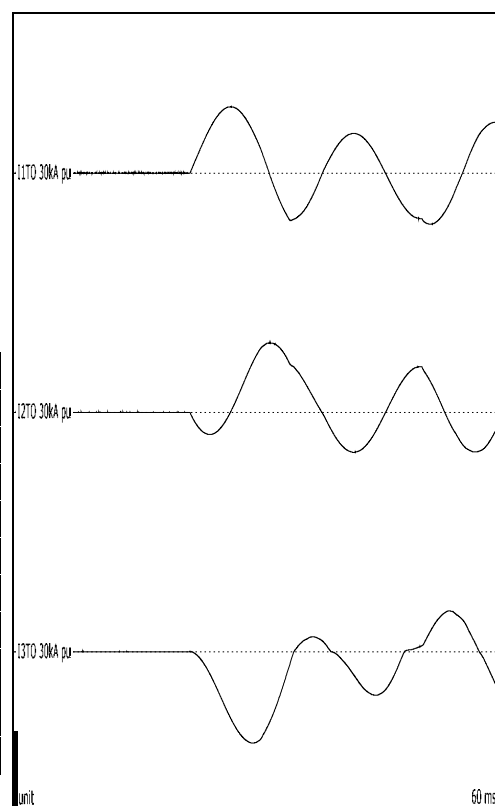
-

Sample 2-13 (C) - 600 V, 13.5 kA



Test number: 190827-7002

Phase		A	B	C
Applied voltage, phase-to-ground	V _{RMS}	356	356	356
Applied voltage, phase-to-phase	V _{RMS}	617		
Making current	kA _{peak}	25.0	26.1	-34.4
Current, a.c. component, beginning	kA _{RMS}	13.4	13.2	11.0
Current, a.c. component, middle	kA _{RMS}	8.92	9.14	10.2
Current, a.c. component, end	kA _{RMS}	7.93	4.10	8.05
Current, a.c. component, average	kA _{RMS}	11.5	10.2	9.09
Current, a.c. component, three-phase average	kA _{RMS}	10.3		
Duration	s	0.405	0.405	0.404
Arc energy	kJ	705	342	601



Observations: Emission of flames and gas observed.

18.4 Condition / inspection after test

Switchgear sustained minimal damage. Arc self-extinguished.

19 SAMPLE 2-13 (D) - 600 V, 13.5 KA

Standard and date

Standard	Client's instructions
Test date	27 August 2019

19.1 Condition before test

Switchgear in same condition as after trial 190827-7002. Arc to be initiated by two #10 AWG stranded wires.

Pressure transducers # 1 & 2 located on right side of switchgear (when facing the front of the gear).

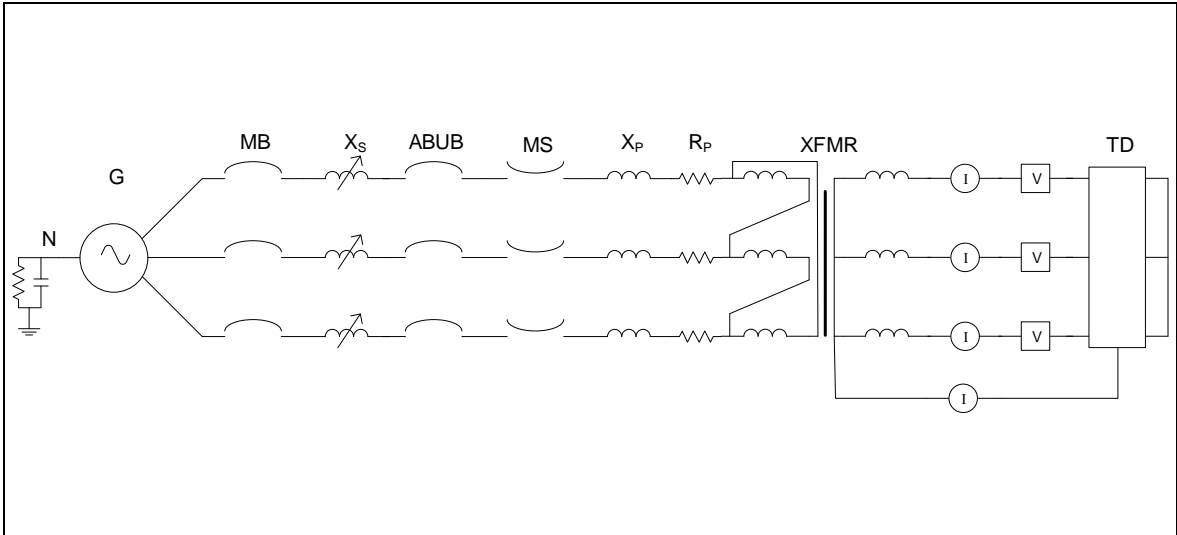
Pressure transducers # 3 & 4 located on left side of switchgear (when facing the front of the gear).

Pressure transducers # 1 & 3 are 0-50 PSI transducers.

Pressure transducers # 2 & 4 are 0-30 PSI transducers.



19.2 Test circuit S07



G	= Generator	ABUB	= Aux. Breaker	R	= Resistance
N	= Neutral	XFMR	= Transformer	C	= Capacitance
MB	= Main Breaker	TD	= Test Device	V	= Voltage Measurement
MS	= Make Switch	X	= Inductance	I	= Current Measurement

Supply		
Power	MVA	14.4
Frequency	Hz	60
Phase(s)		3
Voltage	V	616
Sym. Current	kA	13.5
Peak current	kA	35.6
Impedance	Ω	0.026

Remarks: -

19.3 Test results and oscillograms

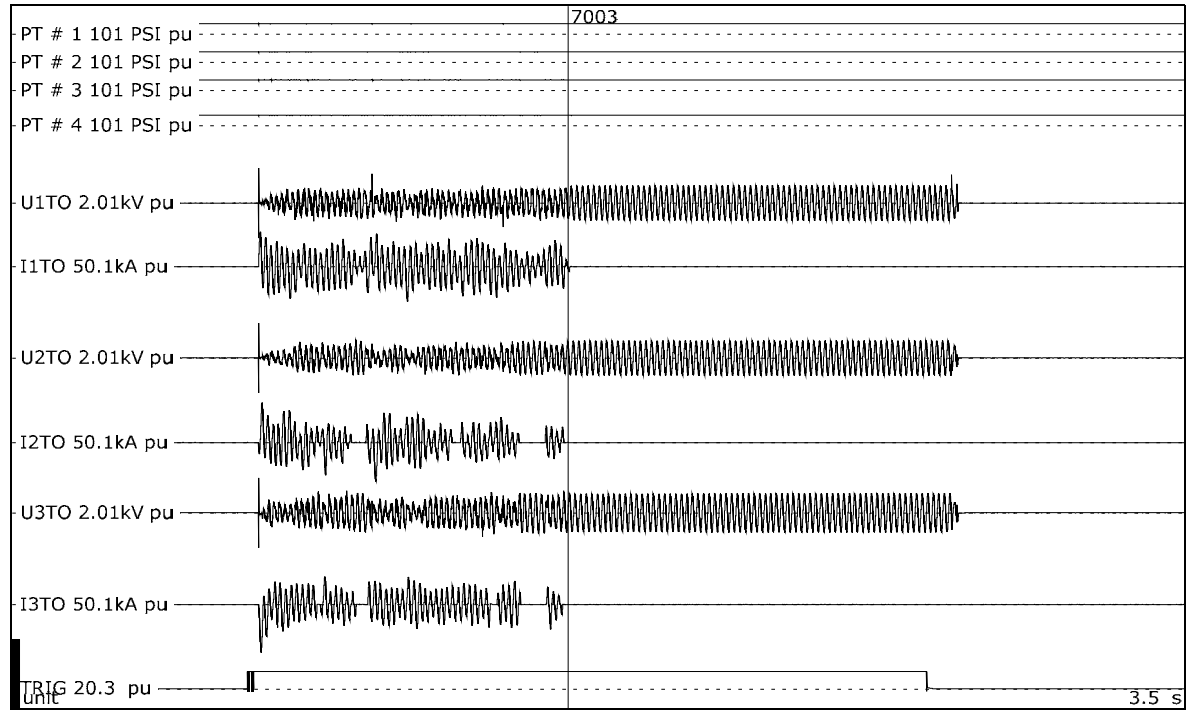
Overview of test numbers

190827-7003

Remarks

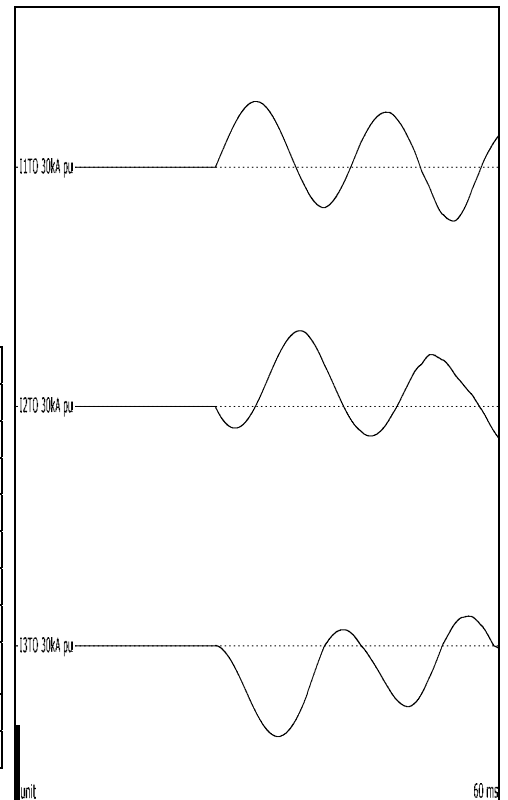
-

Sample 2-13 (D) - 600 V, 13.5 kA



Test number: 190827-7003

Phase		A	B	C
Applied voltage, phase-to-ground	V _{RMS}	356	356	356
Applied voltage, phase-to-phase	V _{RMS}	617		
Making current	kA _{peak}	24.7	28.4	-34.3
Current, a.c. component, beginning	kA _{RMS}	13.4	13.5	12.2
Current, a.c. component, middle	kA _{RMS}	9.05	13.7	11.8
Current, a.c. component, end	kA _{RMS}	10.9	8.03	8.49
Current, a.c. component, average	kA _{RMS}	11.2	10.1	9.88
Current, a.c. component, three-phase average	kA _{RMS}	10.4		
Duration	s	0.924	0.924	0.924
Arc energy	kJ	1754	1031	1356



Observations: Emission of flames and gas observed.

19.4 Condition / inspection after test

Switchgear sustained minimal damage. Arc self-extinguished.

20 SAMPLE 2-13 (E) - 600 V, 13.5 KA

Standard and date

Standard	Client's instructions
Test date	27 August 2019

20.1 Condition before test

Switchgear in same condition as after trial 190827-7003. Arc to be initiated by two #10 AWG stranded wires.

Pressure transducers # 1 & 2 located on right side of switchgear (when facing the front of the gear).

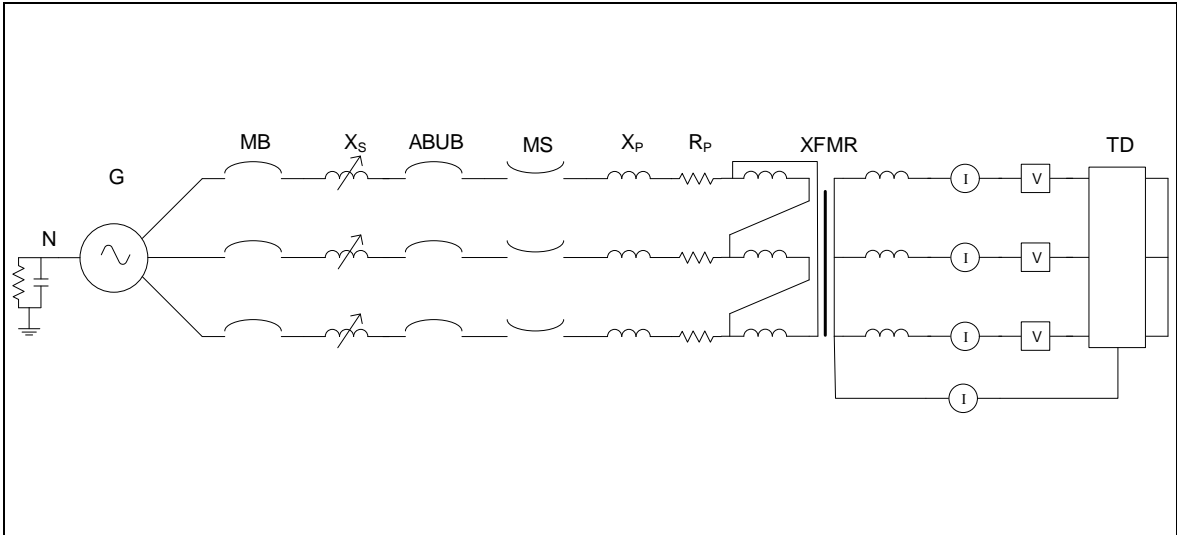
Pressure transducers # 3 & 4 located on left side of switchgear (when facing the front of the gear).

Pressure transducers # 1 & 3 are 0-50 PSI transducers.

Pressure transducers # 2 & 4 are 0-30 PSI transducers.



20.2 Test circuit S07



G	= Generator	ABUB	= Aux. Breaker	R	= Resistance
N	= Neutral	XFMR	= Transformer	C	= Capacitance
MB	= Main Breaker	TD	= Test Device	V	= Voltage Measurement
MS	= Make Switch	X	= Inductance	I	= Current Measurement

Supply		
Power	MVA	14.4
Frequency	Hz	60
Phase(s)		3
Voltage	V	616
Sym. Current	kA	13.5
Peak current	kA	35.6
Impedance	Ω	0.026

Remarks: -

20.3 Test results and oscillograms

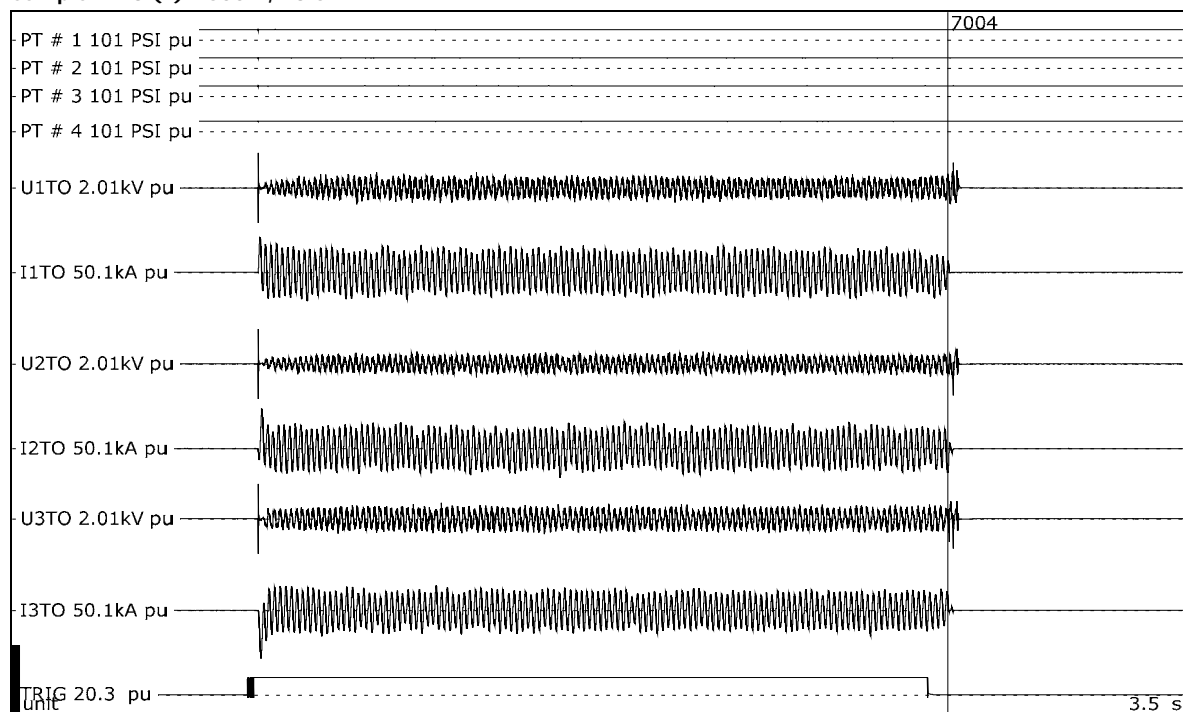
Overview of test numbers

190827-7004

Remarks

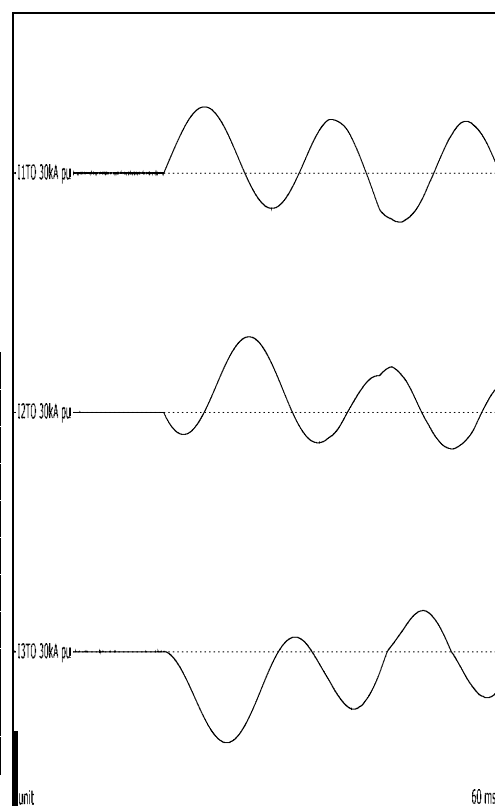
-

Sample 2-13 (E) - 600 V, 13.5 kA



Test number: 190827-7004

Phase		A	B	C
Applied voltage, phase-to-ground	V _{RMS}	356	356	356
Applied voltage, phase-to-phase	V _{RMS}	617		
Making current	kA _{peak}	24.9	28.4	-34.3
Current, a.c. component, beginning	kA _{RMS}	12.6	13.5	11.6
Current, a.c. component, middle	kA _{RMS}	10.4	10.5	9.79
Current, a.c. component, end	kA _{RMS}	10.2	9.35	9.26
Current, a.c. component, average	kA _{RMS}	11.1	10.8	10.00
Current, a.c. component, three-phase average	kA _{RMS}	10.6		
Duration	s	2.06	2.06	2.06
Arc energy	kJ	3497	2815	3289



Observations: Emission of flames and gas observed.

20.4 Condition / inspection after test

Evidence of arcing found around the outside of the switchgear (burning and charring). No complete burn-throughs. Two of the breaker doors opened.

21 SAMPLE 2-13 (F) - 480 V, 13.5 KA

Standard and date

Standard	Client's instructions
Test date	28 August 2019

21.1 Condition before test

Switchgear in same condition as after trial 190827-7004. Arc to be initiated by two #10 AWG stranded wires.

Pressure transducers # 1 & 2 located on right side of switchgear (when facing the front of the gear).

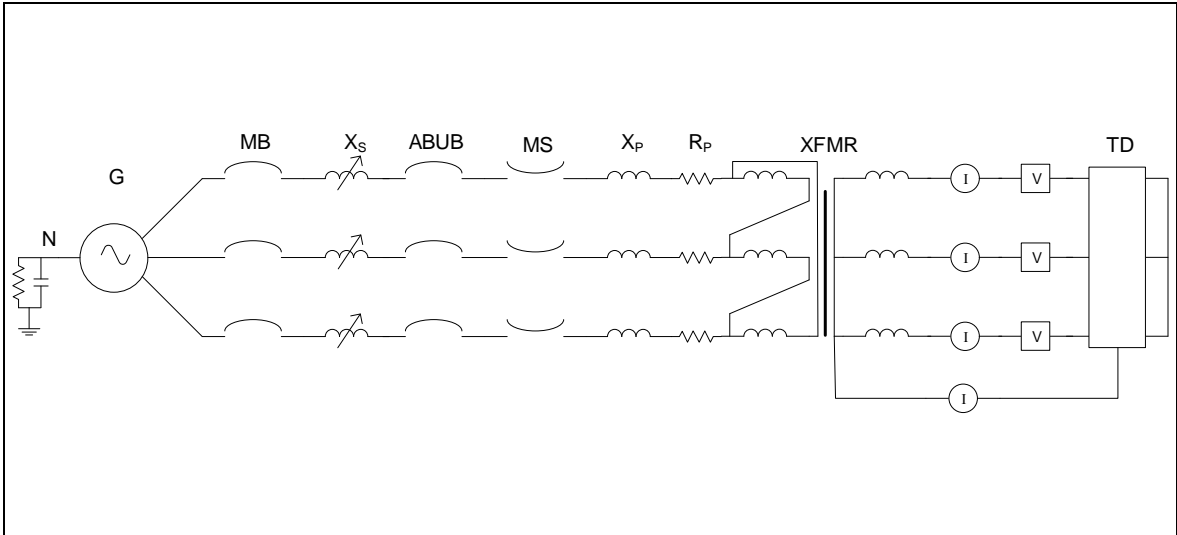
Pressure transducers # 3 & 4 located on left side of switchgear (when facing the front of the gear).

Pressure transducers # 1 & 3 are 0-50 PSI transducers.

Pressure transducers # 2 & 4 are 0-30 PSI transducers.



21.2 Test circuit S06



G	= Generator	ABUB	= Aux. Breaker	R	= Resistance
N	= Neutral	XFMR	= Transformer	C	= Capacitance
MB	= Main Breaker	TD	= Test Device	V	= Voltage Measurement
MS	= Make Switch	X	= Inductance	I	= Current Measurement

Supply		
Power	MVA	11.4
Frequency	Hz	60
Phase(s)		3
Voltage	V	489
Sym. Current	kA	13.5
Peak current	kA	35.5
Impedance	Ω	0.021

Remarks: -

21.3 Test results and oscillograms

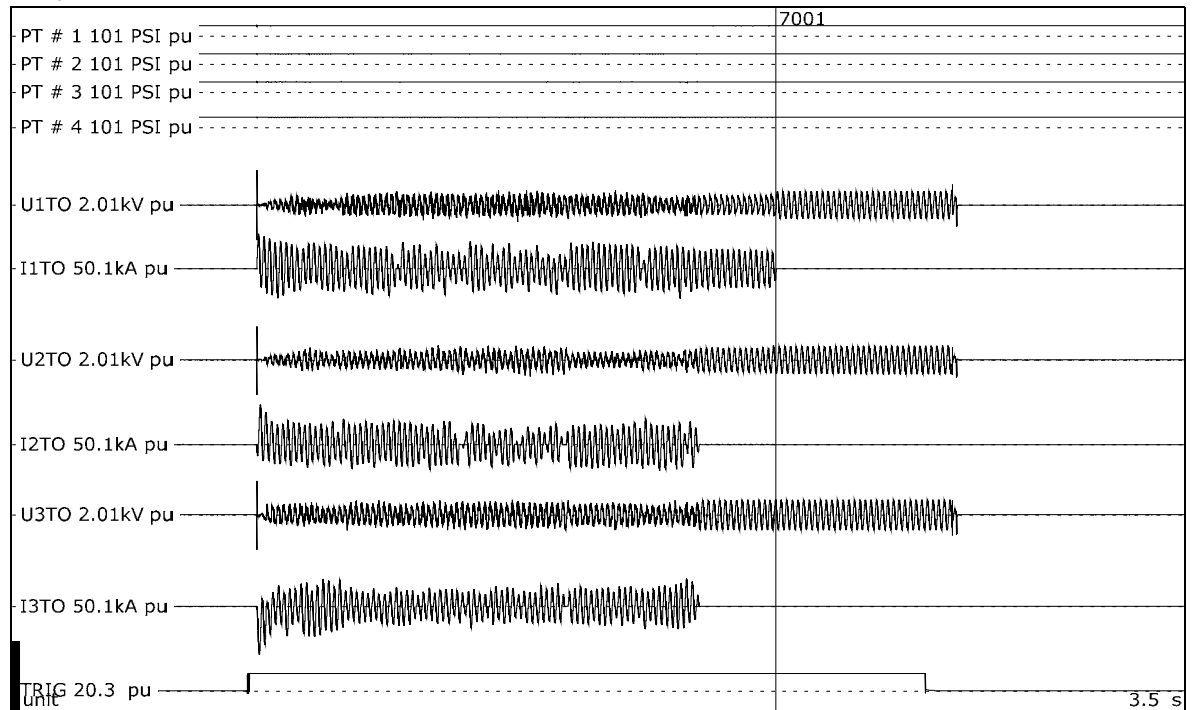
Overview of test numbers

190828-7001

Remarks

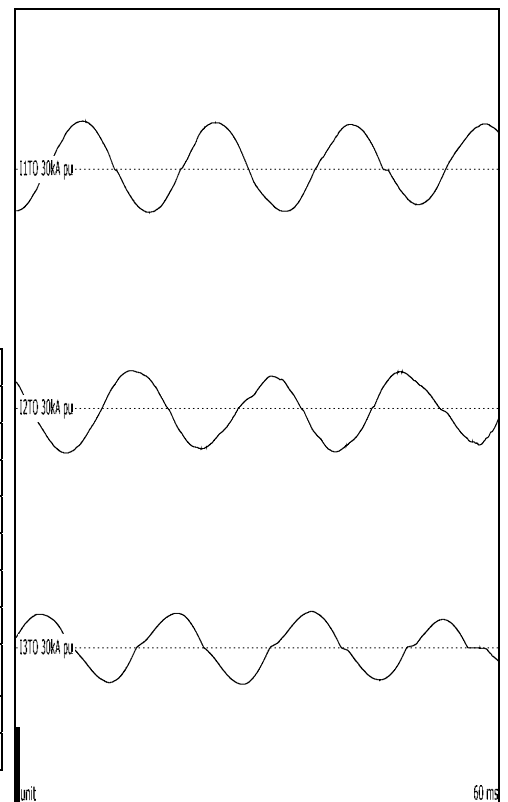
-

Sample 2-13 (F) - 480 V, 13.5 kA



Test number: 190828-7001

Phase		A	B	C
Applied voltage, phase-to-ground	V _{RMS}	282	282	282
Applied voltage, phase-to-phase	V _{RMS}	488		
Making current	kA _{peak}	24.7	28.4	-34.2
Current, a.c. component, beginning	kA _{RMS}	13.1	13.6	12.8
Current, a.c. component, middle	kA _{RMS}	8.32	9.92	7.61
Current, a.c. component, end	kA _{RMS}	9.46	10.4	8.55
Current, a.c. component, average	kA _{RMS}	10.3	9.95	9.26
Current, a.c. component, three-phase average	kA _{RMS}	9.84		
Duration	s	1.55	1.32	1.32
Arc energy	kJ	2119	1518	1732



Observations: Emission of flames and gas observed.

21.4 Condition / inspection after test

Cable connected from enclosure of switchgear to neutral of supply transformer was ejected during test.

22 SAMPLE 2-13 (G) - 600 V, 13.5 KA

Standard and date

Standard	Client's instructions
Test date	28 August 2019

22.1 Condition before test

Switchgear in same condition as after trial 190828-7001. Arc to be initiated by two #10 AWG stranded wires.

Pressure transducers # 1 & 2 located on right side of switchgear (when facing the front of the gear).

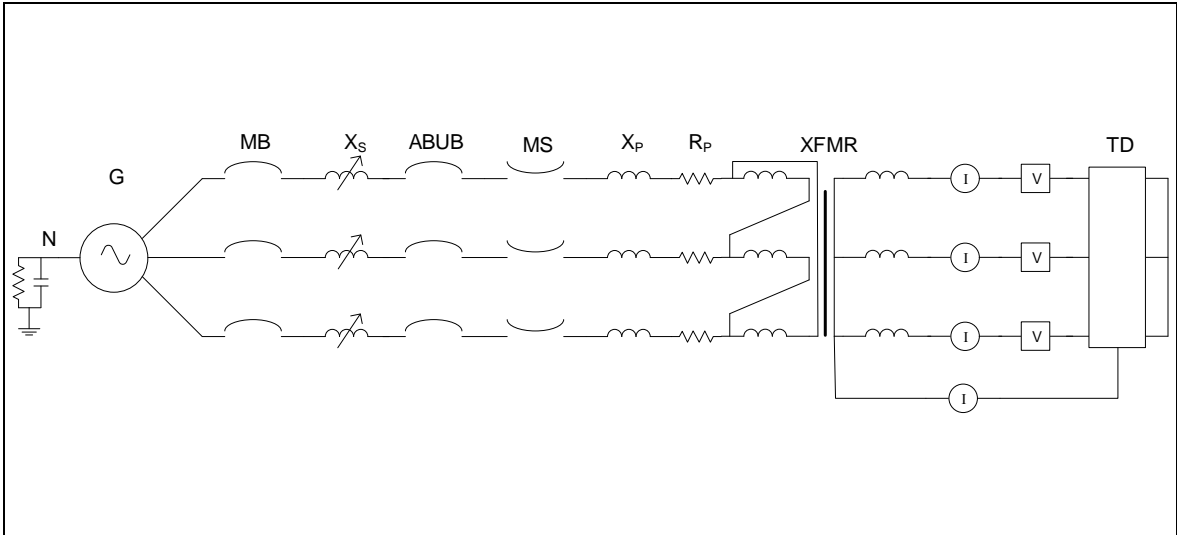
Pressure transducers # 3 & 4 located on left side of switchgear (when facing the front of the gear).

Pressure transducers # 1 & 3 are 0-50 PSI transducers.

Pressure transducers # 2 & 4 are 0-30 PSI transducers.



22.2 Test circuit S07



G	= Generator	ABUB	= Aux. Breaker	R	= Resistance
N	= Neutral	XFMR	= Transformer	C	= Capacitance
MB	= Main Breaker	TD	= Test Device	V	= Voltage Measurement
MS	= Make Switch	X	= Inductance	I	= Current Measurement

Supply		
Power	MVA	14.4
Frequency	Hz	60
Phase(s)		3
Voltage	V	616
Sym. Current	kA	13.5
Peak current	kA	35.6
Impedance	Ω	0.026

Remarks: -

22.3 Test results and oscillograms

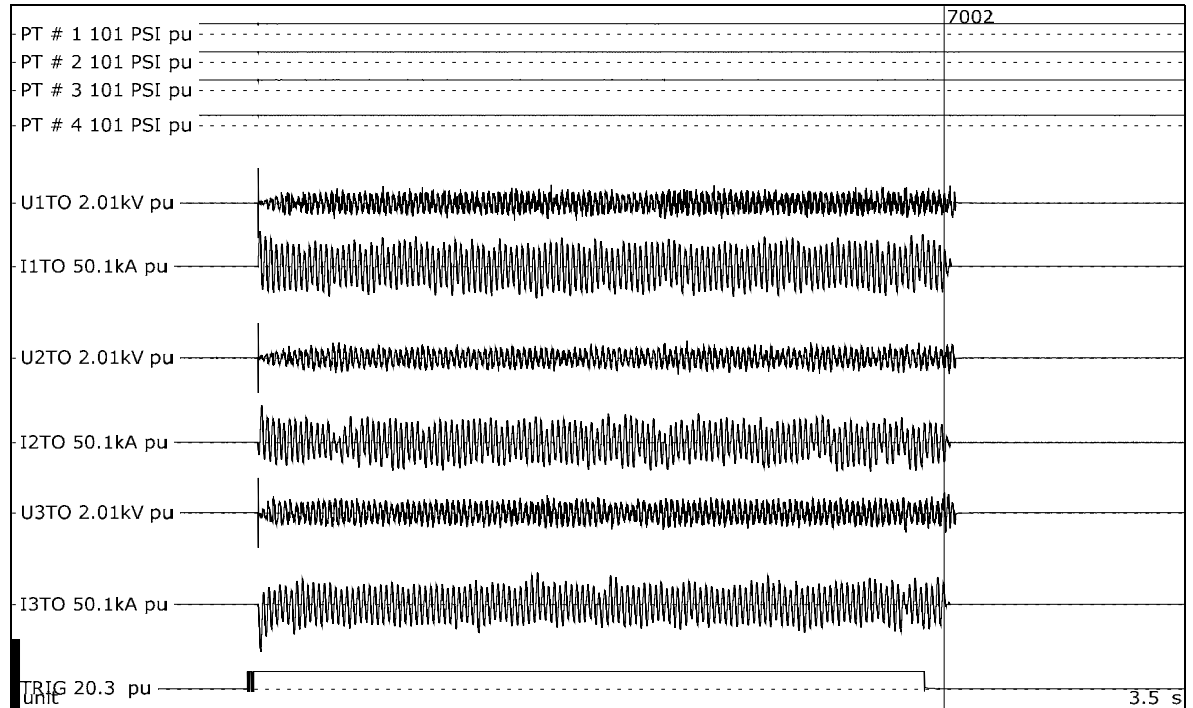
Overview of test numbers

190828-7002

Remarks

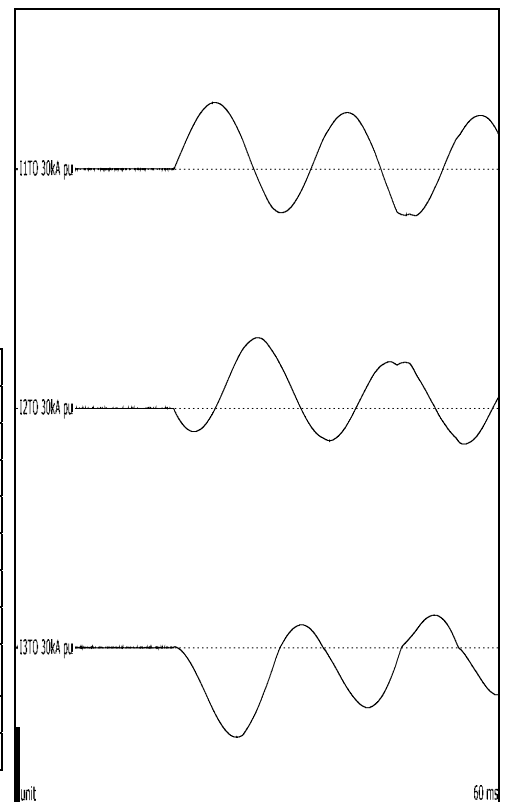
-

Sample 2-13 (G) - 600 V, 13.5 kA



Test number: 190828-7002

Phase		A	B	C
Applied voltage, phase-to-ground	V _{RMS}	356	356	356
Applied voltage, phase-to-phase	V _{RMS}	617		
Making current	kA _{peak}	25.1	26.6	-33.8
Current, a.c. component, beginning	kA _{RMS}	14.0	13.1	13.0
Current, a.c. component, middle	kA _{RMS}	9.62	12.1	9.18
Current, a.c. component, end	kA _{RMS}	12.1	8.87	11.1
Current, a.c. component, average	kA _{RMS}	12.3	10.8	11.0
Current, a.c. component, three-phase average	kA _{RMS}	11.4		
Duration	s	2.04	2.04	2.04
Arc energy	kJ	3525	3106	3646



Observations: Emission of flames and gas observed.

22.4 Condition / inspection after test

Switchgear burned, but otherwise structurally intact.

23 CHECKING THE PROSPECTIVE CURRENT

Standard and date

Standard	Client's instructions
Test date	29 August 2019

23.1 Condition before test

Shorting bar connected at station terminals directly prior to test device.

23.2 Test results and oscillograms

Overview of test numbers

190829-7001 to 7004

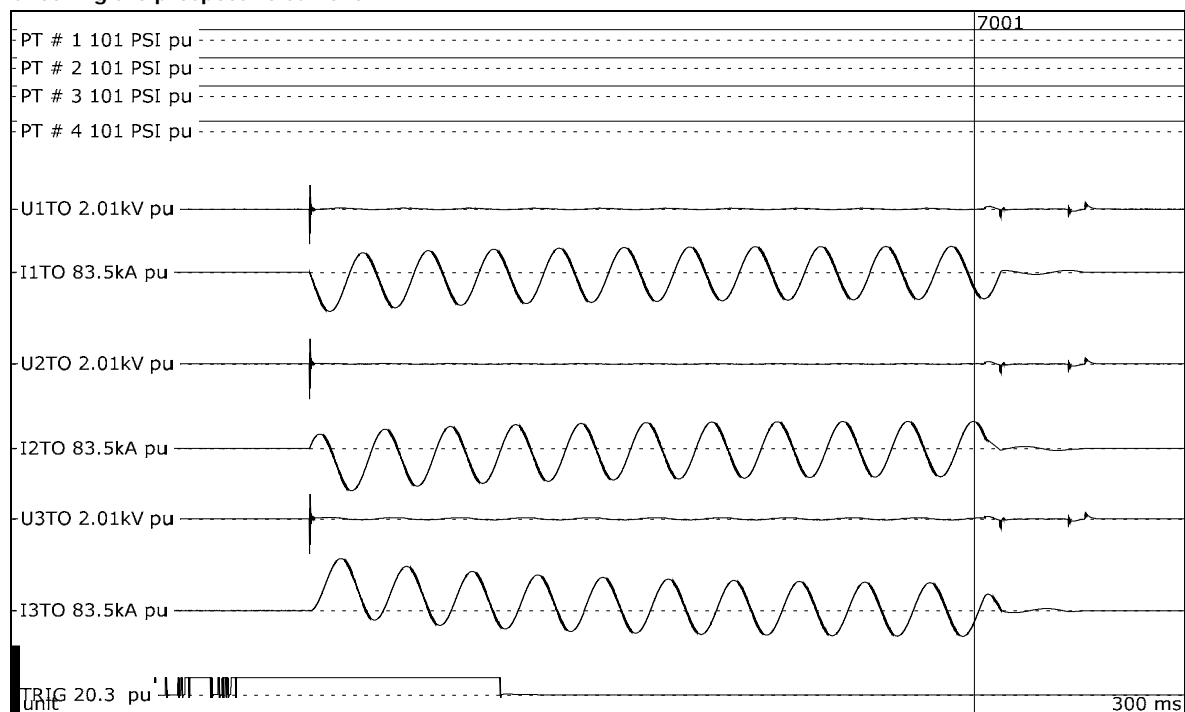
Remarks

Prospective circuit parameters calibrated in this test duty:

190829-7001 and 190829-7002: 619 V, 25.0 kA, 63.3 kA peak.

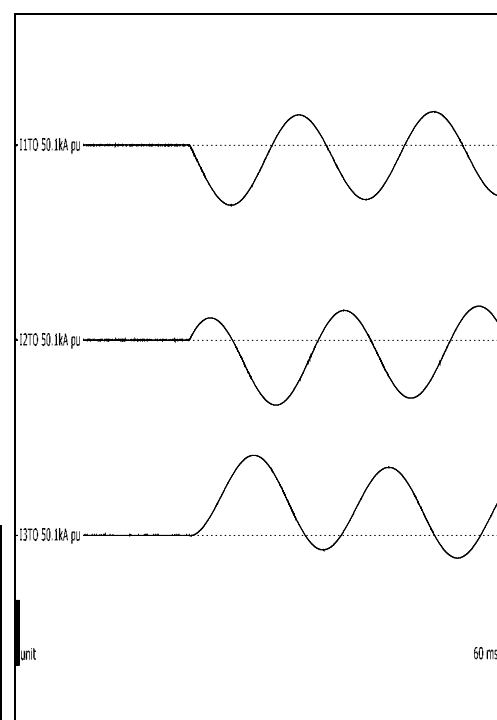
190829-7003 and 190829-7004: 480 V, 25.6 kA, 64.5 kA peak.

Checking the prospective current



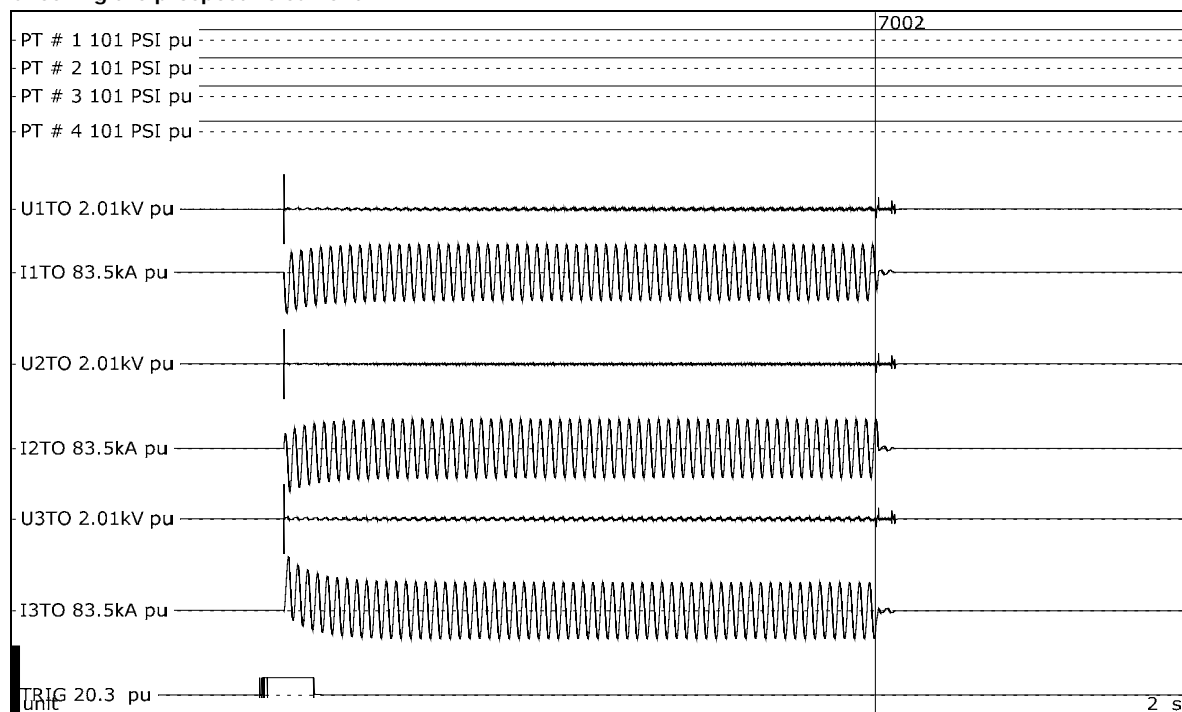
Test number: 190829-7001

Phase		A	B	C
Current	kA _{peak}	-46.4	-50.1	61.5
Current, a.c. component	kA _{RMS}	23.8	24.8	24.1
Current, a.c. component, three-phase average	kA _{RMS}	24.2		
Duration, current	s	0.170	0.170	0.169



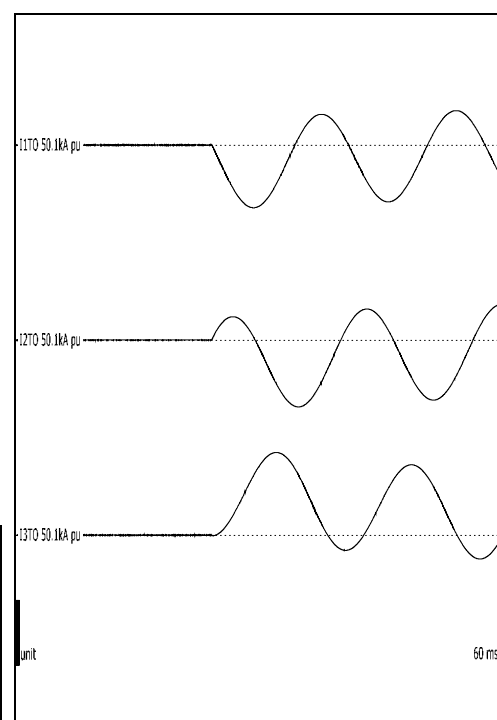
Observations: No visible disturbance.

Checking the prospective current



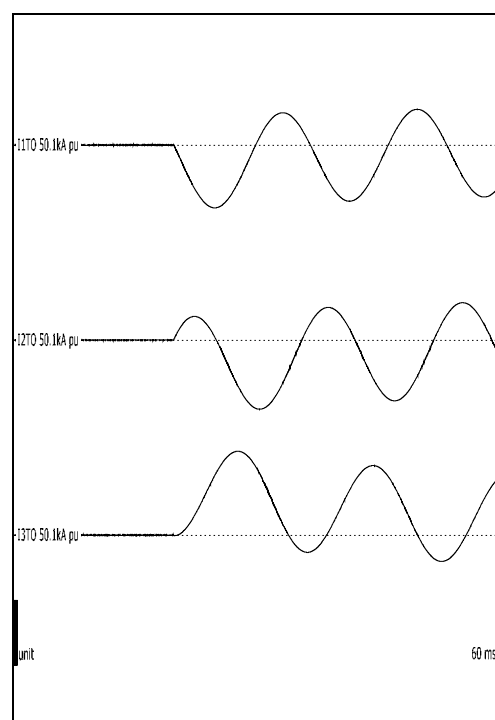
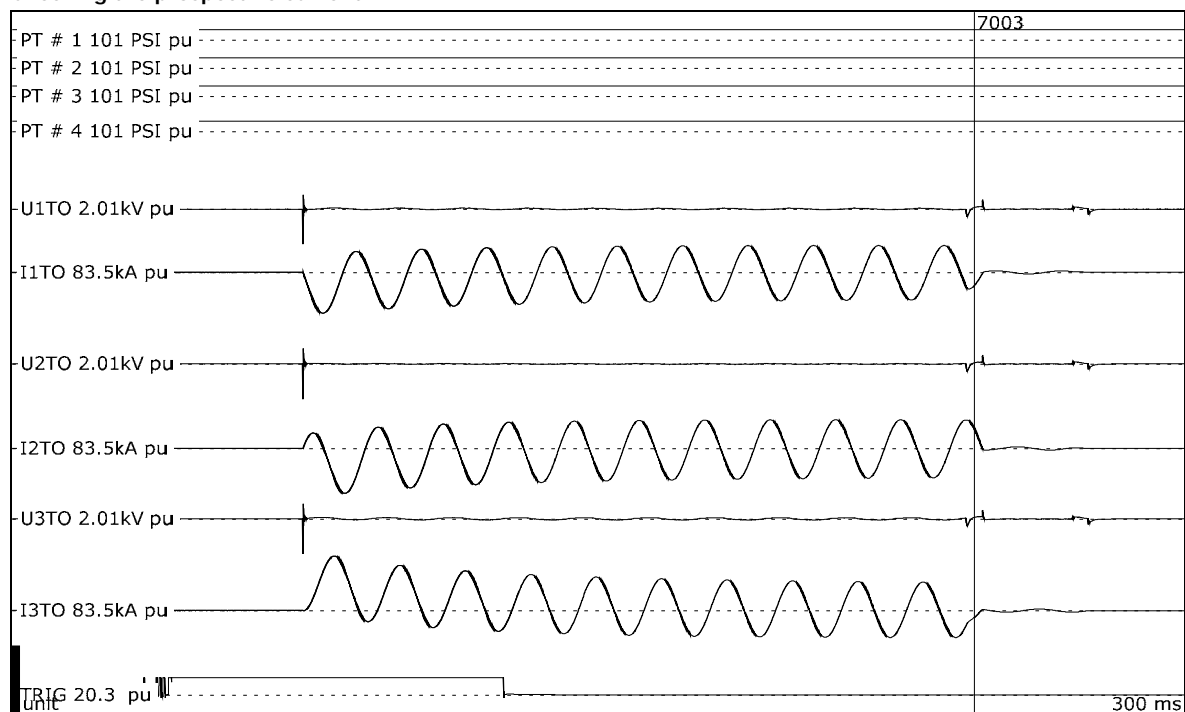
Test number: 190829-7002

Phase		A	B	C
Current	kA _{peak}	33.3	34.9	-33.7
Current, a.c. component	kA _{RMS}	24.6	25.6	25.0
Current, a.c. component, three-phase average	kA _{RMS}	25.1		
Duration, current	s	1.01	1.01	1.01



Observations: No visible disturbance. One second calibration to test super excitation.

Checking the prospective current

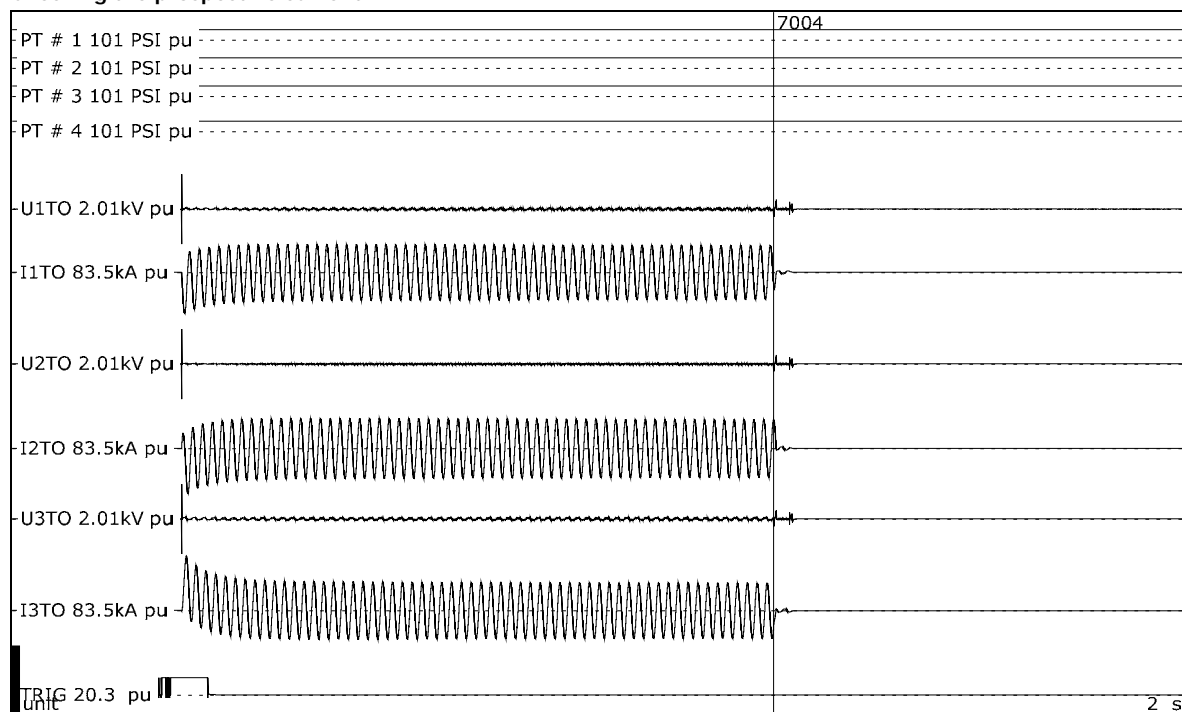


Test number: 190829-7003

Phase		A	B	C
Current	kA _{peak}	-48.4	-53.2	64.6
Current, a.c. component	kA _{RMS}	25.0	26.5	25.5
Current, a.c. component, three-phase average	kA _{RMS}	25.7		
Duration, current	s	0.171	0.172	0.170

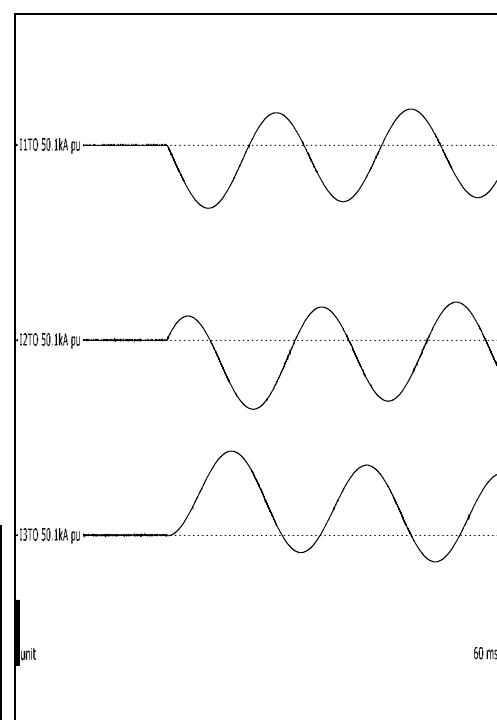
Observations: No visible disturbance.

Checking the prospective current



Test number: 190829-7004

Phase		A	B	C
Current	kA _{peak}	33.0	-35.3	-33.7
Current, a.c. component	kA _{RMS}	24.7	26.2	25.0
Current, a.c. component, three-phase average	kA _{RMS}	25.3		
Duration, current	s	1.01	1.01	1.01



Observations: No visible disturbance. One second calibration to check super excitation.

24 SAMPLE 2-18 (A) - 480 V, 25 KA

Standard and date

Standard	Client's instructions
Test date	29 August 2019

24.1 Condition before test

Switchgear new. Arc to be initiated by #10 AWG stranded wire.

Pressure transducers # 1 & 2 located on right side of switchgear (when facing the front of the gear).

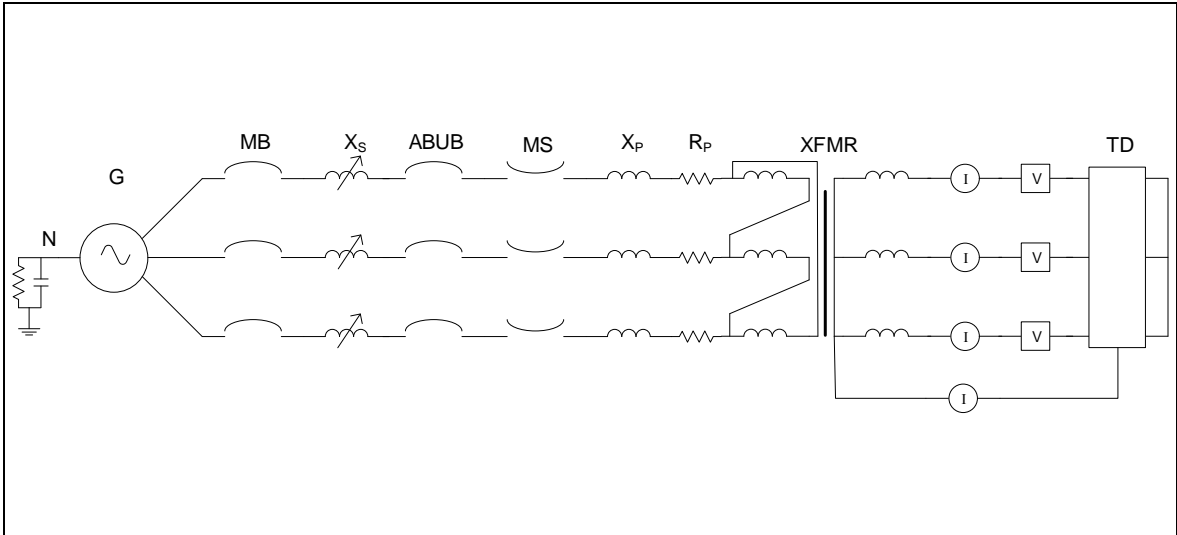
Pressure transducers # 3 & 4 located on left side of switchgear (when facing the front of the gear).

Pressure transducers # 1 & 3 are 0-50 PSI transducers.

Pressure transducers # 2 & 4 are 0-30 PSI transducers.



24.2 Test circuit S09



G	= Generator	ABUB	= Aux. Breaker	R	= Resistance
N	= Neutral	XFMR	= Transformer	C	= Capacitance
MB	= Main Breaker	TD	= Test Device	V	= Voltage Measurement
MS	= Make Switch	X	= Inductance	I	= Current Measurement

Supply		
Power	MVA	21.2
Frequency	Hz	60
Phase(s)		3
Voltage	V	480
Sym. Current	kA	25.6
Peak current	kA	64.5
Impedance	Ω	0.011

Remarks: -

24.3 Test results and oscillograms

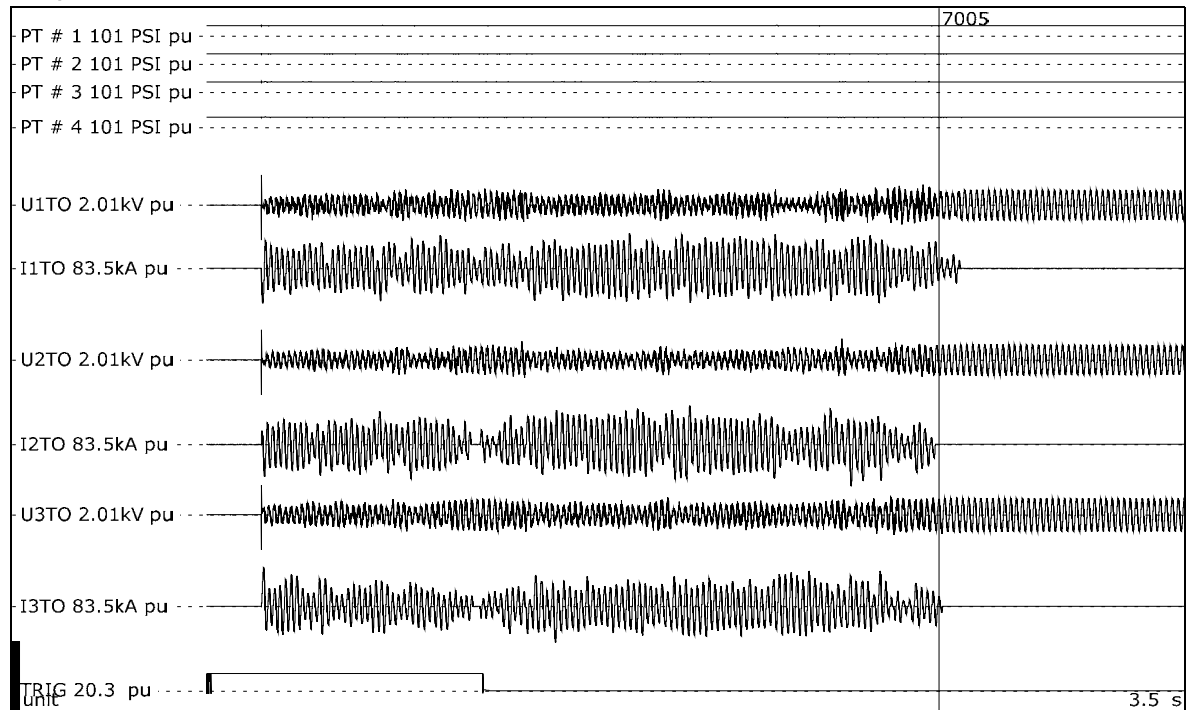
Overview of test numbers

190829-7005

Remarks

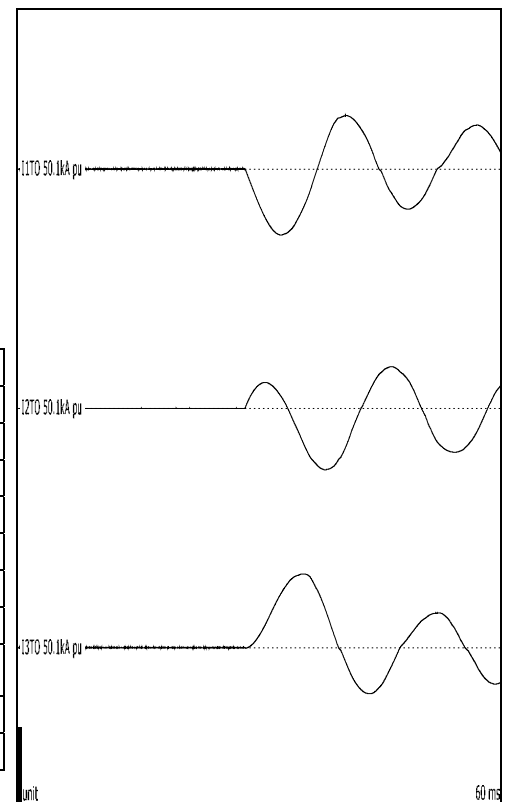
-

Sample 2-18 (A) - 480 V, 25 kA



Test number: 190829-7005

Phase		A	B	C
Applied voltage, phase-to-ground	V _{RMS}	277	277	277
Applied voltage, phase-to-phase	V _{RMS}	480		
Making current	kA _{peak}	-41.4	-38.5	46.2
Current, a.c. component, beginning	kA _{RMS}	23.5	21.0	22.4
Current, a.c. component, middle	kA _{RMS}	20.7	23.5	16.6
Current, a.c. component, end	kA _{RMS}	15.9	18.2	12.5
Current, a.c. component, average	kA _{RMS}	19.8	17.3	17.9
Current, a.c. component, three-phase average	kA _{RMS}	18.3		
Duration	s	2.02	2.02	2.02
Arc energy	kJ	5925	5509	5597



Observations: Emission of flames and gas observed.

24.4 Condition / inspection after test

Evidence of arcing and burning found within the switchgear. Exterior of switchgear mostly intact.

25 SAMPLE 2-18 (B) - 600 V, 25 KA

Standard and date

Standard	Client's instructions
Test date	29 August 2019

25.1 Condition before test

Switchgear in same condition as after trial 190829-7005. Arc to be initiated by two #10 AWG stranded wires.

Pressure transducers # 1 & 2 located on right side of switchgear (when facing the front of the gear).

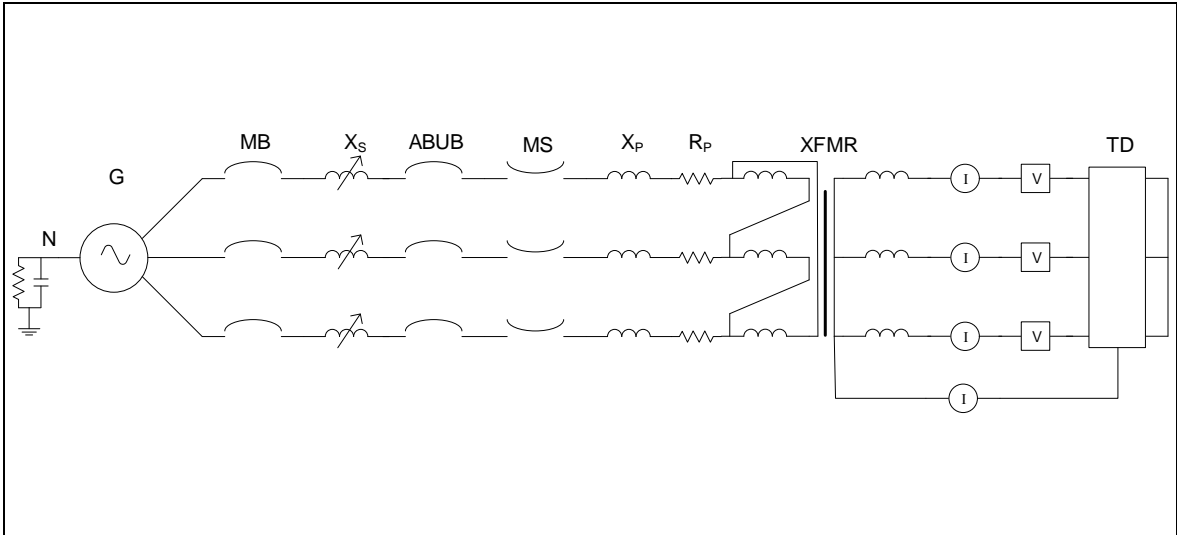
Pressure transducers # 3 & 4 located on left side of switchgear (when facing the front of the gear).

Pressure transducers # 1 & 3 are 0-50 PSI transducers.

Pressure transducers # 2 & 4 are 0-30 PSI transducers.



25.2 Test circuit S08



G	= Generator	ABUB	= Aux. Breaker	R	= Resistance
N	= Neutral	XFMR	= Transformer	C	= Capacitance
MB	= Main Breaker	TD	= Test Device	V	= Voltage Measurement
MS	= Make Switch	X	= Inductance	I	= Current Measurement

Supply		
Power	MVA	26.8
Frequency	Hz	60
Phase(s)		3
Voltage	V	619
Sym. Current	kA	25.0
Peak current	kA	63.3
Impedance	Ω	0.014

Remarks: -

25.3 Test results and oscillograms

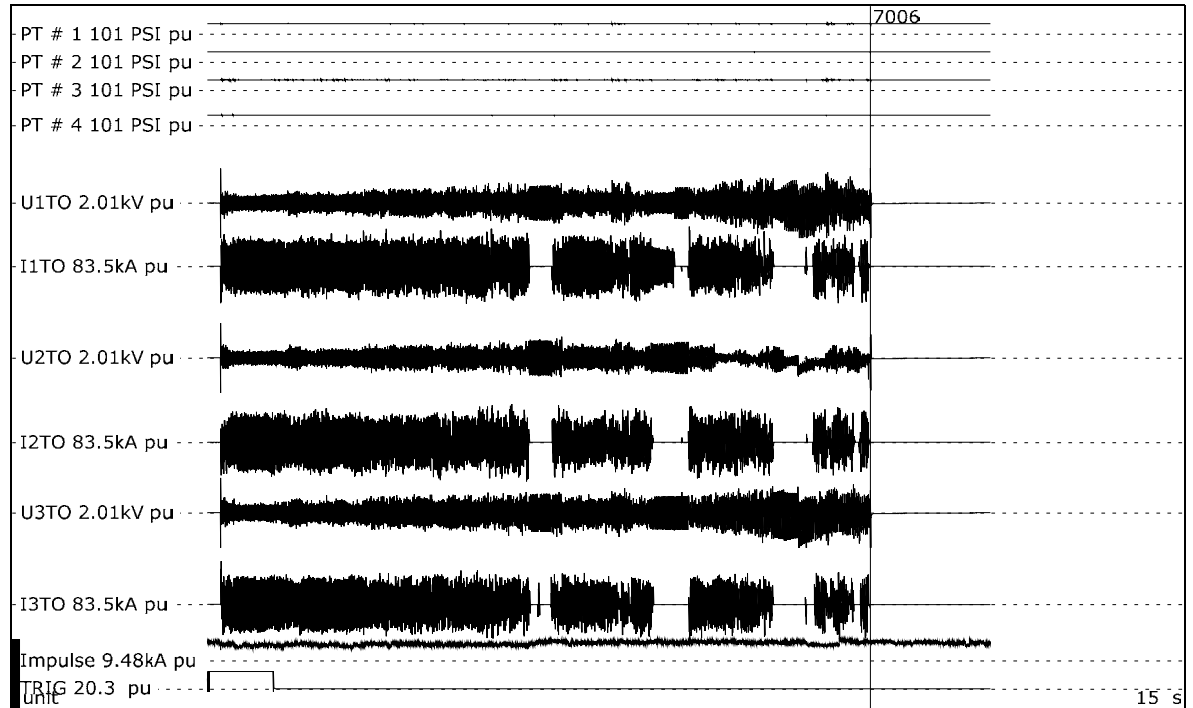
Overview of test numbers

190829-7006

Remarks

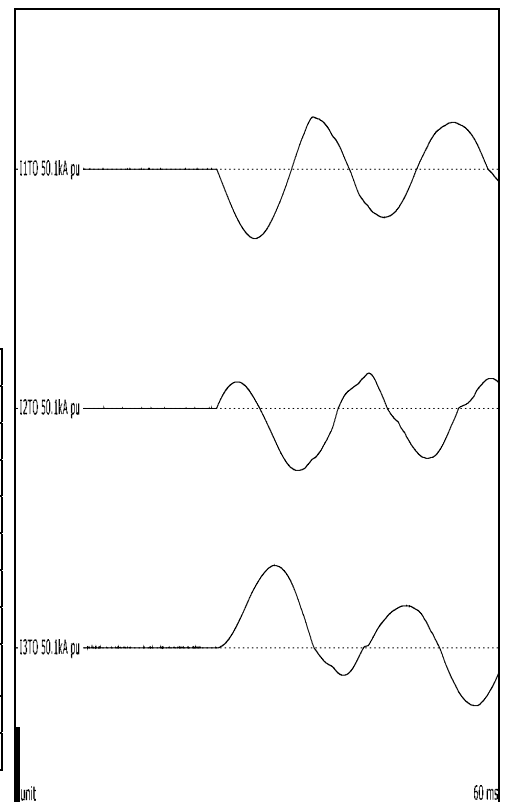
-

Sample 2-18 (B) - 600 V, 25 kA



Test number: 190829-7006

Phase		A	B	C
Applied voltage, phase-to-ground	V _{RMS}	357	357	357
Applied voltage, phase-to-phase	V _{RMS}	618		
Making current	kA _{peak}	35.4	-38.8	-32.4
Current, a.c. component, beginning	kA _{RMS}	22.6	20.9	22.0
Current, a.c. component, middle	kA _{RMS}	25.8	23.6	21.9
Current, a.c. component, end	kA _{RMS}	15.6	22.2	24.3
Current, a.c. component, average	kA _{RMS}	21.1	20.0	19.6
Current, a.c. component, three-phase average	kA _{RMS}	20.2		
Duration	s	8.30	8.30	8.30
Arc energy	MJ	26.1	19.3	27.1



Observations: Emission of flames and gas observed.

25.4 Condition / inspection after test

Switchgear heavily damaged.

26 OPEN BOX TEST # 10 (OB02) - 1000 V, 15 KA

Standard and date

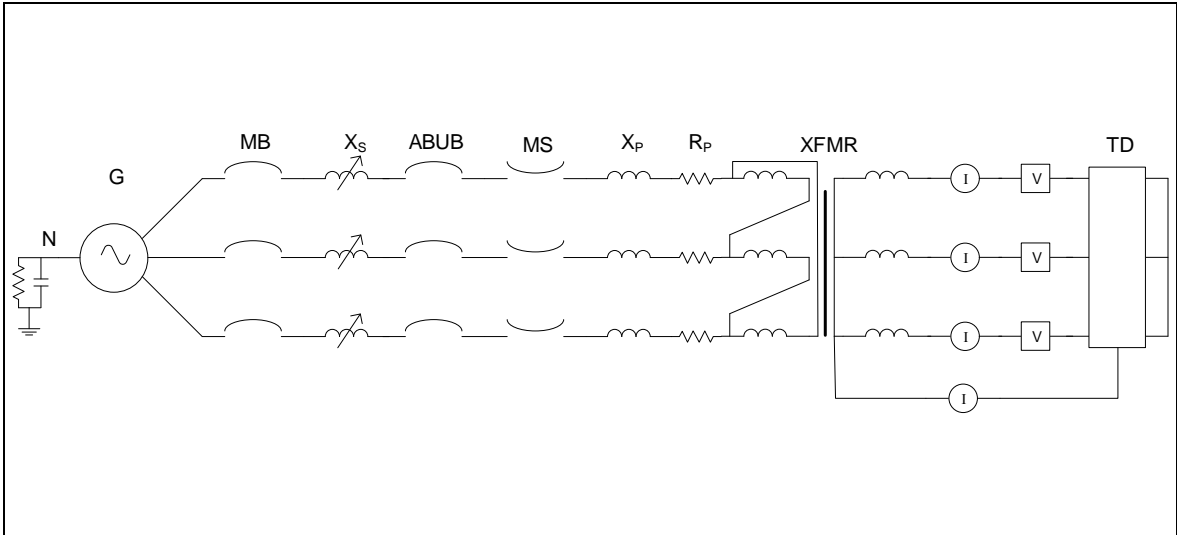
Standard	Client's instructions
Test date	30 August 2019

26.1 Condition before test

Test device new. Arc to be initiated by #24 AWG wire. Arc wire connected to 1" diameter copper rods.
Test duration is 2 seconds.



26.2 Test circuit S03



G	= Generator	ABUB	= Aux. Breaker	R	= Resistance
N	= Neutral	XFMR	= Transformer	C	= Capacitance
MB	= Main Breaker	TD	= Test Device	V	= Voltage Measurement
MS	= Make Switch	X	= Inductance	I	= Current Measurement

Supply		
Power	MVA	26.2
Frequency	Hz	60
Phase(s)		3
Voltage	V	1009
Sym. Current	kA	15
Peak current	kA	40.4
Impedance	Ω	0.014

Remarks: -

26.3 Test results and oscillograms

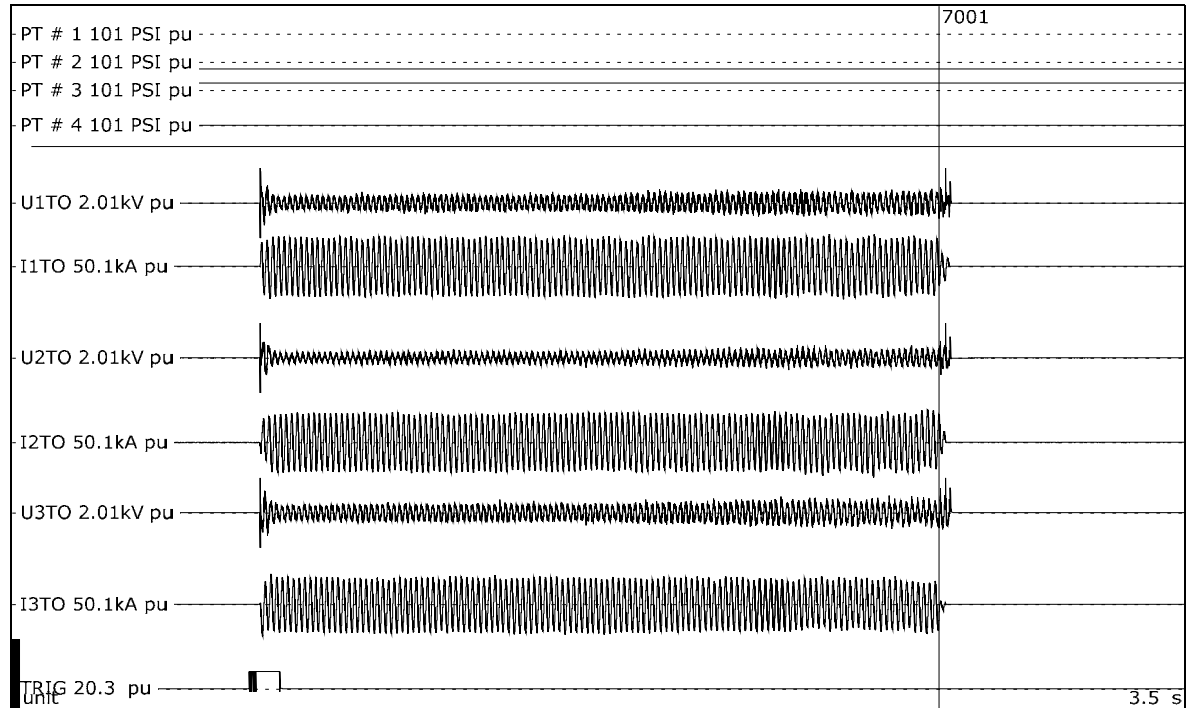
Overview of test numbers

190830-7001

Remarks

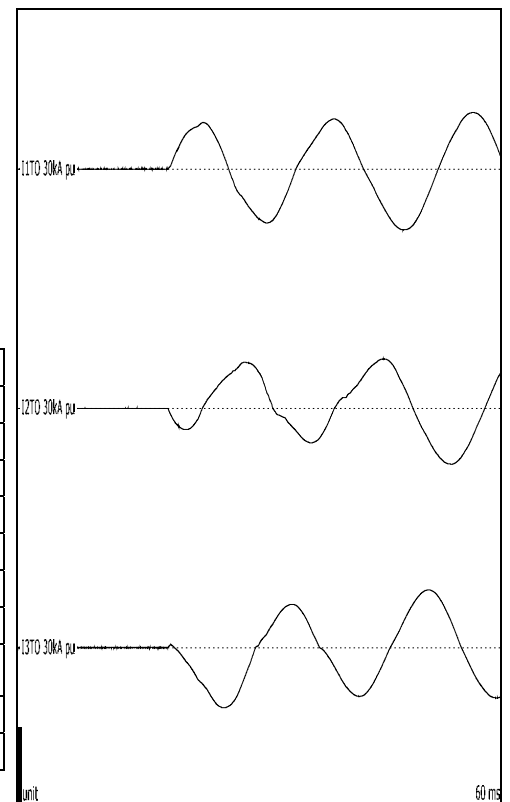
-

Open Box Test # 10 - 1000 V, 15 kA



Test number: 190830-7001

Phase		A	B	C
Applied voltage, phase-to-ground	V _{RMS}	583	583	583
Applied voltage, phase-to-phase	V _{RMS}	1010		
Making current	kA _{peak}	-22.9	18.6	-22.7
Current, a.c. component, beginning	kA _{RMS}	14.6	14.5	13.7
Current, a.c. component, middle	kA _{RMS}	14.7	14.6	13.9
Current, a.c. component, end	kA _{RMS}	13.7	14.2	12.4
Current, a.c. component, average	kA _{RMS}	14.4	13.7	13.5
Current, a.c. component, three-phase average	kA _{RMS}	13.9		
Duration	s	2.02	2.02	2.02
Arc energy	kJ	4395	3277	4317



Observations: Emission of flames and gas observed.

26.4 Condition / inspection after test

Hole burned through bottom of box. Sides and rear of box heavily burned, but not completely through.

27 OPEN BOX TEST # 11 (OB03) - 1000 V, 15 KA

Standard and date

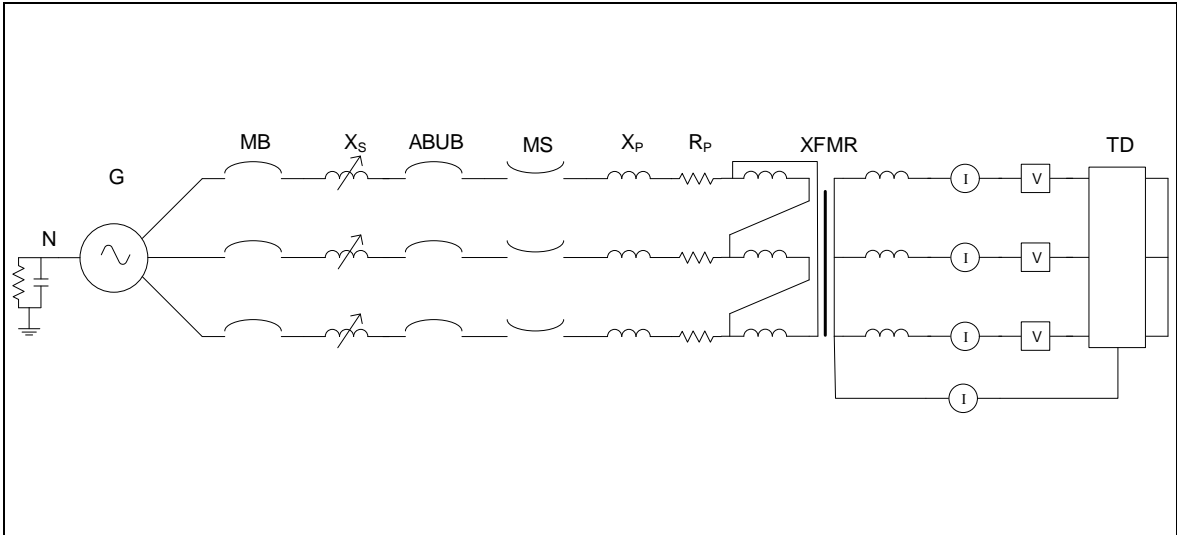
Standard	Client's instructions
Test date	30 August 2019

27.1 Condition before test

Test device new. Arc to be initiated by #24 AWG wire. Arc wire connected to 1" diameter copper rods.
Test duration is 3 seconds.



27.2 Test circuit S03



G	= Generator	ABUB	= Aux. Breaker	R	= Resistance
N	= Neutral	XFMR	= Transformer	C	= Capacitance
MB	= Main Breaker	TD	= Test Device	V	= Voltage Measurement
MS	= Make Switch	X	= Inductance	I	= Current Measurement

Supply		
Power	MVA	26.2
Frequency	Hz	60
Phase(s)		3
Voltage	V	1009
Sym. Current	kA	15
Peak current	kA	40.4
Impedance	Ω	0.014

Remarks: -

27.3 Test results and oscillograms

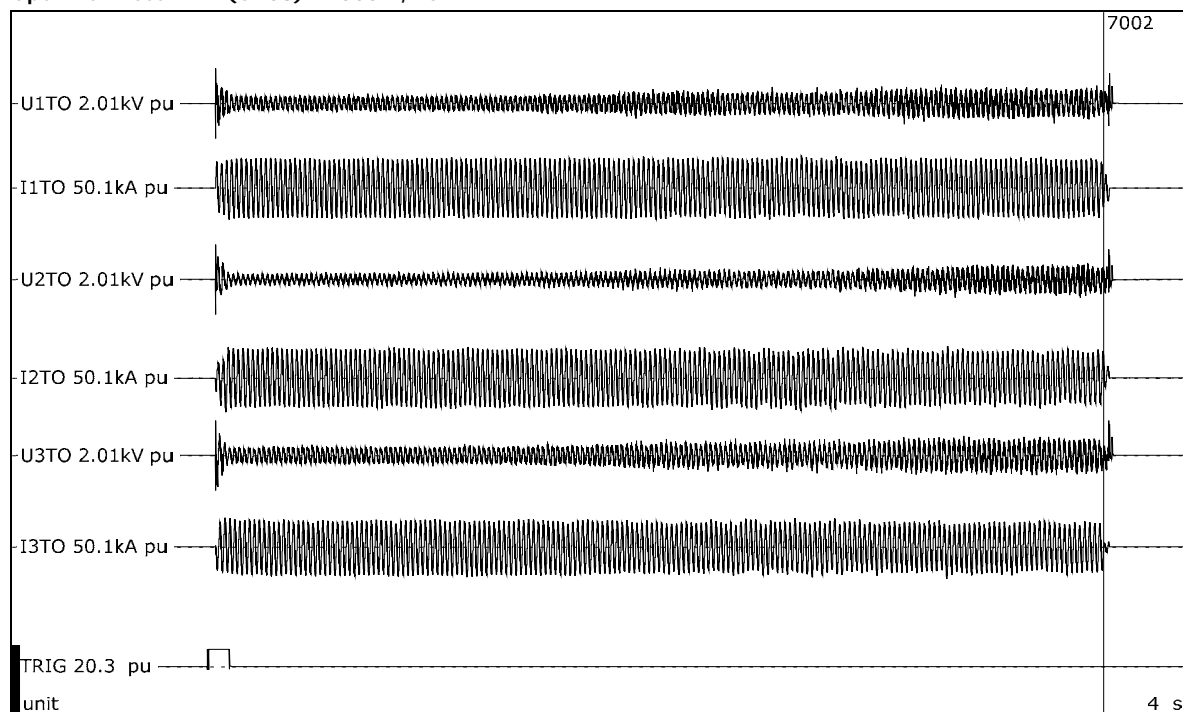
Overview of test numbers

190830-7002

Remarks

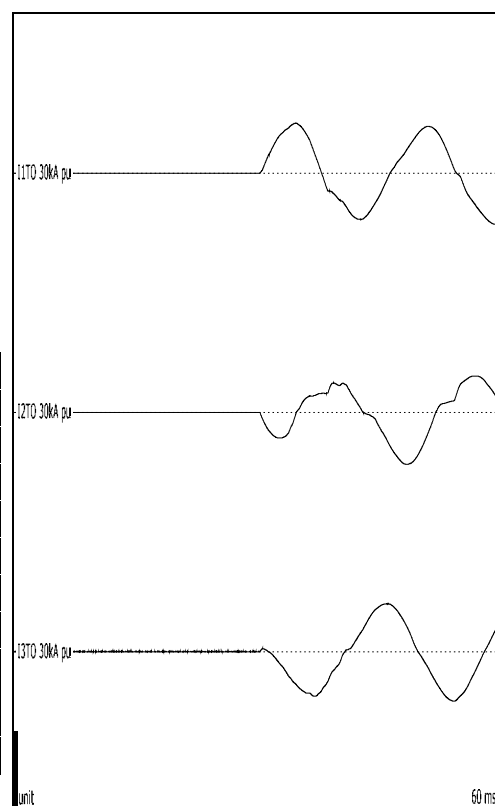
-

Open Box Test # 11 (OB03) - 1000 V, 15 kA



Test number: 190830-7002

Phase		A	B	C
Applied voltage, phase-to-ground	V _{RMS}	583	583	583
Applied voltage, phase-to-phase	V _{RMS}	1010		
Making current	kA _{peak}	-19.4	-19.6	20.9
Current, a.c. component, beginning	kA _{RMS}	14.7	14.6	13.4
Current, a.c. component, middle	kA _{RMS}	14.9	14.2	12.4
Current, a.c. component, end	kA _{RMS}	14.3	13.0	12.4
Current, a.c. component, average	kA _{RMS}	14.4	13.5	13.1
Current, a.c. component, three-phase average	kA _{RMS}	13.6		
Duration	s	3.03	3.03	3.02
Arc energy	kJ	7347	5517	7022



Observations: Emission of flames and gas observed.

27.4 Condition / inspection after test

Bottom of box completely burned through. Sides of box towards bottom of box also burned through.

28 OPEN BOX TEST # 12 (OB04) - 1000 V, 30 KA

Standard and date

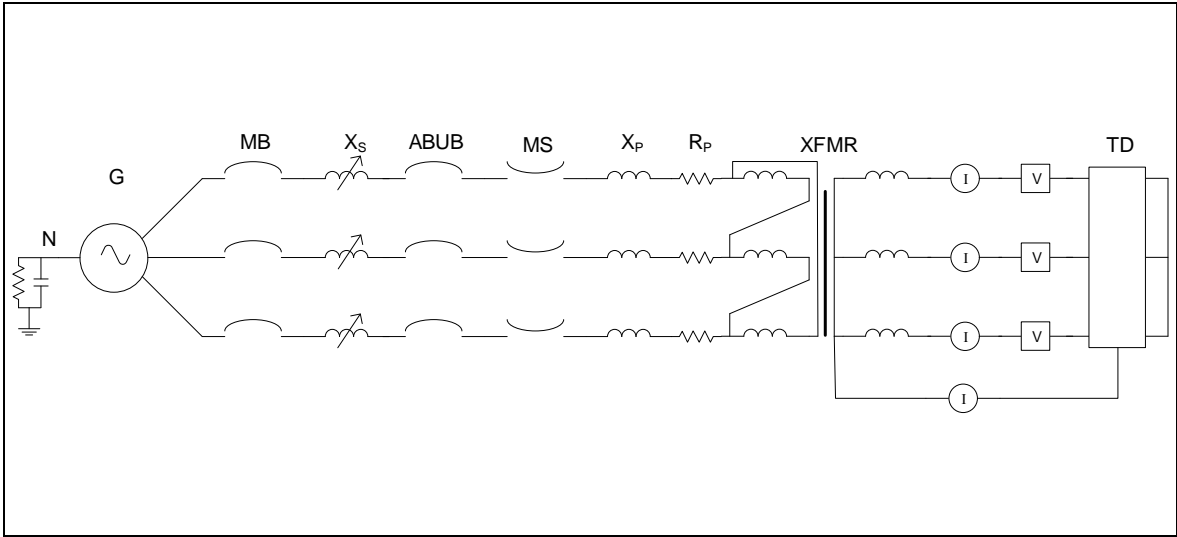
Standard	Client's instructions
Test date	30 August 2019

28.1 Condition before test

Test device new. Arc to be initiated by #24 AWG wire. Arc wire connected to 1" diameter copper rods.
Test duration is 1 seconds.



28.2 Test circuit S04



G	= Generator	ABUB	= Aux. Breaker	R	= Resistance
N	= Neutral	XFMR	= Transformer	C	= Capacitance
MB	= Main Breaker	TD	= Test Device	V	= Voltage Measurement
MS	= Make Switch	X	= Inductance	I	= Current Measurement

Supply		
Power	MVA	55.3
Frequency	Hz	60
Phase(s)		3
Voltage	V	1064
Sym. Current	kA	30
Peak current	kA	79.1
Impedance	Ω	0.020

Remarks: -

28.3 Test results and oscillograms

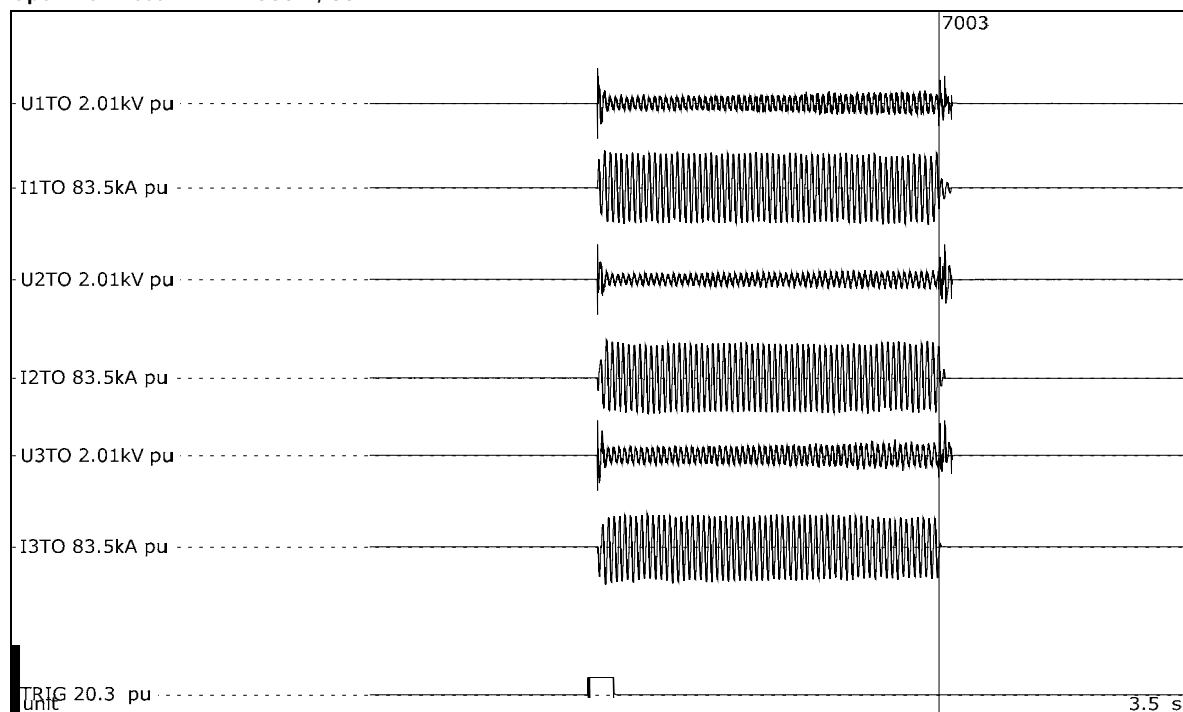
Overview of test numbers

190830-7003

Remarks

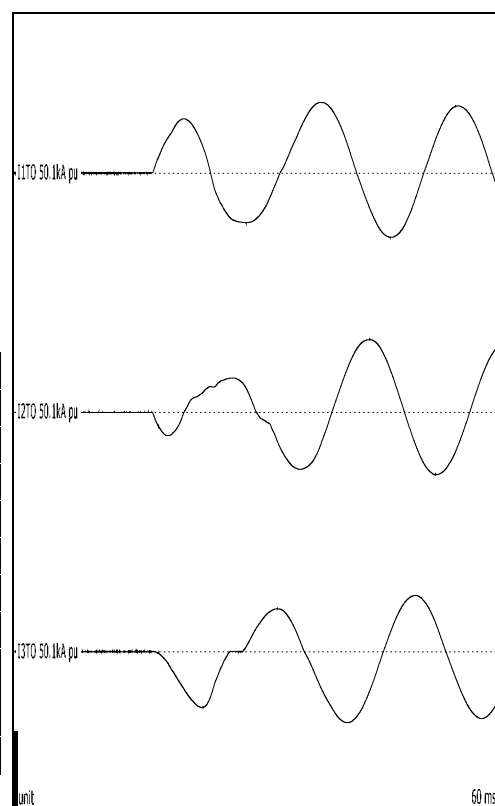
-

Open Box Test # 12 - 1000 V, 30 kA



Test number: 190830-7003

Phase		A	B	C
Applied voltage, phase-to-ground	V _{RMS}	614	614	614
Applied voltage, phase-to-phase	V _{RMS}	1063		
Making current	kA _{peak}	44.4	45.7	-44.6
Current, a.c. component, beginning	kA _{RMS}	29.2	28.9	28.1
Current, a.c. component, middle	kA _{RMS}	29.1	28.5	27.0
Current, a.c. component, end	kA _{RMS}	28.0	28.5	25.1
Current, a.c. component, average	kA _{RMS}	28.1	26.9	26.3
Current, a.c. component, three-phase average	kA _{RMS}	27.1		
Duration	s	1.02	1.02	1.02
Arc energy	kJ	4311	3419	4598



Observations: Emission of flames and gas observed.

28.4 Condition / inspection after test

Small hole burned through bottom of box. Sides of box heavily burned, but not completely through.

29 OPEN BOX TEST # 13 (OB16) - SINGLE PHASE INVESTIGATION

Standard and date

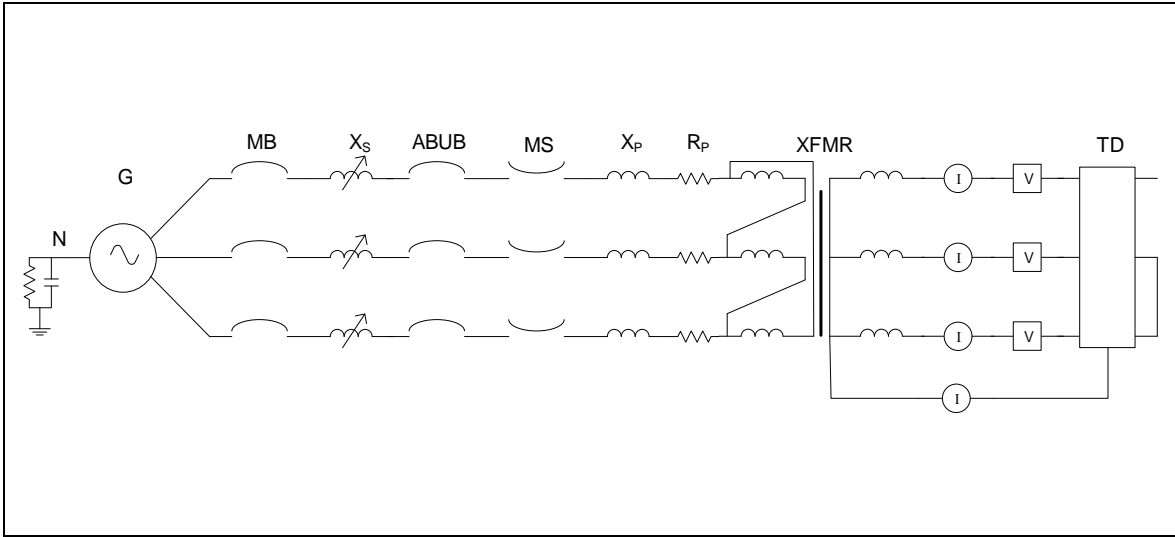
Standard	Client's instructions
Test date	30 August 2019

29.1 Condition before test

Test box new. Copper rods new. Arc to be initiated by #24 AWG wire. Arc wire connected to 1" diameter copper rods on A & B phase only. Test duration is 100 milliseconds. Purpose of the test is to measure how long it takes for arc to propagate to third phase.



29.2 Test circuit S05



G	= Generator	ABUB	= Aux. Breaker	R	= Resistance
N	= Neutral	XFMR	= Transformer	C	= Capacitance
MB	= Main Breaker	TD	= Test Device	V	= Voltage Measurement
MS	= Make Switch	X	= Inductance	I	= Current Measurement

Supply		
Power	MVA	26.2
Frequency	Hz	60
Phase(s)		3
Voltage	V	1009
Sym. Current	kA	15
Peak current	kA	40.4
Impedance	Ω	0.014

Remarks: Test conducted with arc wire only between two phases. Supply table above shows the available 3-phase circuit when arc propagated from 1-phase arc to 3-phase arc.

29.3 Test results and oscillograms

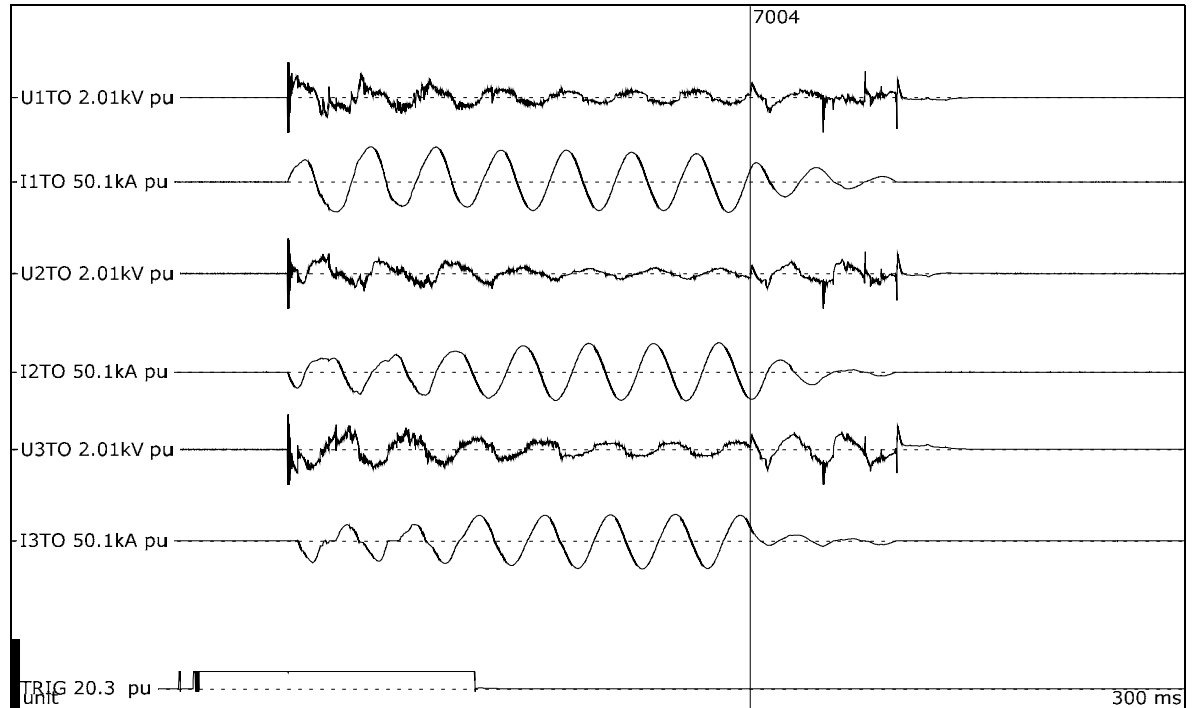
Overview of test numbers

190830-7004

Remarks

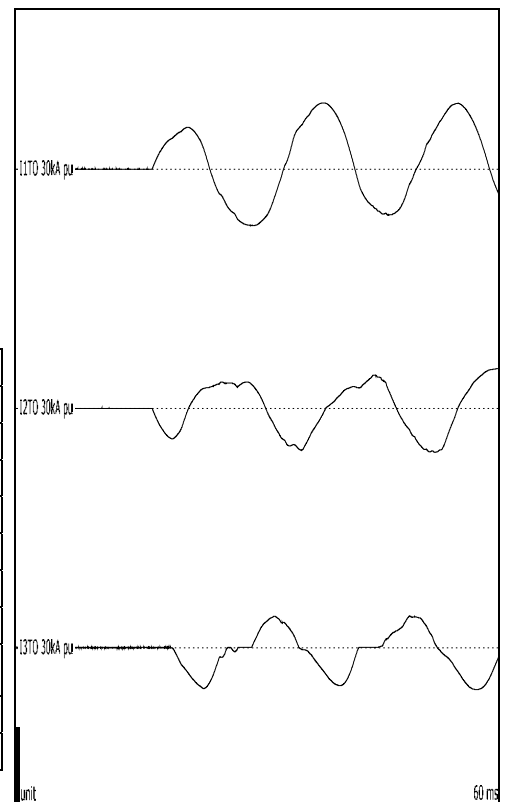
-

Open Box Test # 13 - Single Phase Investigation



Test number: 190830-7004

Phase		A	B	C
Applied voltage, phase-to-ground	V _{RMS}	583	583	583
Applied voltage, phase-to-phase	V _{RMS}	1010		
Making current	kA _{peak}	24.9	-15.7	-15.3
Current, a.c. component, beginning	kA _{RMS}	16.0	9.35	8.47
Current, a.c. component, middle	kA _{RMS}	15.2	14.1	13.4
Current, a.c. component, end	kA _{RMS}	15.2	14.1	13.4
Current, a.c. component, average	kA _{RMS}	14.9	11.1	11.7
Current, a.c. component, three-phase average	kA _{RMS}	12.6		
Duration	s	0.118	0.118	0.116
Arc energy	kJ	296	186	254



Observations: Emission of flames and gas observed. Arc propagation time is approximately 2.52 ms.

29.4 Condition / inspection after test

Minimal damage to test box observed.

30 OPEN BOX TEST # 14 (OB12(A)) - SINGLE PHASE INVESTIGATION

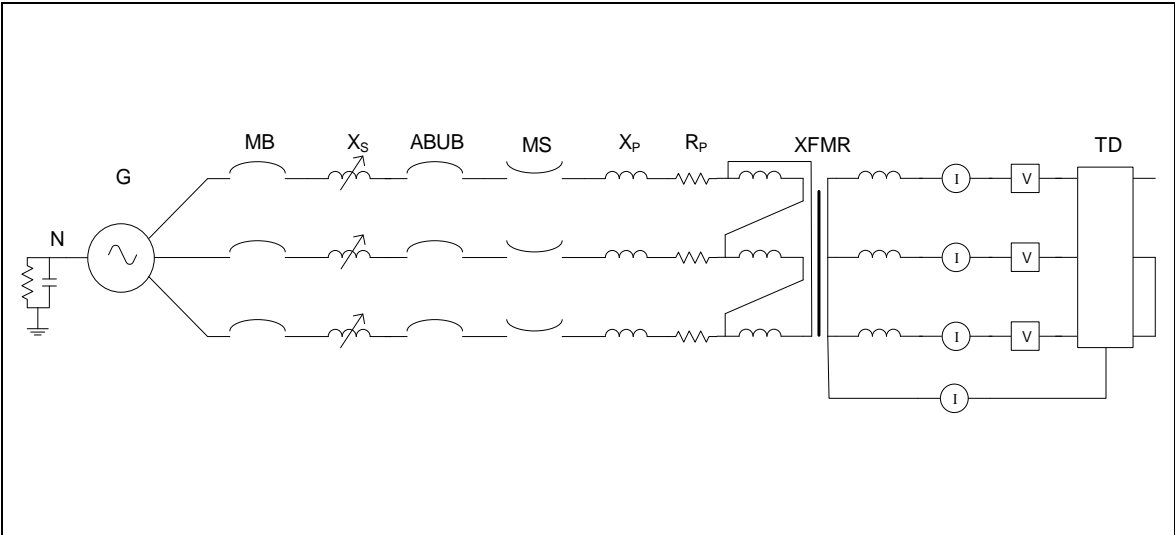
Standard and date

Standard	Client's instructions
Test date	30 August 2019

30.1 Condition before test

Test box in same condition as after trial 190830-7004. Arc to be initiated by #24 AWG wire. Arc wire connected to 1" diameter copper rod on C-phase & enclosure of box. Test duration is 100 milliseconds. Purpose of the test is to measure how long it takes for arc to propagate to other two phases.

30.2 Test circuit S05



G	= Generator	ABUB	= Aux. Breaker	R	= Resistance
N	= Neutral	XFMR	= Transformer	C	= Capacitance
MB	= Main Breaker	TD	= Test Device	V	= Voltage Measurement
MS	= Make Switch	X	= Inductance	I	= Current Measurement

Supply		
Power	MVA	26.2
Frequency	Hz	60
Phase(s)		3
Voltage	V	1009
Sym. Current	kA	15
Peak current	kA	40.4
Impedance	Ω	0.014

Remarks: Test conducted with arc wire only between two phases. Supply table above shows the available 3-phase circuit when arc propagated from 1-phase arc to 3-phase arc.

30.3 Test results and oscillograms

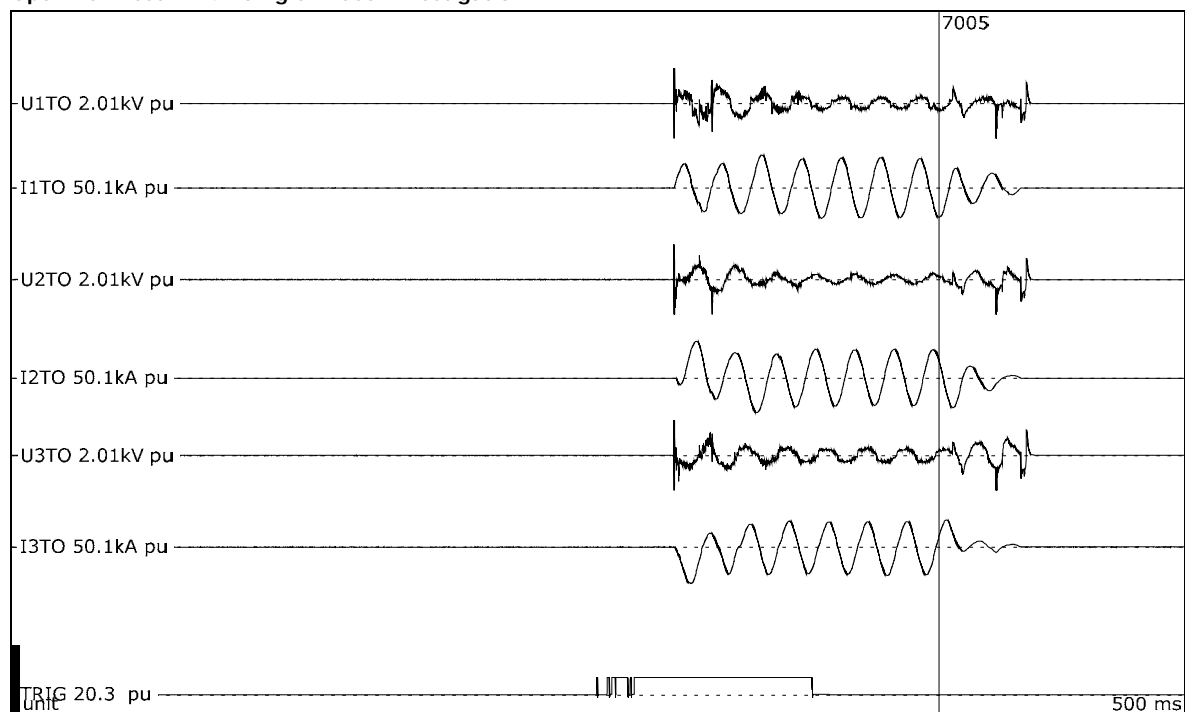
Overview of test numbers

190830-7005

Remarks

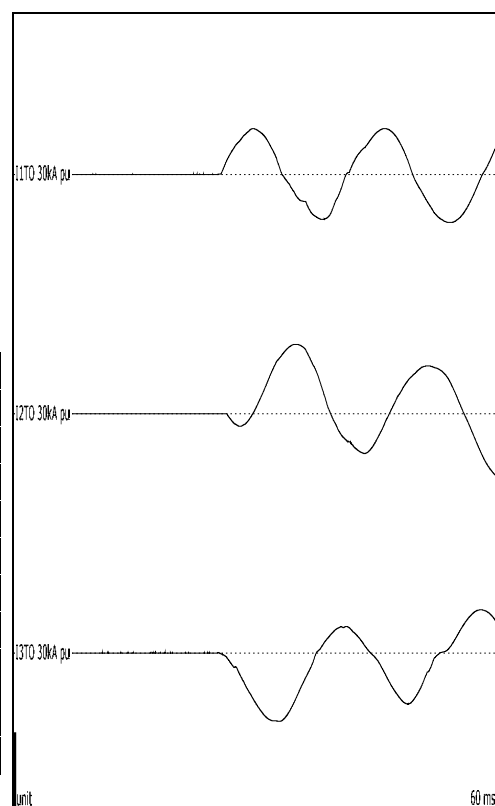
-

Open Box Test # 14 - Single Phase Investigation



Test number: 190830-7005

Phase		A	B	C
Applied voltage, phase-to-ground	V _{RMS}	583	583	583
Applied voltage, phase-to-phase	V _{RMS}	1010		
Making current	kA _{peak}	-18.2	26.1	-25.8
Current, a.c. component, beginning	kA _{RMS}	12.1	12.5	11.4
Current, a.c. component, middle	kA _{RMS}	15.1	14.2	13.1
Current, a.c. component, end	kA _{RMS}	15.1	14.2	13.1
Current, a.c. component, average	kA _{RMS}	14.0	13.7	12.7
Current, a.c. component, three-phase average	kA _{RMS}	13.5		
Duration	s	0.113	0.112	0.113
Arc energy	kJ	267	206	230



Observations: Emission of flames and gas observed. Arc propagation time was approximately 400 us.

30.4 Condition / inspection after test

Minimal damage to test box observed.

31 OPEN BOX TEST # 15 (OB15) - SINGLE PHASE INVESTIGATION

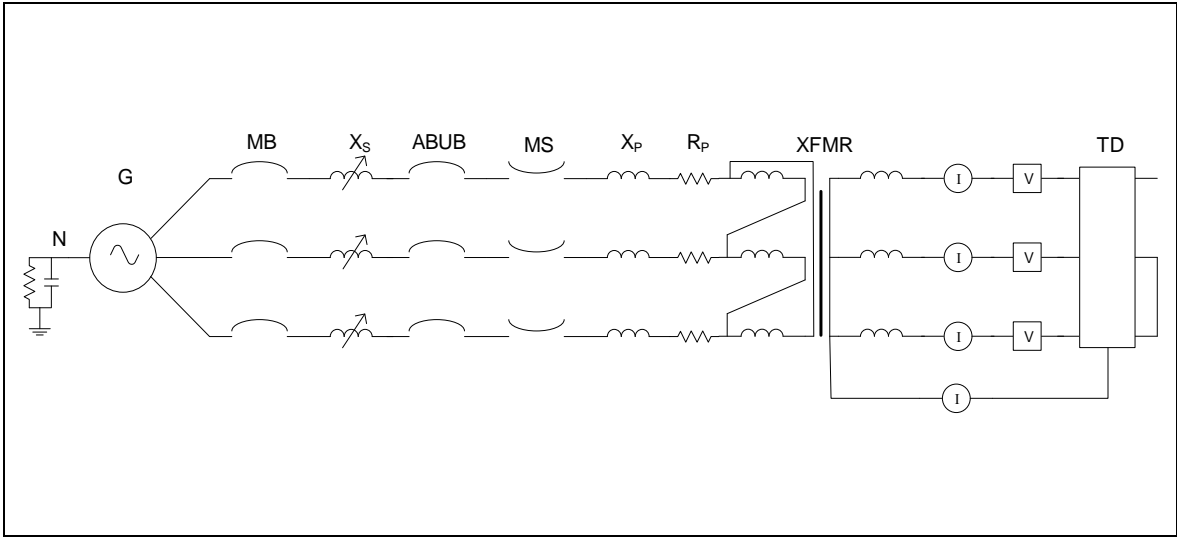
Standard and date

Standard	Client's instructions
Test date	30 August 2019

31.1 Condition before test

Test box in same condition as after trial 190830-7005. Arc to be initiated by #24 AWG wire. Arc wire connected to 1" diameter aluminum rod on B-phase & enclosure of box. Test duration is 100 milliseconds. Purpose of the test is to measure how long it takes for arc to propagate to other two phases.

31.2 Test circuit S05



G	= Generator	ABUB	= Aux. Breaker	R	= Resistance
N	= Neutral	XFMR	= Transformer	C	= Capacitance
MB	= Main Breaker	TD	= Test Device	V	= Voltage Measurement
MS	= Make Switch	X	= Inductance	I	= Current Measurement

Supply		
Power	MVA	26.2
Frequency	Hz	60
Phase(s)		3
Voltage	V	1009
Sym. Current	kA	15
Peak current	kA	40.4
Impedance	Ω	0.014

Remarks: Test conducted with arc wire only between two phases. Supply table above shows the available 3-phase circuit when arc propagated from 1-phase arc to 3-phase arc.

31.3 Test results and oscillograms

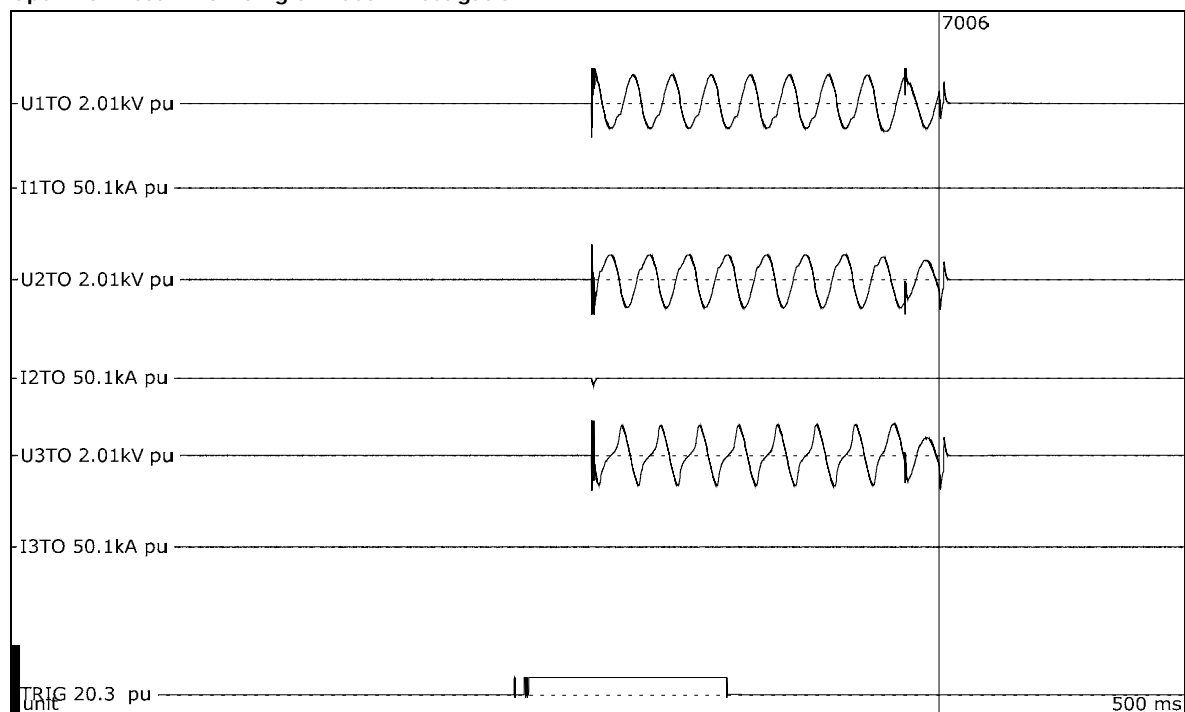
Overview of test numbers

190830-7006

Remarks

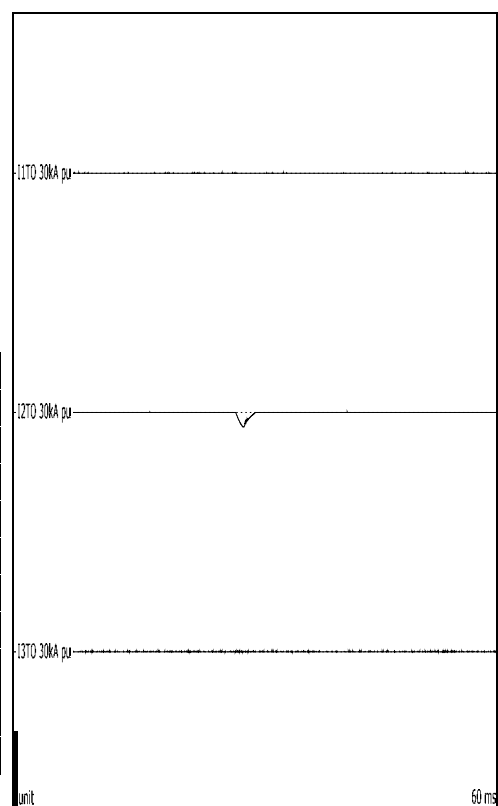
-

Open Box Test # 15 - Single Phase Investigation



Test number: 190830-7006

Phase		A	B	C
Applied voltage, phase-to-ground	V _{RMS}	583	583	583
Applied voltage, phase-to-phase	V _{RMS}	1010		
Making current	kA _{peak}	-	-5.51	-
Current, a.c. component, beginning	kA _{RMS}	-	0.974	-
Current, a.c. component, middle	kA _{RMS}	-	0.000	-
Current, a.c. component, end	kA _{RMS}	0.000	0.000	0.000
Current, a.c. component, average	kA _{RMS}	-	-	-
Current, a.c. component, three-phase average	kA _{RMS}	-		
Duration	s	-	0.148	-
Arc energy	kJ	-		



Observations: Small flash observed. Arc did not propagate to other phases.

31.4 Condition / inspection after test

Arc failed to propagate to other phases.

32 OPEN BOX TEST # 16 (OB14) - SINGLE PHASE INVESTIGATION

Standard and date

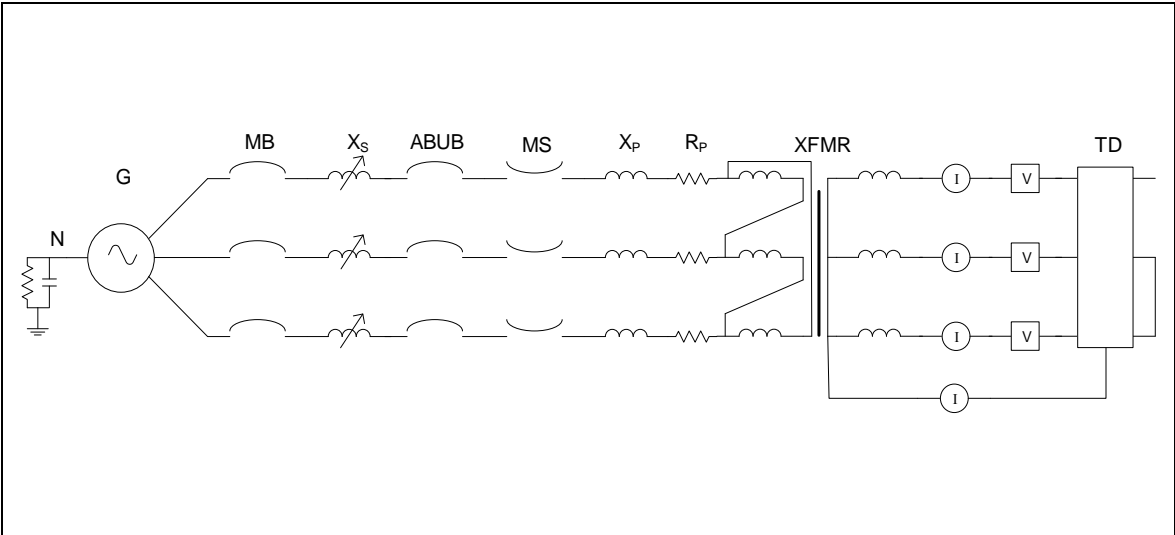
Standard	Client's instructions
Test date	30 August 2019

32.1 Condition before test

Test box in same condition as after trial 190830-7006. Arc to be initiated by #24 AWG wire. Arc wire connected to 1" diameter aluminum rod on A-phase & enclosure of box. Test duration is 100 milliseconds. Purpose of the test is to measure how long it takes for arc to propagate to other two phases.



32.2 Test circuit S05



G	= Generator	ABUB	= Aux. Breaker	R	= Resistance
N	= Neutral	XFMR	= Transformer	C	= Capacitance
MB	= Main Breaker	TD	= Test Device	V	= Voltage Measurement
MS	= Make Switch	X	= Inductance	I	= Current Measurement

Supply		
Power	MVA	26.2
Frequency	Hz	60
Phase(s)		3
Voltage	V	1009
Sym. Current	kA	15
Peak current	kA	40.4
Impedance	Ω	0.014

Remarks: Test conducted with arc wire only between two phases. Supply table above shows the available 3-phase circuit when arc propagated from 1-phase arc to 3-phase arc.

32.3 Test results and oscillograms

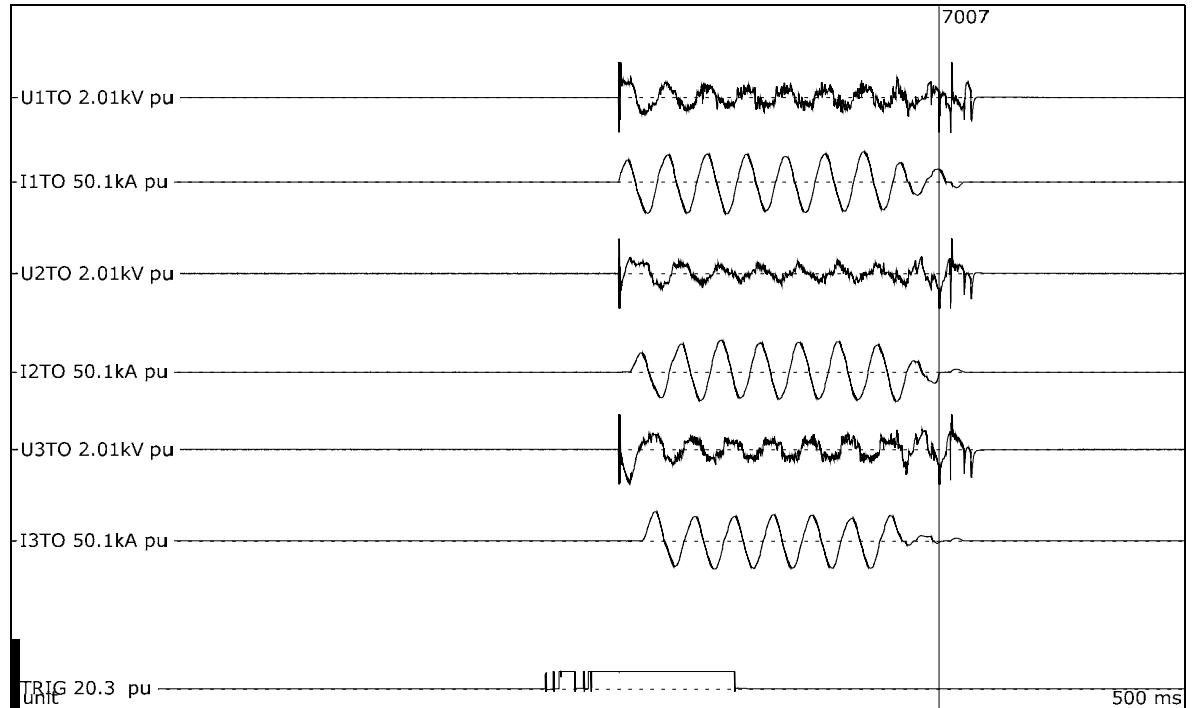
Overview of test numbers

190830-7007

Remarks

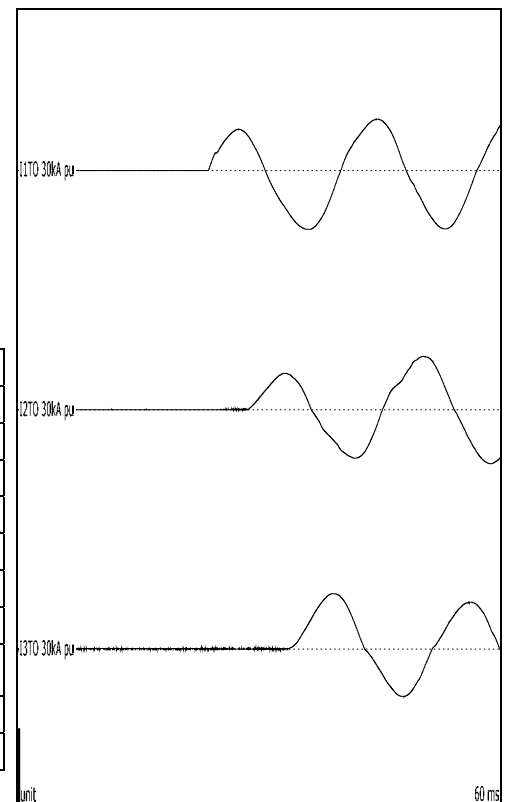
-

Open Box Test # 16 - Single Phase Investigation



Test number: 190830-7007

Phase		A	B	C
Applied voltage, phase-to-ground	V _{RMS}	583	583	583
Applied voltage, phase-to-phase	V _{RMS}	1010		
Making current	kA _{peak}	-22.3	-20.3	20.8
Current, a.c. component, beginning	kA _{RMS}	14.0	12.4	13.1
Current, a.c. component, middle	kA _{RMS}	14.4	14.3	13.4
Current, a.c. component, end	kA _{RMS}	14.5	14.5	13.0
Current, a.c. component, average	kA _{RMS}	14.4	13.9	13.0
Current, a.c. component, three-phase average	kA _{RMS}	13.8		
Duration	s	0.137	0.132	0.126
Arc energy	kJ	373	257	300



Observations: Emission of flames and gas observed. Arc propagated to B-phase in approximately 4.8 ms. Arc propagated to C-phase in approximately 10 ms.

32.4 Condition / inspection after test

Minimal damage to test box observed.

33 OPEN BOX TEST # 17 (OB12(B) & OB12(C)) - SINGLE PHASE INVESTIGATION

Standard and date

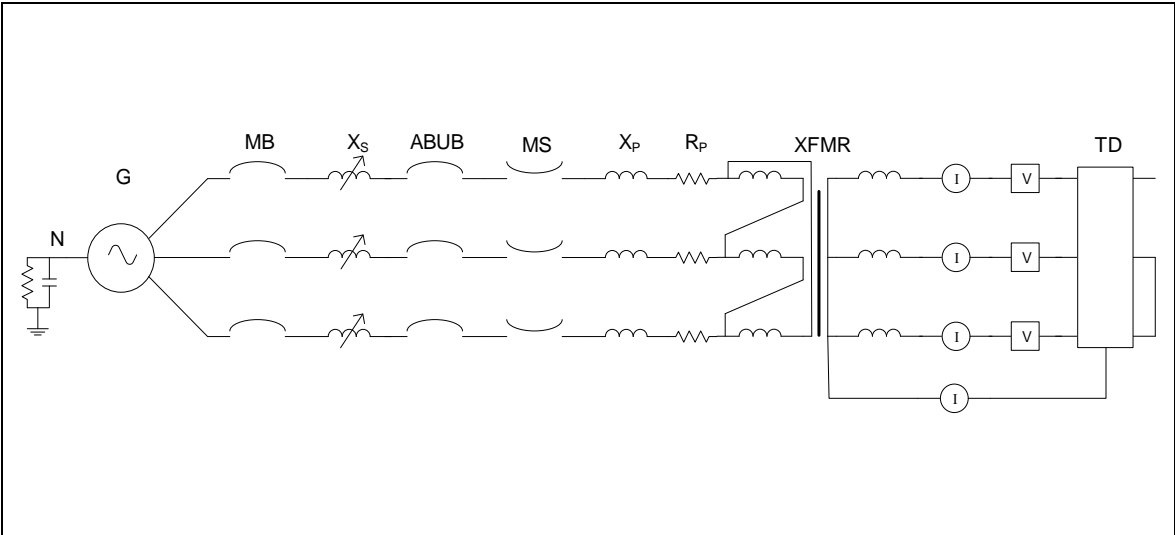
Standard	Client's instructions
Test date	30 August 2019

33.1 Condition before test

Test box in same condition as after trial 190830-7007. Arc to be initiated by #24 AWG wire. Arc wire connected to 1" diameter copper rod on C-phase & enclosure of box. Test duration is 100 milliseconds. Purpose of the test is to measure how long it takes for arc to propagate to other two phases.



33.2 Test circuit S05



G	= Generator	ABUB	= Aux. Breaker	R	= Resistance
N	= Neutral	XFMR	= Transformer	C	= Capacitance
MB	= Main Breaker	TD	= Test Device	V	= Voltage Measurement
MS	= Make Switch	X	= Inductance	I	= Current Measurement

Supply		
Power	MVA	26.2
Frequency	Hz	60
Phase(s)		3
Voltage	V	1009
Sym. Current	kA	15
Peak current	kA	40.4
Impedance	Ω	0.014

Remarks: Test conducted with arc wire only between two phases. Supply table above shows the available 3-phase circuit when arc propagated from 1-phase arc to 3-phase arc.

33.3 Test results and oscillograms

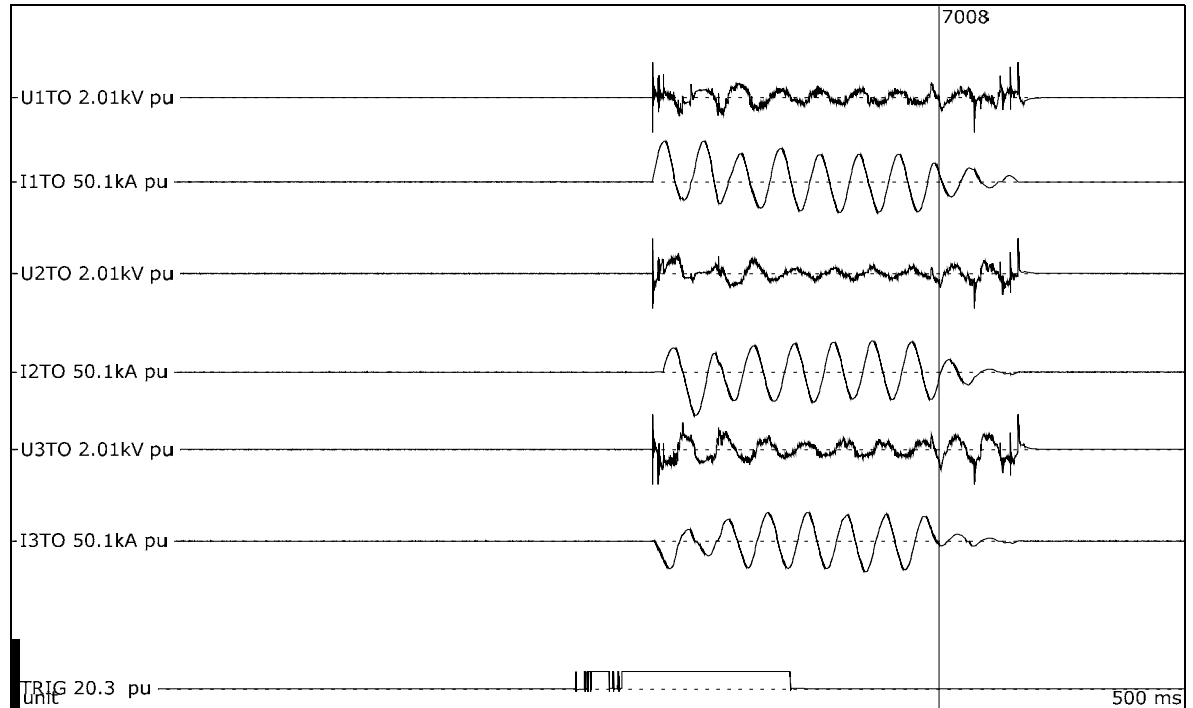
Overview of test numbers

190830-7008, 7009

Remarks

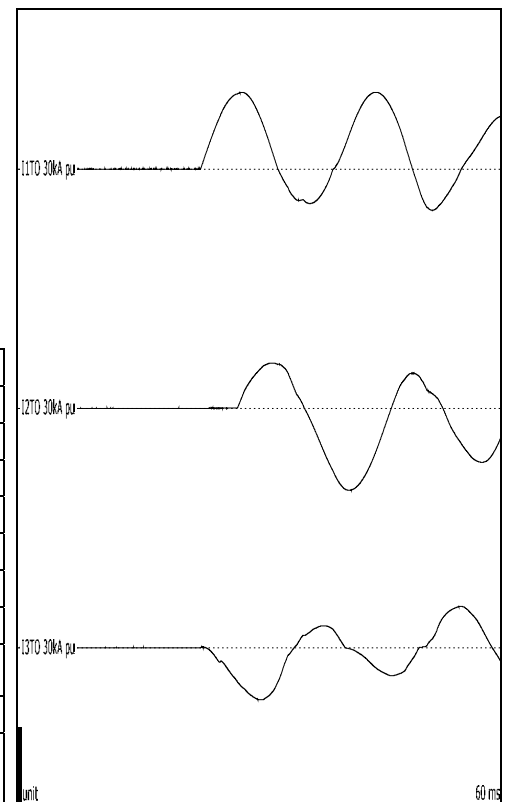
-

Open Box Test # 17 - Single Phase Investigation



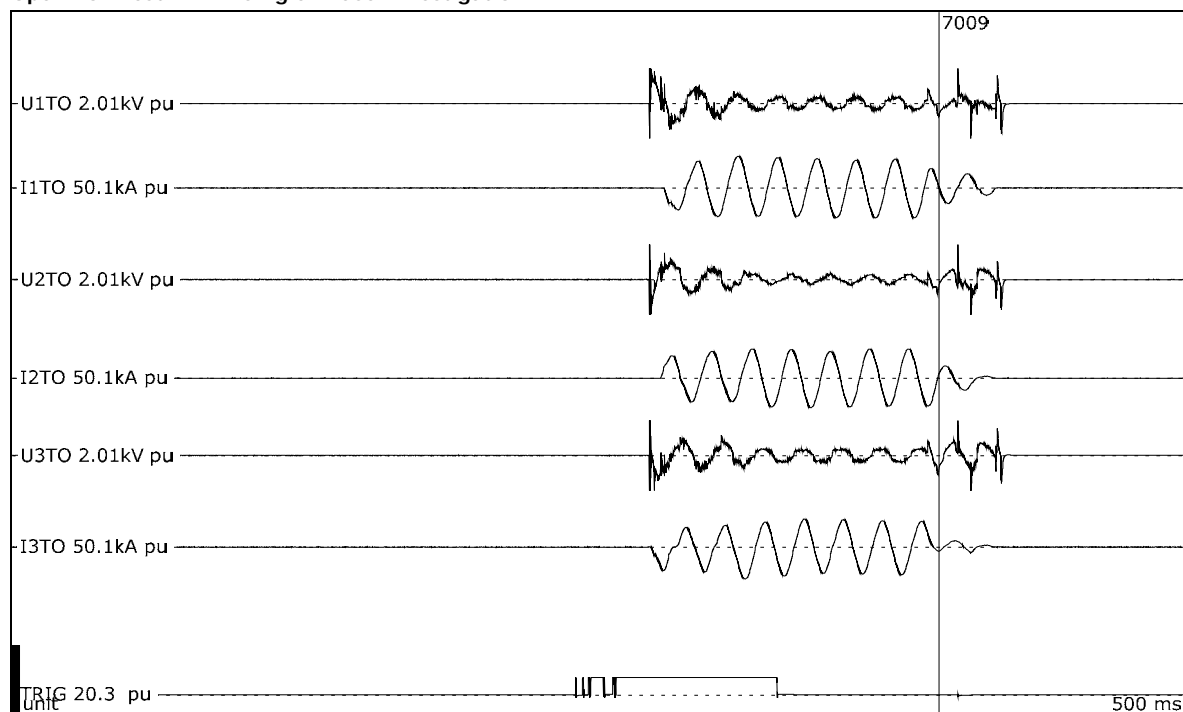
Test number: 190830-7008

Phase		A	B	C
Applied voltage, phase-to-ground	V _{RMS}	583	583	583
Applied voltage, phase-to-phase	V _{RMS}	1010		
Making current	kA _{peak}	28.9	-30.9	-19.7
Current, a.c. component, beginning	kA _{RMS}	14.8	16.2	8.35
Current, a.c. component, middle	kA _{RMS}	14.3	14.7	13.8
Current, a.c. component, end	kA _{RMS}	14.6	14.7	13.8
Current, a.c. component, average	kA _{RMS}	14.6	14.5	12.4
Current, a.c. component, three-phase average	kA _{RMS}	13.8		
Duration	s	0.122	0.118	0.121
Arc energy	kJ	269	211	267



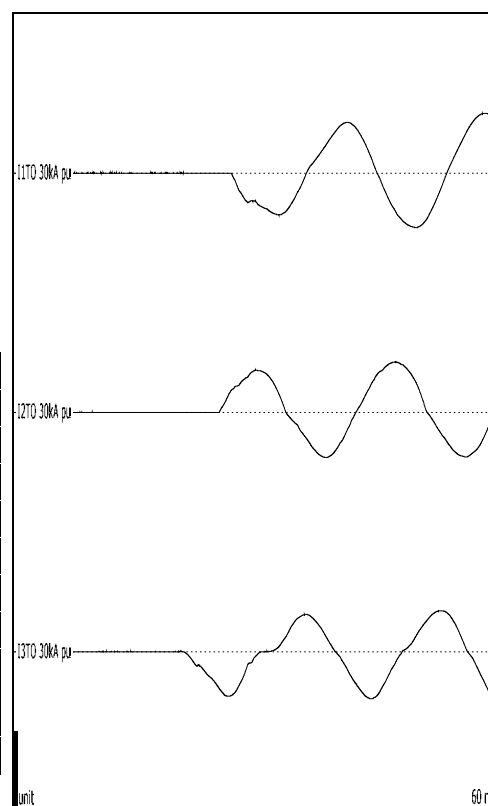
Observations: Emission of flames and gas observed. Current was present on both A and C phases immediately upon closing onto the test device. This test will be repeated.

Open Box Test # 17 - Single Phase Investigation



Test number: 190830-7009

Phase		A	B	C
Applied voltage, phase-to-ground	V _{RMS}	583	583	583
Applied voltage, phase-to-phase	V _{RMS}	1010		
Making current	kA _{peak}	22.5	19.0	-17.8
Current, a.c. component, beginning	kA _{RMS}	13.1	12.2	11.1
Current, a.c. component, middle	kA _{RMS}	14.7	14.1	13.6
Current, a.c. component, end	kA _{RMS}	14.7	14.1	13.6
Current, a.c. component, average	kA _{RMS}	14.5	13.7	13.1
Current, a.c. component, three-phase average	kA _{RMS}	13.8		
Duration	s	0.117	0.119	0.123
Arc energy	kJ	269	206	258



Observations: Emission of flames and gas observed. Arc propagated to B phase in 4.4 ms, to A phase in 5.9 ms.

33.4 Condition / inspection after test

Box sustained minimal damage.

34 OPEN BOX TEST # 18 - 480 V, 13.5 KA

Standard and date

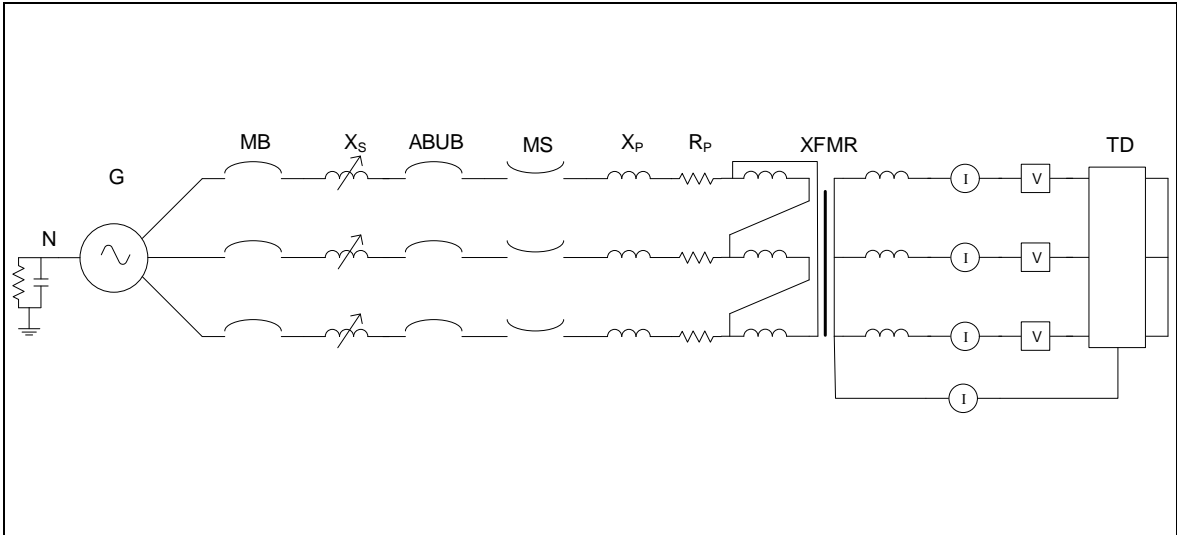
Standard	Client's instructions
Test date	30 August 2019

34.1 Condition before test

Test box in same condition as after trial 190830-7009. Arc to be initiated by #10 AWG wire. Arc wire connected to 1" diameter copper rods. Test duration is 2 seconds.



34.2 Test circuit S06



G	= Generator	ABUB	= Aux. Breaker	R	= Resistance
N	= Neutral	XFMR	= Transformer	C	= Capacitance
MB	= Main Breaker	TD	= Test Device	V	= Voltage Measurement
MS	= Make Switch	X	= Inductance	I	= Current Measurement

Supply		
Power	MVA	11.4
Frequency	Hz	60
Phase(s)		3
Voltage	V	489
Sym. Current	kA	13.5
Peak current	kA	35.5
Impedance	Ω	0.021

Remarks: -

34.3 Test results and oscillograms

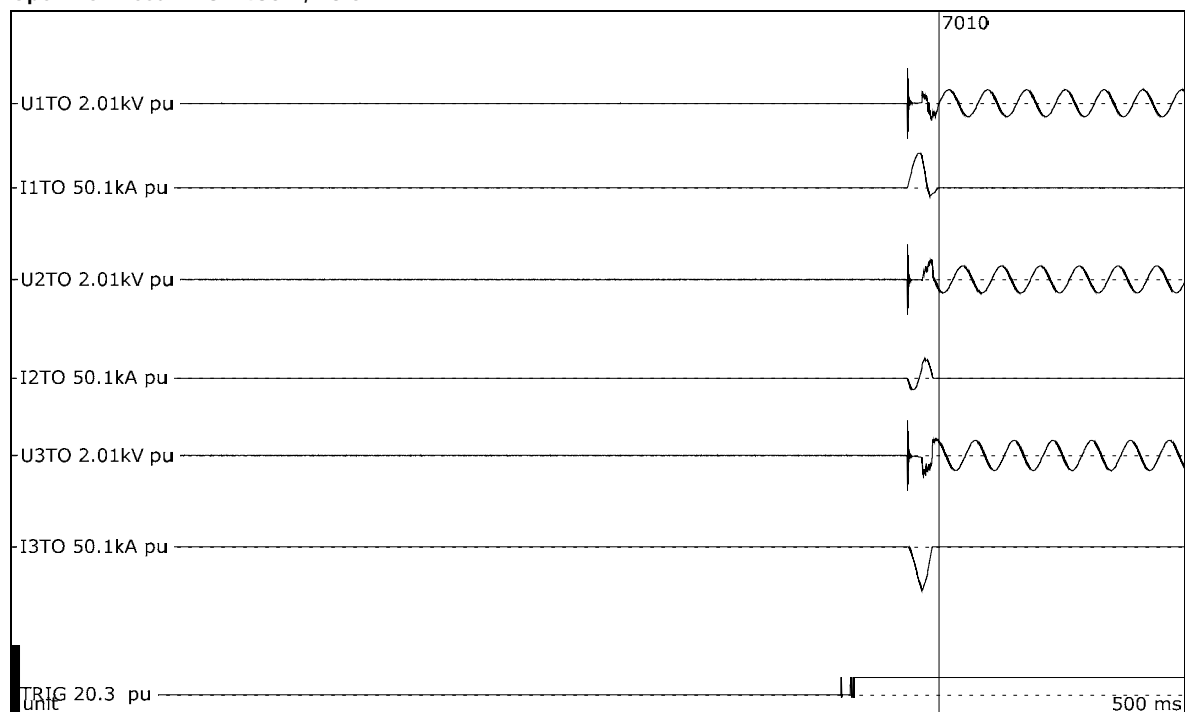
Overview of test numbers

190830-7010

Remarks

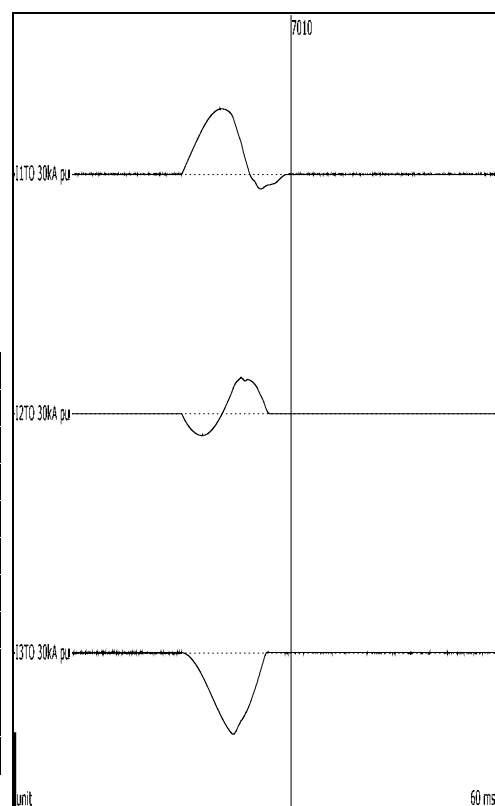
-

Open Box Test # 18 - 480 V, 13.5 kA



Test number: 190830-7010

Phase		A	B	C
Applied voltage, phase-to-ground	V _{RMS}	282	282	282
Applied voltage, phase-to-phase	V _{RMS}	488		
Making current	kA _{peak}	24.7	13.1	-30.6
Current, a.c. component, beginning	kA _{RMS}	3.19	5.07	5.41
Current, a.c. component, middle	kA _{RMS}	0.975	2.32	0.000
Current, a.c. component, end	kA _{RMS}	0.000	0.000	0.000
Current, a.c. component, average	kA _{RMS}	0.000	0.000	-
Current, a.c. component, three-phase average	kA _{RMS}	-		
Duration	ms	12.7	10.9	10.6
Arc energy	kJ	11.4	13.2	34.9



Observations: Emission of flames and gas observed.

34.4 Condition / inspection after test

Box sustained minimal damage. Arc self-extinguished.

35 CHECKING THE PROSPECTIVE CURRENT

Standard and date

Standard	Client's instructions
Test date	16 September 2019

35.1 Condition before test

Shorting bar connected at station terminals directly prior to test device.

35.2 Test results and oscillograms

Overview of test numbers

190916-9002 to 9005

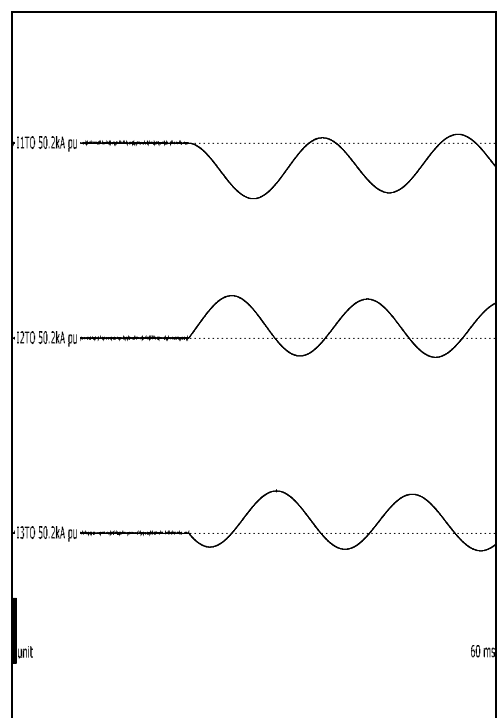
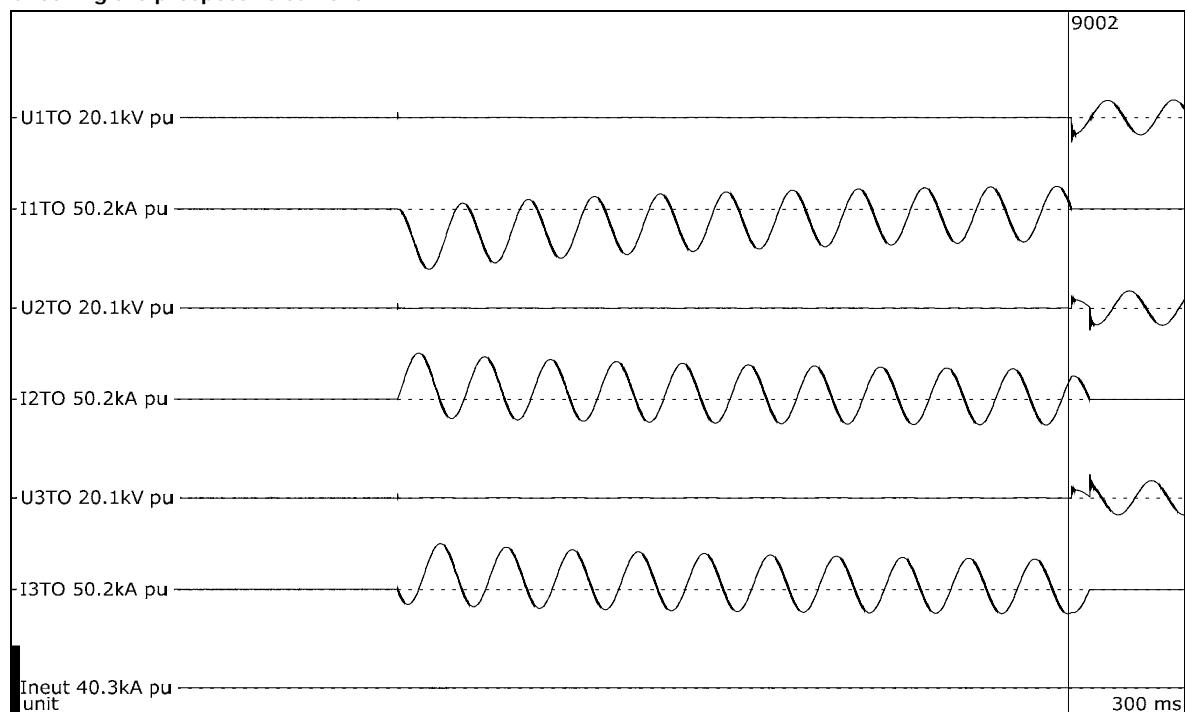
Remarks

Prospective circuit parameters calibrated in this test duty:

190916-9002→9003: 6900 V, 15.3 kA, 42.9 kA peak.

190916-9004→9005: 6900 V, 30.6 kA, 86.5 kA peak.

Checking the prospective current

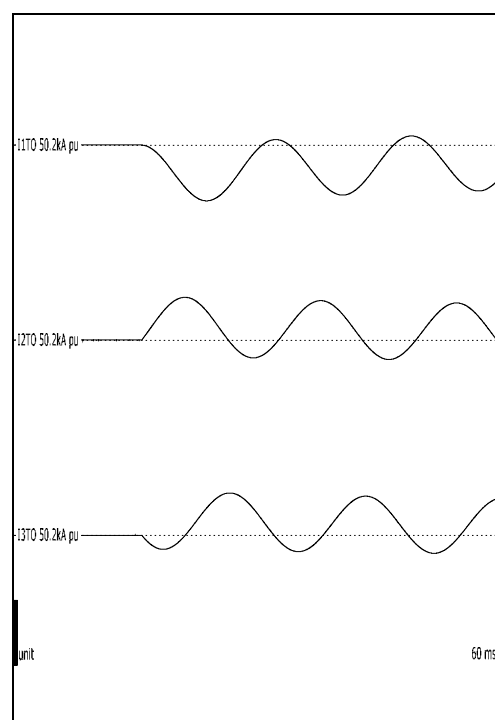
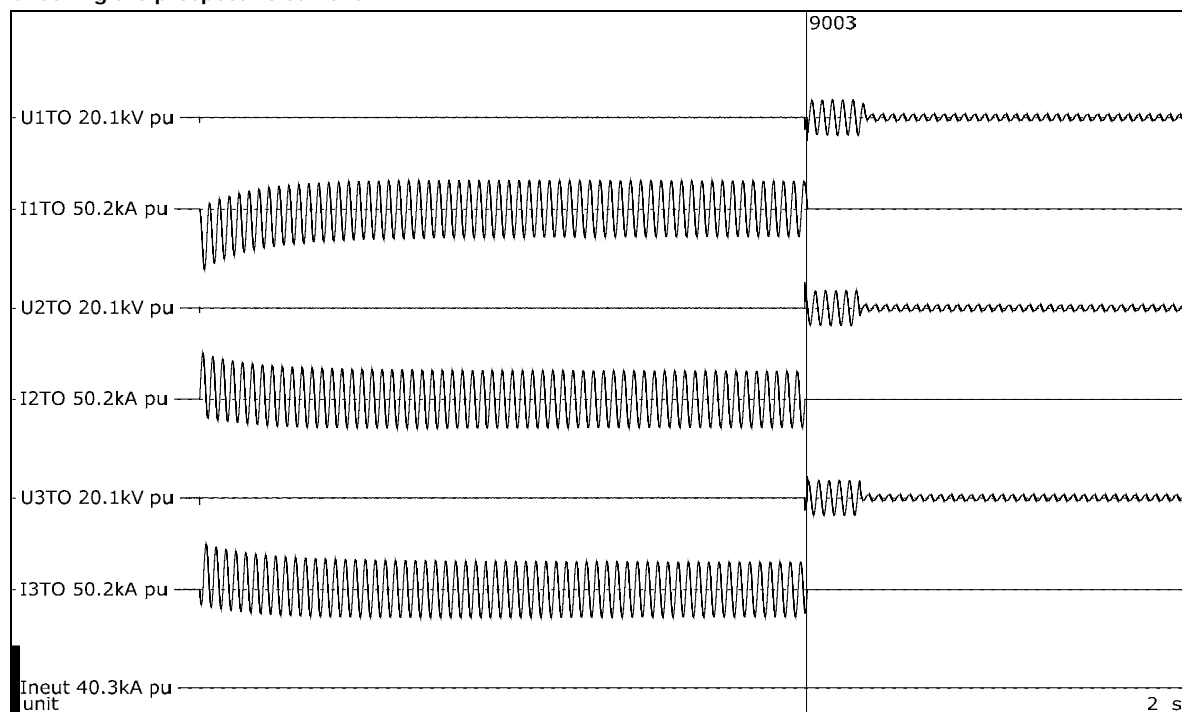


Test number: 190916-9002

Phase		A	B	C
Current	kA _{peak}	42.9	32.8	32.6
Current, a.c. component	kA _{RMS}	15.4	15.5	15.1
Current, a.c. component, three-phase average	kA _{RMS}	15.3		
Duration, current	s	0.171	0.171	0.171

Observations: No visible disturbance.

Checking the prospective current

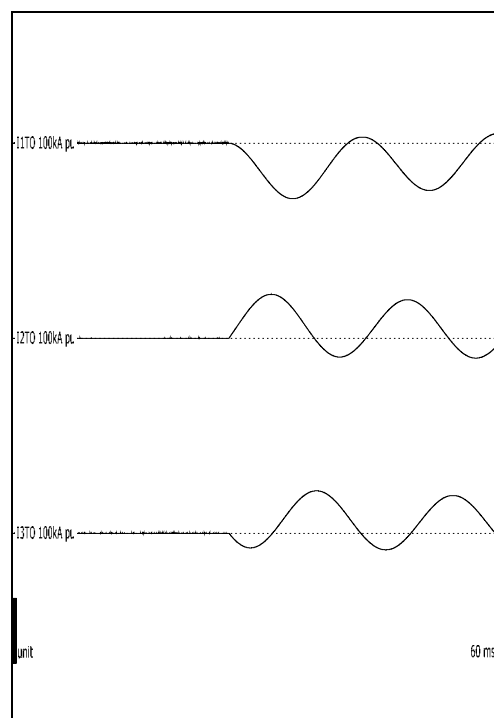
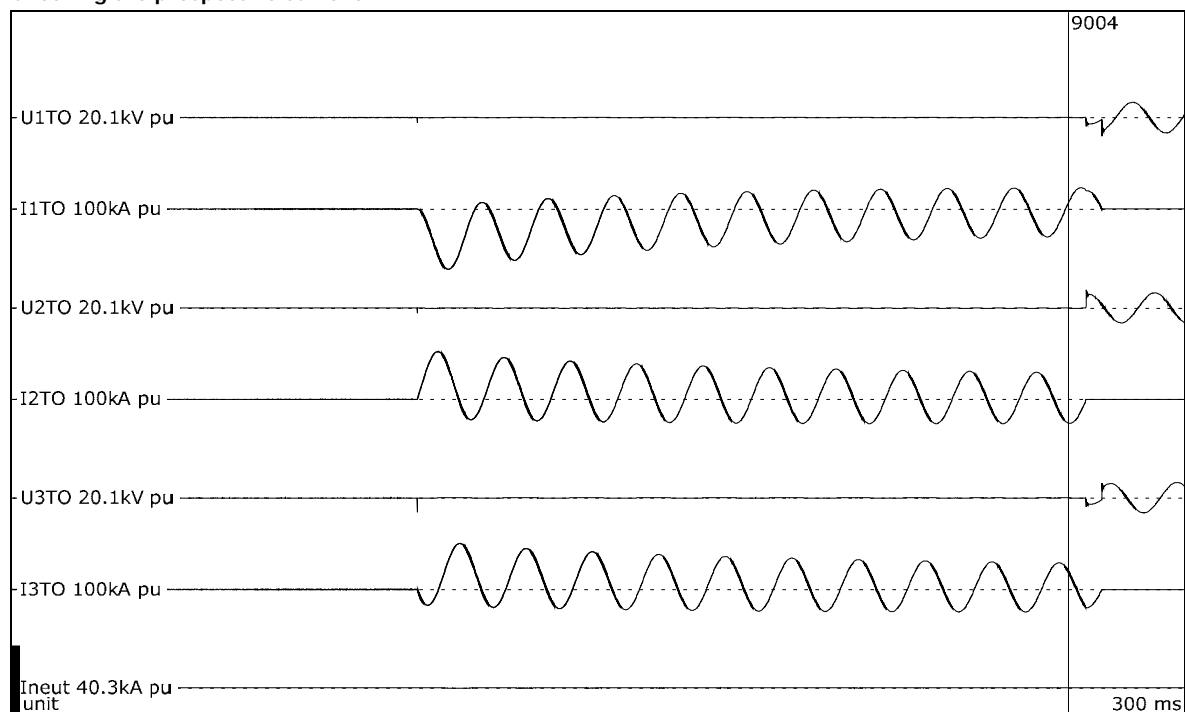


Test number: 190916-9003

Phase		A	B	C
Current	kA _{peak}	43.0	33.1	32.5
Current, a.c. component	kA _{RMS}	14.0	14.2	13.4
Current, a.c. component, three-phase average	kA _{RMS}	13.9		
Duration, current	s	1.03	1.03	1.03

Observations: No visible disturbance.

Checking the prospective current

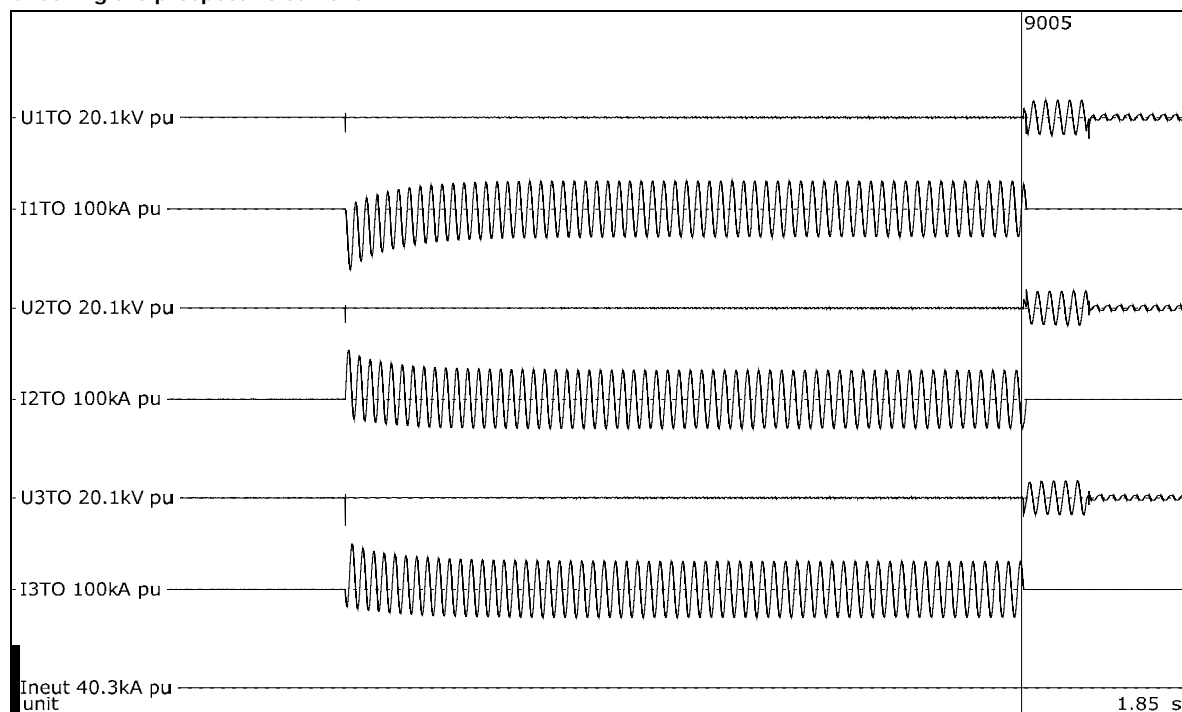


Test number: 190916-9004

Phase		A	B	C
Current	kA _{peak}	85.8	67.7	65.4
Current, a.c. component	kA _{RMS}	30.2	31.6	30.0
Current, a.c. component, three-phase average	kA _{RMS}	30.6		
Duration, current	s	0.166	0.166	0.166

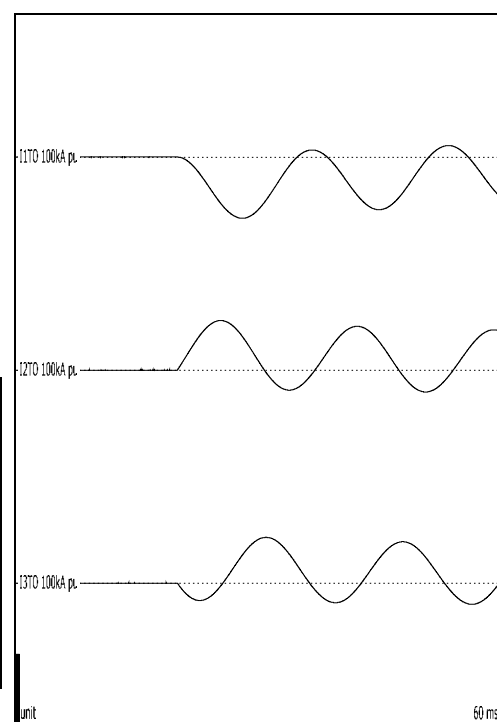
Observations: No visible disturbance.

Checking the prospective current



Test number: 190916-9005

Phase		A	B	C
Current	kA _{peak}	-86.5	70.0	64.6
Current, a.c. component, beginning	kA _{RMS}	30.1	31.3	30.2
Current, a.c. component, middle	kA _{RMS}	28.2	29.4	28.3
Current, a.c. component, end	kA _{RMS}	28.0	29.2	28.1
Current, a.c. component, average	kA _{RMS}	29.0	30.2	29.1
Current, a.c. component, three-phase average	kA _{RMS}	29.4		
Duration, current	s	1.07	1.07	1.07



Observations: No visible disturbance.

36 OBMV # 5

Standard and date

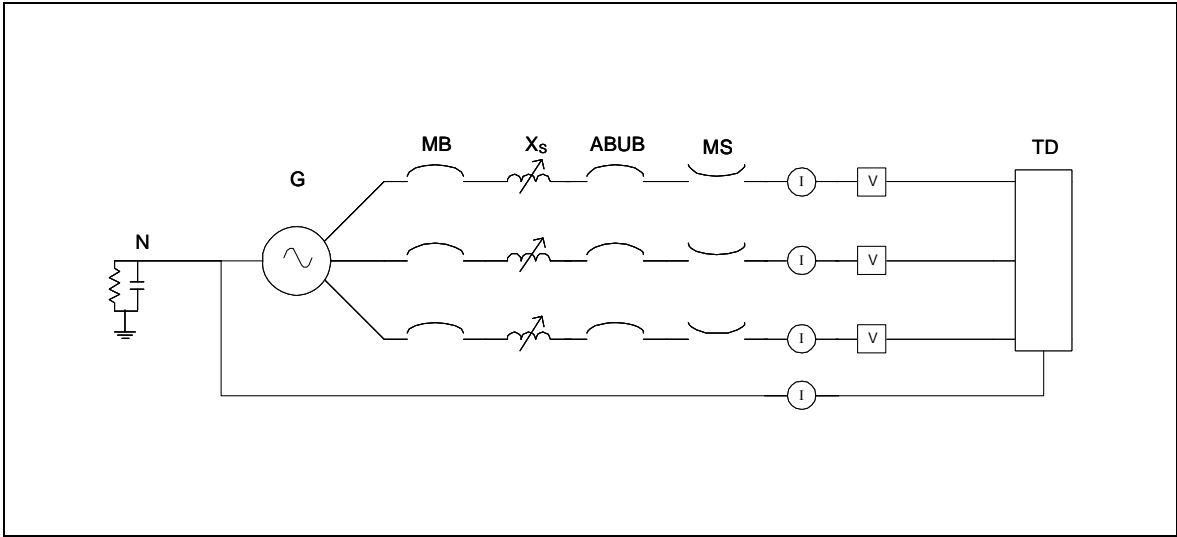
Standard	Client's instructions
Test date	16 September 2019

36.1 Condition before test

Test device new. Arc to be initiated by #24 AWG wire. Arc wire connected to copper bus. Test duration is 2 seconds.



36.2 Test circuit S11



G	= Generator	ABUB	= Aux. Breaker	R	= Resistance
N	= Neutral	XFMR	= Transformer	C	= Capacitance
MB	= Main Breaker	TD	= Test Device	V	= Voltage Measurement
MS	= Make Switch	X	= Inductance	I	= Current Measurement

Supply		
Power	MVA	366
Frequency	Hz	60
Phase(s)		3
Voltage	V	6900
Sym. Current	kA	30.6
Peak current	kA	86.5
Impedance	Ω	0.130

Remarks: -

36.3 Test results and oscillograms

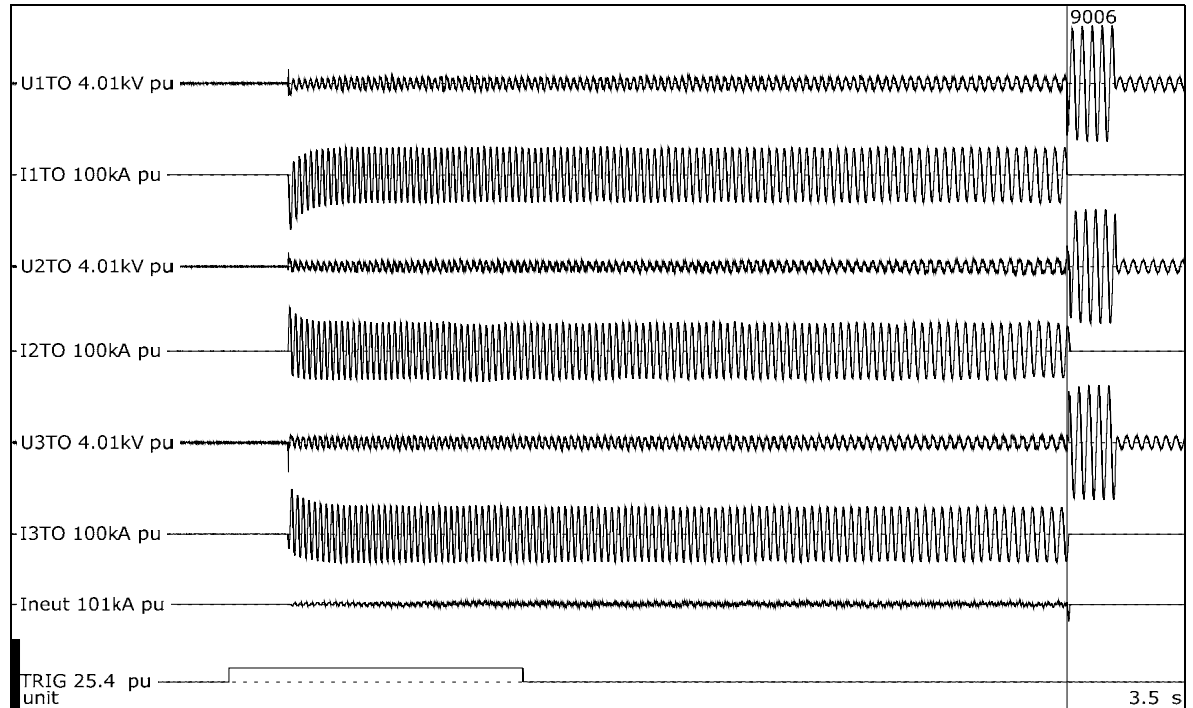
Overview of test numbers

190916-9006

Remarks

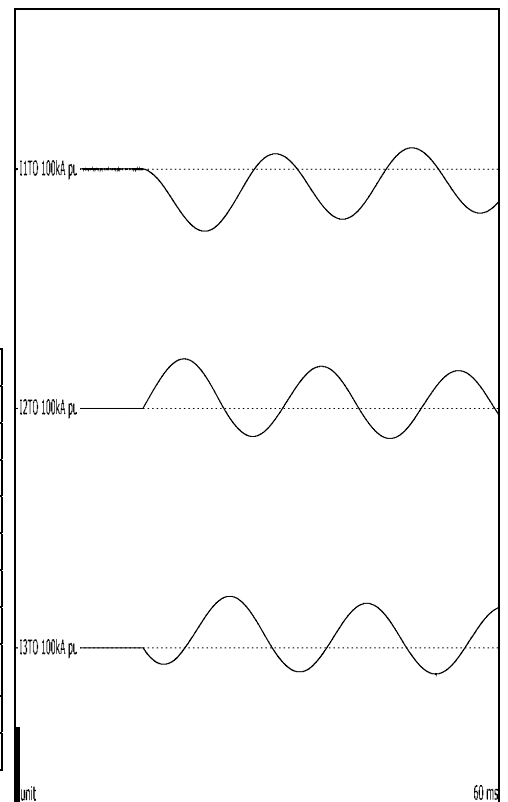
-

OBMV # 5



Test number: 190916-9006

Phase		A	B	C
Applied voltage, phase-to-ground	kV _{RMS}	3.98	3.98	3.98
Applied voltage, phase-to-phase	kV _{RMS}	6.90		
Making current	kA _{peak}	-78.3	62.1	64.5
Current, a.c. component, beginning	kA _{RMS}	31.7	32.9	31.9
Current, a.c. component, middle	kA _{RMS}	27.3	28.3	27.9
Current, a.c. component, end	kA _{RMS}	27.4	28.2	27.4
Current, a.c. component, average	kA _{RMS}	28.3	29.1	28.6
Current, a.c. component, three-phase average	kA _{RMS}	28.7		
Duration	s	2.32	2.32	2.32
Arc energy	MJ	15.7	12.7	15.1



Observations: Emission of flames and gas observed.

36.4 Condition / inspection after test

Left and right side of box burned through. Bottom of box melted and heavily distorted, but no burn-throughs evident.

37 OBMV # 2

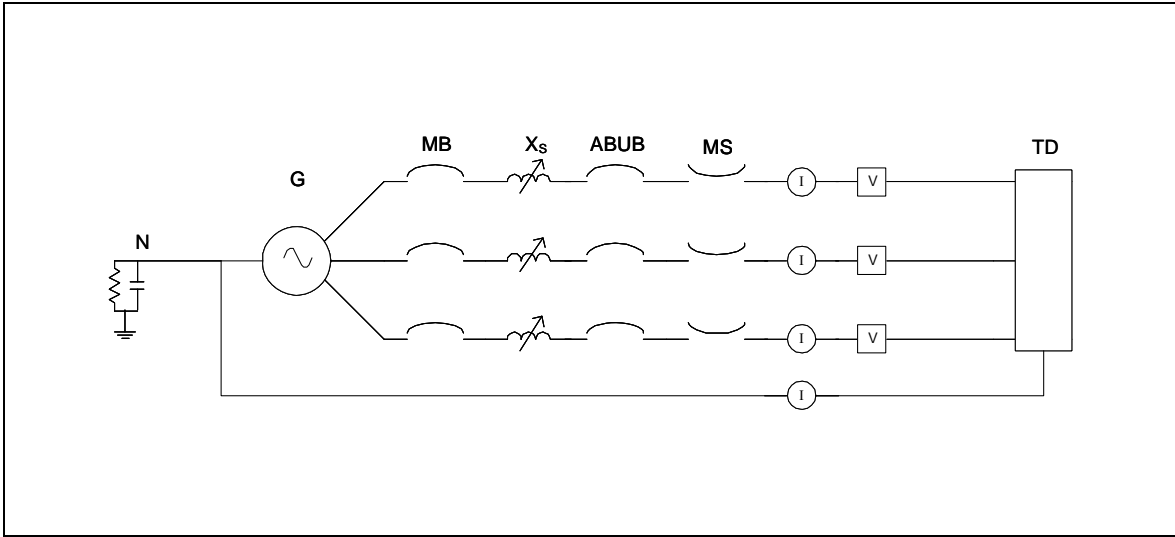
Standard and date

Standard	Client's instructions
Test date	17 September 2019

37.1 Condition before test

Test device new. Arc to be initiated by #24 AWG wire. Arc wire connected to aluminum bus. Test duration is 1 seconds.

37.2 Test circuit S11



G	= Generator	ABUB	= Aux. Breaker	R	= Resistance
N	= Neutral	XFMR	= Transformer	C	= Capacitance
MB	= Main Breaker	TD	= Test Device	V	= Voltage Measurement
MS	= Make Switch	X	= Inductance	I	= Current Measurement

Supply		
Power	MVA	366
Frequency	Hz	60
Phase(s)		3
Voltage	V	6900
Sym. Current	kA	30.6
Peak current	kA	86.5
Impedance	Ω	0.130

Remarks: -

37.3 Test results and oscillograms

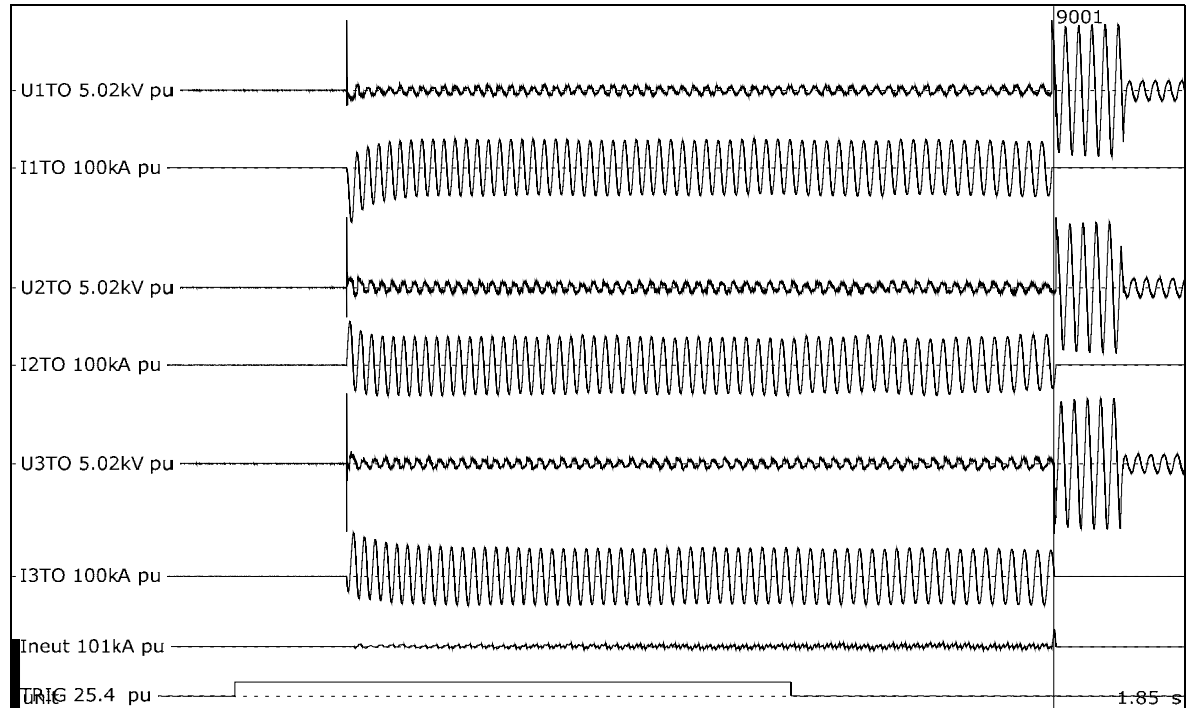
Overview of test numbers

190917-9001

Remarks

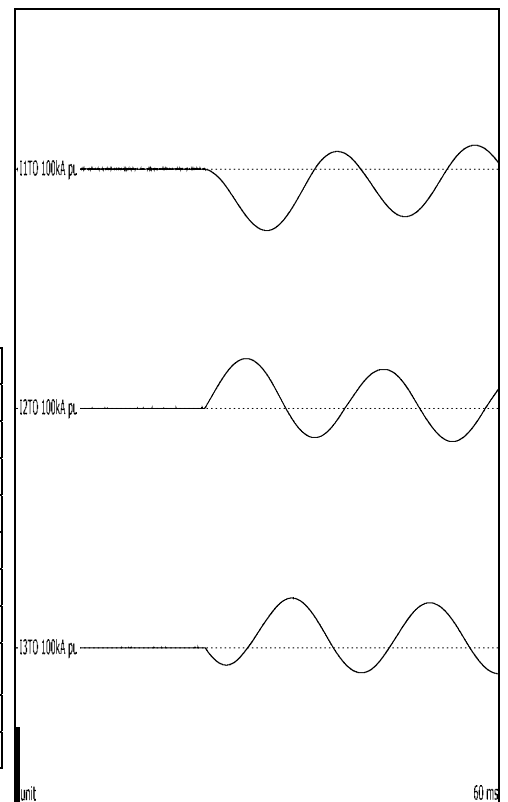
-

OBMV # 2



Test number: 190917-9001

Phase		A	B	C
Applied voltage, phase-to-ground	kV _{RMS}	3.98	3.98	3.98
Applied voltage, phase-to-phase	kV _{RMS}	6.89		
Making current	kA _{peak}	-77.4	62.5	62.2
Current, a.c. component, beginning	kA _{RMS}	32.0	32.7	31.5
Current, a.c. component, middle	kA _{RMS}	27.7	28.5	28.5
Current, a.c. component, end	kA _{RMS}	27.8	28.5	27.9
Current, a.c. component, average	kA _{RMS}	28.7	29.5	29.0
Current, a.c. component, three-phase average	kA _{RMS}	29.0		
Duration	s	1.11	1.11	1.11
Arc energy	MJ	6.58	8.07	6.77



Observations: Emission of flames and gas observed.

37.4 Condition / inspection after test

No complete burn throughs evident.

38 OBMV # 4

Standard and date

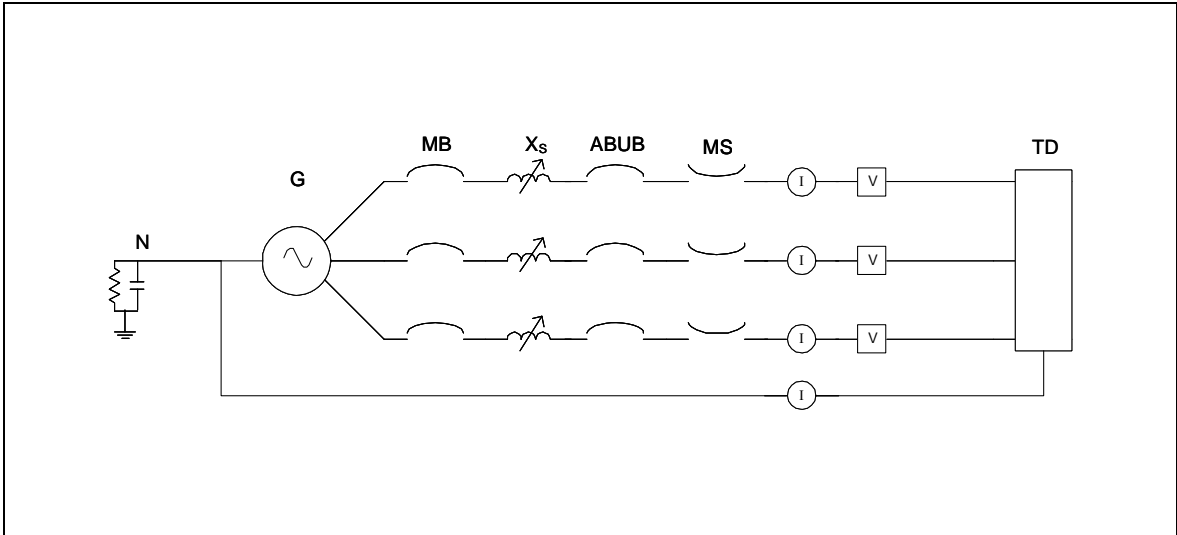
Standard	Client's instructions
Test date	17 September 2019

38.1 Condition before test

Test device new. Arc to be initiated by #24 AWG wire. Arc wire connected to copper bus. Test duration is 5 seconds.



38.2 Test circuit S10



G	= Generator	ABUB	= Aux. Breaker	R	= Resistance
N	= Neutral	XFMR	= Transformer	C	= Capacitance
MB	= Main Breaker	TD	= Test Device	V	= Voltage Measurement
MS	= Make Switch	X	= Inductance	I	= Current Measurement

Supply		
Power	MVA	182
Frequency	Hz	60
Phase(s)		3
Voltage	V	6900
Sym. Current	kA	15.3
Peak current	kA	42.9
Impedance	Ω	0.260

Remarks: -

38.3 Test results and oscillograms

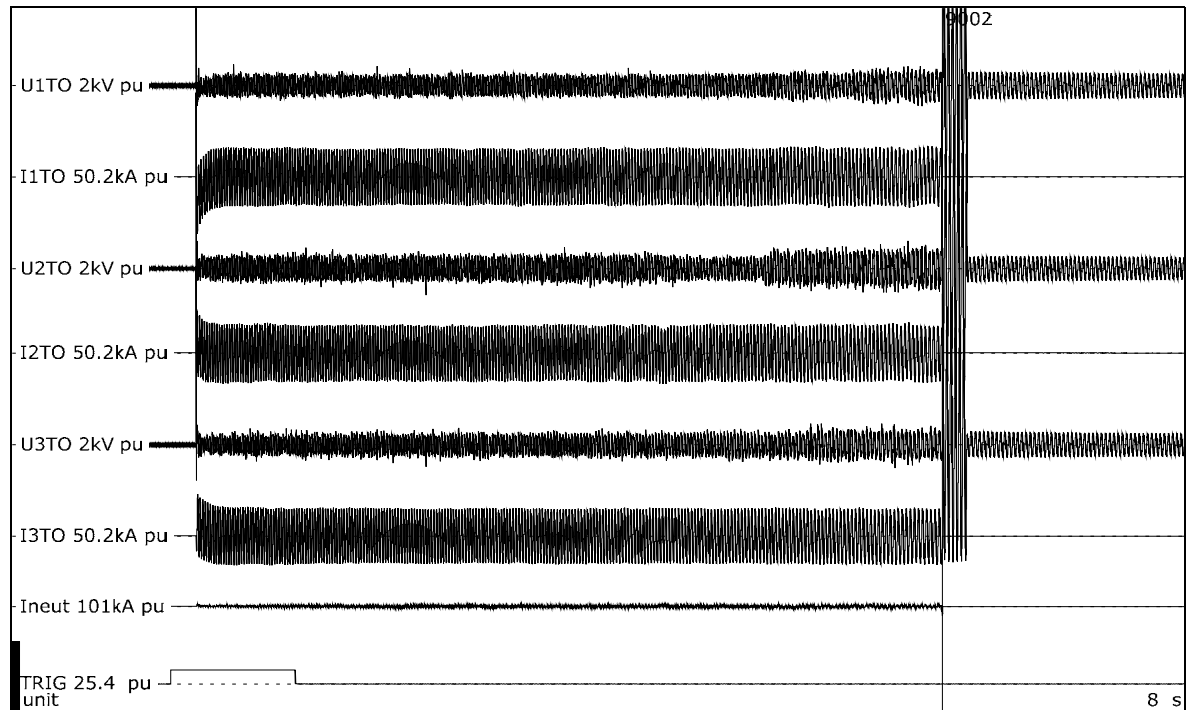
Overview of test numbers

190917-9002

Remarks

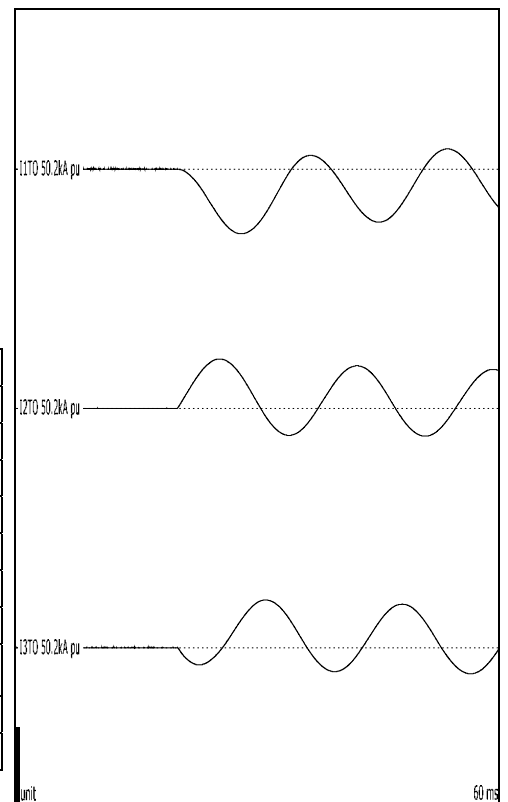
-

OBMV # 4



Test number: 190917-9002

Phase		A	B	C
Applied voltage, phase-to-ground	kV _{RMS}	3.98	3.98	3.98
Applied voltage, phase-to-phase	kV _{RMS}	6.89		
Making current	kA _{peak}	-40.7	31.0	29.9
Current, a.c. component, beginning	kA _{RMS}	16.1	16.2	15.2
Current, a.c. component, middle	kA _{RMS}	14.1	14.0	13.7
Current, a.c. component, end	kA _{RMS}	14.5	14.2	14.0
Current, a.c. component, average	kA _{RMS}	14.6	14.5	14.1
Current, a.c. component, three-phase average	kA _{RMS}	14.4		
Duration	s	5.08	5.08	5.08
Arc energy	MJ	16.7	19.1	16.0



Observations: Emission of flames and gas observed.

38.4 Condition / inspection after test

Bottom of box burned completely through. Large burn throughs evident on sides of box.

39 OBMV # 1

Standard and date

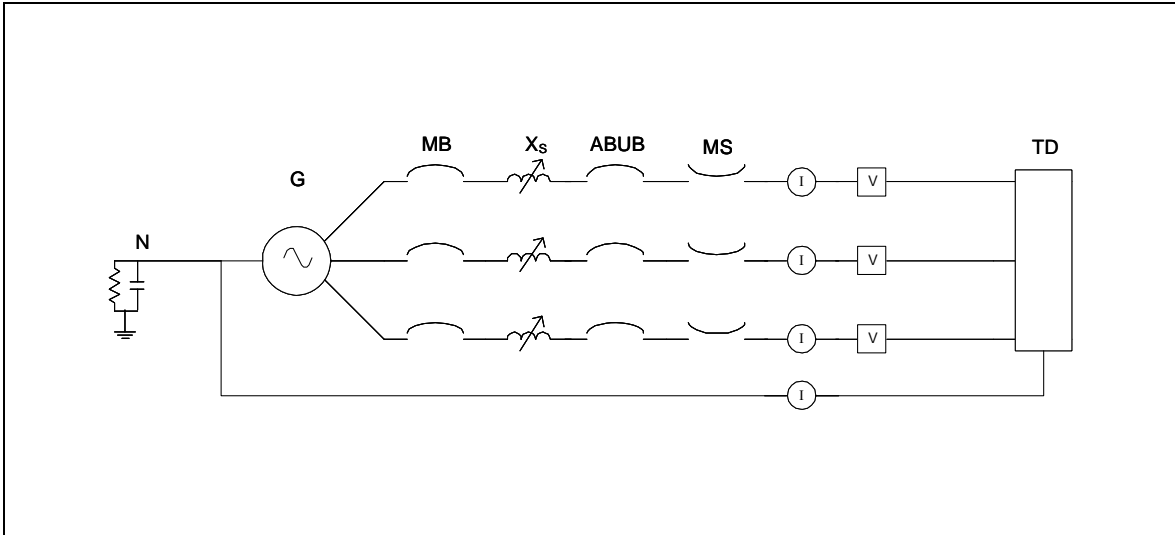
Standard	Client's instructions
Test date	18 September 2019

39.1 Condition before test

Test device new. Arc to be initiated by #24 AWG wire. Arc wire connected to aluminum bus. Test duration is 2 seconds.



39.2 Test circuit S10



G	= Generator	ABUB	= Aux. Breaker	R	= Resistance
N	= Neutral	XFMR	= Transformer	C	= Capacitance
MB	= Main Breaker	TD	= Test Device	V	= Voltage Measurement
MS	= Make Switch	X	= Inductance	I	= Current Measurement

Supply		
Power	MVA	182
Frequency	Hz	60
Phase(s)		3
Voltage	V	6900
Sym. Current	kA	15.3
Peak current	kA	42.9
Impedance	Ω	0.260

Remarks: -

39.3 Test results and oscillograms

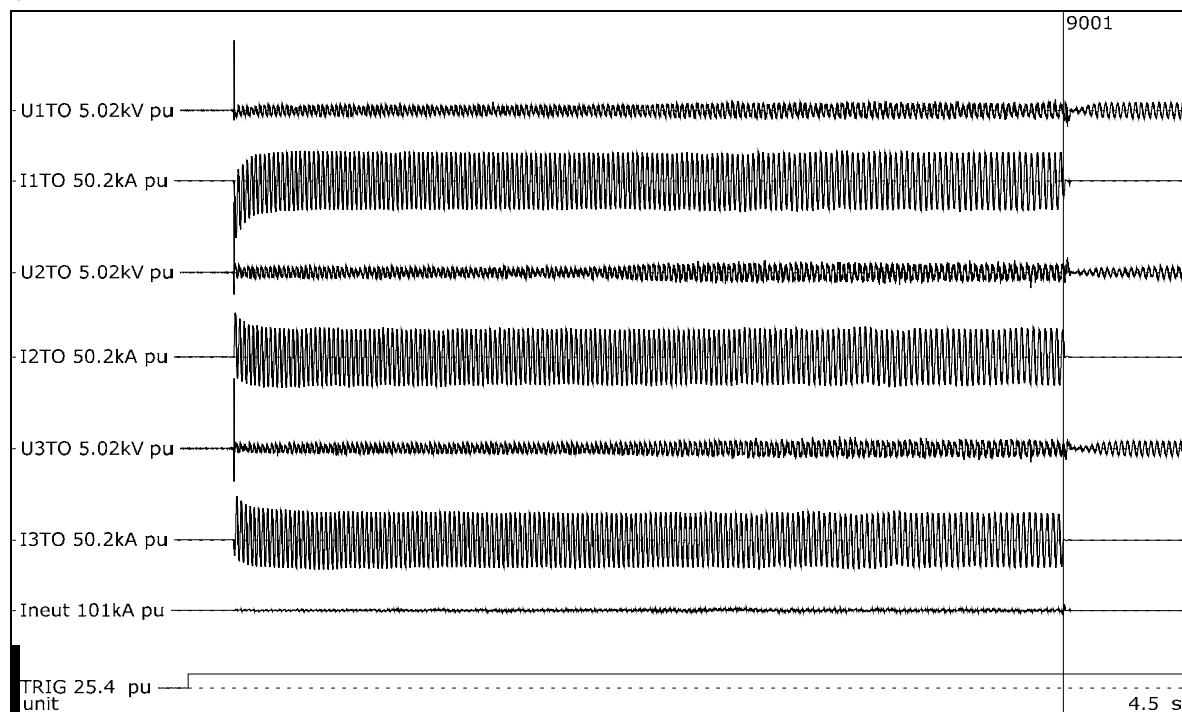
Overview of test numbers

190918-9001

Remarks

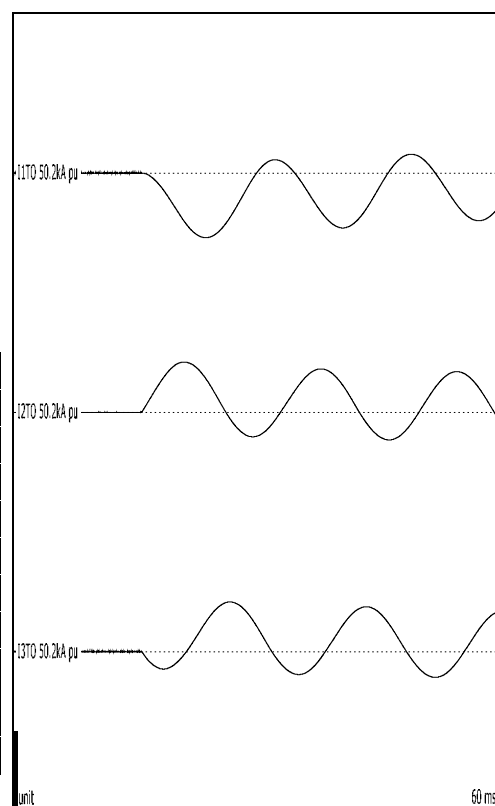
-

OBMV # 1



Test number: 190918-9001

Phase		A	B	C
Applied voltage, phase-to-ground	kV _{RMS}	3.98	3.98	3.98
Applied voltage, phase-to-phase	kV _{RMS}	6.89		
Making current	kA _{peak}	-40.6	31.6	31.2
Current, a.c. component, beginning	kA _{RMS}	16.2	15.8	15.5
Current, a.c. component, middle	kA _{RMS}	14.2	14.2	13.6
Current, a.c. component, end	kA _{RMS}	14.3	14.4	13.6
Current, a.c. component, average	kA _{RMS}	14.7	14.5	14.1
Current, a.c. component, three-phase average	kA _{RMS}	14.4		
Duration	s	3.18	3.18	3.18
Arc energy	MJ	12.4	13.3	11.8



Observations: Emission of flames and gas observed. Station timer malfunctioned during test, causing duration to be extended to 3.18 seconds.

39.4 Condition / inspection after test

Bottom and sides of box completely burned through. Test duration was longer than expected due to station timer malfunction.

40 OBMV # 3

Standard and date

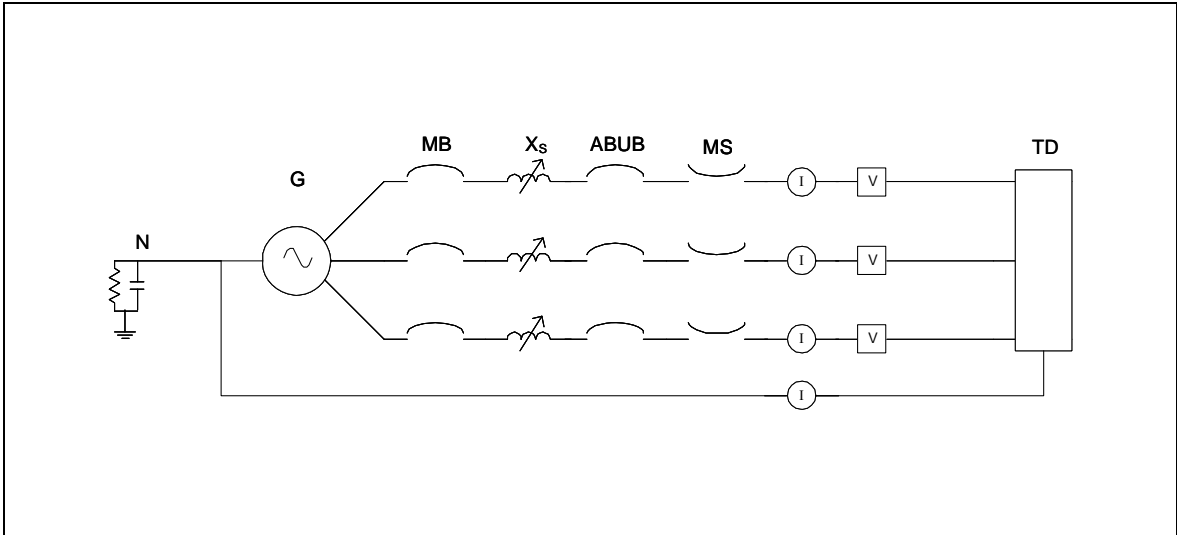
Standard	Client's instructions
Test date	18 September 2019

40.1 Condition before test

Test device new. Arc to be initiated by #24 AWG wire. Arc wire connected to aluminum bus. Test duration is 5 seconds.



40.2 Test circuit S10



G	= Generator	ABUB	= Aux. Breaker	R	= Resistance
N	= Neutral	XFMR	= Transformer	C	= Capacitance
MB	= Main Breaker	TD	= Test Device	V	= Voltage Measurement
MS	= Make Switch	X	= Inductance	I	= Current Measurement

Supply		
Power	MVA	182
Frequency	Hz	60
Phase(s)		3
Voltage	V	6900
Sym. Current	kA	15.3
Peak current	kA	42.9
Impedance	Ω	0.260

Remarks: -

40.3 Test results and oscillograms

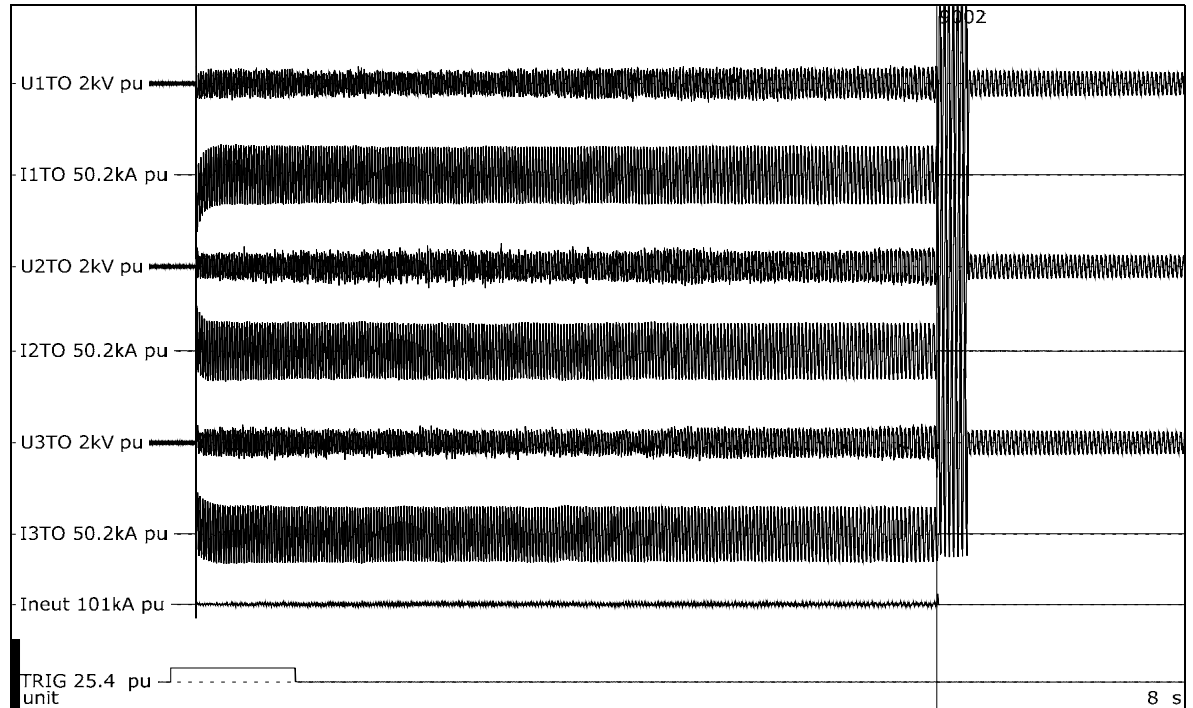
Overview of test numbers

190918-9002

Remarks

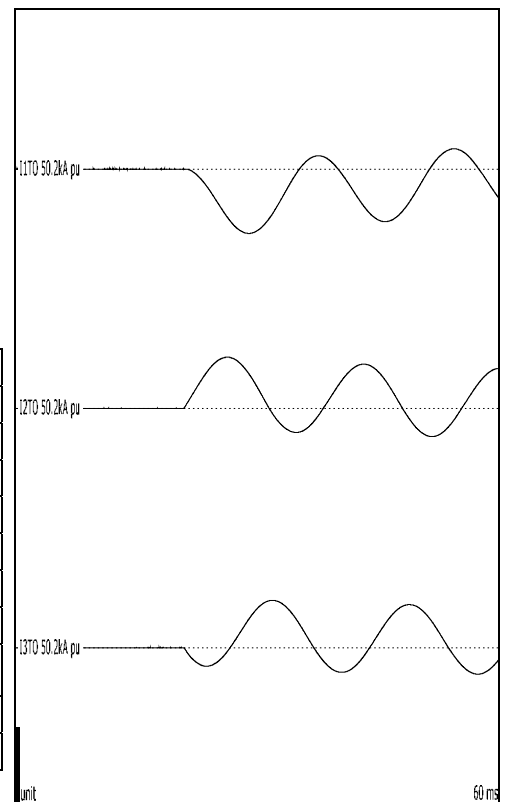
-

OBMV # 3



Test number: 190918-9002

Phase		A	B	C
Applied voltage, phase-to-ground	kV _{RMS}	3.98	3.98	3.98
Applied voltage, phase-to-phase	kV _{RMS}	6.89		
Making current	kA _{peak}	-40.5	32.1	29.7
Current, a.c. component, beginning	kA _{RMS}	15.9	15.9	15.3
Current, a.c. component, middle	kA _{RMS}	14.2	14.0	13.9
Current, a.c. component, end	kA _{RMS}	14.7	14.1	14.1
Current, a.c. component, average	kA _{RMS}	14.7	14.4	14.1
Current, a.c. component, three-phase average	kA _{RMS}	14.4		
Duration	s	5.05	5.05	5.05
Arc energy	MJ	19.1	19.6	17.0



Observations: Emission of flames and gas observed.

40.4 Condition / inspection after test

Bottom and sides of box completely burned through.

41 OBMV # 6

Standard and date

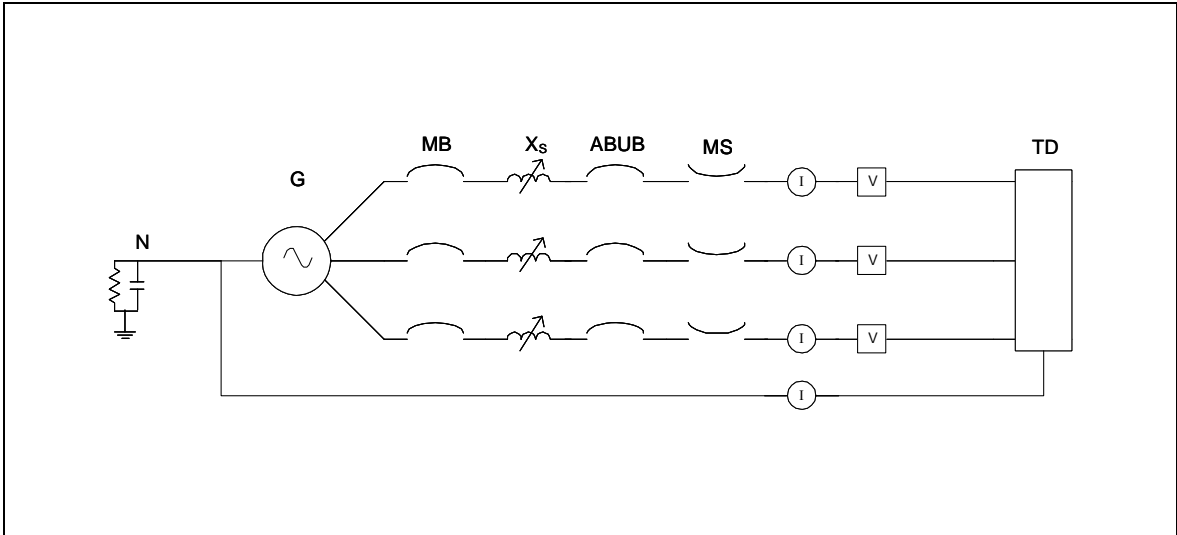
Standard	Client's instructions
Test date	18 September 2019

41.1 Condition before test

Test device new. Arc to be initiated by #24 AWG wire. Arc wire connected to aluminum bus. Test duration is 2 seconds.



41.2 Test circuit S10



G	= Generator	ABUB	= Aux. Breaker	R	= Resistance
N	= Neutral	XFMR	= Transformer	C	= Capacitance
MB	= Main Breaker	TD	= Test Device	V	= Voltage Measurement
MS	= Make Switch	X	= Inductance	I	= Current Measurement

Supply		
Power	MVA	182
Frequency	Hz	60
Phase(s)		3
Voltage	V	6900
Sym. Current	kA	15.3
Peak current	kA	42.9
Impedance	Ω	0.260

Remarks: -

41.3 Test results and oscillograms

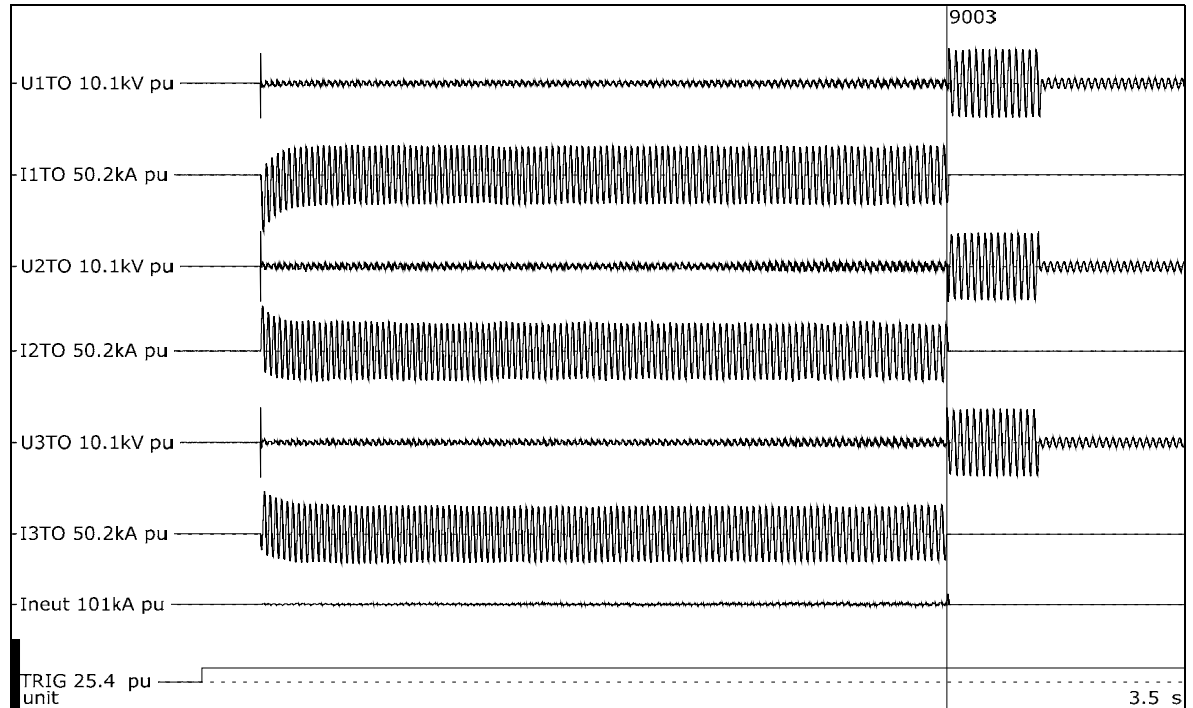
Overview of test numbers

190918-9003

Remarks

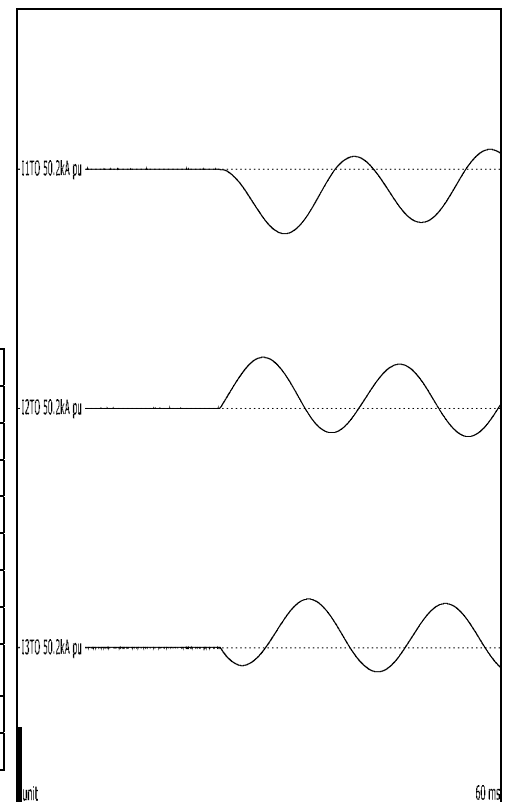
-

OBMV # 6



Test number: 190918-9003

Phase		A	B	C
Applied voltage, phase-to-ground	kV _{RMS}	3.98	3.98	3.98
Applied voltage, phase-to-phase	kV _{RMS}	6.89		
Making current	kA _{peak}	-40.7	32.1	30.5
Current, a.c. component, beginning	kA _{RMS}	15.9	16.0	15.5
Current, a.c. component, middle	kA _{RMS}	14.5	14.1	13.9
Current, a.c. component, end	kA _{RMS}	14.7	13.9	13.9
Current, a.c. component, average	kA _{RMS}	14.8	14.6	14.3
Current, a.c. component, three-phase average	kA _{RMS}	14.6		
Duration	s	2.05	2.05	2.05
Arc energy	MJ	7.66	7.89	7.17



Observations: Emission of flames and gas observed.

41.4 Condition / inspection after test

Bottom and sides of box completely burned through.

42 ATTACHMENTS

1. Calorimeter Data Records [15 PAGES]
2. Instrumentation Information Sheets [2 PAGES]
3. Photographs (269) [135 PAGES]

Test Number:

24512323 Date and Time:

Trial Number:

190826-7003

8/26/2019

DAS Operator:

Joe Duffy

4:18:00 PM

Calorimeter	Avg Start Temp (°C)	Max Temp (°C)	Time to max heat (sec)	Comments
A	44.6	44.6	N/A	1,2
B	23.8	23.8	N/A	1
C	23.9	23.9	N/A	1
D	23.3	23.3	N/A	1
E	24.6	24.6	N/A	1
F	40.7	40.7	N/A	1,2
G	24.8	24.8	N/A	1
H	43.7	43.7	N/A	1,2
I	50.7	50.7	N/A	1,2
J	24.5	24.5	N/A	1

Comments: 1) Due to the arc self-extinguishing, no noticeable differences in temperature during the event were recorded. 2) Ambient temperature readings were much higher than actual ambient, client agreed to proceed with testing despite this difference.

Test Number: 24512323 Date and Time: 8/27/2019
Trial Number: 190827-7001
DAS Operator: Joe Duffy 9:16:00 AM

Calorimeter	Avg Start Temp (°C)	Max Temp (°C)	Time to max heat (sec)	Comments
A	32.0	32.1	N/A	1,2
B	18.2	18.2	N/A	1
C	18.9	18.9	N/A	1
D	18.4	18.9	N/A	1
E	18.5	19.0	N/A	1
F	26.3	26.8	55	2
G	19.7	20.8	30	
H	29.8	31.0	58	2
I	36.0	36.8	23	2
J	19.0	19.4	11	

Comments: 1) Due to the arc self-extinguishing, no noticeable differences in temperature during the event were recorded. 2) Ambient temperature readings were much higher than actual ambient, client agreed to proceed with testing despite this difference.

Test Number: 24512323 Date and Time: 8/27/2019
Trial Number: 190827-7002
DAS Operator: Joe Duffy 10:25:00 AM

Calorimeter	Avg Start Temp (°C)	Max Temp (°C)	Time to max heat (sec)	Comments
A	41.3	41.7	N/A	1,2
B	20.1	20.3	N/A	1
C	20.5	20.6	N/A	1
D	19.7	19.8	N/A	1
E	20.1	21.0	101	
F	34.7	35.6	110	2
G	20.4	21.4	9	
H	38.4	39.6	17	2
I	44.4	45.1	30	2
J	20.5	21.2	33	

Comments: 1) Due to the arc self-extinguishing, no noticeable differences in temperature during the event were recorded. 2) Ambient temperature readings were much higher than actual ambient, client agreed to proceed with testing despite this difference.

Test Number:

24512323 Date and Time:

Trial Number:

190827-7003

8/27/2019

DAS Operator:

Joe Duffy

1:24:00 PM

Calorimeter	Avg Start Temp (°C)	Max Temp (°C)	Time to max heat (sec)	Comments
A	50.0	50.4	N/A	1,2
B	23.1	23.2	N/A	1
C	23.8	23.8	N/A	1
D	22.4	22.5	N/A	1
E	23.7	26.7	158	
F	43.1	45.2	151	2
G	23.5	26.4	80	
H	46.6	50.3	171	2
I	52.3	54.1	99	2
J	23.2	24.2	140	

Comments: 1) Due to the arc self-extinguishing, no noticeable differences in temperature during the event were recorded. 2) Ambient temperature readings were much higher than actual ambient, client agreed to proceed with testing despite this difference.

Test Number: 24512323 Date and Time: 8/27/2019
Trial Number: 190827-7004
DAS Operator: Joe Duffy 2:54:00 PM

Calorimeter	Avg Start Temp (°C)	Max Temp (°C)	Time to max heat (sec)	Comments
A	53.6	53.8	N/A	1,2
B	24.6	24.7	N/A	1
C	24.8	26.2	11	
D	23.8	24.9	137	
E	24.7	25.5	33	
F	47.1	50.0	>10 minutes	2,3
G	24.6	40.5	9	
H	50.8	57.0	147	2
I	56.7	56.5	11	2
J	25.4	28.7	9	

Comments: 1) No significant difference in temperature during the event were recorded. 2) Ambient temperature readings were much higher than actual ambient, client agreed to proceed with testing despite this difference. 3) Temperature appears to still be rising at the end of the data capture window.

Test Number: 24512323 Date and Time: 8/28/2019
Trial Number: 190828-7001
DAS Operator: Joe Duffy 10:14:00 AM

Calorimeter	Avg Start Temp (°C)	Max Temp (°C)	Time to max heat (sec)	Comments
A	64.5	70.9	7	1
B	30.5	41.2	4	
C	26.3	27.0	260	
D	24.8	25.3	260	
E	29.5	30.5	124	
F	56.5	58.1	290	1,2
G	27.2	28.5	135	
H	59.1	60.4	101	1
I	63.7	64.4	160	1
J	27.3	28.2	290	2

Comments: 1) Ambient temperature readings were much higher than actual ambient, client agreed to proceed with testing despite this difference. 2) Temperature appears to still be rising at the end of the data capture window.

Test Number: 24512323 Date and Time: 8/28/2019
Trial Number: 190828-7002
DAS Operator: Joe Duffy 10:53:00 AM

Calorimeter	Avg Start Temp (°C)	Max Temp (°C)	Time to max heat (sec)	Comments
A	61.2	74.3	6	2
B	28.1	47.5	6	
C	27.8	27.9	N/A	1
D	26.9	27.0	N/A	1
E	27.8	29.4	6	
F	54.6	56.3	290	2,3
G	27.7	30.7	47	
H	58.0	63.0	10	2
I	63.9	65.6	58	2
J	27.8	29.7	9	

Comments: 1) No significant difference in temperature during the event were recorded. 2) Ambient temperature readings were much higher than actual ambient, client agreed to proceed with testing despite this difference. 3) Temperature appears to still be rising at the end of the data capture window.

Test Number: 24512323 Date and Time: 8/29/2019
 Trial Number: 190829-7005
 DAS Operator: Joe Duffy 11:21:00 AM

Calorimeter	Avg Start Temp (°C)	Max Temp (°C)	Time to max heat (sec)	Comments
A	62.8	73.0	6	1
B	31.8	46.6	5	
C	27.1	28.0	>7 minutes	2
D	26.3	27.1	>7 minutes	2
E	28.7	33.4	234	
F	54.3	58.5	>7 minutes	1,2
G	28.7	40.2	176	
H	59.3	75.3	21	1
I	64.0	68.7	277	1
J	30.1	35.2	9	
K	30.0	32.5	268	
L	28.0	30.7	>7 minutes	2

Comments: 1) Ambient temperature readings were much higher than actual ambient, client agreed to proceed with testing despite this difference. 2) Temperature appears to still be rising at the end of the data capture window.

Test Number: 24512323 Date and Time: 8/29/2019
 Trial Number: 190829-7006
 DAS Operator: Joe Duffy 2:31:00 PM

Calorimeter	Avg Start Temp (°C)	Max Temp (°C)	Time to max heat (sec)	Comments
A	56.2	120.0	10	1
B	28.6	108.1	9	
C	27.9	33.6	15	
D	27.4	31.5	>17 minutes	2
E	28.2	60.4	84	
F	51.0	86.0	632	1
G	28.7	145.3	15	
H	53.9	219.5	15	1
I	59.5	102.1	19	1
J	29.4	80.4	15	
K	27.6	58.9	325	
L	27.6	58.8	507	

Comments: 1) Ambient temperature readings were much higher than actual ambient, client agreed to proceed with testing despite this difference. 2) Temperature appears to still be rising at the end of the data capture window.



Test Number:	24512323	Date and Time:	
Trial Number:	190916-9006		9/16/2019
DAS Operator:	Joe Duffy		2:10:00 PM

Calorimeter	Avg Start Temp (°C)	Max Temp (°C)	Time to max heat (sec)	Comments
A	28.6	378.8	4	
B	28.7	135.4	34	

Comments:

Test Number: 24512323 Date and Time: 9/17/2019
Trial Number: 190917-9001
DAS Operator: Joe Duffy 10:03:00 AM

Calorimeter	Avg Start Temp (°C)	Max Temp (°C)	Time to max heat (sec)	Comments
A	26.6	402.3	2	
B	N/A	N/A	N/A	1

Comments: 1) Calorimeter B was not available for this test. Prior to test, it was discovered that thermocouple was reading as an open circuit. It was confirmed in the test cell that the issue was with the thermocouple wire, and not the data system. Client agreed to proceed with the test without calorimeter B due to the time it would take to replace the thermocouple wire.



Test Number: 24512323 Date and Time: 9/17/2019
Trial Number: 190917-9002
DAS Operator: Joe Duffy 3:35:00 PM

Calorimeter	Avg Start Temp (°C)	Max Temp (°C)	Time to max heat (sec)	Comments
A	25.9	227.5	6	
B	25.5	480.4	8	

Comments:



Test Number: 24512323 Date and Time: 9/18/2019
Trial Number: 190918-9001
DAS Operator: Joe Duffy 9:20:00 AM

Calorimeter	Avg Start Temp (°C)	Max Temp (°C)	Time to max heat (sec)	Comments
A	22.2	155.1	6	
B	28.7	>836	5	1

Comments: 1) Maximum temperature that can be recorded by thermal data system is 836° C.



Test Number: 24512323 Date and Time: 9/18/2019
Trial Number: 190918-9002
DAS Operator: Joe Duffy 10:04:00 AM

Calorimeter	Avg Start Temp (°C)	Max Temp (°C)	Time to max heat (sec)	Comments
A	22.5	281.0	9	
B	23.2	388.7	32	

Comments:



Test Number: 24512323 Date and Time: 9/18/2019
Trial Number: 190918-9003
DAS Operator: Joe Duffy 2:49:00 PM

Calorimeter	Avg Start Temp (°C)	Max Temp (°C)	Time to max heat (sec)	Comments
A	22.9	106.4	8	
B	22.8	405.7	4	

Comments:

KEMA-Powertest, Inc.

Instrumentation Information Sheet

TEST NO: 24512323

DATE: 09/19/2019

TEST DEVICE: Medium & Low Voltage Switchgear

TESTED BY: J. Duffy, B. Swartz

CODE#	TYPE	MANUFACTURER	MODEL#	SERIAL#	CALIBRATION	
					LAST	DUE
DAS20	DAS	NI/DEWETRON	DEWE-30-16	V08X02F33	10/16/2019	5/3/2020
PAV37	PNL.VOLTMTR	SIMPSON	F45-1-34	N/A	6/17/2019	1/3/2020
PAV24	PNL.VOLTMTR	WESTON	1234	N/A	6/17/2019	1/3/2020
ISO141	ISO AMP	DEWETRON	HIS-LV	504659	10/16/2019	5/3/2020
ISO142	ISO AMP	DEWETRON	HIS-LV	504660	10/16/2019	5/3/2020
ISO143	ISO AMP	DEWETRON	HIS-LV	504661	10/16/2019	5/3/2020
ISO144	ISO AMP	DEWETRON	HIS-LV	504662	10/16/2019	5/3/2020
ISO145	ISO AMP	DEWETRON	HIS-LV	508022	10/16/2019	5/3/2020
ISO146	ISO AMP	DEWETRON	HIS-LV	508021	10/16/2019	5/3/2020
ISO147	ISO AMP	DEWETRON	HIS-LV	508020	10/16/2019	5/3/2020
ISO149	ISO AMP	DEWETRON	HIS-LV	416717	10/16/2019	5/3/2020
ISO150	ISO AMP	DEWETRON	HIS-LV	416728	10/16/2019	5/3/2020
ISO151	ISO AMP	DEWETRON	HIS-LV	416698	10/16/2019	5/3/2020
CTX15	C.T.	ITE	TR	56571	1/17/2019	1/17/2021
CTX16	C.T.	ITE	TR	56573	1/17/2019	1/17/2021
CTX17	C.T.	ITE	TR	56572	1/17/2019	1/17/2021
CTX214	ROGOWSKI CT	PEM	CWT75LFxB	37226-29255	10/16/2019	5/3/2020
CTX215	ROGOWSKI CT	PEM	CWT75LFxB	37226-29256	10/16/2019	5/3/2020
CTX216	ROGOWSKI CT	PEM	CWT75LFxB	37226-29257	10/16/2019	5/3/2020
CTS51	CT SHUNT	DALE	NH-250	N/A	7/8/2019	1/24/2020
CTS52	CT SHUNT	DALE	NH-250	N/A	7/8/2019	1/24/2020
CTS53	CT SHUNT	DALE	NH-250	N/A	7/8/2019	1/24/2020
VDR38	RES.VOL.DIV	POWERTEST	189:1	38	7/8/2019	1/24/2020
VDR39	RES.VOL.DIV	POWERTEST	189:1	39	7/8/2019	1/24/2020
VDR40	RES.VOL.DIV	POWERTEST	189:1	40	7/8/2019	1/24/2020
VDR92	V.DIVIDER	NORTH STAR	PVM-11	1716317	6/21/2019	1/7/2020
VDR93	V.DIVIDER	NORTH STAR	PVM-11	1716417	10/16/2019	5/3/2020
VDR94	V.DIVIDER	NORTH STAR	PVM-11	1716517	10/16/2019	5/3/2020
KPT101	PRESS.TRANS	OMEGA	PX329	0303181148	7/16/2019	2/1/2020
KPT102	PRESS.TRANS	OMEGA	PX329	0303181131	7/16/2019	2/1/2020
AMP41	FO ISO AMP	AAA LAB SYST	AFL-300	1	8/12/2019	2/28/2020
AMP43	FO ISO AMP	AAA LAB SYST	AFL-300	3	8/12/2019	2/28/2020
AMP44	FO ISO AMP	AAA LAB SYST	AFL-300	4	8/12/2019	2/28/2020
AMP45	FO ISO AMP	AAA LAB SYST	AFL-300	5	8/12/2019	2/28/2020
KPT87	PRES.TRANS.	OMEGA	PX329	072613I064	10/24/2019	5/11/2020
KPT98	PRESS.TRANS	OMEGA	PX329	071114I076	4/5/2019	10/22/2019

KEMA-Powertest, Inc.

Instrumentation Information Sheet

TEST NO: 24512323*

DATE: 09/19/2019

TEST DEVICE: Low & Medium Voltage Switchgear

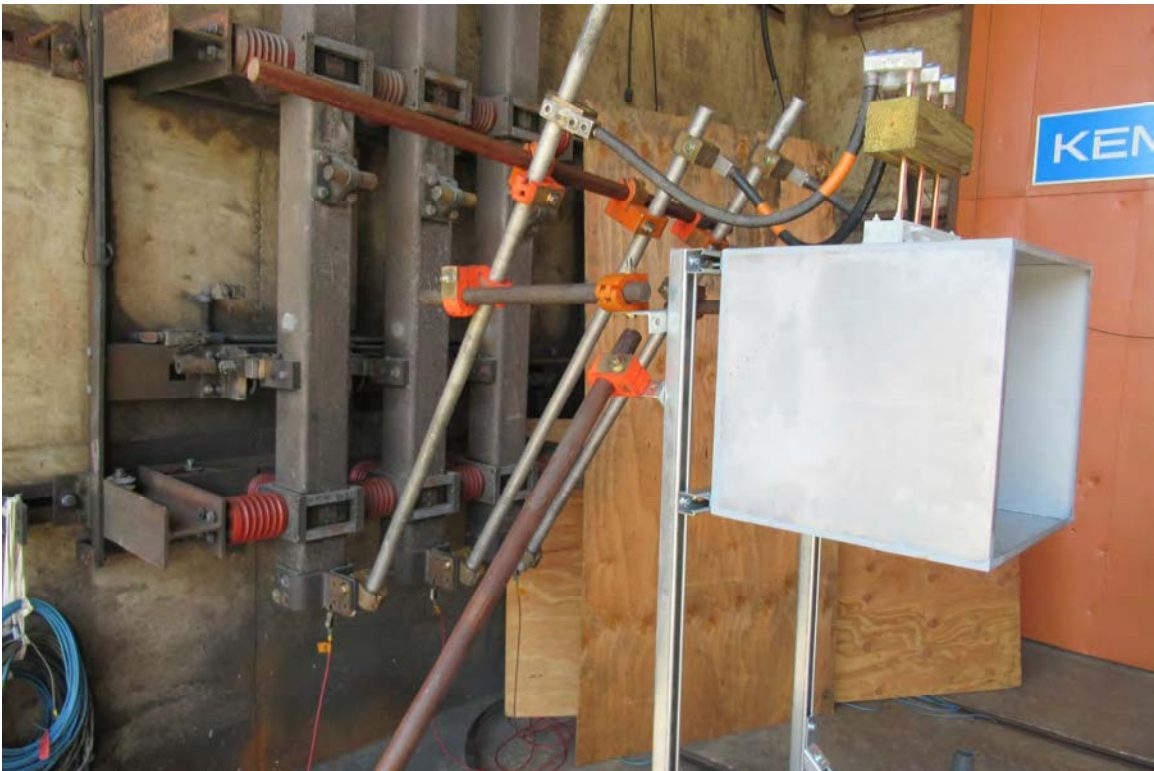
TESTED BY: J. Duffy, B. Swartz

CODE#	TYPE	MANUFACTURER	MODEL#	SERIAL#	CALIBRATION	
					LAST	DUE
TEM89	TEMP.LOGGER	DEWESoft	KRYPTONi	D05980d869	5/30/2019	12/16/2019
TEM92	TEMP.LOGGER	DEWESoft	KRYPTONi	D05980F2EB	5/30/2019	12/16/2019
DAS17	DAS	NI/DEWETRON	DEWE-30-16	0195BB69	9/23/2019	4/10/2020
ISO132	ISO AMP	DEWETRON	HIS-LV	437726	9/23/2019	4/10/2020
ISO117	ISO AMP	DEWETRON	HIS-LV	437711	9/23/2019	4/10/2020
ISO118	ISO AMP	DEWETRON	HIS-LV	437712	9/23/2019	4/10/2020
ISO119	ISO AMP	DEWETRON	HIS-LV	437713	9/23/2019	4/10/2020
ISO124	ISO AMP	DEWETRON	HIS-LV	437718	9/23/2019	4/10/2020
ISO125	ISO AMP	DEWETRON	HIS-LV	437719	9/23/2019	4/10/2020
ISO126	ISO AMP	DEWETRON	HIS-LV	437720	9/23/2019	4/10/2020
CTX172	ROGOWSKI CT	PEM	SDS0680	0002-0100A	10/11/2019	4/28/2020
CTX173	ROGOWSKI CT	PEM	SDS0680	0002-0100B	10/11/2019	4/28/2020
CTX174	ROGOWSKI CT	PEM	SDS0680	0002-0100C	10/11/2019	4/28/2020
CTX175	ROGOWSKI CT	PEM	SDS0680	0002-0100D	10/11/2019	4/28/2020
VDR84	V.DIVIDER	NORTH STAR	VD-150	1	6/21/2019	1/7/2020
VDR86	V.DIVIDER	NORTH STAR	VD-150	3	6/21/2019	1/7/2020
VDR90	V.DIVIDER	NORTH STAR	VD-150	7	6/21/2019	1/7/2020

DATE:	QUOTE #:
8/22/19	24512323
TRIAL #:	SAMPLE #:
7003	
NOTES:	
1kA 1kV	
BEFORE TEST	











DATE: 8/22/19	QUOTE #: 24512323
TRIAL #: 7003	SAMPLE #:
NOTES: 1kA 1kV	
AFTER TEST	



DATE:	QUOTE #:
8/22/19	245/2323
TRIAL #:	SAMPLE #:
7004	
NOTES:	
1 kA 1 kV	
BEFORE TEST	



DATE: 8/22/19	QUOTE #: 24512323
TRIAL #: 7004	SAMPLE #:
NOTES: 1 kA 1 kV	
AFTER TEST	



DATE: 8/22/19	QUOTE #: 24512323
TRIAL #: 7005	SAMPLE #:
NOTES:	
BEFORE TEST	



DATE: 8/22/19	QUOTE #: 24512323
TRIAL #: 7005	SAMPLE #:
NOTES:	
AFTER TEST	



DATE: 8/22/19	QUOTE #: 24512323
TRIAL #: 7006	SAMPLE #:
NOTES:	
BEFORE TEST	

DATE: 8/22/19	QUOTE #: 24512323
TRIAL #: 7006	SAMPLE #:
NOTES: 5KA	
BEFORE TEST	



DATE:	QUOTE #:
8/22/19	24512323
TRIAL #:	SAMPLE #:
7006	
NOTES:	5KA
AFTER TEST	





DATE:	QUOTE #:
8/22/19	245/2323
TRIAL #:	SAMPLE #:
7007	
NOTES:	5KA
BEFORE TEST	



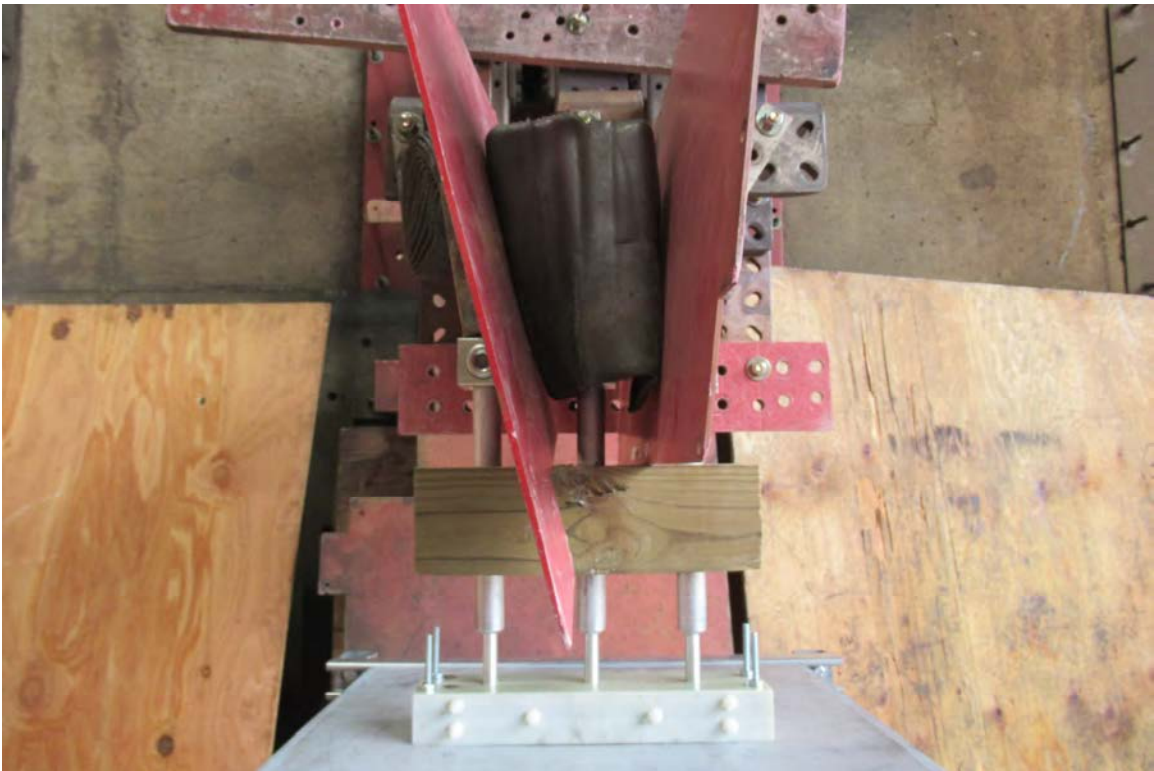
DATE:	QUOTE #:
8/22/19	24512323
TRIAL #:	SAMPLE #:
7007	
NOTES:	
5KA	
AFTER TEST	

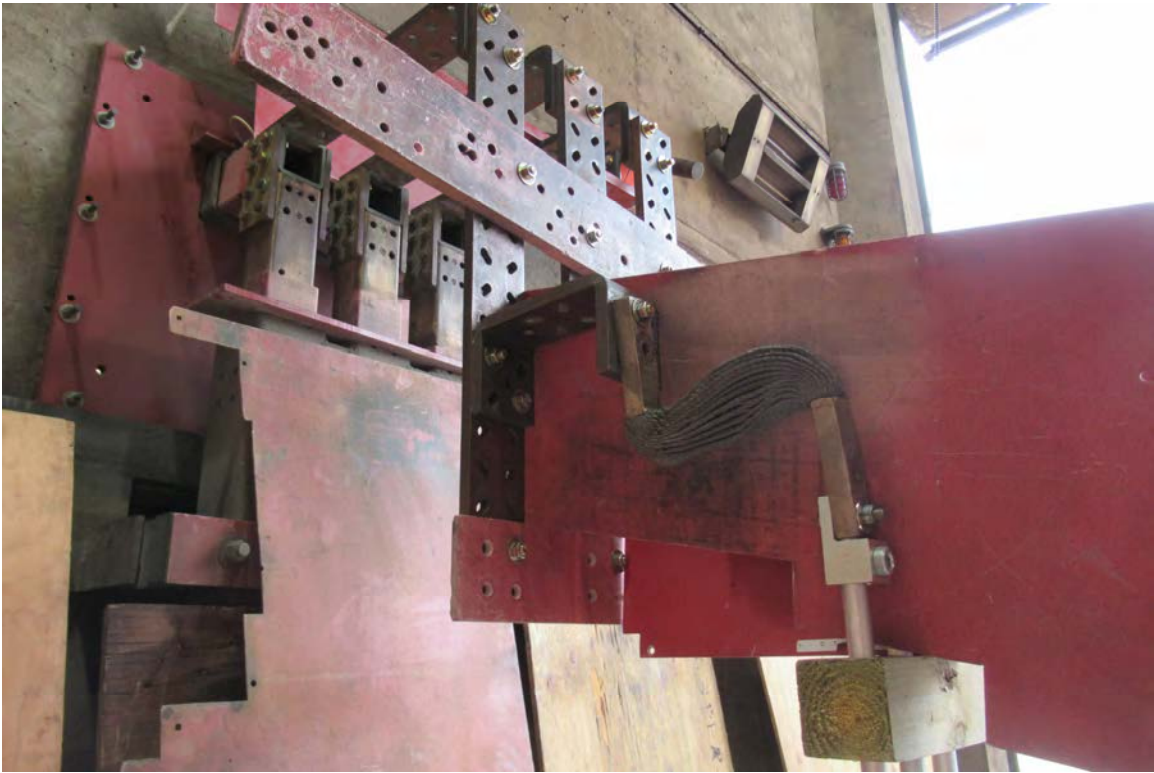


DATE:	QUOTE #:
8/23/19	245/2323
TRIAL #:	SAMPLE #:
7003	
NOTES:	
1000 V 15 kA	
BEFORE TEST	





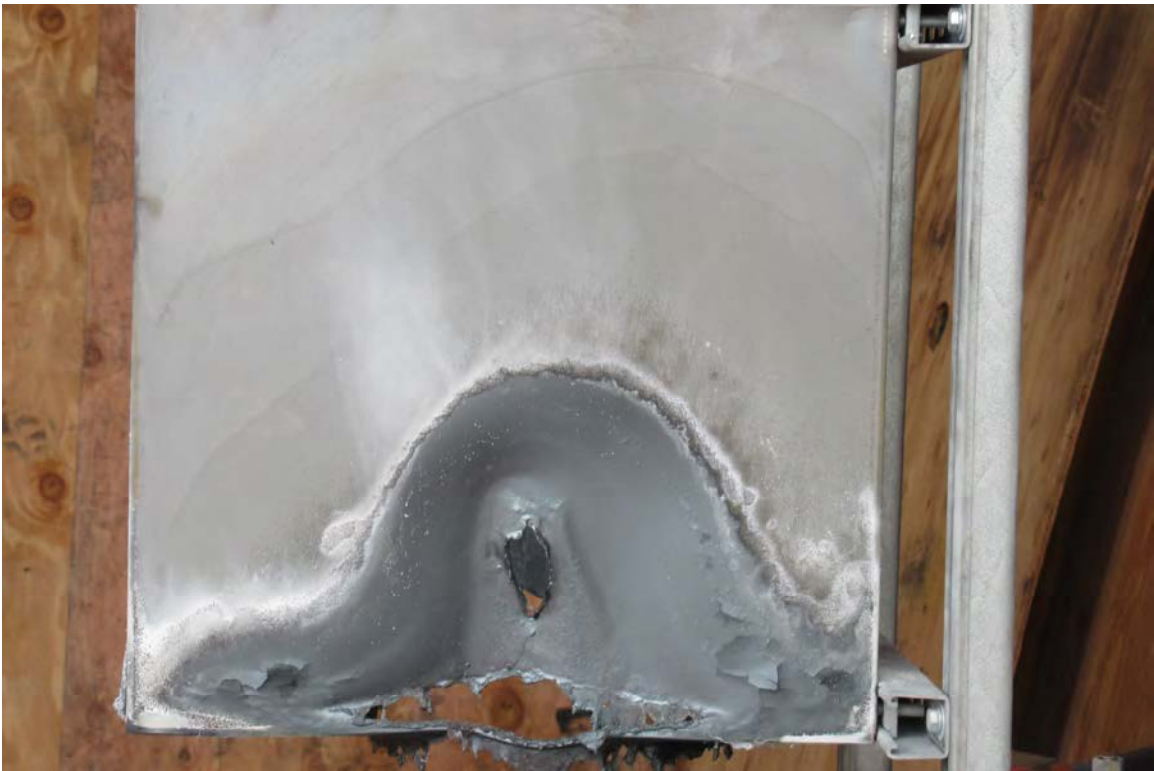




DATE:	QUOTE #:
8/23/19	24512323
TRIAL #:	SAMPLE #:
7003	
NOTES:	
1000 V 15 kA	
AFTER TEST	









DATE:	QUOTE #:
8/23/19	245/2323
TRIAL #:	SAMPLE #:
7004	
NOTES:	
1000 V 15 kA	
BEFORE TEST	



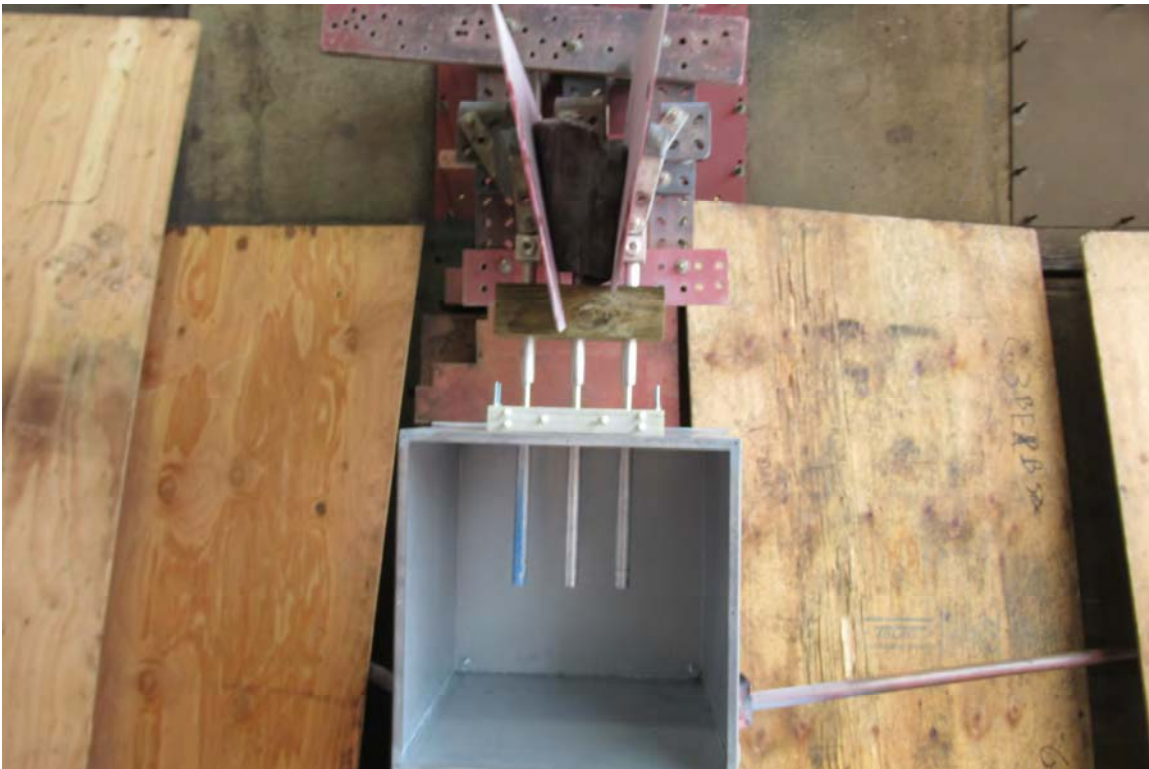


8/23/19	24512323
TRIAL #:	SAMPLE #:
7004	
NOTES:	
1000 V 15 kA	
AFTER TEST	





DATE:	QUOTE #:
8/23/19	24512323
TRIAL #:	SAMPLE #:
7005	
NOTES:	
1000 V 30 kA	
BEFORE TEST	





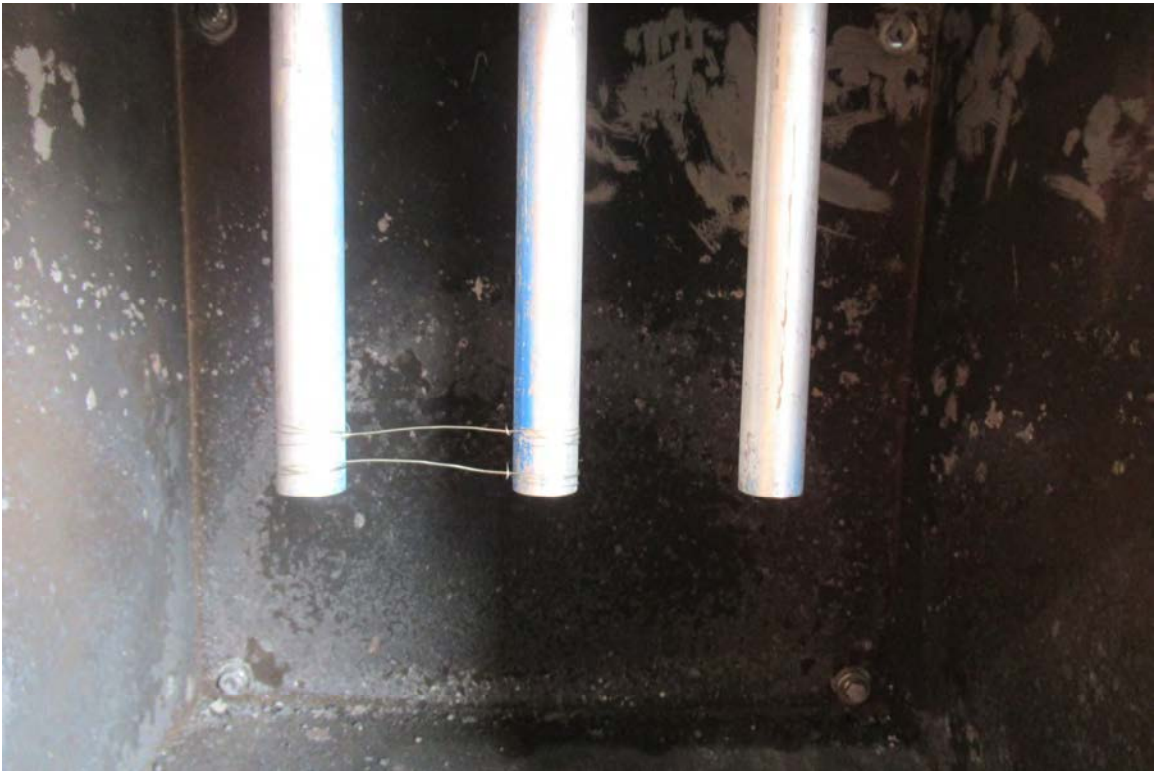
DATE:	QUOTE #:
8/23/19	24512323
TRIAL #:	SAMPLE #:
7005	
NOTES:	
1000 V 30 kA	
AFTER TEST	







DATE:	QUOTE #:
8/23/19	245/2323
TRIAL #:	SAMPLE #:
7006	
NOTES:	
1000 V 15 kA	
BEFORE TEST	

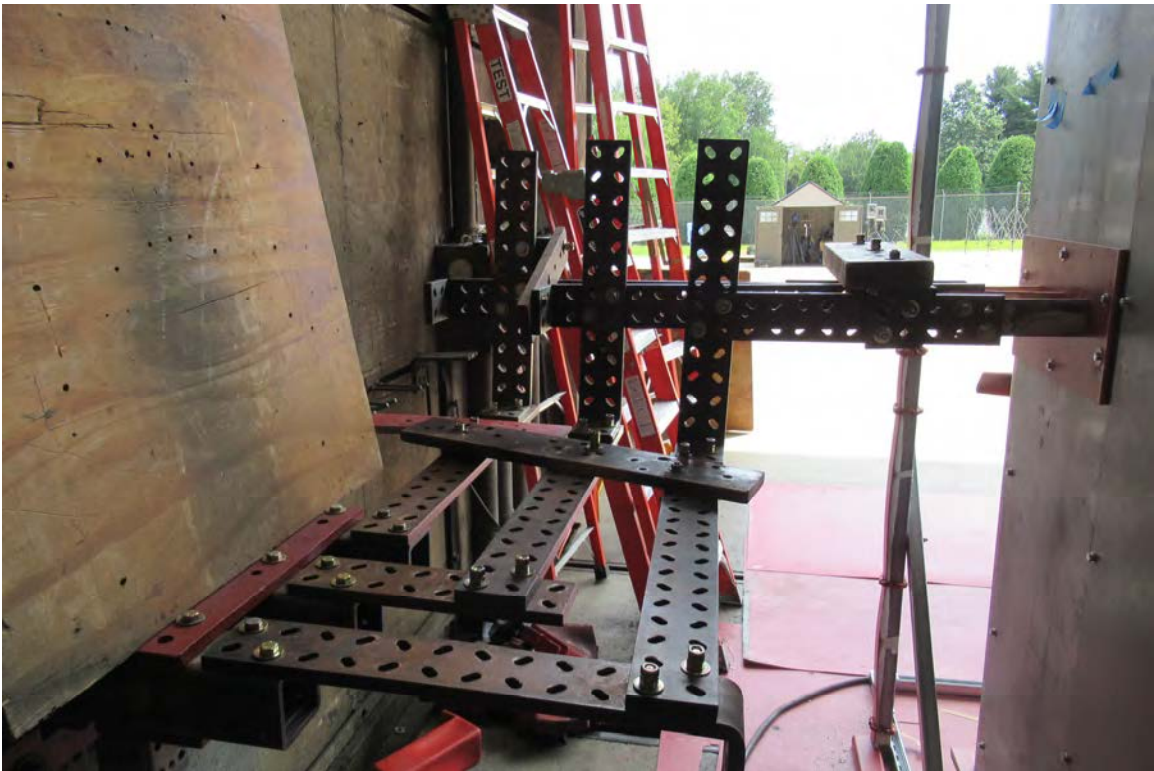


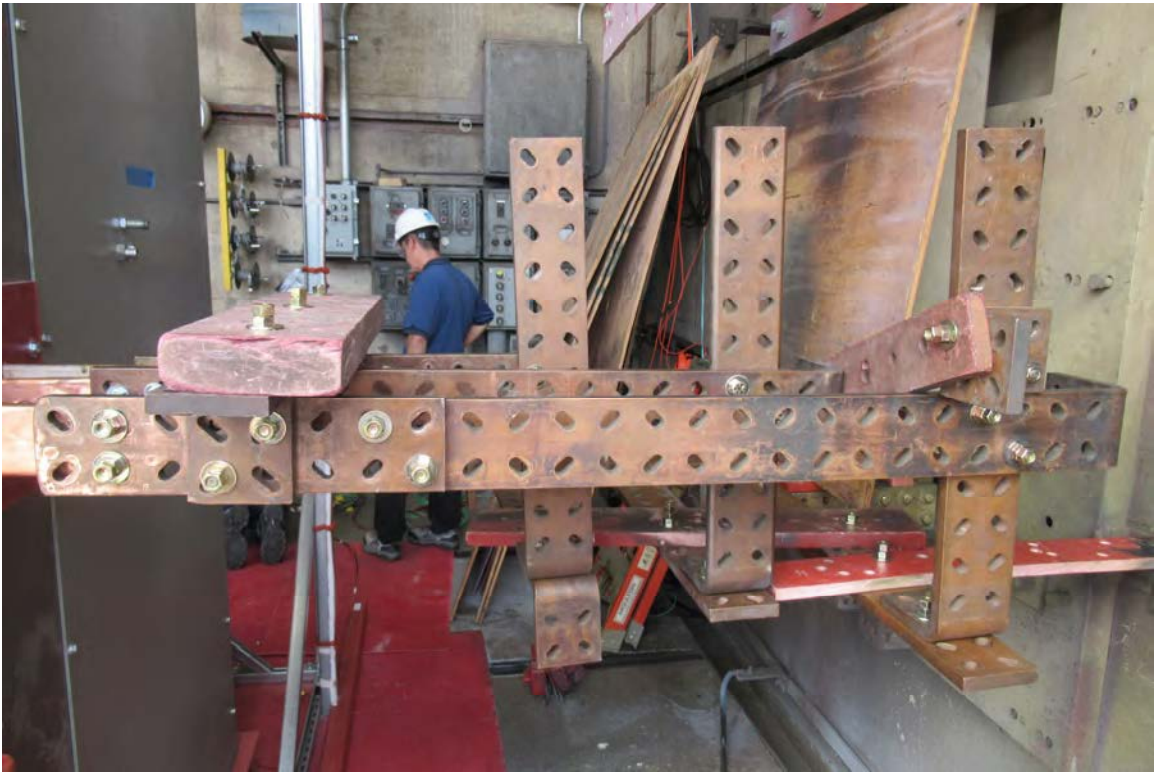
DATE:	QUOTE #:
8/23/19	245/2323
TRIAL #:	SAMPLE #:
7006	
NOTES:	
1000 V 15 kA	
AFTER TEST	





DATE:	QUOTE #:
8/26/19	24512323
TRIAL #:	SAMPLE #:
7003	
NOTES:	
BEFORE TEST	













DATE:	QUOTE #:
8/26/19	24512323
TRIAL #:	SAMPLE #:
7003	
NOTES:	
AFTER TEST	



DATE: 8/27/19	QUOTE #: 24512323
TRIAL #: 7001	SAMPLE #:
NOTES:	

BEFORE TEST





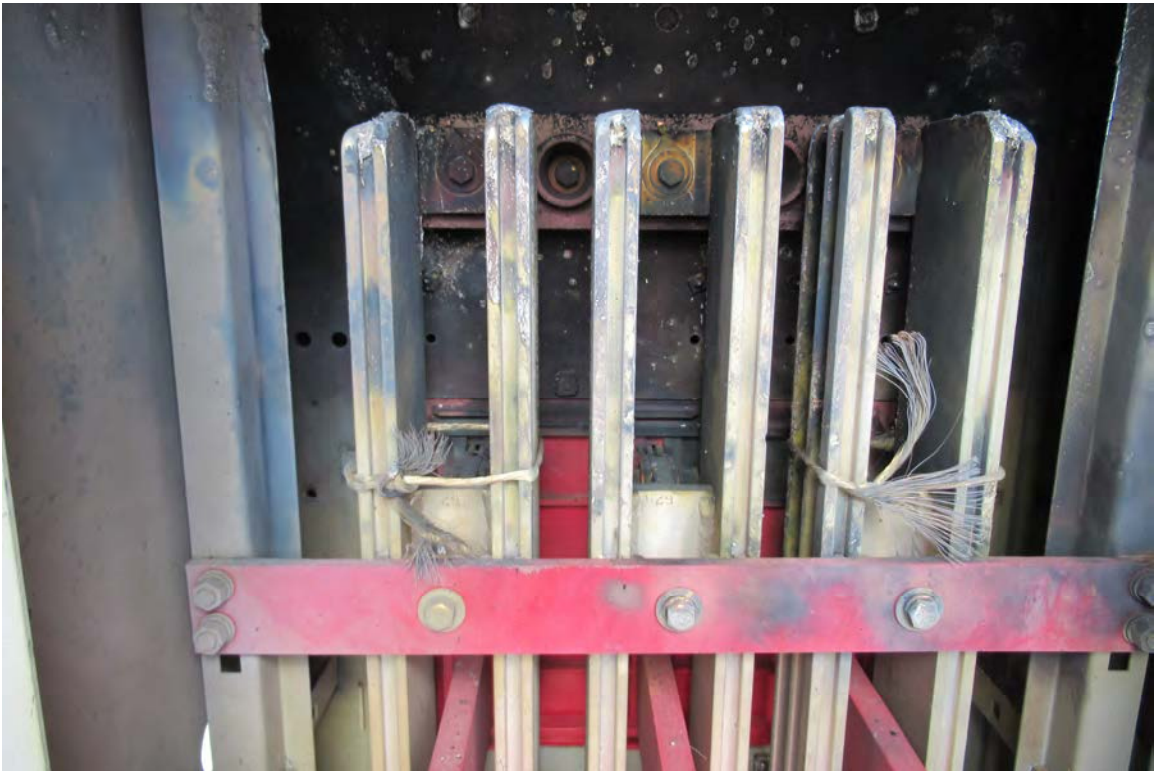
DATE: 8/27/19	QUOTE #: 24512323
TRIAL #: 7001	SAMPLE #:
NOTES:	
AFTER TEST	



DATE:	QUOTE #:
8/27/19	24512323
TRIAL #:	SAMPLE #:
7002	
NOTES:	
BEFORE TEST	



DATE:	QUOTE #:
8/27/19	24512323
TRIAL #:	SAMPLE #:
7002	
NOTES:	
AFTER TEST	



DATE:	QUOTE #:
8/27/19	24512323
TRIAL #:	SAMPLE #:
7003	
NOTES:	
BEFORE TEST	



DATE:	QUOTE #:
8/27/19	24512323
TRIAL #:	SAMPLE #:
7003	
NOTES:	
AFTER TEST	





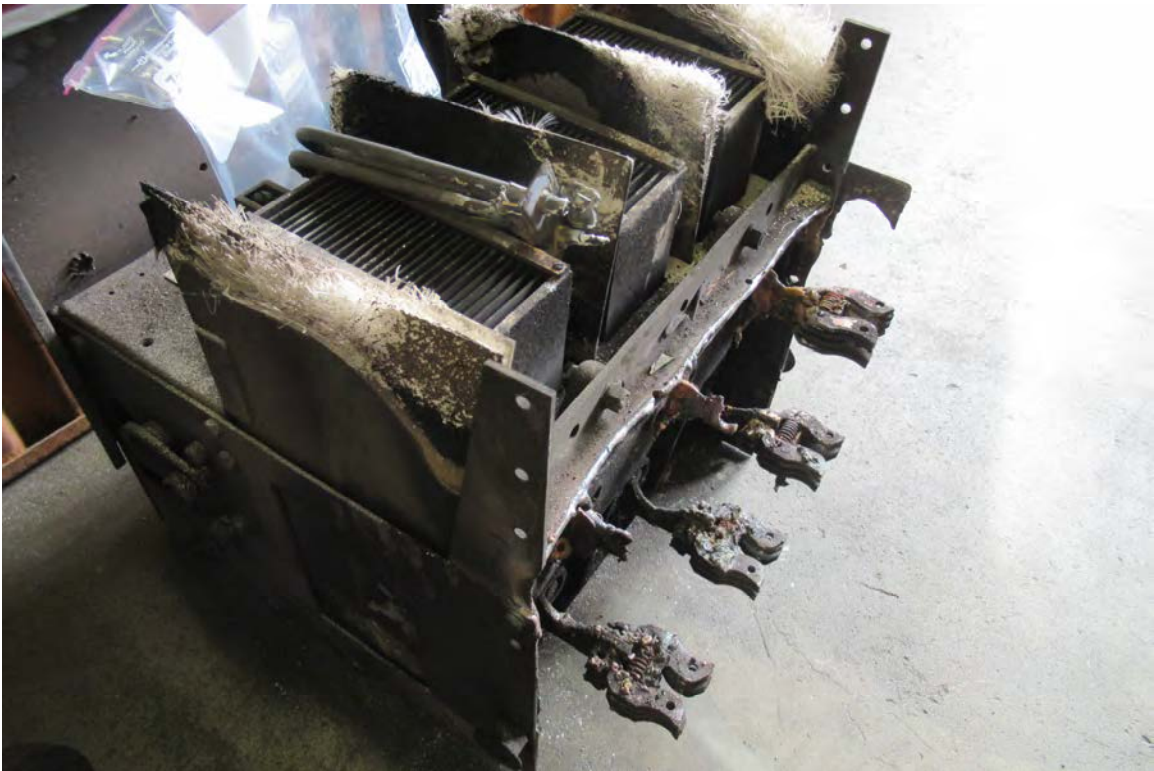
DATE: 8/27/19	QUOTE #: 24512323
TRIAL #: 7004	SAMPLE #:
NOTES:	
BEFORE TEST	



DATE:	QUOTE #:
8/28/19	24512323
TRIAL #:	SAMPLE #:
7001	
NOTES:	
BEFORE TEST	



DATE:	QUOTE #:
8/28/19	24512323
TRIAL #:	SAMPLE #:
7001	
NOTES:	
AFTER TEST	







DATE:	QUOTE #:
8/28/19	24512323
TRIAL #:	SAMPLE #:
7002	
NOTES:	
BEFORE TEST	





DATE:	QUOTE #:
8/29/19	24512323
TRIAL #:	SAMPLE #:
7005	
NOTES:	
BEFORE TEST	













DATE: 8/29/19	QUOTE #: 24512323
TRIAL #: 7005	SAMPLE #:
NOTES:	
AFTER TEST	









DATE: 8/29/19	QUOTE #: 24512323
TRIAL #: 7006	SAMPLE #:
NOTES:	
AFTER TEST	



DATE:	QUOTE #:
8/30/19	24512323
TRIAL #:	SAMPLE #:
7001	
NOTES:	
1000 V, 15 kA	
BEFORE TEST	



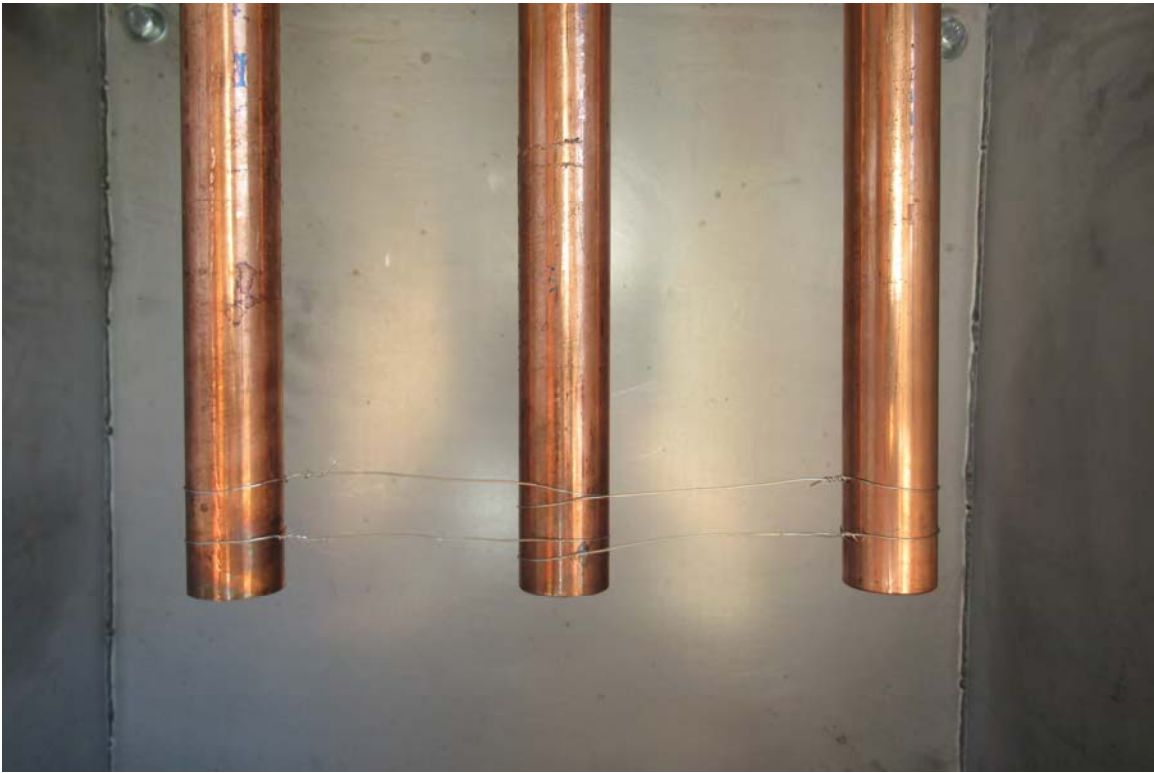




DATE:	QUOTE #:
8/30/19	24512323
TRIAL #:	SAMPLE #:
7001	
NOTES:	
1000 V, 15 KA	
AFTER TEST	



DATE:	QUOTE #:
8/30/19	24512323
TRIAL #:	SAMPLE #:
7002	
NOTES:	
1000 V, 15 KA	
3 SEC	
BEFORE TEST	



DATE:	QUOTE #:
8/30/19	24512323
TRIAL #:	SAMPLE #:
7002	
NOTES:	
1000 V, 15 KA	
3 SEC	
AFTER TEST	





DATE:	QUOTE #:
8/30/19	24512323
TRIAL #:	SAMPLE #:
7003	
NOTES:	
1000 V, 30KA	
1 SEC	
BEFORE TEST	



DATE:	QUOTE #:
8/30/19	24512323
TRIAL #:	SAMPLE #:
7003	
NOTES:	
1000 V, 30KA	
1 SEC	
AFTER TEST	





DATE:	QUOTE #:
8/30/19	24512323
TRIAL #:	SAMPLE #:
700.4	
NOTES:	
1000 V, 15 kA AΦ - BΦ	
BEFORE TEST	



DATE:	QUOTE #:
8/30/19	24512323
SERIAL #:	SAMPLE #:
700.4	
NOTES:	
1000 V, 15 KA AΦ - BΦ	
AFTER TEST	



DATE:	QUOTE #:
8/30/19	24512323
TRIAL #:	SAMPLE #:
7005	
NOTES:	
1000 V, 15 KA CΦ → ENC	
BEFORE TEST	



DATE:	QUOTE #:
8/30/19	24512323
MATERIAL #:	SAMPLE #:
7005	
NOTES:	
1000 V, 15 KA CØ → ENC	
AFTER TEST	



DATE:	QUOTE #:
8/30/19	24512323
TRIAL #:	SAMPLE #:
7006	
NOTES:	
1000 V, 15 KA Bφ → ENC	
BEFORE TEST	



DATE:	QUOTE #:
8/30/19	24512323
TRIAL #:	SAMPLE #:
7006	
NOTES:	
1000 V, 15 KA BØ → ENC	
AFTER TEST	



DATE:	QUOTE #:
8/30/19	24512323
TRIAL #:	SAMPLE #:
7007	
NOTES:	
1000 V, 15 KA C:Φ → ENC	
BEFORE TEST	



DATE: 8/30/19	QUOTE #: 24512323
TRIAL #: 7007	SAMPLE #:
NOTES: 1000 V, 15 KA C: ϕ \rightarrow ENC	
AFTER TEST	



DATE:	QUOTE #:
8/30/19	24512323
TRIAL #:	SAMPLE #:
7008	
NOTES:	
1000 V, 15 KA C Φ \rightarrow ENC	
BEFORE TEST	



DATE:	QUOTE #:
8/30/19	24512323
TRIAL #:	SAMPLE #:
7008	
NOTES:	
1000 V, 15 KA C Φ \rightarrow ENC	
AFTER TEST	



DATE:	QUOTE #:
8/30/19	24512323
TRIAL #:	SAMPLE #:
7009	
NOTES:	
1000 V, 15 KA C Φ \rightarrow ENC	
BEFORE TEST	



DATE:	QUOTE #:
8/30/19	24512323
TRIAL #:	SAMPLE #:
7009	
NOTES:	
1000 V, 15 KA C Φ \rightarrow ENC	
AFTER TEST	



DATE:	QUOTE #:
8/30/19	24512323
TRIAL #:	SAMPLE #:
7010	
NOTES:	
480 V, 13.5	
BEFORE TEST	



DATE:	QUOTE #:
8/30/19	24512323
TRIAL #:	SAMPLE #:
7010	
NOTES:	
480 V, 13.5	
AFTER TEST	



DATE:	QUOTE #:
9/16/19	24512323
TRIAL #:	SAMPLE #:
9006	03MV5
NOTES:	
BEFORE TEST	

09/16/2019













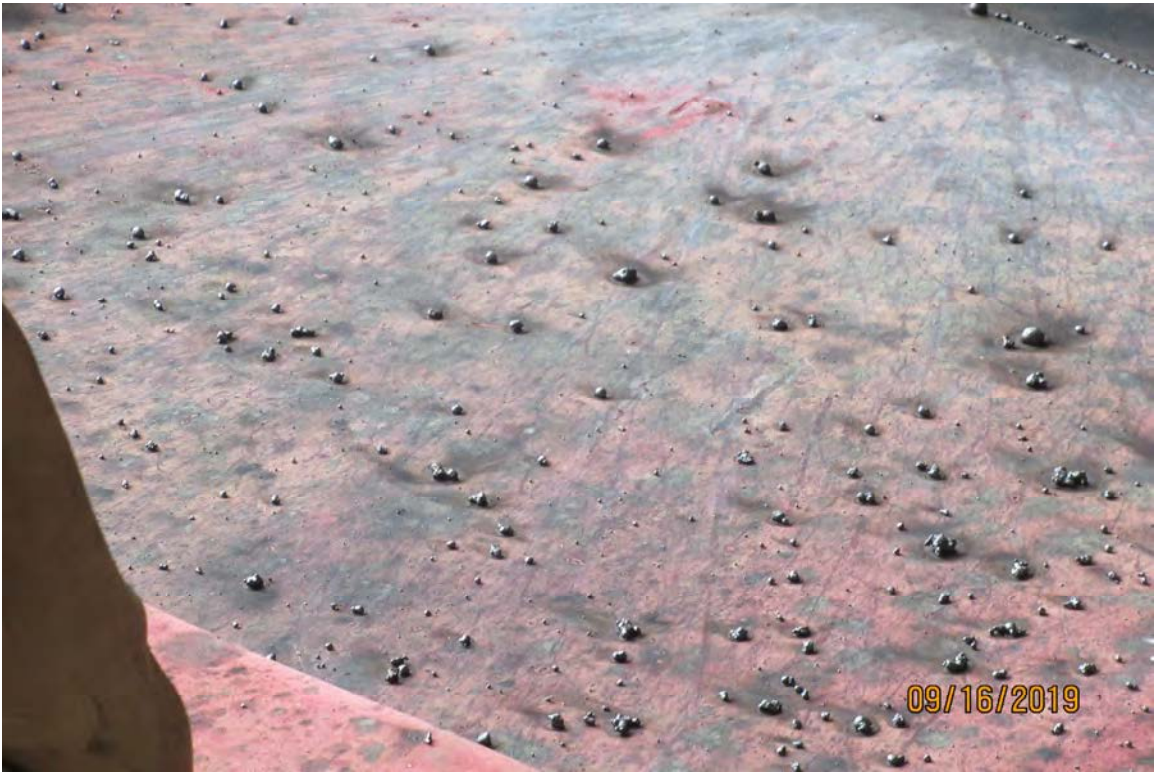
DATE:	QUOTE #:
9/16/19	245/2323
TRIAL #:	SAMPLE #:
9006	OBMV5
NOTES:	
AFTER TEST	

09/16/2019









DATE:	QUOTE #:
9/17/19	24512323
TRIAL #:	SAMPLE #:
9001	OBMV 2
NOTES:	
BEFORE TEST	

09/17/2019

















DATE:	QUOTE #:
9/17/19	245/2323
TRIAL #:	SAMPLE #:
9002	03MV4
NOTES:	
BEFORE TEST	

09/17/2019







DATE:	QUOTE #:
9/17/19	24512323
TRIAL #:	SAMPLE #:
9002	03MV4
NOTES:	
BEFORE TEST	

09/17/2019

DATE:	QUOTE #:
9/17/19	245/2323
TRIAL #:	SAMPLE #:
9002	03MV4
NOTES:	
AFTER TEST	

09/17/2019









DATE:	QUOTE #:
9/18/19	24512323
TRIAL #:	SAMPLE #:
9001	03MVI
NOTES:	
BEFORE TEST	

09/18/2019









DATE:	QUOTE #:
9/18/19	245/2323
TRIAL #:	SAMPLE #:
9001	03Mv1
NOTES:	
AFTER TEST	

09/18/2019



DATE:	QUOTE #:
9/18/19	245/2323
TRIAL #:	SAMPLE #:
9002	03Mv3
NOTES:	

BEFORE TEST

09/18/2019













DATE:	QUOTE #:
9/18/19	245/2323
TRIAL #:	SAMPLE #:
9003	03MV6
NOTES:	
BEFORE TEST	

09/18/2019







DATE:	QUOTE #:
9/18/19	24512323
TRIAL #:	SAMPLE #:
9003	03MV6
NOTES:	

09/18/2019

AFTER TEST





END OF DOCUMENT